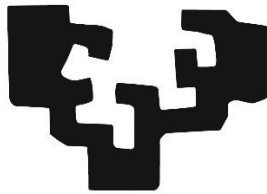eman ta zabal zazu

Universidad
del País Vasco

Euskal Herriko
Unibertsitatea

Cannabinoid modulation of the cortical information processing through the basal ganglia circuits in physiological and hypodopaminergic states

Doctoral thesis presented by Mario Antonazzo Soler

Leioa, 2021

INDEX

5. DISCUSSION   123

ABBREVIATION LIST

6-OHDA	6-Hydroxydopamine
ACC	Anterior Cingulate Cortex
AMPA	Ionotropic glutamatergic α-amino-3-hydroxy-5-methyl-4-isoxazolepropionate receptors
ANOVA	Analysis of the variance
AP	Anteroposterior
AUC	Area Under the Curve
BG	Basal Ganglia
CB$_1$	Cannabinoid receptor 1
CB$_2$	Cannabinoid receptor 2
CV	Coefficient of Variation
D$_1$-D$_5$	Dopaminergic D$_1$-D$_5$ receptor
DA	Dopamine / Dopaminergic
DAB	3,3′-diaminobenzidine
DV	Dorsoventral
ECoG	Electrocorticogram
EE	Early Excitation
FR	Firing Rate
GP	*Globus pallidus*
GPe	external *globus pallidus*
GPi	internal *globus pallidus*
Hz	Hertz
i.p.	intraperitoneal
i.v.	intravenous
INH	Inhibition
ISI	Inter-Spike Interval
KPBS	Potassium Phosphate Buffer

L-DOPA	Levodopa or 3,4-Dihydroxy-L-phenylalanine methyl ester
LE	Late Excitation
LFP	Local Field Potential
MC	Motor Cortex
MFB	Medial Forebrain Bundle
ML	Mediolateral
mPF	medial prefrontal
MPTP	l-methyl-4-phenyl-l,2,3,6-tetrahydropyridine
MSN	Medium Spiny Neuron
NGS	Normal Goat Serum
NMDA	Ionotropic glutamatergic N-methyl-D-aspartate (NMDA) receptor
OD	Optical Density
PB	Phosphate Buffer
PBS	Phosphate Buffer Saline
PD	Parkinson's disease
PPAR	peroxisome proliferator-activated receptors
S.E.M	Standard Error of the Mean
SM	*Sensorimotor*
SN	*Substantia nigra*
SNc	Substantia nigra *pars compacta*
SNr	Substantia nigra *pars reticulata*
STN	Subthalamic nucleus
SWA	Slow-wave Activity
TBS	Tris-HCl Buffered Saline
TH	Tyrosine hydroxylase
TRP	transient receptor potential channels
WIN	WIN 55,2l2-2
Δ⁹-THC	delta-9-Tetrahydrocannabinol

1. INTRODUCTION

1. INTRODUCTION

1.1. Cortico-basal ganglia circuits

The basal ganglia (BG) form a highly organized network of subcortical nuclei implicated in a vast array of functions influencing movement, learning, cognition and motivation (Pennartz et al., 2009). Therefore, disturbances in this complex network could lead to a wide range of behavioural disorders like schizophrenia, drug abuse or Parkinson's disease (PD) (Tremblay et al., 2015). Moreover, cortex and thalamus are tightly associated with the BG, giving place to the so called cortico-BG circuits, destined to integrate multi-modal information, in order to fine-tune behavioural output. Following, the more relevant structures in cortico-BG circuits are detailed.

1.1.1. Main structures involved in cortico-basal ganglia circuit function

1.1.1.1. Cortex

Cortical neurons can be divided in two fundamental types: pyramidal and non-pyramidal cells. Generally, these neurons in the cerebral cortex are disposed in six layers, forming a characteristic laminar pattern (Pandya et al., 2014). Most of these neurons are pyramidal neurons using glutamate as neurotransmitter, with ~20% being GABAergic interneurons, important in keeping balance between excitatory and inhibitory inputs, that otherwise may end up in disorders such as epilepsy (Chu & Anderson, 2015; Defelipe et al., 2013; Marín, 2012). Pyramidal neurons, depending on the layer they are located, form different synapses thus having different functions (Pandya et al., 2014). Pyramidal neurons in layers 2 and 3 form axonal projections within the cerebral cortex, not just between layers (i.e., 4, 5 and 6), but also with different cortical areas. Pyramidal neurons in layer 4 convey a source of information entering cortex receiving, for instance, inputs from thalamic projections, thus closing the cortico-BG-thalamic loops (Gerfen et al., 2018; Shepherd, 2013).

Of great importance in cortico-BG circuits are pyramidal neurons in layers 5 and 6, especially those in layer 5. According to their projections, these neurons can be classified as intratelencephalic or pyramidal tract neurons. Intratelencephalic neurons (i.e., layers 5 and 6) project ipsi- or bilaterally to cortical and striatal targets, whilst pyramidal tract neurons (i.e., layer 5) ipsilaterally innervate BG nuclei like the striatum and the subthalamic nucleus (STN), on their way to their targets in the brain stem and the spinal cord. Finally, another group of pyramidal neurons in the layer 6, would project exclusively to the ipsilateral thalamus (Shepherd, 2013).

1.1.1.2. Striatum

The striatum is considered the main input structure of the BG, whose main theorized function is to integrate a wide range of inputs from cortex, thalamus, hippocampus, and amygdala, among others. The striatum is composed in a ~95% of GABAergic projection neurons called medium spiny neurons (MSN). According to their projection patterns, approximately half of MSNs project to the *substantia nigra pars reticulata* (SNr) or entopeduncular nucleus (internal *globus pallidus* (GPi) in primates) forming the so-called 'direct' or striato-nigral pathway, while the other half projects to the *globus pallidus* (GP; external *globus pallidus* (GPe) in primates) stablishing the so-called 'indirect' or striato-pallidal pathway (Albin et al., 1989). In terms of their molecular profile, MSNs belonging to the direct pathway express substance P, dynorphin, and the dopamine (DA) D_1 receptor, while MSNs from the indirect pathway express enkephalin and the DA D_2 receptor (Gerfen & Young, 1988). Striatal interneurons, despite their small number, comprise several neuronal populations with distinct electrophysiological, molecular and synaptic profiles. According to the neurotransmitter used, these interneurons can be classified as cholinergic or GABAergic, although they might release other signalling molecules as well, like glutamate (Higley et al., 2011). GABAergic interneurons can be further classified as fast-spiking, low-threshold, calretinin-expressing, tyrosine hydroxylase (TH)-expressing, neurogliaform, fast adapting or spontaneous active bursty interneurons (Assous et al., 2018; Faust et al., 2015; Ibáñez-Sandoval et al., 2010, 2011; Kawaguchi et al., 1995).

Different criteria have been used to partition the striatum, in order to study it. Based on certain molecular markers (i.e., opioid μ receptors, acetyltransferase), the striatum can be divided in patches and matrix (Graybiel & Ragsdale, 1978; Herkenham & Pert, 1981). Attending to anatomical criteria (i.e., cortical inputs), this nucleus can be divided in functional territories. The dorsal striatum comprises what would be the caudate and putamen in primates, and can be further divided in dorsolateral, and dorsomedial striatum. On the other hand, the ventral striatum would refer to the *nucleus accumbens*, both core and shell. Cortical projections onto the striatum follow a highly organized pattern, following a dorsolateral-ventromedial distribution (Figure 1.1). The dorsolateral striatum receives mostly afferents from sensorimotor (SM)-related cortical areas, while the dorsomedial striatum receives principally projections from the dorsal part of the medial prefrontal (mPF) cortex (i.e., anterior cingulate cortex (ACC) and dorsal prelimbic cortex). On the other hand, the *nucleus accumbens* principally receives afferents from ventral areas of the mPF cortex (i.e., ventral prelimbic and infralimbic cortices) and insular cortices, sharing some cortical projection areas with the dorsomedial striatum, especially in its core (Berendse et al., 1992; McGeorge & Faull, 1989). Despite this highly organized pattern, there is no clear-cut division between projections from different cortical areas, showing some degree of overlapping (Heilbronner et al., 2016). Thalamic nuclei also project to the striatum in a patterned manner, as each thalamic nuclei innervate mainly a striatal region (Van der Werf et al., 2002). Basal amygdaloid complex innervation of the striatum especially innervate its ventral tiers, with some fibres reaching the dorsomedial striatum, and sparse innervation of the dorsolateral striatum (Wright et al., 1996). In addition, the hippocampus projects almost exclusively to the *nucleus accumbens* shell (Groenewegen et al., 1999). Furthermore, monoaminergic areas of the brain, like the *substantia nigra pars compacta* (SNc) and ventral tegmental area, dorsal raphe nucleus, and to some extent the *locus coeruleus* also project to the striatum, conveying important neuromodulation to striatal circuits (Joel & Weiner, 2000; Mason & Fibiger, 1979; Steinbusch et al., 1981). Regarding striatal DA innervation, SNc and ventral tegmental area projections are arranged in a compartmentalized fashion. Dorsolateral striatum receives mainly DA inputs from the lateral SNc, while the dorsomedial striatum receives afferents especially from the medial SNc, but also from the ventral

tegmental area. On the other hand, the ventral striatum receives DA inputs especially from the ventral tegmental area, and to some extent from the medial SNc (Joel & Weiner, 2000).
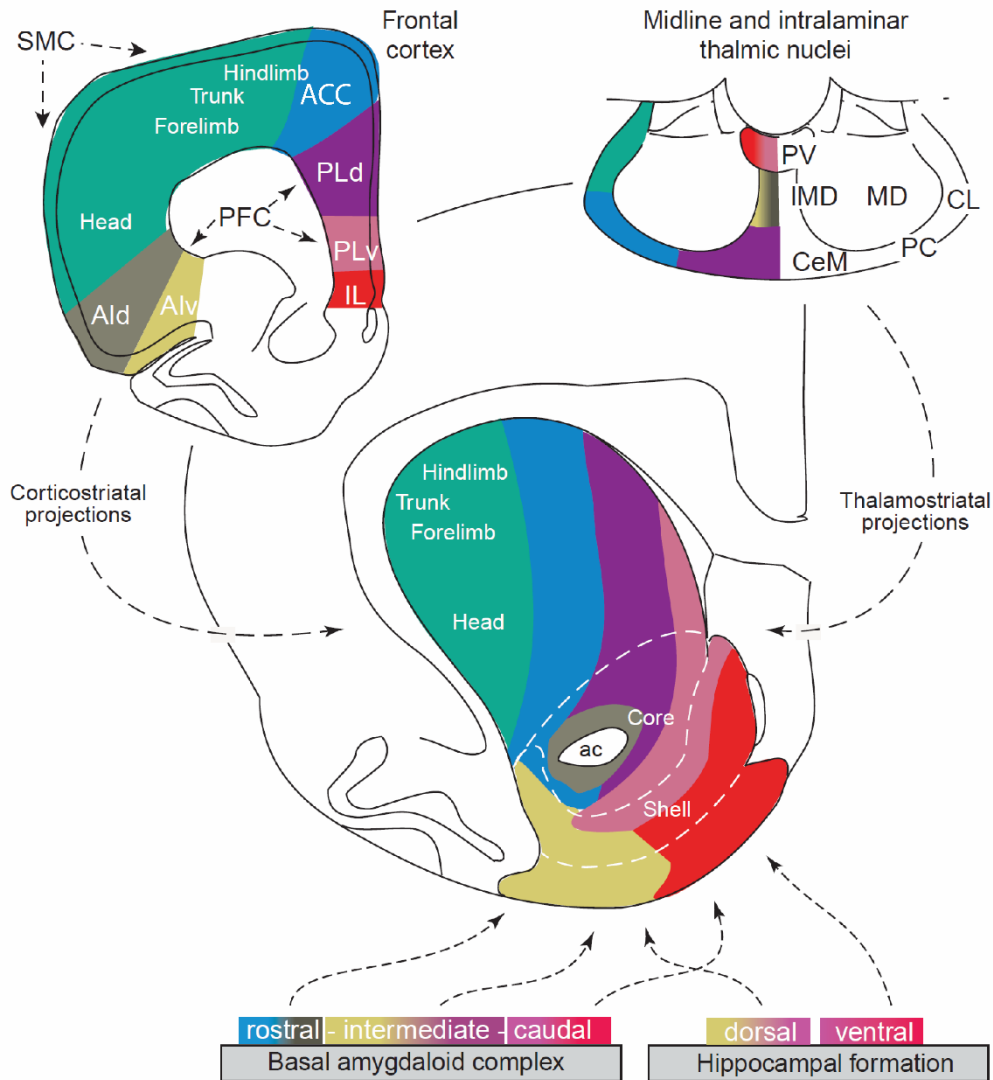
Figure 1.1: Patterned distribution of cortical, thalamic, amygdaloid and hippocampal inputs to the rodent striatum. Note the dorsolateral-ventromedial characteristic organization of cortico-striatal projections. ac, anterior commissure; ACC, anterior cingulate cortex; AId, dorsal agranular insular cortex; AIv, ventral agranular insular cortex; CeM, central medial thalamic nucleus; CL, central lateral thalamic nucleus; IL, infralimbic cortex; IMD, intermediodorsal thalamic nucleus; MD, mediodorsal thalamic nucleus; PC, paracentral thalamic nucleus; PFC, prefrontal cortex; PLd, dorsal prelimbic cortex; PLv, ventral prelimbic cortex; PV, paraventricular thalamic nucleus; SMC, sensorimotor cortex. (Voorn et al., 2004).

Altogether, striatal neurons would stablish contacts with each other, as well as with incoming terminals to the striatum, forming a complex circuitry, that will ultimately shape striatal output conveyed by MSNs.

1.1.1.3. *Globus pallidus*

The GP is a GABAergic nucleus, and key component of the indirect pathway in cortico-BG circuits. Principal inputs to this nucleus come from GABAergic MSNs belonging to the indirect pathway, and glutamatergic inputs from the STN, as well as collaterals from GP neurons (Kita, 2007; Parent & Hazrati, 1995; Sadek et al., 2007). On the other hand, GP neurons mainly send efferents to the striatum, STN and SNr (Chang et al., 1983; Gerfen et al., 1990; Smith & Bolam, 1989). Striatal inputs to the GP follow a functional organization, as shown by their calbindin expression pattern, lateral tiers of the GP would receive inputs from the dorsolateral striatum, while medial tiers of the GP would receive afferents from the dorsomedial striatum (Fujiyama et al., 2016; Rajakumar, Rushlow, et al., 1994). GP input/output seem to be defined by two distinct electrophysiological and molecularly characterized neuronal subpopulations: prototypical and arkypallidal GP neurons (Mallet et al., 2012). Prototypical neurons are characterized by Nkx2.1 expression, accounting for more than the 70% of GP neurons. This GP neuronal population receive innervation from striato-pallidal MSNs and STN neurons. In turn, these neurons project to nuclei such as the STN, both parts of the SN, the entopeduncular nucleus, and the striatum (Abdi et al., 2015; Bevan et al., 1998; Fujiyama et al., 2016; Saunders et al., 2016). On the other hand, arkypallidal neurons are characterized for expressing FoxP2, and constitute ~20% of GP neurons. These neurons receive external inputs from striato-pallidal MSNs, although to a lesser extent than prototypical neurons. Additionally, arkypallidal GP neurons exclusively project their axons to the striatum (Dodson et al., 2015; Mallet et al., 2012; Yuan et al., 2017). This GP circuitry is regulated by serotonergic and DA neurotransmission systems, coming from the *raphe nuclei* and the SNc, respectively (Perkins & Stone, 1983; Rommelfanger & Wichmann, 2010).

1.1.1.4.   Subthalamic nucleus

Together with the striatum, the STN represents a station of external excitatory inputs into the BG. The STN is integrated by densely packed glutamatergic projection neurons, mainly receiving GABAergic contacts from the GP, and glutamatergic contacts from thalamus and cortex, the latter constituting the so-called hyperdirect pathway (Afsharpour, 1985a; Chang et al., 1983; Groenewegen & Berendse, 1990; Kita et al., 1983; Parent & Hazrati, 1995). Excitatory projections onto the STN seem to be topographically arranged, with SM related cortical areas projecting to the lateral part of this nucleus, while mPF cortical areas innervate the medial tier (Afsharpour, 1985b; Berendse & Groenewegen, 1991; Janssen et al., 2017). Moreover, the thalamus sparsely innervates the STN, also showing a mediolateral distribution. Similarly, pallidal innervation show this mediolateral distribution as well, in this case heavily innervating the STN (Groenewegen et al., 1993; Groenewegen & Berendse, 1990; Parent & Hazrati, 1995). Additionally, DA and serotonergic neurotransmitter systems project to the STN modulating its neuronal activity (Canteras et al., 1990; Steinbusch, 1981). Regarding its efferences, STN neurons send projections especially to the GP, but also to both sections of the SN, and to some extent to the striatum and cortex (Koshimizu et al., 2013). STN neurons project to the GP and the SNr profusely and in a topographical way, following a mediolateral distribution (Groenewegen & Berendse, 1990; Parent & Hazrati, 1995; Van Der Kooy & Hattori, 1980). In addition, some STN projections will reach SNc DA neurons, modulating DA release (Koshimizu et al., 2013; Rosales et al., 1994; Smith & Grace, 1992). Moreover, STN axon collaterals contact with other STN neurons, providing an amplification mechanism (Gouty-Colomer et al., 2018).

1.1.1.5.   *Substantia nigra*

The SN is a large midbrain structure composed by a dorsal region called *pars compacta,* and a ventral region called *pars reticulata*. This anatomically and functionally diverse structure stablish relevant synapses with nuclei outside and inside the BG, therefore being involved in several physiological and pathological processes.

1.1.1.5.1.   *Substantia nigra pars compacta*

The SNc correspond to an elongated and densely packed DA nucleus dorsal to the SNr. Its DA neurons project long axons to the striatum and other brain areas forming the nigrostriatal pathway, which is included in the medial forebrain bundle (MFB). Besides DA neurons, the SNc also has GABAergic and glutamatergic neurons (Morales & Root, 2014). This way the SNc provides DA to the striatum, the STN and the GP, among other nuclei (Canteras et al., 1990; Joel & Weiner, 2000; Rommelfanger & Wichmann, 2010). Most of the afferences to this nucleus are GABAergic, coming from the SNr, the GP, and the striatum (Grofová, 1975; Hattori et al., 1975; Tepper et al., 1995). In turn, glutamatergic projections from the mPF cortex and the STN, in addition to serotonergic projections from medial and dorsal raphe nuclei, reach the SNc (Hauber, 1998; Koshimizu et al., 2013; Naito & Kita, 1994).

1.1.1.5.2.   *Substantia nigra pars reticulata*

Ventral to the SNc, there is the SNr, formed mainly by GABAergic projection neurons, with the occasional infiltration of DA neuron groups (González-Hernández & Rodríguez, 2000). GABAergic neurons in the SNr show molecular diversity with neurons subsets expressing parvalbumin, calretinin, nitric oxide and acetylcholine transferase (González-Hernández & Rodríguez, 2000; Martínez-Murillo et al., 1989). Parvalbumin-expressing SNr neurons are mainly located in the lateral aspects of the nucleus, involved in the processing of information from SM-related cortical areas (Rajakumar, Elisevich, et al., 1994).

Together with the entopeduncular nucleus, the SNr constitutes one of the output nuclei of the BG, where information from distinct cortical and thalamic inputs abandons the BG after adequate integration. In line with this, afferents to the SNr come mainly from BG structures, maintaining the mediolateral distribution seen in other BG nuclei afferents (Deniau et al., 1996). The main GABAergic input to the SNr comes from MSNs in the striatum (both dorsal and ventral) conforming the direct-pathway, as well as from other sources such as the GP, and the ventral pallidum (Chevalier & Deniau, 1990; Deniau et al., 1994;

Groenewegen et al., 1993; Smith & Bolam, 1989). Moreover, SNr neurons receive important glutamatergic inputs from the STN, constituting the last step in the hyperdirect pathway (Kita & Kitai, 1987). Additionally, serotonergic and DA innervation from the dorsal raphe nucleus and the SNc respectively, reaches the SNr (Cheramy et al., 1981; Corvaja et al., 1993). SNr neurons send projections mainly to the thalamus, which in turn, projects back to the BG or the cortex closing the cortico-BG-thalamic loops (Kha et al., 2001). In addition to the thalamus, SNr neurons also reach the superior colliculus, the pedunculopontine nucleus, and the periaqueductal grey, offering tonic inhibition on these structures. Projections out of the SNr are carried out by four specific neuronal populations, that projects to different combinations of these nuclei (Cebrián et al., 2005; Kha et al., 2001). Besides this, these neurons display collaterals, playing a dual role as inter- and projection neurons in the SNr (Deniau et al., 1982, 2007).

1.1.2. Sensorimotor and medial prefrontal basal ganglia circuits

The BG nuclei provide the substrate for a complex network that links cortex and thalamus, creating the known as cortico-BG-thalamo-cortical loops or circuits (Figure 1.2). As mentioned above, almost the entire cortex projects to the striatum following an anatomo-functional organization, thus allowing us to establish functional subdivisions of this nucleus, depending on the cortical areas innervating that region. Moreover, this apparent anatomo-functional compartmentalization is not exclusive of the striatum, as it is conserved throughout the BG nuclei. This suggests the existence of parallel and closed cortico-BG circuits through which specific functional information flow back to cortex, after being processed within the BG nuclei. Alexander and colleagues (1986) proposed a cortico-BG-thalamo-cortical organization in non-human primates, including five functionally-distinct parallel loops (Alexander et al., 1986). Later, evidences suggested the involvement of associative/limbic BG territories in motor behaviour (Belin & Everitt, 2008; Sawada et al., 2015), observations further supported by anatomical and functional studies (Aoki et al., 2019; McFarland & Haber, 2002), thus opening a gateway in these 'closed' cortico-BG circuits for information exchange between functionally distinct circuits. Nowadays, is generally

accepted to group these circuits in three functional domains (Tremblay et al., 2015). The 'motor' and 'oculomotor' circuits fall into the SM domain, including premotor, motor and somatosensory cortices; the 'dorsolateral prefrontal' and 'lateral orbitofrontal' circuits belong in the 'associative' domain; and the 'anterior cingulate' circuit pertain to the 'limbic' domain. In rodents, a distinction can be made between the 'sensorimotor' circuits, that would belong to the 'sensorimotor' domain, and the mPF circuits, which would represent a mixed 'associative/limbic' domain (Aliane et al., 2009; Beyeler et al., 2010).
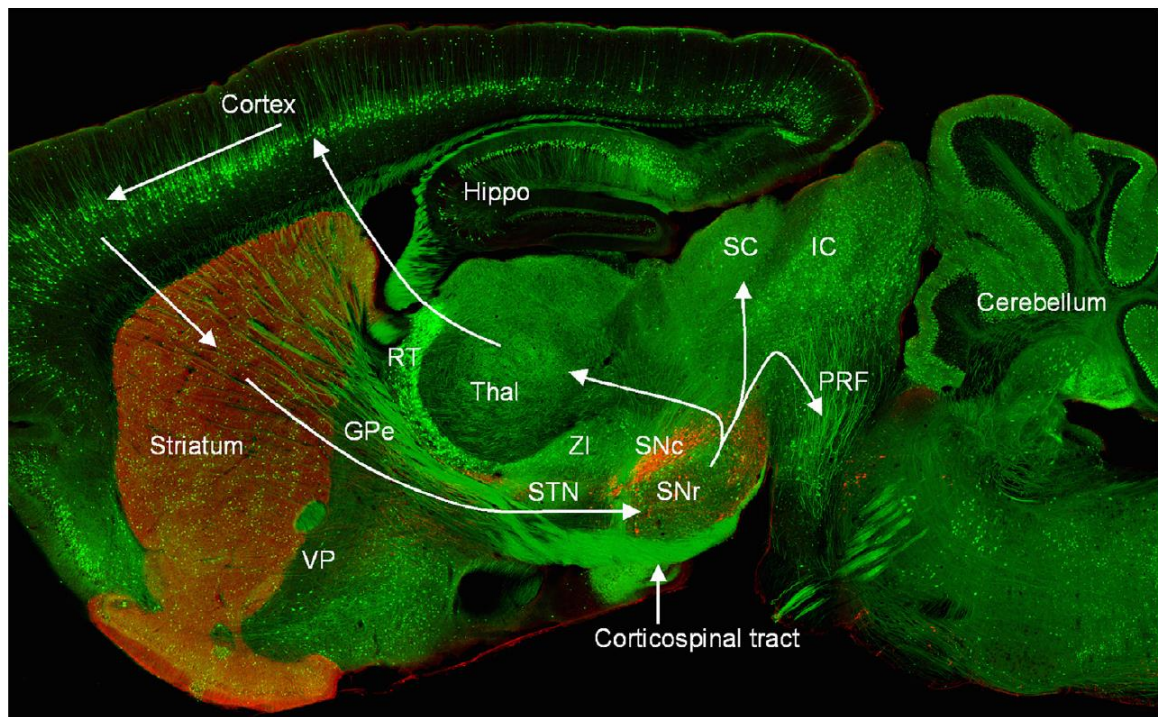
Figure 1.2: Sagittal view of the nuclei involved in the cortico-BG-thalamo-cortical loops. Arrows schematically show the information flow within these circuits. Cortical pyramidal neurons are labelled with Thy1-controlled YFP, GABAergic neurons expressing GAD65 and GAD67 co-express GFP (all shown in green). Red indicated tyrosine hydroxylase immunostaining. GPe, external *globus pallidus*; Hippo, hippocampus; IC, inferior *colliculus*; PRF, midbrain and pontine reticular formation; RT, reticular thalamus; SC, superior *colliculus*; SNc, *substantia nigra pars compacta;* SNr, *substantia nigra pars reticulata;* STN, subthalamic nucleus; Thal, thalamus; VP, ventral pallidum; ZI, zona incerta (Zhou, 2016).

In a simplified way, cortical information through the SM and mPF BG circuits is transmitted to the output structures (i.e., SNr and entopeduncular nucleus) of the BG through three pathways, the hyperdirect trans-subthalamic pathway, and the direct and indirect trans-striatal pathways (Albin et al., 1989; Kita, 1994; Maurice et al., 1999). Inputs from SM and mPF cortices enter the BG through the striatum and the STN. Glutamatergic projections from SM/mPF cortices make contact with lateral/medial STN neurons, which in turn send glutamatergic projections to the lateral/medial SNr, constituting the hyperdirect pathway. Moreover, SM and mPF cortices send glutamatergic projections onto the dorsolateral/dorsomedial-ventral striatum. MSNs from these regions of the striatum send GABAergic projections to the lateral/medial SNr, forming the direct pathway. Ultimately, MSNs from the dorsolateral/dorsomedial-ventral striatum send GABAergic projections to prototypical neurons in the lateral/medial GP. From the GP, GABAergic neurons will project to the lateral/medial STN, which sends glutamatergic projections to the lateral/medial SNr (Figure 1.3). The way these pathways are constituted set the neural substrates for BG circuits function.
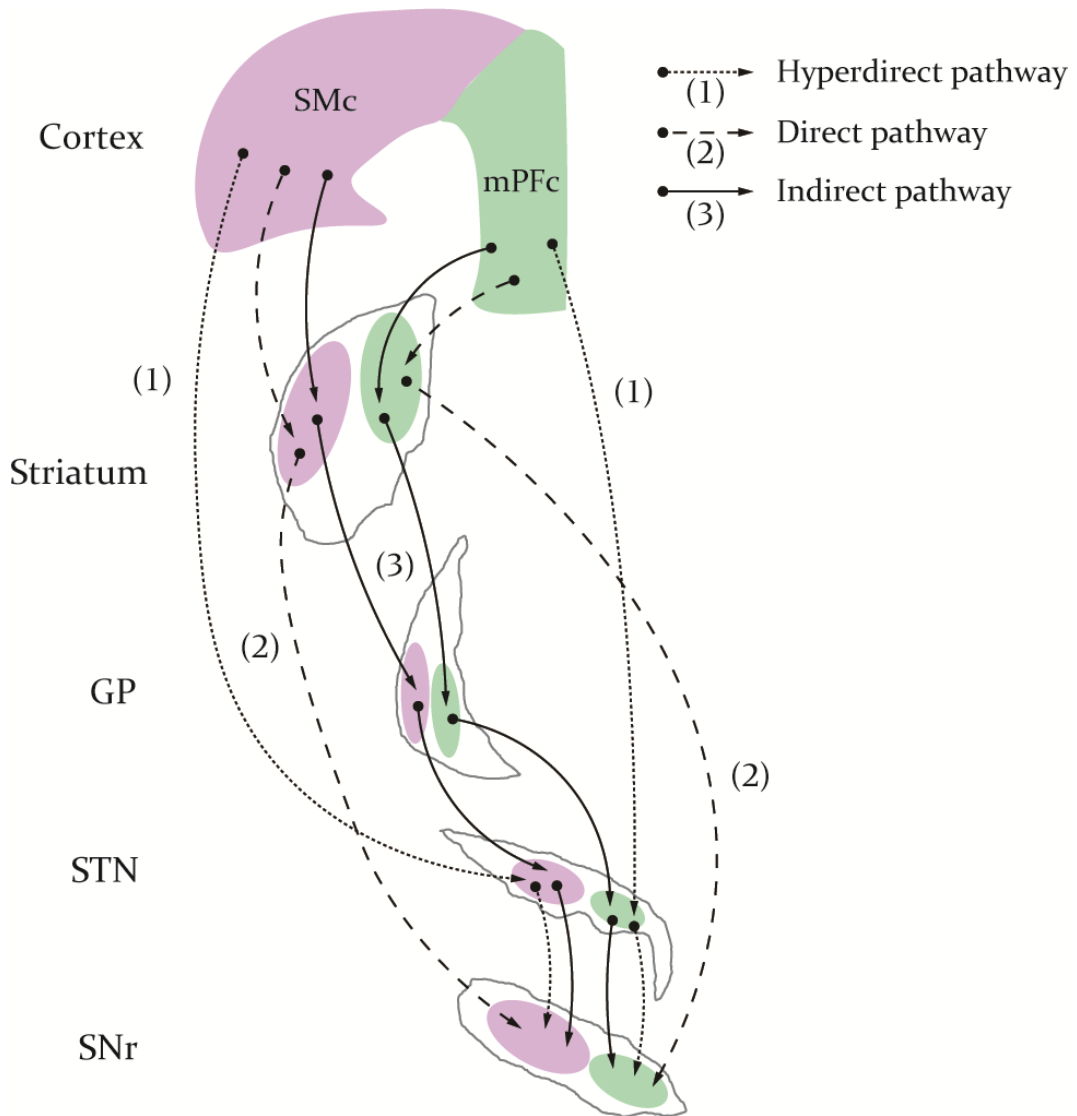
Figure 1.3: Schematic representation of the sensorimotor (SM, purple) and medial prefrontal (mPF, green) basal ganglia circuits (BG). These circuits convey cortical information to the BG output nuclei through three pathways: the hyperdirect (cortex-STN-SNr; (1) dotted line), the direct (cortex-striatum-SNr; (2) dashed line) and the indirect pathways (cortex-striatum-GP-STN-SNr; (3) solid line). However, SM and mPF BG circuits are anatomically segregated. While the SM circuits course through the lateral parts of the BG nuclei, the mPF circuits go through the medial parts of these nuclei. GP, *globus pallidus*; mPFc, medial prefrontal cortex; SMc, sensorimotor cortex; SNr, *substantia nigra pars reticulata;* STN, subthalamic nucleus.

As its name suggests, the SM BG circuits process SM information provided by the motor and somatosensory cortices. These circuits are involved in modulating motor and sensory cortices in order to control motor output, allowing precise movement execution, learning motor sequences, and their correct expression (Gremel & Costa, 2013; Jin et al., 2014; Phillips et al., 1993). According to the classical functioning model of the BG, the direct and indirect pathways play opposite roles in movement control (Albin et al., 1989). This model predicts that activation of direct-pathway MSNs by cortical projection neurons, leads to inhibition of the BG output nuclei. This would decrease the GABAergic inhibitory drive of these nuclei onto the thalamus, which in turn increases the excitatory thalamo-cortical pathway, leading to excitation of the motor cortex, and ultimately, movement facilitation. On the other hand, activation of indirect-pathway MSNs by cortical excitatory inputs reduces GP activity, leading to STN disinhibition, and increases STN glutamatergic input onto the BG output nuclei. This would end up inhibiting thalamic neurons, thus reducing excitatory input onto the motor cortex, and promoting movement suppression. Beyond this model, manipulation of direct or indirect-pathway MSNs has confirmed the hypothesized functions for these SM BG circuits pathways (Kravitz et al., 2010). Theoretically, activation of STN neurons in the hyperdirect pathway by cortical inputs, would increase excitatory drive onto the BG output nuclei, resulting in reduced thalamo-cortical input, inducing movement suppression. In agreement with this, ablation of this pathway induces hyperactivity in rodents, probably by increasing thalamo-cortical input (Koketsu et al., 2021). The specific role of this pathway in movement execution has been hypothesized to be the inhibition of competing motor programs, thus contributing to correct expression of motor patterns (Nambu et al., 2002). A similar role has been proposed for the indirect pathway in the inhibition of competing motor programs, while the direct pathway would be involved in selecting the desired motor programs (Mink, 2003). In line with this, direct- and indirect-pathway MSNs are active during the initiation and termination of action sequences, with mainly direct-pathway MSNs being activated during sustained motor activity. Thus, revealing that balanced activity between both pathways is needed for correct motor program selection (Cui et al., 2013; Jin et al., 2014).

On the other hand, mPF circuits process information coming from mPF cortical areas (i.e., anterior cingulate, prelimbic and infralimbic cortices), and are involved in 'associative/limbic' aspects of behaviour like goal-directed and drug-seeking behaviour, evaluation and revaluation of outcome values, and action selection update after outcome revaluation (Balleine & O'Doherty, 2010; Gremel & Costa, 2013; Nakanishi et al., 2014; Nonomura et al., 2018). Activation of the pathways constituting these circuits would provoke physiological responses in the BG nuclei similar to those described above for the SM circuits, although their behavioural correlates are not well understood. Evidence suggests that accumbal direct-pathway MSNs are involved in positive outcome learning, but not in negative outcome learning, for which participation of indirect-pathway MSNs is necessary (Hikida et al., 2010, 2013; Kravitz et al., 2012). Similar pathway-specificity is seen in the dorsomedial striatum, where direct-pathway MSNs code positive outcomes, and indirect-pathway MSNs code for negative outcomes, and switch in action selection (Nonomura et al., 2018). Similarly, accumbal indirect-pathway MSNs are required for flexible learning (Yawata et al., 2012).

1.2. The endocannabinoid system in the basal ganglia

The psychotropic effects of *Cannabis sativa* extracts fuelled the investigation about the compounds of this plant, which ultimately lead to the discovery of the endocannabinoid system. Identification of the Δ^9-Tetrahydrocannabinol (Δ^9-THC) as the main responsible for the plant psychotropic effects made possible the development of synthetic cannabinoids, that allowed the identification of the CB_1 receptor (Devane et al., 1988; Gaoni & Mechoulam, 1964). The existence of CB_1 receptors was the start point for the search of endogenous ligands, culminating with the first isolation of an endocannabinoid: the anandamide (Devane et al., 1992). Nowadays, the endocannabinoid system represents a widely distributed neuromodulatory system, constituted by receptors, and synthesis, degradation and transport pathways for endogenous ligands (Piomelli, 2003).

Besides its relationship with the psychotropic effects of cannabis, this system has been gaining attention over the last decades regarding its potential therapeutic use. The endocannabinoid system has been proposed as a useful target for neuroprotection, which could be especially useful in modifying the progression of neurodegenerative BG disorders, such as PD (Fernández-Ruiz et al., 2011). Activation of cannabinoid receptors (i.e., CB_1 and CB_2) can lead to neuroprotection by reducing glutamatergic excitotoxicity, proinflammatory molecule release, and gliosis (Smith et al., 2000; Van Der Stelt et al., 2001; Walter et al., 2003). Additionally, certain cannabinoids have anti-inflammatory and anti-oxidant properties, given their chemical structure containing phenolic groups, or by acting on other non-cannabinoid receptors, such as peroxisome proliferator-activated receptors (Marsicano et al., 2002; O'Sullivan, 2016).

1.2.1. Cannabinoid receptors distribution

The distribution of the CB_1 receptor is principally in the central nervous system, being present in neurons, astrocytes, oligodendrocytes, and neuronal precursors (Aguado et al., 2005; Gomez et al., 2011; Molina-Holgado et al., 2002). In neurons, CB_1 receptors are located mainly presynaptically, and its presence has been described in the external mitochondrial membrane (Bénard et al., 2012; Szabo & Schlicker, 2005). In the brain, CB_1 receptor expression is not homogeneous, and is observed especially in the BG nuclei, cerebellum and hippocampus, showing moderate expression in cortex (Mailleux & Vanderhaeghen, 1992). Outside the brain, this receptor is located in adrenal glands, heart, lung, liver, thymus, bone marrow, tonsils, gastrointestinal tract, and urinary and reproductive systems (Galiègue et al., 1995; Gérard et al., 1991; Pertwee, 2001).

Putting the focus on the structures related with cortico-BG circuit function, the mPF cortex is one of cortical areas showing a higher mRNA of this receptor, while lateral cortical areas (i.e., motor and somatosensory areas) show less CB_1 receptor mRNA and binding (Heng et al., 2011; Herkenham, Lynn, Johnson, et al., 1991; Mailleux & Vanderhaeghen, 1992). CB_1 receptor expression in the striatum follows a dorsolateral-ventromedial gradient, resembling cortical afferents onto this nucleus. This way, there is an intense CB_1 receptor mRNA and

binding in the dorsolateral part, with lower mRNA and binding in the dorsomedial/ventral striatum (Herkenham, Lynn, Johnson, et al., 1991; Julian et al., 2003; Mailleux & Vanderhaeghen, 1992). The relatively moderate mRNA in cortex, together with the high striatal mRNA and preferential presynaptic location of this receptor, argues for the CB_1 receptor observed in binding studies to be in striatal neuron collateral terminals (Van Waes et al., 2012). GP neurons lack CB_1 receptor mRNA, although it shows intense CB_1 receptor labelling, suggesting that the CB_1 receptor present in this nucleus, is located specially in striato-pallidal, and to some extent subthalamo-pallidal terminals. Consistent with the striato-pallidal projection pattern, lateral tiers of the GP have more CB_1 receptor presence than the medial parts of the GP (Herkenham, Lynn, de Costa, et al., 1991; Herkenham, Lynn, Johnson, et al., 1991; Julian et al., 2003; Mailleux & Vanderhaeghen, 1992). Regarding the STN, it shows moderate mRNA, together with sparse CB_1 receptor binding. Given the lack of CB_1 receptor mRNA in GP neurons –main contributor of STN afferents–, the slight binding observed in the STN, is likely coming from cortical afferents and STN neuron collaterals. In these studies, no gradient in CB_1 receptor mRNA or binding was observed in the STN (Herkenham, Lynn, Johnson, et al., 1991; Julian et al., 2003; Mailleux & Vanderhaeghen, 1992). SNr neurons lack CB_1 receptor mRNA, but shows a high density of this receptor (Herkenham, Lynn, Johnson, et al., 1991; Mailleux & Vanderhaeghen, 1992). Thus, CB_1 receptor in this nucleus is likely located in striato-nigral terminals, and to some extent in subthalamo-nigral terminals (Herkenham, Lynn, de Costa, et al., 1991). CB_1 receptor presence in the SNr shows a mediolateral gradient, resembling the striato-nigral projection pattern, with low CB_1 receptor presence in medial tiers of the SNr, and high presence in lateral portions (Julian et al., 2003) (Figure 1.4).

The second cannabinoid receptor described was the CB_2 receptor (Munro et al., 1993). This receptor was first described in spleen; thus, it has been attributed with immune functions. In line with this, is located mainly in immune cells like macrophages, NK cells, B and T lymphocytes, monocytes and neutrophils (Galiègue et al., 1995). Besides immune cells, this receptor has also been described in other peripheral tissues like lung, gastrointestinal tract, heart, adipocytes, bone cells and meiotic cells (Grimaldi et al., 2009; Joyeux et al., 2002; Ofek et al., 2006; Roche et al., 2006; Storr et al., 2002; Zoratti et al., 2003). CB_2

receptor presence in the central nervous system has been questioned, although several authors have described its presence mainly in microglia and astrocytes, especially after an inflammatory, infectious, traumatic or toxic insult, which places this receptor in a privileged spot as a therapeutic target for neurodegenerative processes (Benito et al., 2008; Fernández-Ruiz et al., 2007). Moreover, CB_2 receptor expression has been found in neurons in the BG, brainstem, and cerebellum (Gong et al., 2006; Lanciego et al., 2011; Van Sickle et al., 2005).

Besides CB_1 and CB_2 receptors, cannabinoids also act upon other targets including orphan G protein-coupled receptors (i.e., GPR18 and GPR55), peroxisome proliferator-activated receptors (i.e., PPARα and γ) and transient receptor potential channels (i.e., TRPV1, TRPV2 y TRPA1) (Di Marzo et al., 1998; Jordt et al., 2004; McHugh et al., 2012; O'Sullivan & Kendall, 2010; Qin et al., 2008; Sylantyev et al., 2013).
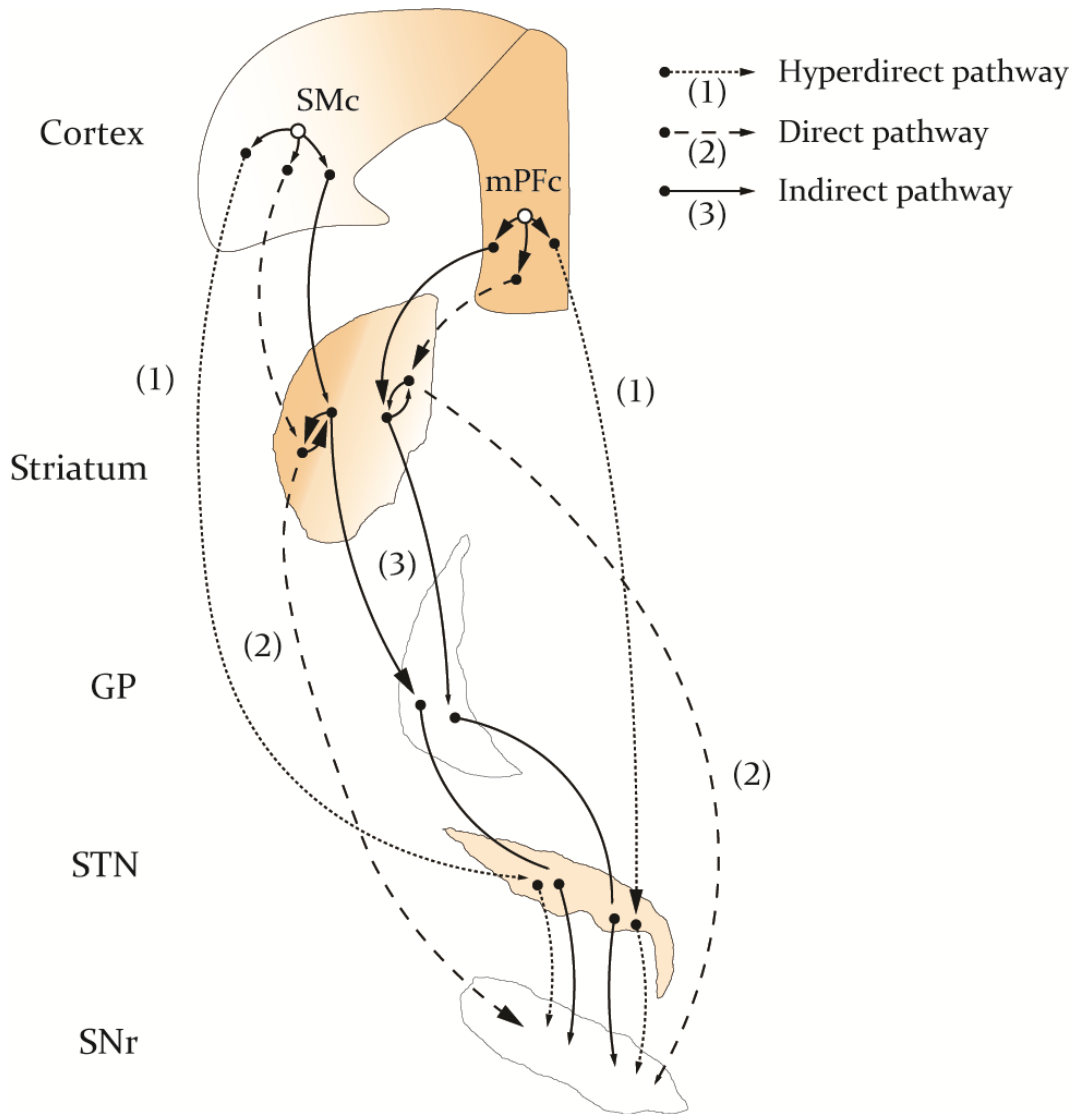
Figure 1.4: Schematic representation of the CB$_1$ receptor presence in the pathways and nuclei involved in the BG circuits. In cortex, most of the observed CB$_1$ receptor binding is due to the presence of this receptor at interneuron terminals, represented as white circles, where most of this receptor is expressed; CB$_1$ receptor is abundantly expressed in the mPFc (medial prefrontal cortex), while moderate to sparse expression is observed in sensorimotor cortices (SMc). In the striatum, there is a dorsolateral-ventromedial gradient in CB$_1$ receptor expression and binding; principal contribution to binding is from medium spiny neuron collaterals. In the *globus pallidus* (GP), there is no CB$_1$ receptor expression and binding comes mostly from striato-pallidal terminals. In the subthalamic nucleus (STN), CB$_1$ receptor is moderately expressed and mild binding is observed, presumably from cortical terminals. In the *substantia nigra pars reticulata* (SNr), there is no CB$_1$ receptor expression, but shows an intense binding coming mainly from striato-nigral, but also from subthalamo-nigral terminals. Intensity of the orange shade represents the relative level, within that nucleus, of CB$_1$ receptor mRNA transcripts; more intense colour means higher presence of transcripts. The size of the arrow point indicates the amount of CB$_1$ receptor located on that terminal and, therefore, its contribution to the binding detected in the nucleus where the terminal is present; the bigger the arrow the higher the presence of CB$_1$ receptor at that terminal.

1.2.2. CB1 receptor and its function in the basal ganglia

Transmission between BG nuclei rely on GABA and glutamate, which cannabinoids have proven to interfere with, by acting mainly on the CB_1 receptor. Most of the CB_1 receptor expression in cortex is in GABAergic interneurons, and to a lesser extent pyramidal projection neurons (Bodor et al., 2005; Mailleux & Vanderhaeghen, 1992; Marsicano & Lutz, 1999). Therefore, most of the effects seen in cortex after CB_1 receptor manipulation would be restricted to local GABAergic neurotransmission, decreasing GABA release, and supressing pyramidal projection neuron inhibition (Bodor et al., 2005; Pistis et al., 2002; Trettel & Levine, 2002). Another important role is modulation of synaptic plasticity. Within cortex, cannabinoids mainly intervene in long term depression development in excitatory and inhibitory synapses, as well as in depolarization-induced suppression of inhibition (Auclair et al., 2000; Chiu et al., 2010; Trettel & Levine, 2003). Despite the apparent low CB_1 receptor expression in cortical projection neurons, it is an important modulator of cortico-striatal synapses, decreasing glutamate release at both direct- and indirect-pathway cortico-MSN contacts (Gerdeman & Lovinger, 2001; Kreitzer & Malenka, 2007). This receptor is involved in depolarization-induced suppression of excitation, and long term depression induction in cortico-MSN synapses, although this latter form of plasticity seems to preferentially involve indirect-pathway MSNs (Lovinger & Mathur, 2016; Uchigashima et al., 2007). GABAergic neurotransmission in the striatum is modulated by CB_1 receptor activation, reducing MSNs GABA currents, in a mechanism likely involving MSNs axon collaterals (Hoffman & Lupica, 2001; Szabo et al., 1998). Moreover, this receptor is also involved in GABAergic synaptic plasticity in the striatum, where CB_1 receptors located in MSN-MSN and fast spiking interneurons-MSN synapses, participate in long term depression induction (Mathur et al., 2013). Additionally, cannabinoid-dependent depolarization-induced suppression of inhibition has been described in fast spiking interneurons-MSN synapses (Narushima et al., 2006). CB_1 receptors expressed in striato-pallidal terminals reduce GABA release upon activation, and participate in depolarization-induced suppression of inhibition induction at these synapses (Engler et al., 2006; Miller & Walker, 1996). Besides striatal inputs, subthalamo-pallidal terminals contain CB_1 receptors that reduce glutamate release onto GP

neurons upon activation (Freiman & Szabo, 2005). Regarding the STN, CB$_1$ receptor activation caused inhibition or excitation of STN neurons in the lateral or medial part of this nucleus, respectively. Therefore, suggesting cannabinoid modulation mainly on glutamatergic inputs in the medial STN, and on GABAergic inputs in the lateral STN (Morera-Herreras et al., 2010). In the SNr, CB$_1$ receptor activation decreases both GABA and glutamate release from striato-nigral and subthalamo-nigral terminals, respectively, although the net effect of cannabinoids on SNr neuron activity is excitatory (Miller & Walker, 1995; Sañudo-Peña & Walker, 1997; Szabo et al., 2000; Wallmichrath & Szabo, 2002a, 2002b). Similar to that observed in the GP, CB$_1$ receptor in striato-nigral terminals participates in depolarization-induced suppression of inhibition induction (Yanovsky et al., 2003). Moreover, the CB$_1$ receptor control serotonergic, noradrenergic and DA neurotransmitter systems, which in turn control BG function (Carvalho & Van Bockstaele, 2012; Fitzgerald et al., 2012; Haj-Dahmane & Shen, 2011).

In the case of the DA system within the BG, cannabinoids by activating the CB$_1$ receptor can influence DA neurotransmission indirectly, modulating other neurotransmitter systems since DA neurons lack CB$_1$ receptor mRNA (Julian et al., 2003). Cannabinoids are thought to indirectly modulate DA release disinhibiting DA neurons in the midbrain (i.e., SNc and ventral tegmental area neurons). Several mechanisms involving suppression of GABA release by cannabinoids have been proposed to explain this, such as inhibition of GABA release from interneurons or GABAergic afferents expressing CB$_1$ receptor, as well as modulation of other BG nuclei activity, like the STN, resulting in DA neuron net excitation after cannabinoid administration (Cheer et al., 2000; Lupica & Riegel, 2005; Morera-Herreras et al., 2008; Szabo et al., 2002; Yanovsky et al., 2003). Therefore, disinhibition of midbrain DA neurons would produce an increase in DA release in both dorsal and ventral striatum, as it happens after cannabinoid systemic administration (Cheer et al., 2004; Polissidis et al., 2014). Although the net effect of systemic cannabinoid administration is increased DA neuron activity, and subsequent DA release, there is an additional modulatory effect mediated through CB$_1$ receptors expressed in glutamatergic terminals in midbrain DA nuclei. CB$_1$ receptor activation in this terminals would hinder glutamate release, subsequently suppressing excitatory drive onto DA neurons (Lupica & Riegel, 2005). Locally,

at the target nuclei of DA neurons, cannabinoids can modulate DA release as well. In the ventral striatum, CB_1 receptors located in mPF cortical terminals reduce DA release induced by acetylcholine or glutamate release from cholinergic interneurons or cortical terminals, respectively (Mateo et al., 2017). Although the exact circuit components involved in CB_1 receptor-mediated DA release in the dorsal striatum have not been stablish yet, activation of this receptor can locally inhibit DA release as well (Sidló et al., 2008). The role of cannabinoids on DA release in the striatum has been thoroughly explored, but the participation that this receptor might have on DA neurotransmission in other BG nuclei where cannabinoid and DA systems coexist, is yet to be determined.

In line with the effects CB_1 receptor activation has on BG neurotransmission, behavioural traits related with BG function are affected by cannabinoids. Cannabis users display motor (i.e., fine motor control) and cognitive deficits (i.e., impulsivity, memory, learning), functions that are related to cortico-BG circuits (Boggs et al., 2018; Ramaekers et al., 2006; Schreiner & Dunn, 2012; Tremblay et al., 2015). In preclinical studies, systemic administration of CB_1 receptor agonists induces motor impairments, like hypokinesia and fine motor control disruption (De Fonseca et al., 1994; Di Marzo et al., 2001; Mclaughlin et al., 2000; Romero, de Miguel, et al., 1995; Romero, García, et al., 1995; Wickens & Pertwee, 1993). In line with this, cortico-BG circuit efficiency during motor tasks is reduced in humans after cannabis consumption (Filbey & Yezhuvath, 2013). However, direct administration of CB_1 receptor agonists into different BG nuclei, induce different effects on motor behaviour in animals, hinting at the specific contribution of the endocannabinoid system in each BG nuclei. Activation of the CB_1 receptor specifically in the striatum or the SNr, increases rotatory behaviour in rodents, while receptor activation in the GP or STN decreased it (Miller et al., 1998; Sañudo-Peña et al., 1998, 1999; Sañudo-Peña & Walker, 1998; Souilhac et al., 1995).

Regarding associative/limbic functions, systemic CB_1 receptor agonist administration impairs strategy update based on reward, therefore persevering in behaviours without taking into account changes in cue-reward association (Egerton et al., 2005; Hill et al., 2006). Activation of this receptor in the mPF cortex or the *nucleus accumbens* impairs aversive

learning and aversive-related responses (Hikida et al., 2013; Lisboa et al., 2010). In line with this, heavy cannabis users have a decreased ACC-striatum functional connectivity, as observed between the prefrontal cortex and the striatum after Δ^9-THC administration (Bhattacharyya et al., 2015; Blanco-Hinojo et al., 2017).

Distribution of cannabinoid receptors within the BG, together with their ability to modulate the principal neurotransmitters involved in its function, and their actions on inflammatory processes, place them in a privileged spot as disease-modifying and symptomatology treatment targets in BG disorders such as PD.

1.3. Parkinson's Disease

PD was first described by Dr. James Parkinson in 1817, which referred to it as 'shaking palsy', describing some of the key motor symptoms (Parkinson, 2002). Afterwards, a more in-detail description of the disease, including a clinical definition and further description of the motor symptoms, was made by Jean-Martin Charcot which put its final name: Parkinson's disease (Charcot, 1892). In the early 20th century, Frederick Lewy described the presence of intracellular inclusion bodies in PD patients' brains, which he called 'Lewy bodies' (Lewy, 1912). Later, the SNc was targeted as the main brain structure affected by these cellular inclusions (Holdorff, 2019). After a few decades, a link was stablished between PD pathology and DA, with the observation of a DA deficit in the striatum and SNc of PD patients (Ehringer & Hornykiewicz, 1998). Making such link between central DA deficiency and PD symptoms led to the development of DA replacement therapies, which now constitute the main treatment for alleviating motor symptomatology (Birkmayer & Hornykiewicz, 1961). Despite this, not all patients respond to such therapy, and after a few years into treatment, the vast majority begin to develop serious adverse effects (i.e., dyskinesia) (Marsden & Parkes, 1977). At this moment, symptomatology treatment strategies without such side effects, together with disease-modifying treatments that hinder the neurodegenerative process are the aim of the actual efforts in developing PD effective treatments.

1.3.1. Epidemiology, aetiology and pathology

PD is the most common neurodegenerative disorder after Alzheimer's Disease, affecting 2% of the population over 60 years old (Tysnes & Storstein, 2017). Increase in life expectancy has led to a rise in neurodegenerative disorders prevalence, such as PD (Lee & Gilbert, 2016). However, prevalence is not homogeneous, depending on race, ethnicity and gender, among other factors (Ascherio & Schwarzschild, 2016; Van Den Eeden et al., 2003).

PD presentation consists in two major neuropathological traits: SNc DA neuronal loss and widespread Lewy body inclusions –mainly constituted by α-synuclein– are necessary for a formal PD diagnosis (Poewe et al., 2017). Loss of DA neurons begins in the ventrolateral SNc, principally affecting DA neurons involved in motor behaviour; other DA midbrain neurons remain more or less unaffected (Damier et al., 1999; Fearnley & Lees, 1991). Before motor symptoms start taking place, a dramatic loss of DA neurons and the subsequent DA striatal denervation are necessary (Dijkstra et al., 2014; Iacono et al., 2015). Together with this, α-synuclein aggregation and subsequent Lewy body formation appear in several brain regions. According to Braak's theory, Lewy bodies start to build up in cholinergic and monoaminergic midbrain neuron populations, as well as in the olfactory system. As the neurodegeneration progresses, Lewy bodies start to appear in neocortical and limbic regions (Braak et al., 2003, 2004).

Although the exact aetiology for PD is still unknown, several cellular and molecular mechanisms are known to be involved in its pathology (Figure 1.5), among which are:

Mitochondrial dysfunction is caused by gene mutations (i.e., *SNCA*, parkin, *PINK1*, among others), but also morphological and functional alterations have been described in PD patients (Surmeier, 2018; Zhang et al., 2018). These alterations affect mitochondrial electron chain complex I, and are related with the aggregation of α-synuclein in SNc neurons (Poewe et al., 2017; Schapira et al., 1990). This, together with the presence of iron deposits in PD patients' brain, could favour the over-exposition of these patients to oxidative stress (Gu et al., 1998; Jomova et al., 2010).

Mounting evidence indicate that **oxidative stress** is an important contributor of PD pathology. Together with deficits in the main antioxidant enzymes (i.e., catalase, superoxide dismutase, glutathione peroxidase), further evidence of an oxidant environment is found in lipid peroxidation, DNA oxidation and oxidised proteins (Alam, Daniel, et al., 1997; Alam, Jenner, et al., 1997; Dexter et al., 1994; Hornykiewicz & Kish, 1987; Saggu et al., 1989). The source of this oxidative stress, is linked to mitochondrial malfunction, altered iron metabolism and pathological α-synuclein forms (Schapira & Jenner, 2011).

Protein homeostasis seems to be altered in PD patients' brain. Under-expression of proteasome subunits, is accompanied by elevated levels of ubiquitinated proteins, indicating decreased protein elimination (Lonskaya et al., 2013; McNaught & Jenner, 2001; Toulorge et al., 2016). Moreover, proteasome alterations in PD have been linked to deleterious α-synuclein degradation (Tofaris et al., 2001). In addition, parkin mutations –known to be involved in protein metabolism– are linked to PD (Seirafi et al., 2015). Furthermore, autophagy-related genes present mutations in PD, hindering even more protein metabolism (Schapira & Jenner, 2011; Toulorge et al., 2016).

Neuroinflammation is present in PD and is related with DA degeneration and PD worsening (Kaur et al., 2017; Ouchi et al., 2005). It can be mainly attributed to glial activation, as is shown in activated microglia and astrocytosis in PD patients' brains (McGeer et al., 1988). As a consequence of glial activation pro-inflammatory agents such as TNF-α, IL-1α, IL-1β, inducible nitric oxide and cyclooxygenase 2 are released, inducing cellular injury and further promoting neuroinflammation (Ramsey & Tansey, 2014; Teismann & Schulz, 2004).

Excitotoxicity caused by high glutamate levels in PD could increase neuronal calcium permeability, inducing a cascade of events resulting in cell apoptosis (Surmeier et al., 2017). The source of this elevated glutamatergic tone is thought to be the STN hyperactivity well documented in PD, which innervates the SNc, and would be directly implicated in DA neuronal loss (Steigerwald et al., 2008). Moreover, neuroinflammation and

α-synuclein aggregates promote glutamate release, which in turn, act on the microglia feeding pro-inflammatory processes, further contributing to cell loss (Ambrosi et al., 2014).
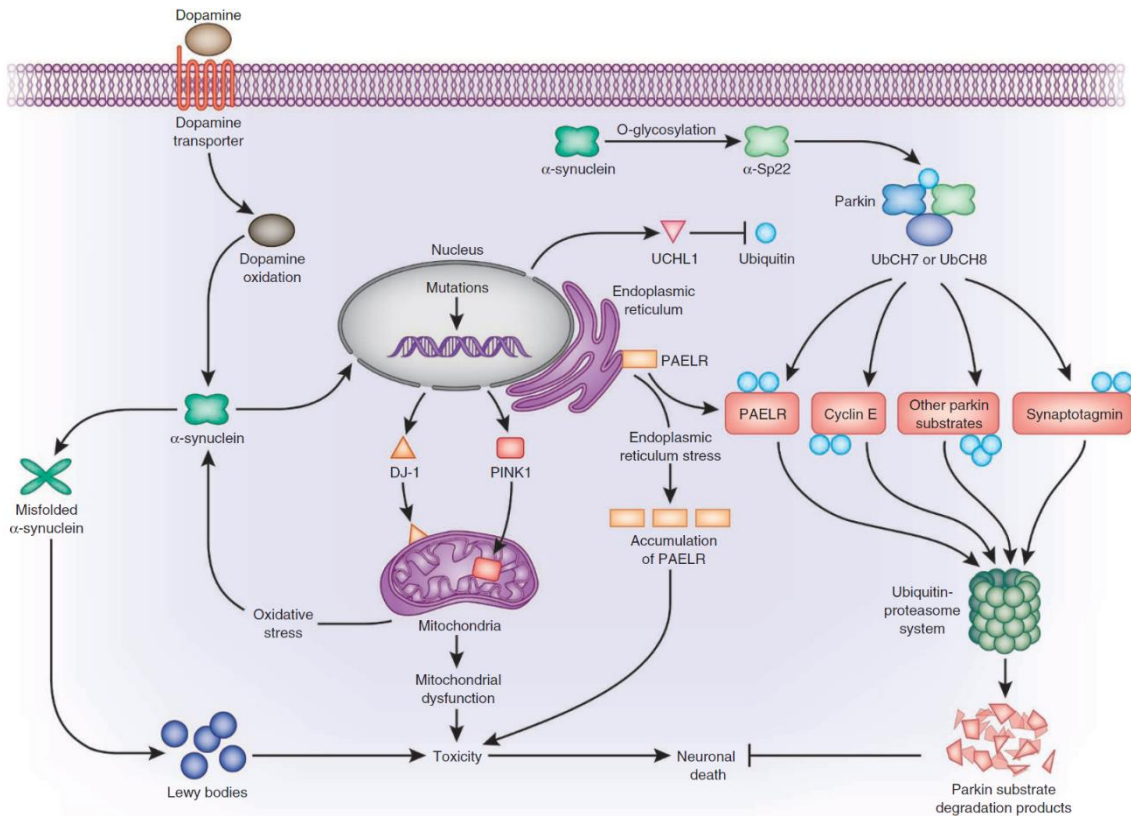
Figure 1.5: Schematic summary of the mechanisms involved in the aetiology of Parkinson's disease. Aggregation of α-synuclein, mitochondrial dysfunction and subsequent oxidative stress, proteosomal dysfunction leading to altered protein homeostasis, neuroinflammation and excitotoxicity (not shown) contribute to dopaminergic neuron cell death and progressive degeneration. α-Sp22, a 22-kilodalton glycosylated form of α-synuclein; PAELR, parkin-associated endothelin receptor-like receptor; UbCH7, ubiquitin-conjugating enzyme 7; UbCH8, ubiquitin-conjugating enzyme 8; UCHL1, ubiquitin carboxy-terminal hydrolase L1. (Obeso et al., 2010).

PD can be classified as idiopathic or genetic PD (Tysnes & Storstein, 2017). Idiopathic PD accounts for ~90% of the total PD cases, and it is thought to be caused by aging, as well as environmental factors and genetic predisposition. Although aging is the main PD risk factor, several environmental agents like toxin exposure (i.e., MPTP, rotenone, paraquat) or lifestyle, have been linked to PD (Ascherio & Schwarzschild, 2016; Ball et al., 2019). Genetic PD accounts for ~10% of total cases, they are characterized by an early symptomatology onset (< 50 years old), and a strong heritable genetic component. There are 23 loci and 19 causative

genes linked to PD like parkin and *UCH-L1*, affecting protein homeostasis; *PINK1* and *LRRK2* interfering with phosphorylation, or *DJ-1* provoking oxidative stress (Del Rey et al., 2018; Van Der Brug et al., 2015). Moreover, epigenetic alterations (i.e., DNA methylation, histone modification and microRNA's) have been linked to PD (Coupland et al., 2014; Kim et al., 2007; Park et al., 2016). Despite its low prevalence, heritable forms of PD have provided an understanding of the mechanisms involved in PD pathology, as genes affected in these forms are also affected in idiopathic PD (Nalls et al., 2014).

1.3.2. Parkinson's disease treatment

At this moment, only symptomatic treatment of motor and non-motor symptoms is available for PD, with no therapy aimed at slowing down progression, although the sooner treatment starts, patients have a better prognosis. Currently, DA replacement therapies are the first choice in PD treatment. In some cases, surgical approaches are necessary, as some patients develop strong side effects, or show small benefits from medication (Lang & Espay, 2018; Olanow, 2008).

1.3.2.1. Pharmacological treatments

The golden-standard for motor symptoms treatment in PD is L-DOPA. This is a DA precursor, therefore replacing DA deficits in PD patients' brains. This is possible by the L-DOPA ability to cross the blood-brain barrier, reaching the brain where is going to be transformed to DA (Kageyama et al., 2000). L-DOPA is administered concomitantly with carbidopa or benserazide, DA decarboxylase inhibitors unable to cross the blood-brain barrier, thus preventing peripheral transformation of L-DOPA into DA. This way, biodisponibility increases and side effects caused by peripheral circulating DA are avoided. Unfortunately, L-DOPA treatment is unable to modify disease progression and over time decreases in efficacy. Moreover, long-term treatment produces serious motor complications such as L-DOPA-induced dyskinesia (Fahn, 2008). Besides L-DOPA, other treatments targeting the DA system to control motor symptoms are available including DA agonists,

monoamine oxidase B inhibitors, catechol-O-methyltransferase inhibitors and anticholinergic drugs.

Regarding PD cognitive impairments, primavanserin, an atypical antipsychotic with inverse-agonist actions at the 5-HT$_{2A}$ receptor, is indicated for PD psychosis since it lacks effects upon the DA system (Markham, 2016). L-DOPA treatment is able to address some psychiatric symptoms (i.e., apathy, anhedonia), but could induce impulse control disorders, hypersexuality or eating disorders, among others (Weintraub et al., 2010). Moreover, rivastigmine, an acetylcholinesterase inhibitor, is often used for cognitive decline treatment in PD patients (Pagano et al., 2015).

Other PD therapeutic strategies addressing mainly motor symptoms include: Surgery (i.e., mechanical or ultrasound ablation of BG nuclei) and STN stimulation (Lang & Lozano, 1998; Martínez-Fernández et al., 2018; Starr et al., 1998).

1.3.2.2. Cannabinoids as neuroprotective agents in Parkinson's Disease

Cannabinoid receptors distribution within the BG and components of the immune system (reviewed in 1.2.1) place them in a privileged spot for neuroprotection, and they have indeed shown ability to modulate some of the pathological features observed in PD (Fernández-Ruiz et al., 2011). Cannabinoids have a direct impact on neuroinflammation, likely by tackling glial activity, since this cellular type is necessary for the neuroprotective effects of these compounds (Chung et al., 2011; Lastres-Becker et al., 2005). Both CB$_1$ and CB$_2$ receptors seem to be involved in neuroprotection. CB$_1$ receptor activation offered protection against toxic insults to DA neurons (i.e., MPTP, LPS), decreasing microglial activation, TNF-α, IL-1β and inducible nitric oxide levels, and oxidative stress markers, such as DNA and protein oxidized species (Chung et al., 2011; Vrechi et al., 2018). Other studies, suggest that antagonism of this receptor could lead to neuroprotective effects against 6-hydroxydopamine (6-OHDA), by astroglial activation (Cerri et al., 2014). As reviewed in 1.2.2, CB$_1$ receptor activation modulates glutamate release, therefore hindering the main mechanism by which excitotoxicity occurs in PD. In fact, activating the CB$_1$ receptor reduces

ouabain-induced excitotoxicity (Van Der Stelt et al., 2001). CB_1-related protection against excitotoxicity is thought to be mediated by induction of BDNF mRNA, which has shown to protect against 6-OHDA-induced DA degeneration (Blázquez et al., 2015; Herrán et al., 2014; Khaspekov et al., 2004; Marsicano et al., 2003). CB_2 receptor involvement in neuroprotection seems more straightforward, with mounting evidence indicating that its activation prevents neurodegeneration in several animal models of PD (i.e., MPTP, rotenone, LPS), as well as decreasing inflammatory factors and increasing antioxidant enzymes and molecules (Chung et al., 2016; Javed et al., 2016; Malek et al., 2015; Ojha et al., 2016). Moreover, Δ^9-THC by activating PPAR-γ receptors protect against MPTP toxicity in an *in vitro* model, as well as increasing mitochondrial biogenesis markers and decreasing oxidative stress (Carroll et al., 2012; Zeissler et al., 2016). Cannabidiol, another phytocannabinoid, protects against 6-OHDA DA insult in PD animal models, an effect that could be mediated by the positive impact this compound has in mitochondrial function, as well as in oxidative stress in *in vitro* models (Lastres-Becker et al., 2005; Liu et al., 2015; Sun et al., 2017; Yang et al., 2014).

1.3.3. Motor and non-motor symptoms of Parkinson's disease: relationship with the dysfunction of basal ganglia circuits

The main motor symptoms in PD are often unilateral or asymmetrical at the beginning, finally becoming bilateral. These include resting tremor (rhythmic tremor that disappears during voluntary movement), rigidity (muscle stiffness, reducing movement range) and bradykinesia (reduction in movement speed, movement initiation difficulties and postural instability) (Louis, 2016; Postuma et al., 2015). In advanced stages gait and balance impairments may appear (Bloem et al., 2004). Although motor symptoms draw most of the attention, PD patients experience several non-motor dysfunctions. During the first stages of the disease, and before motor symptoms start, PD patients show hyposmia, autonomic dysfunctions (i.e., constipation) and mood and sleep disorders (Poewe et al., 2017). The most frequent non-motor symptom in PD is psychosis, as it is experienced by more than a half of PD patients (Fénelon & Alves, 2010). Another very frequent non-motor symptoms in PD are

mood disorders such as anxiety, depression or apathy, that can appear throughout the disease course (Aarsland et al., 2009; Pontone et al., 2009; Reijnders et al., 2008). Other non-motor symptoms arise as neurodegeneration makes its way through the brain, such as cognitive decline and dementia or autonomic dysfunction (McGregor & Nelson, 2019; Poewe et al., 2017). Moreover, PD patients show planning, working memory and set-shifting deficits (Robbins & Cools, 2014).

Classical models of BG function during PD stablish that, after nigrostriatal DA pathway degeneration, direct-pathway MSNs –expressing D_1 receptor– and indirect-pathway MSNs –expressing D_2 receptor– activities are imbalanced (Albin et al., 1989; DeLong, 1990). According to this model, direct-pathway MSNs activity would be reduced, thus disinhibiting neurons in BG output nuclei. On the other hand, indirect-pathway MSNs would be hyperactive, therefore inhibiting GP neurons which in turn would be disinhibiting STN neurons, which would ultimately excite neurons in BG output nuclei. According to this model, BG output nuclei during PD would be hyperactive, which would end up inhibiting thalamic nuclei, relieving thalamo-cortical glutamatergic input, and finally, inhibiting behaviour development at a cortical level that would result in PD symptomatology. In agreement with this theoretical model, STN and GPe neurons are hyperactive and hypoactive, respectively, in PD patients (Filion & Tremblay, 1991; Miller & DeLong, 1987). Moreover, parkinsonian symptoms can be alleviated by GPi or STN stimulation (Lang & Lozano, 1998). Despite the usefulness of this model –known as 'rate model'– in understanding some PD traits, and developing surgical strategies for PD symptomatology treatment, it fails to explain some BG changes during PD, as well as in explaining PD symptom development. Moreover, this model represents general BG function in PD without accounting for differential pathological processes happening in different cortico-BG circuits. As it happens, DA neuron loss starts in lateral parts of the SNc, principally affecting motor behaviours by putamen DA denervation, while degeneration of other midbrain DA neurons is spared, partially affecting caudate, and barely affecting *nucleus accumbens*, regions that are involved in spatial working memory, reward and impulsive behaviour (Damier et al., 1999; Kish et al., 1988).

Beyond the rate model, other pathophysiological changes in PD may help to explain PD symptoms. Neurons in BG nuclei display burst firing pattern in addition to changes in its tonic activity. Bursting has been observed throughout the BG circuits, with burst patterns being displayed in GPe, STN and GPi neurons of PD patients (Bergman et al., 1994; Hutchison et al., 1994; Soares et al., 2004). This abnormal firing pattern has been linked to PD symptoms, since they were alleviated with L-DOPA, which also reduced burst firing in GPe and GPi neurons of primate PD models and PD patients (Boraud et al., 1998; Filion et al., 1991). Moreover, both experimental PD models and PD patients, present aberrant activity (i.e., burst and synchronized firing) in STN, GPe and GPi neurons, that are linked to bradykinesia and tremor (Hutchison et al., 1997; Levy et al., 2002; Pan et al., 2016). Oscillatory changes, emerge as another alteration of BG nuclei in PD. The main oscillatory change in PD patients is the appearance of oscillations in the β frequency range (i.e., ~ 20 Hz) in the STN and GPi, which is treatment responsive, and correlates with bradykinesia and rigidity (Brown et al., 2001; Kühn et al., 2009; Levy et al., 2002). Besides changes in the β frequency range activity, γ band frequency activity is decreased in PD patients, and it is restored after L-DOPA treatment, thus this band has been considered to be prokinetic (Brown & Williams, 2005).

Neurophysiological representations of non-motor symptoms in PD are even less understood that those for motor symptoms. Most non-motor symptoms are unaffected or worsened by DA replacement therapy, which points towards a different neurobiological substrate than that observed for motor symptoms (Sethi, 2008). However, L-DOPA treatment improves some non-motor symptoms in PD patients, such as spatial and verbal working memory, planning and task-set switching, likely by acting on cortico-BG circuitry (Cools et al., 2001; Lange et al., 1992; Lewis et al., 2004, 2005). Therefore, similar mechanisms than those linked to PD motor symptoms might be involved in these DA-dependent non-motor symptoms. In line with the DA deficit pattern observed in the BG of PD patients, is thought that L-DOPA causes a hyperdopaminergic state in other, still DA-competent circuits, such as the associative/limbic BG circuits (Cools et al., 2001). In line with this, patients without L-DOPA learn more when they receive negative feedback, but when they are on L-DOPA treatment they learn more after receiving a positive feedback,

resembling the ascribed functions for the direct and indirect pathways in the mPF BG circuits of rodents (Frank et al., 2004; Hikida et al., 2010, 2013; Kravitz et al., 2012).

1.3.4. Parkinson's disease and the endocannabinoid system

Although the DA system is greatly affected in PD, the neurodegenerative process taking place affects other neurotransmitter systems such as the serotonergic, noradrenergic, cholinergic and endocannabinoid system (Halliday et al., 1990; McMillan et al., 2011; Müller & Bohnen, 2013). Regarding the endocannabinoid system –specifically their receptors–, its behaviour in PD patients and in animal models has gathered mixed results. Some of the problems faced when determining CB_1 receptor status in PD patients are the different medication and PD progression of the patients being examined. Drug-naïve early-PD patients show decreased CB_1 receptor binding in the SN and an increased receptor binding in putamen and prefrontal cortex, similar to what was found in late-PD patients, measured *in vivo* through positron emission tomography (Van Laere et al., 2012). Such results have been partially replicated in *post mortem* brain tissue from PD patients showing increased binding, together with increased mRNA and G protein coupling, in the putamen. However, no changes in the SN were found in these studies (Lastres-Becker et al., 2001; Navarrete et al., 2018). On the other hand, other studies report conflicting results showing no changes, or decreased CB_1 receptor mRNA in the putamen from *post mortem* tissue (Farkas et al., 2012; Hurley et al., 2003). One study also reported changes in other BG structures showing increased CB_1 receptor binding and G protein coupling in the caudate, and increased G protein coupling in the GPe and SN in *post mortem* brain tissue from PD patients (Lastres-Becker et al., 2001). Additionally, a functional correlate could be stablished between CB_1 receptor and some non-motor symptoms in PD patients, showing that decreased CB_1 receptor binding in some areas of the prefrontal cortex correlates with impaired executive and visuospatial functioning and episodic memory (Ceccarini et al., 2019).

This picture gets more complicated with PD animal models. Neurotoxins have been used widespread to model PD in animals. Administration of known toxins for DA neurons (i.e., MPTP, 6-OHDA), yield different degrees of DA denervation overtime, modelling the hypodopaminergic state observed in PD patients. MPTP-treated non-human primates have gathered conflicting results, showing both increases and decreases in CB_1 receptor presence in the dorsal striatum (Lastres-Becker et al., 2001; Rojo-Bustamante et al., 2018). In the case of rats, 6-OHDA injections have to be made in different points within the DA system anatomy to achieve these results, which further adds variability to this PD model. Injection of 6-OHDA in the MFB is unable to induce any changes in CB_1 receptor binding, immunostaining, G protein coupling or mRNA in different BG nuclei (i.e., dorsal striatum, GP and SN), at different time-points (i.e., 3,4 and 7 weeks) (Romero et al., 1999; Walsh et al., 2010; Zeng et al., 1999). However, other studies find that MFB 6-OHDA injection decreases CB_1 receptor binding 3 weeks after lesion in different BG nuclei, or increases its expression in the striatum 4 and 17 weeks post-surgery (Mackovski et al., 2016; Mailleux & Vanderhaeghen, 1993; Romero et al., 1999). Moreover, 6-OHDA injection into the SN decreases CB_1 receptor binding in the dorsal striatum 6 weeks after lesioning, as intrastriatal 6-OHDA injections does, consistently decreasing CB_1 receptor immunostaining in the SNr 3-4 weeks after surgery, although this is thought to reflect cell loss in the striatum (Casteels et al., 2010; Chaves-Kirsten et al., 2013; Walsh et al., 2010).

Regarding the CB_2 receptor in PD much less is known, but results across patients and animal models seem more consistent. PD patients and MPTP treated non-human primates show increased CB_2 receptor mRNA in the SN, preferentially located in astrocytes (Navarrete et al., 2018; Price et al., 2009). A rodent PD model consisting in 6-OHDA injections into the striatum showed increased mRNA in the striatum, contrary to what was observed in PD patients (Concannon et al., 2015; Navarrete et al., 2018). CB_2 receptor behaviour in PD, together with its intimate relationship with glial cells, reveals the potential utility of manipulating this receptor to modify disease progression.

2. HYPOTHESIS AND OBJETIVES

2.   HYPOTHESIS AND OBJECTIVES

Classically considered to have mainly motor functions, mounting evidence is redefining our view about BG as a highly organized network that, beyond motor behaviour, integrates cognitive and emotional information. Information in the BG is processed through anatomically segregated circuits following a dorsolateral-ventromedial distribution, being the SM and the mPF circuits the two major anatomo-functional entities in the BG of rats. Adding to the anatomical segregation, there are differences in some neurotransmission systems. Several studies find a different presence of the DA and the endocannabinoid systems in these circuits, along with differences in how these neurotransmission systems act on them. Being PD an affection involving several neurotransmission systems and brain regions, plenty of evidence aim at the BG as the main structures behind PD motor and non-motor features. Considering this, we hypothesized that the function of the SM and mPF BG circuits could be differently affected by cannabinoid drugs and DA denervation.

The main objective of this thesis was to characterize the CB_1 receptor modulation on information transmission through the SM and mPF BG circuits, as well as the impact of DA denervation on these circuits, in order to understand their function and cannabinoid drugs usefulness in PD.

Chapter 2. HYPOTHESIS AND OBJECTIVES

To this end, the specific objectives of this study were:

I. To characterize the spontaneous and cortically-evoked activity of the lateral and medial SNr.

II. To study the CB_1 receptor modulation on cortico-nigral information transmission through the SM and mPF BG circuits.

III. To investigate the impact of DA denervation on cortico-nigral information transmission through the SM and mPF BG circuits.

IV. To explore the effect of DA denervation on the cannabinoid regulation of SM and mPF BG circuits.

V. To characterize the SM and mPF cortico-striatal networks and their modulation by the CB_1 receptor.

3. EXPERIMENTAL PROCEDURES

3.   EXPERIMENTAL PROCEDURES

3.1.   Animals
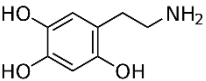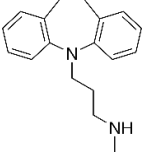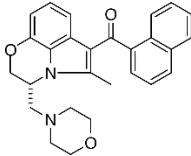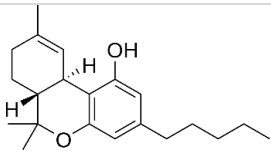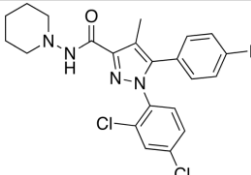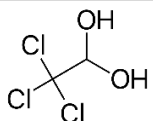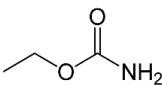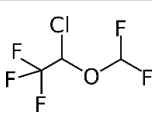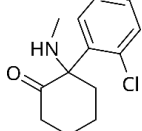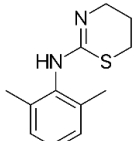
Male (Studies I, II and III; SGiker facilities, University of the Basque Country, UPV/EHU) and female (Study III; ENVIGO, Barcelona, Spain) Sprague-Dawley rats were housed under standard laboratory conditions (22 ± 1°C, 55 ± 5% relative humidity, and 12:12 h light/dark cycle) with food and water provided *ad libitum*. Every effort was made to minimize animal suffering and to use the minimum number of animals per group and experiment. Experimental protocols were reviewed and approved by the Local Ethical Committee for Animal Research of the University of the Basque Country (UPV/EHU, CEEA, M20/2016/176; M20/2019/172). All experiments were performed in accordance with the European Community Council Directive on "The Protection of Animals Used for Scientific Purposes" (2010/63/EU) and with Spanish Law (RD 53/2013) for the care and use of laboratory animals.

3.2.   Drugs

6-OHDA, desipramine hydrochloride, WIN 55,212-2 (WIN), chloral hydrate and urethane were obtained from Sigma-Aldrich. AM251 was obtained from Tocris Bioscience. Δ^9-THC was a generous gift from GW Pharmaceuticals Ltd. Isoflurane was obtained from Ecuphar. Ketamine (100 mg/mL) and xylazine (20 mg/mL) stock solutions were obtain from Richter-Pharma and Calier, respectively. Used drugs and their pharmacological activity are summarized in Table 3.1.

Table 3.1: Pharmacological activity and structure of drugs used

Drug	Pharmacological activity	Structure
6 – OHDA	Neurotoxin	
Desipramine hydrochloride	Noradrenalin reuptake inhibitor	
WIN 55,212-2	CB$_1$/CB$_2$ receptor full agonist	
Δ^9-THC	CB$_1$/CB$_2$ receptor partial agonist	
AM251	CB$_1$ receptor antagonist	
Chloral hydrate	Anaesthetic	
Urethane	Anaesthetic	
Isoflurane	Anaesthetic	
Ketamine	Anaesthetic	
Xylazine	Anaesthetic/Analgesic	

Desipramine, chloral hydrate and urethane were dissolved in a physiological saline solution (0.9% NaCl). 6-OHDA was prepared in Milli-Q water containing 0.02 % ascorbic acid. Cannabinoid drugs (WIN, AM251 and Δ^9-THC) were dissolved in 1:1:18 cremophor/ethanol/saline solution, and if necessary, further diluted with physiological saline until reaching the desired concentration; Δ^9-THC was previously dissolved in ethanol and stored at -20 °C; WIN aliquots were stored at –20 °C, and used within the next 3 weeks. Ketamine and xylazine stock solutions were diluted with physiological saline. Except urethane and ketamine/xylazine mixture, all solutions were freshly prepared immediately prior to use.

3.3. Antibodies

General characteristics of the antibodies employed are summarized in Table 3.2.

Table 3.2: Primary and secondary antibodies characteristics

Antigen	Host	Reference	Manufacturer
Tyrosine Hydroxylase	Rabbit	AB152	Merck Millipore
Rabbit IgG (H+L)	Goat	BA-1000	Vector Laboratories
CB$_1$ receptor	Goat	CB1-Go-Af450	Frontier Institute
Goat IgG (H+L)	Horse	BA-9500	Vector Laboratories
Proenkephalin	Rabbit	LS-C23084	LifeSpan Biosciences
Rabbit IgG (H+L)	Donkey	A-21206	ThermoFisher

3.4. Experimental design

Study I

A total of 177 male Sprague-Dawley rats (250-325 g) were used in this study. Animals were divided into two groups for the characterization of the spontaneous and cortically-evoked activity of SNr neurons: 87 rats were used for electrophysiological recordings in the SM circuits, and 90 for recordings in the mPF circuits. Basal SNr neuron activity was recorded during $\approx$ 200 s, before starting cortical stimulation during another $\approx$ 200 s. When the neuron was challenged with drug, at least 180 s passed before making any measurement on the recorded activity; just one neuron per animal was pharmacologically tested. At the end of the experiment animals were transcardially perfused, brains removed, and prepared for histological processing (i.e. Verification of the stimulation and recording sites) (Figure 3.1).

Study II

A total of 124 male Sprague-Dawley rats (160-215 g at the beginning of the procedures) were used in this study. Animals were divided into four groups according to circuit (i.e. SM or mPF) and neurotoxin or vehicle injection (i.e. 6-OHDA or sham). In the SM group, 17 rats corresponded to the sham group, and 24 in the 6-OHDA-lesioned group. In the mPF group, 28 rats were in the sham group, and 29 in the 6-OHDA-lesioned group. Both circuits were recorded in 4 sham, and 12 6-OHDA-lesioned animals. Rats received 6-OHDA or vehicle injections in the right MFB 4-5 weeks before electrophysiological experiments. The same week electrophysiological experiments were performed, the severity of the DA lesion was assessed using the cylinder test. As the recordings performed in study I, basal SNr neuron activity was recorded during $\approx$ 200 s., before starting cortical stimulation during another $\approx$ 200 s. When the neuron was challenged with drug, at least 180 s passed before making any measurement on the recorded activity; just one neuron per animal was pharmacologically tested. At the end of the experiment animals were transcardially perfused, brains removed, and prepared for histological processing (i.e. Verification of the stimulation

and recording sites, TH immunohistochemistry). A separate group of 10 animals was employed to determine the expression of the CB_1 receptor within the BG. These animals were equally distributed between sham and 6-OHDA-lesioned groups (i.e. Sham: n = 5; 6-OHDA: n = 5). Perfusion of this group of animals took place at the same time after toxin injection (i.e. 4 weeks), than those animals employed for electrophysiology recordings. Thus, after performing the cylinder test to assess lesion severity, animals were perfused and brains prepared for histological processing (Figure 3.1).

Study III

A total of 42 Sprague-Dawley rats (250-360 g) were used in this study. Animals were divided into two groups regarding the studied circuit: SM and mPF. In the SM group, 21 rats were used for electrophysiological recordings in the SM functional territory of the striatum (i.e. dorsolateral striatum). In the mPF group, 21 rats were used for electrophysiological recordings in the mPF functional territory of the striatum (i.e. dorsomedial striatum). Of the total 42 rats used in this study, 6 were female rats that were distributed as follows: SM: n=2; mPF: n=4. During these experiments, the cortex would be stimulated while slowly lowering the electrode upon finding a striatal neuron. Then, stimulation would be stopped, and the spontaneous activity of the neuron recorded. The basal activity was recorded during at least 300 s, before starting cortical stimulation during another $\approx$ 200 s. When the neuron was challenged with drug, at least 180 s passed before making any measurement on the recorded activity; just one neuron per animal was pharmacologically tested. At the end of the experiment, juxtacellular labelling with neurobiotin was attempted, animals transcardially perfused, brains removed, and prepared for histological processing (i.e., Neuronal identification and molecular characterization) (Figure 3.1).
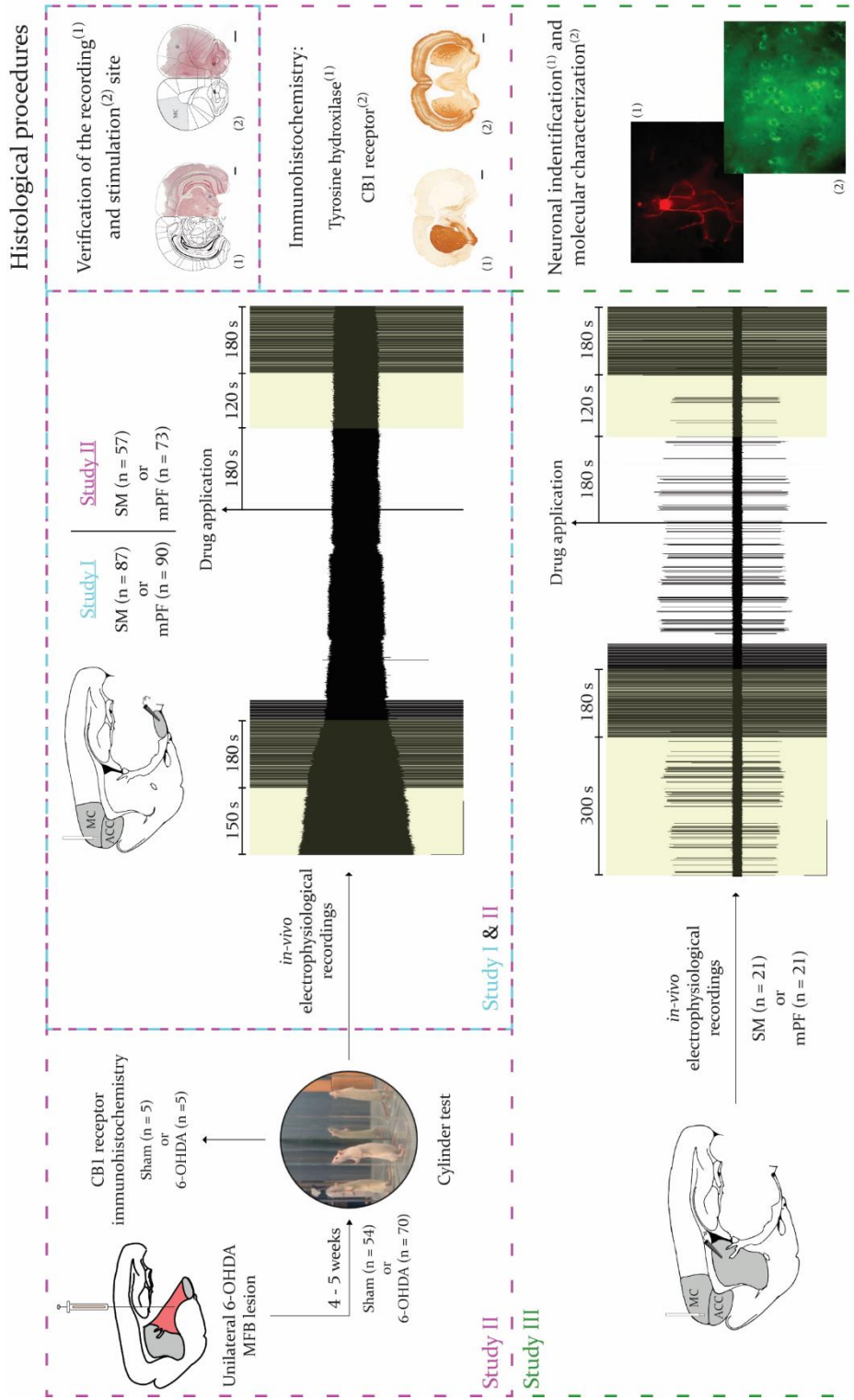
Figure 3.1: Schematic representation of the experimental design in the three studies. In Study I (blue), *in vivo* single-unit extracellular recordings of the lateral and medial territories of the *substantia nigra pars reticulata*, paired with stimulation of the motor (MC) or the anterior cingulate (ACC) cortices, respectively, were performed in control anaesthetized rats. In Study II (purple), rats were injected with 6-OHDA or vehicle (sham) in the right medial forebrain bundle (MFB), and motor asymmetry assessed by the cylinder test. Some rats were employed to evaluate CB$_1$ receptor immunostaining in the basal ganglia, the rest underwent electrophysiological recordings with the same methodology used in Study I. In Study III (green), *in vivo* single-unit extracellular recordings in the dorsolateral or dorsomedial striatum, paired with stimulation of the MC or the ACC, respectively, were performed in control anaesthetized rats. In Studies I and II, recording and stimulation sites were histologically verified. In Study II, dopaminergic denervation was assessed by a tyrosine hydroxylase immunohistochemistry. In Study III, morphological and molecular characterization of some recorded neurons was carried out.

3.5. Dopaminergic denervation with 6-Hydroxydopamine

Thirty minutes prior surgery, rats were pretreated with desipramine (25 mg/kg, i.p.) in order to protect noradrenergic terminals from 6-OHDA toxicity. After that, rats were deeply anaesthetized through isoflurane inhalation (4% for induction; 1.5-2% for maintenance), and placed in a stereotaxic frame (David Kopf® Instruments). A sagittal incision was done on the scalp to reveal the skull, and the connective tissue removed. Two burr holes were drilled over the right MFB coordinates. First, 8.75 µg were injected at anteroposterior (AP) −4.4 mm and mediolateral (ML) +1.2 mm relative to Bregma, and dorsoventral (DV) −7.8 mm relative to dura, with the tooth bar set at −2.4 mm. The second injection of 7 µg was at AP −4.0 mm, ML +0.8 mm, and DV −8 mm, with the tooth bar set at +3.4 mm (Paxinos & Watson, 2006). A total of 4.5 µL of 6-OHDA (3.5 µg/µL; saline with 0.02% ascorbic acid) or vehicle (sham animals) were infused into de MFB through a 10 µL Hamilton syringe coupled to a pump (KDS Scientific, Massachusetts, USA) at a rate of 1 µL/min. After the infusion ended, the syringe needle was left in place for an additional 2-3 minutes to allow diffusion of the neurotoxin in the injection site, before being slowly retracted. The 6-OHDA solution was prepared daily for each surgery session. It was kept in ice and away from light to avoid premature oxidation. The toxin was replaced when oxidation was apparent, as indicated by a change in its colour from clear to pale pink. After surgery, rats were left to recover for 4-5 weeks.

3.6.   Cylinder test

The cylinder test is designed to evaluate asymmetry in forelimb use, by assessing the ability of the animal to stand on the wall of a translucent cylinder with their forelimbs during exploration. 4 – 5 weeks after surgery rats were individually placed in a 20 cm diameter methacrylate cylinder, and allowed to explore freely. Mirrors were placed behind the cylinder to allow a 360° view of the exploratory behaviour. Each animal was left in place until at least 20 supporting front paw touches with open digits were done on the walls of the cylinder. The session was video-recorded for posterior analysis. Touches performed with the forelimb contralateral or ipsilateral to the lesioned hemisphere were counted, and data expressed as the percentage of ipsilateral placement. Rats using the ipsilateral paw about 70% or more were considered to have severe damage of the DA system.

3.7.   Electrophysiological procedures

3.7.1. *In vivo* single-unit extracellular recordings of *substantia nigra pars reticulata* neurons and simultaneous cortical stimulation

3.7.1.1.   Animal preparation and surgery

The animals were anaesthetized with chloral hydrate (420 mg⁄kg, i.p.) for induction, followed by continuous administration of chloral hydrate at a rate of 115.5 mg/kg/h (i.p.) using a peristaltic pump to keep a steady level of anaesthesia. For additional systemic drug administration, the right jugular vein was cannulated with a polyethylene cannula (Clay Adams, Becton Dickinson and Company Division, model PE-240). The rat was placed in a stereotaxic frame and its body temperature was maintained at ~37°C for the entire experiment with a heating pad connected to a rectal probe (Thermoregulator RTC-1, Cibertec). After making a sagittal incision on the scalp to reveal the skull, cleaning the connective tissue, and setting the skull to a 0° plane, two burr-holes were made in the right hemisphere. The first burr-hole was over the motor cortex (MC; AP +3.5 mm and ML -3.2

mm relative to Bregma, and DV -1.6 mm to dura) or the anterior cingulate cortex (ACC; AP +2.9 mm and ML -0.6 mm relative to Bregma, and DV -1.7 to dura) in which an stimulation electrode was placed. The second was over the lateral part (AP -5.8 mm, ML -2.5 mm relative to Bregma, and DV -7/-8 mm to dura), or the medial part (AP -5.4 mm and ML -1.8 mm relative to Bregma, and DV -7/-8 mm to dura) of the SNr, depending on whether the MC or the ACC cortex were being stimulated, respectively.

3.7.1.2. Recording electrode preparation

A thin-wall glass capillary with filament (TW150F-4, World Precision Instruments, UK) was stretched using an automatic vertical electrode stretcher (PE-2, Narishige Scientific Instrument Lab, Japan). Afterwards, the tip of the electrode was broken back to a tip diameter of approximately 1-2.5 μm under visual inspection through a microscopy (CH-2, Olympus Optical Co.) with 40x magnification. The electrode was finally filled with filtered (Minisart® syringe filter, 0.2 μm pore diameter, Sartorius) 2% solution of Pontamine Sky Blue (Sigma-Aldrich) in 0.5% sodium acetate.

3.7.1.3. Electrical stimulation of the cortex

After placement of the stimulation electrode ipsilateral to the recording site, in the coordinates described above, MC and ACC were electrically stimulated at 1 Hz (pulse width 0.6 ms; intensity 1 mA), using a coaxial stainless-steel electrode (diameter, 250 μm; tip diameter, 100 μm; tip-to-barrel distance, 300 μm; Cibertec S.A.). Electrical pulses were generated with a CS-220 Stimulator (Cibertec S.A.) and a stimulus isolator (ISU 165, Cibertec S.A.).

3.7.1.4.   Recording and neuronal identification

The glass electrode was lowered to the above-mentioned stereotaxic coordinates for the SNr by a hydraulic microdrive (David Kopf® Instruments, Tujunga, California, EEUU, model 640). The electrical signal from the electrode was pre-amplified (10x) and amplified (x10) with a high-input impedance amplifier (model AE-2, Cibertec S.A.), notch-filtered at 50 Hz and bandpass-filtered at 300-3000 Hz in a second amplifier (1x; 63AC, Cibertec S.A.). From this amplifier the signal was sent to an oscilloscope (HAMEG® analog digital scope HM507) and on an audio monitor (AUMON 14, Cibertec S.A.) to be monitored, and to an analog-digital interface (CED micro 1401 mk II interface, Cambridge Electronic Design, UK) to allow the digitization of the recorded signals at a rate of 25 kHz.

Neurons from the SNr were identified as GABAergic by their classically defined electrophysiological characteristics: biphasic action potentials with an average duration of 0.5-1.2 ms, regular firing rates above 10 Hz without a decrease in spike amplitude, as described by (Aristieta et al., 2016), and location ventral to SNc neurons, with spikes wider than 2 ms.

Cortical stimulation evoked characteristic triphasic responses in SNr neurons, consisting in different combinations of an early excitation (EE), inhibition (INH) and/or late excitation (LE) (Aliane et al., 2009; Kolomiets et al., 2003; Maurice et al., 1999) (Figure 3.2).
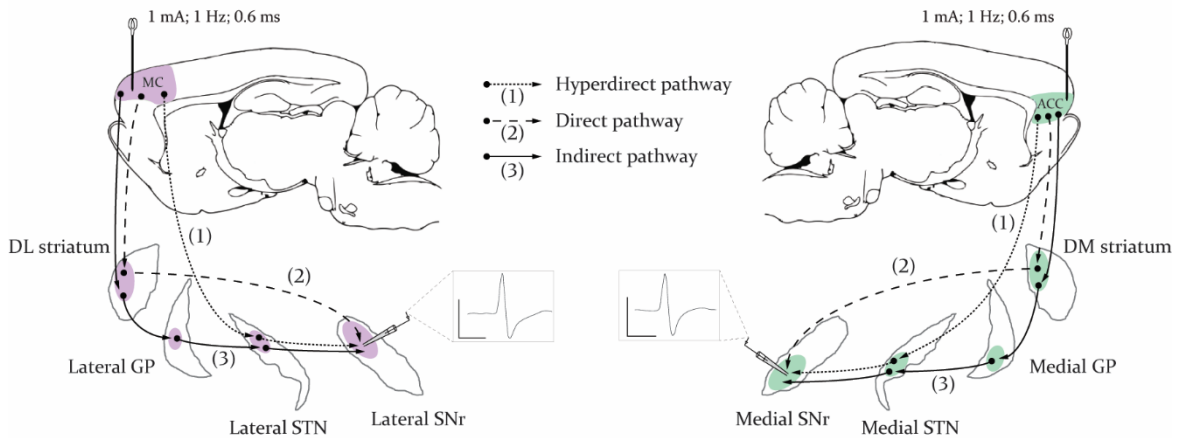
Figure 3.2: Schematic illustration of the cortico-nigral information transmission through the sensorimotor (SM) and medial prefrontal (mPF) basal ganglia (BG) circuits. **A.** Schematic parasagittal sections of the rat brain showing the SM (Left, purple) and mPF (Right, green) circuits of the BG, and representative spike traces from lateral and medial SNr neurons during single-unit extracellular recordings. Additional coronal sections of the different BG nuclei show their involvement in the different pathways that constitute these BG circuits. Cortical information from the motor (MC) and anterior cingulate (ACC) cortex is transferred through the hyperdirect (cortex-STN-SNr; 1, dotted line), direct (cortex-striatum-SNr; 2, dashed line) and indirect pathways (cortex-striatum-GP-STN-SNr; 3, solid line). Scale bars for spike traces are set at 1 V and 1 ms. **B.** Peristimulus time histograms showing the characteristic triphasic responses evoked after MC stimulation in lateral SNr neurons (Left), and after ACC stimulation in medial SNr neurons (Right). Numbers above the responses in the peristimulus time histograms reference the pathway producing that response. Arrows indicate cortical stimulus application. Dashed lines show the threshold above which an excitatory response is considered. DL/DM striatum: dorsolateral/dorsomedial striatum; GP: *globus pallidus*; STN: subthalamic nucleus; SNr: *substantia nigra pars reticulata*.

3.7.2. *In vivo* single-unit extracellular recordings of medium spiny neurons and simultaneous cortical stimulation

3.7.2.1.   Animal preparation and surgery

As described in Sharott et al. (2017), animals were anaesthetized with urethane (1.3 g/kg, i.p.) for induction. To achieve a deeper level of anaesthesia, supplemental doses of ketamine (30 mg/kg, i.p.) and xylazine (3 mg/kg, i.p.) were added throughout the experiment. Proper depth of anaesthesia was assessed regularly by testing the spontaneous electrocorticogram (ECoG), in order to keep the animal in a state of cortical slow-wave activity (SWA; ECoG dominant frequency < 1.6 Hz), which is similar to the observed activity during natural sleep. The right jugular vein was cannulated with a polyethylene cannula, for additional systemic drug administration. A lower gauge polyethylene cannula was used to perform a tracheotomy in order to facilitate the breathing of the rat, and minimize possible vibrations coming from respiratory movements that could interfere with the recordings. Body temperature was maintained at ~37°C for the entire experiment with a heating pad connected to a rectal probe.

The rat was placed in a stereotaxic frame and the body and head of the rat were disposed at the same level to minimize differences in vascular pressure that could compromise recording stability. A sagittal incision was made on the scalp to reveal the skull, the connective tissue cleaned, and the skull set to a 0° plane. The craniotomy was performed as described in Pinault (2005): First, the skull zone in which the stimulation/recording electrode was going to be placed was drilled down until a thin bone membrane remained. This thin bone layer was carefully removed exposing a little section (around 1 mm^2) of the brain underneath. Finally, the dura was removed trying not to disturb any adjacent blood vessels. The first burr-hole was over the MC (3.5 mm anterior to Bregma, 3.2 mm lateral to midline, and 1.6 mm ventral to the dura mater) or the ACC (3.7 mm anterior to Bregma, 0.6 mm lateral to midline, and 1.7 ventral to the dura mater) in which the stimulation electrode was placed. The second burr-hole was targeting the MC (4.7 mm anterior to Bregma, 2 mm

lateral to midline) or the ACC (1.4 mm anterior to Bregma, 0.3 mm lateral to midline) at a different coordinate, where an epidural stainless steel screw was placed. The third was aimed to the lateral (-0.5 to 1 mm relative to Bregma, 3 to 4 mm lateral to midline) or medial (-0.6 to 0.9 mm relative to Bregma, 1.7 to 3 mm lateral to midline) dorsal striatum depending on whether the MC or the ACC were being stimulated, respectively. The fourth was made above the ipsilateral cerebellum, and an additional fifth hole was made above the contralateral cerebellum. Epidural stainless steel screws were placed in these two last holes, acting as reference and ground electrodes for the ECoG, respectively.

3.7.2.2. Recording electrode preparation

A standard-wall glass capillary with filament (G150F-4, Warner Instruments, USA) was stretched, and the tip was broken back as detailed above. The electrode was left in a filtered solution containing 2% neurobiotin (Neurobiotin tracer, SP-1120, Vector Laboratories) in 0.5M sodium chloride, for approximately 2 h to let the tip be filled by capillarity, and avoid bubble formation. Afterwards, the rest of the electrode was filled entirely.

3.7.2.3. Electrical stimulation of the cortex

After placement of the stimulation electrode ipsilateral to the recording site, in the coordinates described above, MC or ACC were electrically stimulated using a coaxial platinum/iridium electrode (diameter, 350 µm; tip diameter, 75 µm; tip-to-barrel distance, 300 µm; MicroProbes). Electrical pulses were generated as previously described. Stimulation of the cortices took place under two different stimulation protocols: search and response protocols.

The search protocol consisted in two square-wave current pulses (each having a duration of 0.3 ms, an amplitude of 1 mA, and a pulse interval of 100 ms) delivered at a frequency of 0.5 Hz. These parameters were chosen as they have demonstrated to evoke

spikes in MSNs, even those not firing spontaneously under urethane anaesthesia (Mallet et al., 2006).

The response protocol consisted in one square-wave current pulse, with a duration of 0.6 ms and an intensity of 1 mA delivered at 1 Hz.

3.7.2.4.   Recording and neuronal identification

The electrical signal from the electrode was pre-amplified (0.1x) and amplified (10x) with a high-input impedance amplifier (AxoClamp 2-B, Axon Instruments), notch-filtered at 50 Hz and bandpass-filtered at 300-3000 Hz in a second amplifier (100x; 63AC; Cibertec S.A.). From this amplifier the signal was sent to an oscilloscope (HAMEG® analog digital scope HM507) and on an audio monitor (AUMON 14; Cibertec S.A.) to be monitored, and to an analog-digital interface (CED micro3 1401 interface, Cambridge Electronic Design, UK) to allow the digitization of the recorded signals at a sampling rate of 25 kHz. The glass electrode was slowly lowered into the striatum at the mentioned coordinates by a hydraulic microdrive (David Kopf® Instruments, Tujunga, California, EEUU, model 640).

While lowering the electrode, the cortex was stimulated with the named "search" protocol until encountering a unit responding consistently and with short latency (<20 ms.) to cortical stimulation; the stimulation would be then stopped. After recording its spontaneous activity, the neuron would be then stimulated with the named "response" protocol, and its evoked activity recorded. Putative MSNs were identified by their consistent response to cortical stimulation and spike waveform. Posterior juxtacellular labelling with neurobiotin would confirm the identity of the recorded neuron. Labelled neurons not identified as MSNs were discarded from all the analyses.

Other filters were applied to the signal coming from the glass electrode to record the striatal local field potential (LFP). In this case the signal was similarly pre-amplified (0.1x) and amplified (10x), and then notch-filtered at 50 Hz, and band-pass filtered at 0.1-100 Hz in the amplifier (100x). The filtered signal was digitized at a sample rate of 2.5 kHz.

The ECoG signal was recorded from the screw placed over the MC or the ACC. The signal was pre-amplified and notch-filtered at 50 Hz. (10x, AmpliBox, Cibertec S.A.), and band-pass filtered at 0.1-400 Hz by the amplifier (200x). The filtered signal was digitized at a sample rate of 2.5 kHz (Figure 3.3).
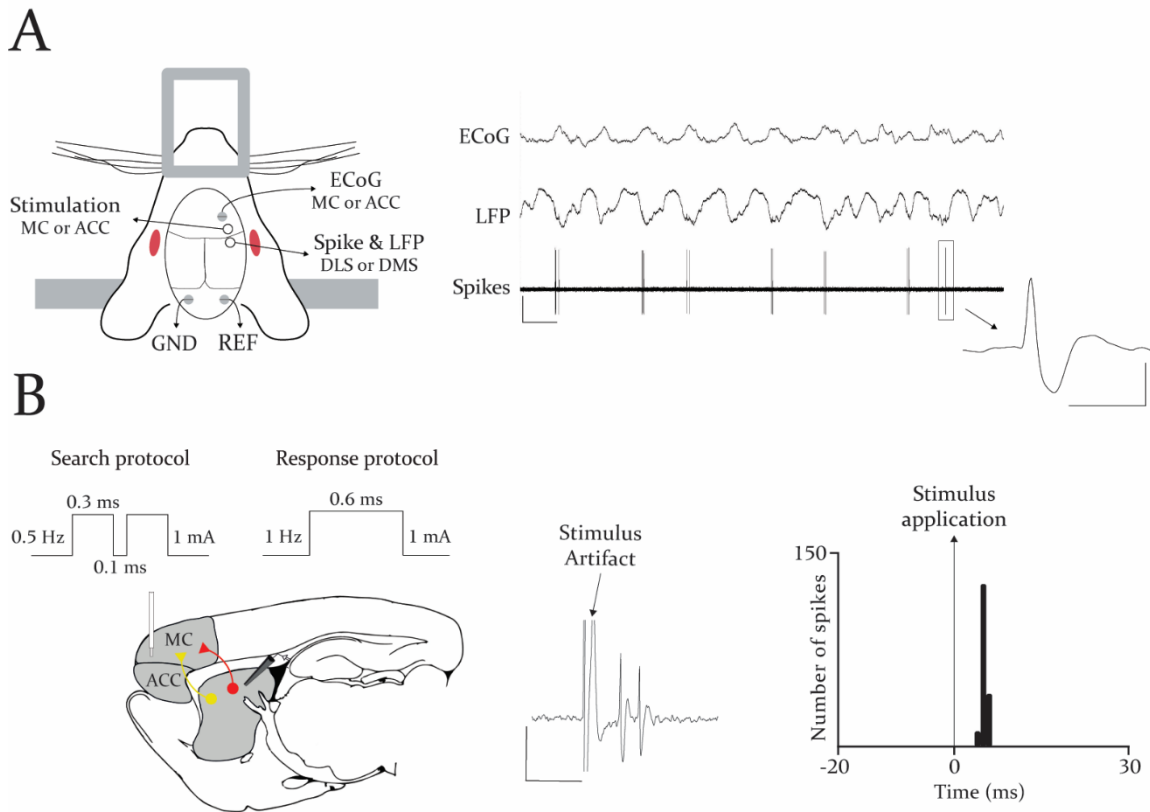
Figure 3.3: Schematic summary of the methodological approach used to study cortico-striatal networks in rats. **A.** Schematic representation of the experimental set-up (Left), and representative recording from a spontaneously active MSN (Right), along with the correspondent electrocorticogram (ECoG) and local filed potential (LFP). Note the synchronicity between firing and oscillatory activity in ECoG and LFP channels. A representative MSN spike trace is shown; scale bar set at 1 V and 2 ms. **B.** Representative scheme of the search and response protocols illustrating the squared pulses delivered to motor cortex (MC) or anterior cingulate cortex (ACC) during recordings, followed by a scheme showing the stimulation and recording sites (Left). Cortical projection neurons make synapses with preproenkephalin+ (yellow) and preproenkephalin- (red) MSNs, among others, in the striatum. After cortical stimulation, MSNs would consistently fire short-latency spikes (Right). Scale bar set at 1 V and 100 ms.

3.7.3. Electrophysiological data analysis

Before data analysis, spike-sorting procedures, such as template matching and principal component analysis, were used to discriminate artefacts from the electrical stimulation that might interfere with the posterior analysis. All analysis were done offline using the Spike2 software (version 7; Cambridge Electronic Design) or MATLAB (v. R2020a, MathWorks Inc.). Electrophysiological data was averaged per animal since more than one neuron (1-15) would usually be recorded during these experiments; this way, each animal would have one value for each electrophysiological parameter. The following parameters were estimated:

Firing rate (FR): Expressed as Hz (number of action potentials per second). The number of action potentials during the recording was grouped in 10 s bins. The mean FR of GABAergic SNr neurons was quantified for 150 s under physiological conditions, and during 120 s after drug administration, to assess the effects of administered drugs. Only neurons above 7 Hz were considered for analysis.

In the case of recordings from striatal neurons, action potentials were grouped in 1 ms bins. Under physiological conditions, firing was quantified during 300 s epochs, and 120 s after drug administration, for drug effect assessment. Only putative MSNs with spontaneous firing ≥ 0.03 Hz (Sharott et al., 2017) were considered for further analysis.

Coefficient of variation (CV): The CV consists on the ratio, expressed as a percentage, between the weighted standard deviation and mean of the inter-spike interval (ISI) histogram of a given neuron. This histogram was made with 1 ms bins, and considering all ISIs ≤ 0.5 ms for SNr neurons (given their relatively high FR) and ≤ 33.33 s for putative MSNs (based on the minimum FR considered for a putative MSN to be spontaneously active). The periods used in either case for the analysis were the same than in the analysis of the FR.

Index of pauses: The index of pauses was analysed as an additional regularity measure for the spontaneous firing of putative MSNs. The analysed time range was divided into four equal

periods, from which ISI histograms considering all ISIs ≤ 33.33 s were made with 1 ms bins. The longest ISI in each of these ISI histograms was used to calculate the mean, which would represent the index of pauses. In other words, the index of pauses is the mean of the longest ISIs in the four periods the analysed time range was divided into. Analysed time epochs were the same than in previous analyses.

Burst firing pattern: Burst-related parameters in SNr neurons (i.e. number of bursts, mean duration of burst, number of spikes per burst, recurrence of bursts and intraburst frequency) were analysed using the Poisson surprise method (Legendy & Salcman, 1985) through a Spike2 script ("surprise"). Depending on whether neurons presented burst firing, they were classified as neurons with or without bursts. Analysed time epochs were the same than in previous analyses.

Spectral analysis: ECoGs and LFPs were smoothed to 1 ms prior to the calculation of the power spectrum using a fast Fourier transform (Block size: 8192; Frequency resolution: 0.3 Hz). Data from these power spectra was used to calculate the coherence spectra between ECoG-LFP pairs. The peak frequency and the frequency band area under the curve (AUC) was analysed for each ECoG, LFP and coherence spectra. The peak frequency was defined as that frequency contributing the most to a given signal. The AUC was analysed in the following frequency bands: δ [0.6 – 4 Hz], θ [4 – 9 Hz], α [9 – 13 Hz], β [13 – 31 Hz], γ [31 – 49 Hz] using the trapezoidal rule. In order to calculate frequency band AUCs that describe actual changes in that band and not in total power, AUC values for each band were normalized to the total AUC of the power spectrum. Thus, frequency band AUCs are expressed as percentages, reflecting the relative contribution of that band to the total AUC of a given power spectrum. The total AUC was calculated as the AUC between 0 and 80 Hz, excluding the electrical noise around 50 Hz. Analysed time epochs were the same than in previous analyses.

Phase-lock analysis: ECoGs and LFPs were down-sampled to 62.5 Hz and band-pass filtered at 0.4-1.6 Hz. Peak events were extracted from the filtered waveform and used to calculate the instantaneous phase of each spike. Descriptive circular statistics and Rayleigh's test for

uniformity were calculated from the instantaneous spike phases using CircStat toolbox (Berens, 2009). In this work, only neurons with ≥ 10 spikes in the recorded period were used for these analyses. Analysed time epochs were the same than in previous analyses.

Cortically-evoked responses: Peristimulus time histograms were generated from 180 stimulation trials using 1 ms bins. In the case of SNr neurons, the criterion used to determine the existence of an excitatory response was an increase of two-fold the standard deviation, plus the mean number of spikes from a pre-stimulus period of 20 ms, for three consecutive bins. An INH was defined as a period in which no spikes were observed for at least three consecutive bins. The duration was equal to the time between the beginning of the first bin, and the end of the last bin in a given response meeting the above criteria. The latency would correspond to the time in which the first bin begins in a given response. The amplitude of the excitations was quantified by calculating the difference between the mean number of spikes evoked within the time window of the excitation, and the mean number of spikes occurring spontaneously in the pre-stimulus period.

Since SM and mPF circuits of the BG in 6-OHDA-lesioned animals are not as thoroughly described as in control ones (Maurice et al., 1999), to better describe the information transmission through these circuits, we set latency ranges based on the latencies of triphasic responses, since they provide full information on transmission through the three pathways that constitute these circuits. Ranges were set up to each cortically-evoked response (i.e. EE, INH, LE), in each circuit (i.e. SM or mPF) and experimental group (i.e. Sham or 6-OHDA). For each response, a range was set according to the minimum and maximum latency observed within the triphasic-respondent neurons of that circuit and experimental group. Hence, cortically-evoked responses whose latency were out of range were excluded from the analyses of the cortically-evoked responses, and neurons with no cortically-evoked response within range were excluded from all the analysis.

For the cortically-evoked responses in striatal neurons, the duration of the response was defined as the beginning of the first bin, and the end of the last bin right after the stimulation. The latency corresponded to the time in which the first bin after the stimulation

begins. The amplitude was defined as the difference between the spike counts during the response duration, and the spike counts in the 20-ms period before the stimulation.

3.8.   Histological and quantification procedures

3.8.1. Histological procedures

At the end of the electrophysiological experiments animals were deeply anaesthetized with chloral hydrate (1 g/kg, i.p.) and transcardially perfused with phosphate buffer saline (PBS; 0.1M, pH = 7.4), followed by 4% ice-cold paraformaldehyde in PBS. Brains were removed and post-fixed in paraformaldehyde for at least 24 h at 4 °C. Afterwards, brains were transferred to a 30% sucrose solution until they sank. Brains were cut in 40-μm coronal sections using a freezing microtome (HM 430, Microm®), and slices were conserved in a cryoprotective solution (30% ethylene glycol and 26% glycerol in PBS) at -20 °C until further processing. All brains were processed this way, unless stated otherwise.

3.8.2. Verification of the recording and stimulation site

In a set of experiments, at the end of SNr recordings a 10 μA cathodic current was constantly applied through the recording electrode for 10 minutes (Digital Midgard precision current source, 515595, Stoelting) to allow the formation of a Pontamine Sky Blue deposit on the recording site. Brains were processed as described above, and coronal brain sections containing the SNr were mounted on gelatinized glass slides, stained with 1% Neutral Red for 10 minutes, washed in distilled water, dehydrated in an ascending series of alcohol, cleared with xylene and coverslipped with DPX (Sigma-Aldrich) mounting medium. A blue dot on the lateral or medial portion of the SNr, examined under a microscope, determined the correct placement of the recording electrode.

To verify the correct placement of the stimulation electrode, a 1 mA cathodic current was passed through the electrode during 10 minutes to allow the deposition of iron at the tip of the electrode. Brains removed after perfusion, were post-fixed in a solution containing an

80% of a 4% paraformaldehyde solution, 20 % of ethanol containing 2% acetic acid, and 1% (w/v) of potassium ferricyanide. This would stain the iron deposit from the electrode in blue, showing the stimulation site. Coronal sections containing the MC or ACC were mounted on gelatinized glass slides, if the blue point was apparent sections were counterstained with Neutral red as described above; otherwise Nissl-thionine stained, to inspect the tract of the electrode in cortex.

To Nissl-thionine-stained slices, after mounting them in gelatine-coated slides, were processed as follows: slides were washed in distilled water twice for 5 min. Then they were dehydrated in 70% ethanol and 96% ethanol for 10 and 2 min, respectively. They were then rinsed in an ethanol-paraformaldehyde mixture for 5 min (4:1, 96% ethanol | 10% paraformaldehyde). They were washed in 96% ethanol for 2 min, to be rinsed in a chloroform-ethyl ether-96% ethanol mixture for 10 min (8:1:1, chloroform | ethyl ether | 96% ethanol). Slides were then washed in 96% ethanol during 2 min, further dehydrated with 100% ethanol twice for 2 min, and xylene for 5 min. Afterwards, slides were rehydrated rinsing them in 100% ethanol for 10 min twice, 96% ethanol for 2 min, then 96% ethanol for 10 min, 70% ethanol for 5 min, and 50% ethanol for 5 min. They were then stained with thionine 1% for 20-45 min, washed in distilled water for 1 min, then rinsed in glacial acetic 0.3% in distilled water for 1.5 min, and glacial acetic 0.3% in 70% ethanol for 1.5 min. Finally, they were dehydrated in 96% ethanol, and 100% ethanol for 2 min each, and xylene for 8 min twice. After that, they were coverslipped with DPX mounting medium. The blue point/tract of the stimulation electrode in MC or ACC cortices served to determine its correct placement (Figure 3.4).
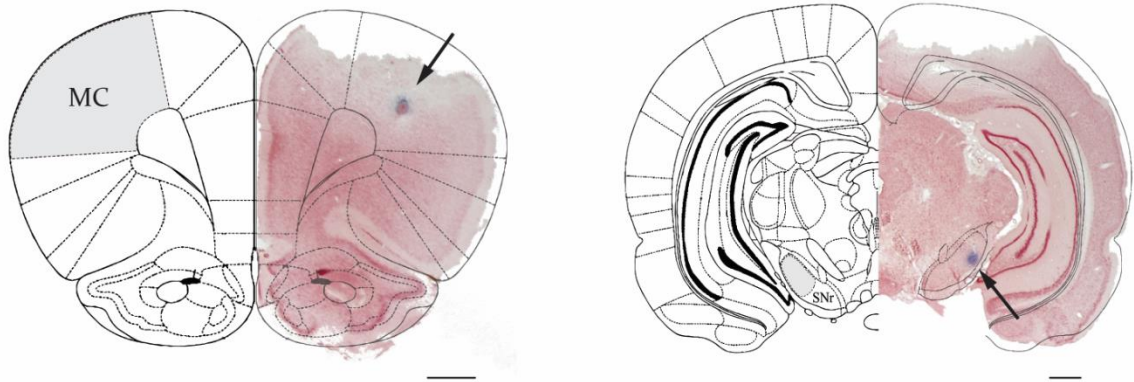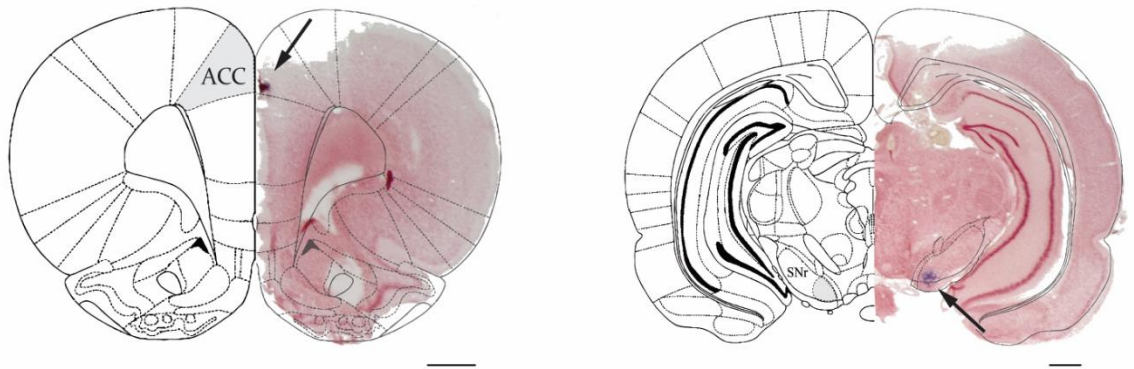
Figure 3.4: Histological verification of the cortical stimulation site and recording place within *substantia nigra pars reticulata* (SNr), for the sensorimotor (lateral SNr) (**A**) and medial prefrontal circuits (medial SNr) (**B**). Cortical and SNr areas targeted in the experiments are shaded in gray. Arrows indicate the exact position of the blue dot in the target area by ferricyanide-iron reaction (Left) or deposition of Pontamine Sky Blue (Right). Scale bar set at 1 mm. ACC: anterior cingulate cortex; MC: motor cortex.

3.8.3. Identification of recorded and juxtacellularly-labelled striatal neurons

At the end of each electrophysiological recording, striatal neurons were juxtacellularly labelled with neurobiotin. In order to achieve that, positive currents pulses ranging from 2 to 10 nA in amplitude, and 200 ms in duration (50% duty cycle) were applied until the activity of the neuron became robustly synchronized with the pulses. After that, the current was rapidly stopped, the amplitude was lowered, and pulses resumed entraining neuron activity. If this was accomplished, the pulses would be maintained for around 1 minute to allow neurobiotin to enter into the recorded neuron; if not, the process would start from the beginning, until the neuron was satisfactory entrained by the pulses. Next, the glass electrode was slowly withdrawn from the brain to ensure no damage to the recently labelled neuron. To allow the neurobiotin disseminate through the perikaryon and dendrites, perfusion was performed two to four hours after the labelling procedure. Brains were processed as described above, and cut in 50-μm parasagittal sections with a freezing microtome.

Floating sections containing the striatum were washed in PBS, and incubated at room temperature a minimum of 7 hours in PBS containing a 0.3% of Triton X-100, and Cy3-conjugated streptavidin (1:1000; ZyMax Streptavidin-Cy3, 43-8315, ThermoFisher Scientific). Afterwards, sections were washed in PBS, mounted in superfrost slides and coverslipped with Vectashield (H-1000, Vector Laboratories), and the striatum inspected under a fluorescence microscope (BX51, Olympus), coupled to a CCD camera (Orca R^2 C10600, Hamamatsu). Labelled neurons with dense spiny dendrites were considered MSNs; these sections were retrieved for further molecular characterization. Sections with labelled neurons presenting aspiny dendrites, or no labelled neurons, were discarded; electrophysiological recordings from neurons with aspiny dendrites were excluded from further analysis.

3.8.4. Immunohistological assays

3.8.4.1.   Tyrosine hydroxylase immunohistochemistry

TH immunostaining was used to examine the degree of DA denervation in the striatum and the SNc. Briefly, free-floating sections of these areas were first washed three times in potassium phosphate buffer saline (KPBS; 0.02M, pH = 7.4). Endogenous peroxidases were quenched using 3% H_2O_2 and 10% methanol in KPBS for 30 min at room temperature. After washing the sections three times in KPBS, these were incubated in the blocking solution consisting of 0.1% Triton X-100, and 5% normal goat serum (NGS) in KPBS for 1 h at room temperature. They were incubated with an anti-TH primary antibody (1:1000, Table 3.2) in the blocking solution overnight at room temperature. Next, slices were washed in KPBS twice, slices were pre-incubated in the blocking solution (2.5% NGS) for 10 min, and incubated for 2 h with a biotinylated antibody (anti-rabbit 1:200, Table 3.2) in blocking solution (2.5% NGS). Sections were washed in KPBS, and incubated with an avidin-biotin-peroxidase complex (PK-6100, Vector Laboratories) in KPBS with 0.1% Triton X-100, for 1 h at room temperature. Peroxidase activity was revealed with 0.05% 3,3′-diaminobenzidine (DAB; Sigma) and 0.03% H_2O_2. The reaction was stopped by washing the sections in mQ water. The sections were then washed three times in KPBS and mounted onto gelatine-coated slides, dehydrated, cleared with xylene and coverslipped with DPX mounting medium.

3.8.4.2.   CB₁ receptor immunohistochemistry

Another series of animals (i.e. sham and 6-OHDA-lesioned rats) different to those used in electrophysiological experiments were used to determine the expression of CB₁ receptors within the BG. Rats were transcardially perfused with a PBS solution followed by a mixture of 4% paraformaldehyde, 0.5 % glutaraldehyde and 0.2% of a saturated solution of picric acid in phosphate buffer (PB; 0.1M, pH = 7.4). Brains were extracted and stored in fixative solution for one week. After that, brains were coronally cut at 50 μm with a cryotome.

Sections were preincubated in blocking solution containing 10% bovine serum albumin, 0.5% Triton X-100 and 0.1% sodium azide in Tris-HCl buffered saline (TBS) for 30 min. Then, sections were incubated in a solution with the primary antibody raised in goat against CB_1 cannabinoid receptor (Table 3.2), at a final concentration of 2 µg/ml in 10% bovine serum albumin, 0.5% Triton X-100, and 0.1% sodium azide in TBS for 20 h. Sections were afterwards rinsed in 1% bovine serum albumin and 0.5% Triton X-100 in TBS, and incubated in biotinylated horse anti-goat secondary antibody (Table 3.2), at a concentration of 15 µg/ml in 1% bovine serum albumin and 0.5% Triton X-100 in TBS for 1 h. After secondary antibody incubation, sections were again rinsed in 1% bovine serum albumin, and 0.5% Triton X-100 in TBS, and reacted for 90 min in ABC complex diluted 1:1:50 in TBS. After several rinses in PB, peroxidase reaction with 0.05 % DAB and 0.003% H_2O_2 in PB was developed for 2 min. Sections were rinsed in PB, mounted onto gelatine-coated slides, dehydrated, cleared in xylene and coverslipped with DPX mounting medium.

3.8.4.3. Preproenkephalin immunofluorescence

Brain sections containing neurobiotin-labelled MSNs were used to determine whether they expressed preproenkephalin or not. Somatic expression of this molecular marker was used to identify MSNs from the indirect pathway, considering those with no preproenkephalin somatic expression to correspond to the direct pathway (Lee et al., 1997; Sharott et al., 2017).

Parasagittal 50-µm brain sections containing Cy3-positive MSNs were washed in PBS, and then incubated in a blocking solution with 10% normal donkey serum and 0.3% Triton X-100 in PBS, for 1 h at room temperature. Following that, sections were washed in PBS and incubated in a 10 mM sodium citrate (pH = 6) solution for 3 h at 80 °C for antigen retrieval (Mallet et al., 2012). After washing sections in PBS, they were incubated with a solution containing an anti-preproenkephalin primary antibody (1:2500, Table 3.2) with 0.3% Triton X-100 in PBS, overnight at 4 °C. Afterwards sections were washed in PBS, and incubated 4 h at room temperature with a donkey anti-rabbit secondary antibody (1:500, Table 3.2), with 0.3% Triton x-100 in PBS. After washing the sections in PBS, these were re-incubated in the

primary antibody solution for 1 h at 4 °C. Following PBS washing of the sections, these were re-incubated in the secondary antibody solution for 1 h at 4 °C. Sections were finally washed in PBS before mounting the sections in Vectashield to determine preproenkephalin expression in Cy3-positive MSNs under a fluorescence microscope.

## 3.8.4.4.	Quantification procedures for the immunohistochemical assays

## 3.8.4.4.1.	Optical densitometry of tyrosine hydroxylase-positive fibres in the striatum

To assess the extent of the DA denervation induced by 6-OHDA injection we performed an optical density (OD) analysis of striatal DA fibres based on TH immunoreactivity. Striatal coronal sections from each animal covering the rostral, medial and caudal striatal levels were digitized using an EPSON V700 scanner at a resolution of 6400 ppp. For each slice, the dorsal striatum was delimited and the mean OD of the ipsilateral or lesioned hemisphere was expressed as a percentage of that in the contralateral or intact non-lesioned hemisphere. The corpus callosum was considered as the background. Images were analysed using FIJI software (Schindelin et al., 2012). Only animals with more than 90% DA degeneration were include in the analysis.

## 3.8.4.4.2.	Optical densitometry of the CB_1 receptor

To analyse the effect of the 6-OHDA lesion on the expression of the CB_1 receptor in the BG nuclei, an OD analysis of the CB_1 immunoreactivity was performed. The analysis had into account the different anatomo-functional BG territories to assess whether expression in them was different, or the lesion affected these territories differently. Microscope slides with the reacted tissue were scanned with the 20× objective (NA 0.8; Carl-Zeiss) of a Pannoramic MIDI II (3DHISTECH) automatic slide scanner coupled to a CMOS camera (pco. edge 4.2, PCO), through an adapter with 1.6× magnification, and the images studied with FIJI software using the Bio-Formats plugin (Linkert et al., 2010).

We defined the regions of interest for each functional division in each nucleus based on previous tracing, molecular and functional reports, in which compartmentalization of the analysed BG nuclei is made depending on the cortical information they process. Regarding the cortex, we focused on MC and ACC areas since they were the target of cortical stimulation in electrophysiological assays. BG nuclei receiving information from MC were considered to belong to the SM circuits, and those receiving ACC information to the mPF circuits of the BG. MC and ACC regions of interest were defined following a rat brain atlas (Paxinos & Watson, 2006). Cortical areas were analysed until 0.4 mm posterior to Bregma, where they were considered small enough to be properly selected. SM and mPF striatal functional territories were limited to those areas receiving afferences from MC and ACC, respectively (Heilbronner et al., 2016; McGeorge & Faull, 1989). SM and mPF GP functional territories were defined based on calbindin expression patterns, which resembles striatal projections from these territories onto the GP (Rajakumar, Rushlow, et al., 1994). SM and mPF SNr functional territories were defined based on functional studies showing connectivity between the MC or the ACC, respectively (Kolomiets et al., 2003). For frontal slices the olfactory tract, forceps minor or corpus callosum, were selected as background. For more caudal slices, the thalamus, geniculate nucleus or reticular formation, were used as background (Figure 3.5).

To analyse changes in CB_1 receptor density between lesion group (i.e. sham *vs.* 6-OHDA) and functional territories (i.e. SM or mPF) of the analysed BG nuclei, background OD from each hemisphere was subtracted from regions of interest ODs in their corresponding hemisphere. Then values from both hemispheres of the same slice, corresponding to a given nucleus and functional territory, were averaged between them; averaged values from all the slices in an animal were averaged, so each animal would have two values per nucleus: one value for the SM territory, and another for the mPF territory. Values corresponding to the same BG functional territory and nucleus were averaged by lesion group.
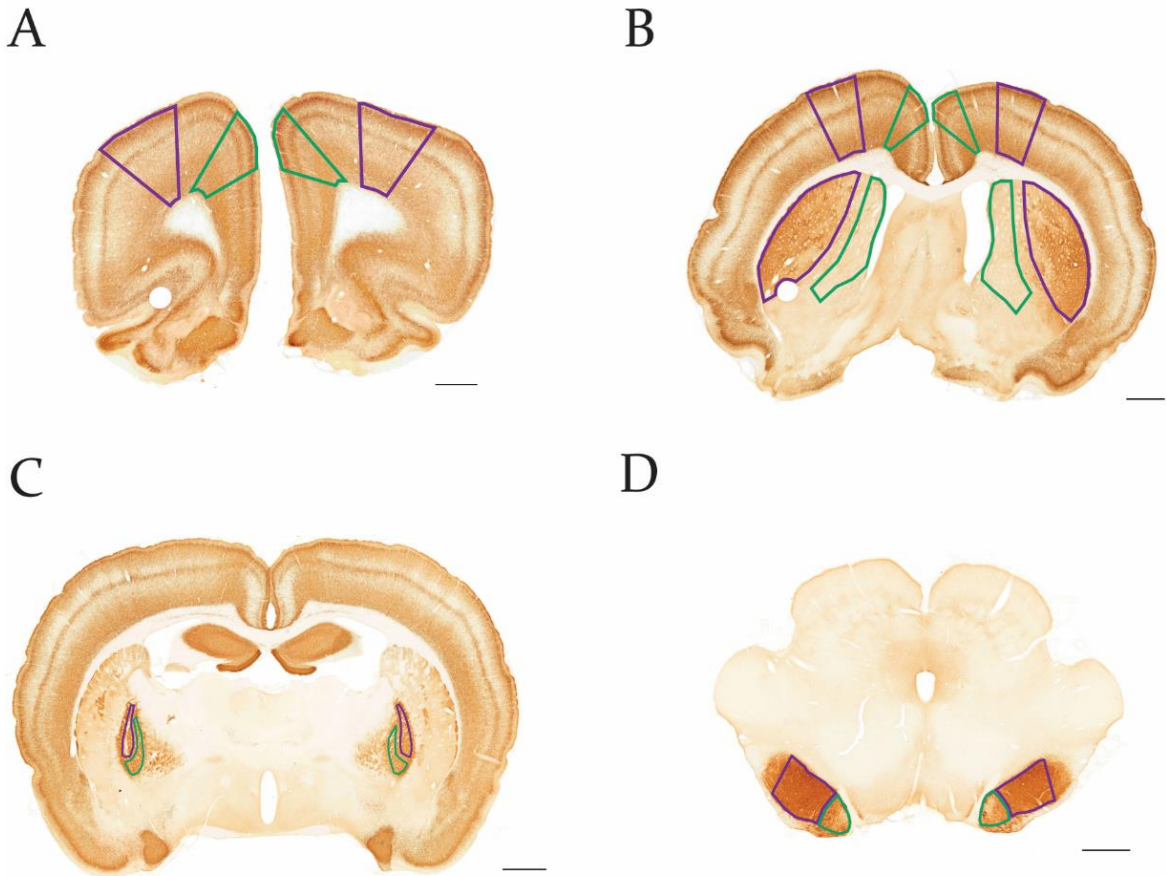
Figure 3.5: Representative coronal sections of a rat brain showing CB_1 receptor immunoreactivity and the regions of interest analysed in each basal ganglia nuclei (**A**, cortex; **B**, cortex and striatum; **C**, *globus pallidus*; **D**, *substantia nigra pars reticulata*). Sensorimotor and medial prefrontal functional territories are marked in purple and green, respectively. Scale bar set at 1 mm.

3.9. Statistical analysis

GraphPad Prism (v. 5.01; GraphPad Software, Inc.), SPSS (v. 25; IBM Corp.) and MATLAB (v. R2020a, MathWorks Inc.) were used for statistical analysis. The level of statistical significance was set at $p < 0.05$. Shapiro-Wilk test was used to determine if variables were normally distributed. Kuiper test was used to assess whether distributions from circular variables were significantly different from a von Mises distribution. Data are presented as group means ± standard error of the mean (S.E.M.) of n rats, unless stated otherwise.

Differences in FR, CV and parameters related to cortically-evoked responses in SNr neurons were analysed using a two-tailed unpaired Student's *t* test. Differences in most burst-related parameters were analysed using Mann-Whitney rank sum test as data were not normally distributed; intra-burst FR was analysed using a two-tailed unpaired Student's *t* test. Likewise, FR, parameters related to cortically-evoked responses of striatal neurons, phase vector length, peak frequency and band frequency AUCs of power spectra were analysed using a Mann-Whitney rank sum test; CV and index of pauses were analysed using a two-tailed unpaired Student's *t* test. Fisher's exact test was used to determine differences in the number of neurons presenting burst firing, and different cortically-evoked response patterns. To assess differences in the mean phase angle of neurons the Watson-Williams test was used.

To assess the effect of the administered drugs (i.e. WIN or Δ^9-THC) in control animals, two-tailed paired Student's *t* test was used to analyse differences in FR, CV, and parameters related to cortically-evoked responses, before and after drug administration. To determine if WIN and Δ^9-THC were differentially affecting the SM or mPF circuits in control animals, cortically-evoked responses before and after drug administration were analysed using a repeated-measures two-way ANOVA (drug × circuit). In sham and 6-OHDA-lesioned animals, a repeated-measures two-way ANOVA was used (drug × lesion) to assess the effects of WIN on FR, CV and parameters related to cortically-evoked responses, before and after drug application. Differences in the number of neurons with burst firing, before and after drug administration, were assessed with Fisher's exact test. Most burst-related parameters before and after drug application were analysed using Wilcoxon matched-pairs signed rank test; intra-burst FR was analysed using a two-tailed paired Student's *t* test. Differences in the FR and cortically-evoked responses of striatal neurons, and peak frequency and band frequency AUCs of power spectra were analysed using Friedman test. When allowable, Bonferroni's (ANOVA) or Dunn's (Friedman) *post hoc* test was used for correction of multiple comparisons.

To study the impact of AM251 on the effect of WIN or Δ^9-THC, FR, CV and parameters related to cortically-evoked responses pre-AM251, post-AM251 and post

AM251+WIN or Δ^9-THC were compared using a repeated-measures one-way ANOVA. In the mPF circuits a repeated-measures two-way ANOVA (drug × lesion) was used. The number of neurons with burst firing was compared using the Chi-squared (χ^2) test. To assess how these drugs would alter burst firing, most burst-related parameters were analysed using Friedman test. Intra-burst FR was analysed using a repeated-measures one-way ANOVA; in the mPF circuits, repeated-measures two-way ANOVA (drug × lesion) was used for this analysis. Geisser-Greenhouse's correction was used if epsilon was below 0.75. When allowable, Bonferroni's *post hoc* test was used for correction of multiple comparisons.

CB$_1$ receptor density averages from sham or 6-OHDA-lesioned rats were compared using a two-way ANOVA (lesion × territory) to assess differences in CB$_1$ receptor density. When allowable, Bonferroni's *post hoc* test was used for correction of multiple comparisons.

Differences in TH OD and ipsilateral forelimb use between sham and 6-OHDA-lesioned rats were analysed using a two-tailed unpaired Student's *t*-test.

4. RESULTS

4. RESULTS

4.1. STUDY I: CB$_1$ receptor control of cortico-nigral transmission through the sensorimotor and medial prefrontal basal ganglia circuits

Neurons from a total of 177 animals were recorded in the SNr, among which 87 were recorded in the lateral SNr, and 90 in the medial SNr. GABAergic neurons within the SNr display typical electrophysiological characteristics (i.e., a narrow spike waveform and a relatively high FR with a regular pattern of discharge). To ensure the belonging of the recorded cells to their corresponding circuits (i.e. SM or mPF), only those responding to cortical stimulation were used in the analysis.

4.1.1. Spontaneous and cortically-evoked activity of *substantia nigra pars reticulata* neurons: Territorial particularities

Recorded neurons from the lateral and medial SNr were not different in terms of their FR or CV, although they showed differences regarding their firing pattern (Table 4.1). A smaller percentage of neurons in the lateral SNr exhibited bursting discharge in comparison to medial SNr neurons. In line with the number and duration of bursts, as well as the recurrence of burst displayed by lateral SNr neurons.

Table 4.1: Firing properties of neurons from the lateral and medial subdivisions of the *substantia nigra pars reticulata* (SNr)

	Lateral SNr (n = 87)	Medial SNr (n = 90)
Firing rate (Hz)	25.2 ± 0.9	22.8 ± 0.9
Coefficient of variation (%)	47.0 ± 1.9	48.3 ± 2.2
Burst firing neurons / recorded neurons	39 / 87	74 / 90
Neurons exhibiting burst firing pattern (%)	44.8	82.2*
Number of bursts	12.4 ± 2.8	21.7 ± 3.0*
Duration of burst (ms)	0.6 ± 0.1	0.9 ± 0.1*
Nº spikes/burst	20.3 ± 3.5	23.2 ± 2.7
Recurrence of burst (nº burst/min)	4.1 ± 0.9	8.7 ± 1.2*
Intraburst frequency (Hz)	49.2 ± 2.8	45.5 ± 2.0

Each value represents the mean ± S.E.M. of (n) recorded rats. *$p<0.05$ *vs.* Lateral SNr (neurons exhibiting burst firing pattern: Fisher's exact test; burst parameters: Mann-Whitney rank sum test).

According to previous publications (Aliane et al., 2009; Kolomiets et al., 2003; Maurice et al., 1999), cortical stimulation of the MC or ACC evoked responses in the SNr neurons that consisted of an EE, followed by an INH and a LE, forming a characteristic triphasic response. The presence of the EE is attributable to the activation of the so-called 'hyperdirect' cortico-subthalamo-nigral pathway. The activation of the 'direct' cortico-striato-nigral pathway produces the observed INH, and the LE derives from the activation of the 'indirect' cortico-striato-pallido-subthalamo-nigral pathway (Maurice et al., 1999). Different patterns of responses were observed in both SNr functional territories, yielding triphasic, biphasic and monophasic responses from the activation of the different pathways along the circuits. The percentage of occurrence of such patterns of responses in lateral SNr and medial SNr neurons is shown in Figure 4.1A.

Regarding the parameters analysed for each of the responses, such as latency of appearance, duration of the response and amplitude of the excitations, the major differences between circuits were observed in latency. In the SM circuits, the appearance of all three responses was significantly advanced in comparison to the mPF circuits, as indicated by an increased latency. Moreover, the duration of the INH was greater in the SM circuits than in the mPF circuits Figure 4.1B.
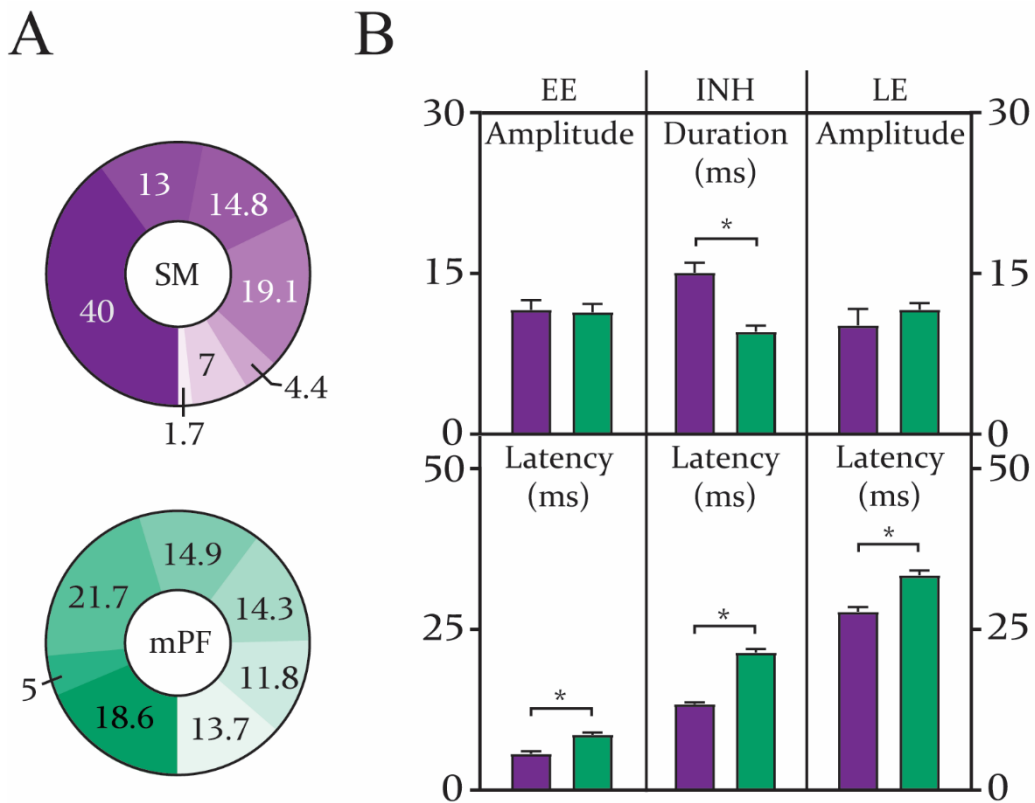
Figure 4.1: Patterns of responses evoked in *substantia nigra pars reticulata* (SNr) neurons by cortical stimulation of the motor cortex or anterior cingulate cortex. **A.** Percentage of occurrence of the different patterns of response evoked in SNr cells by cortical stimulation. From darker to lighter colours: EE + I + LE; EE + I; I + LE; EE + LE; EE; I; LE. **B.** Characteristics of the responses (latency, amplitude of excitations, and duration of the inhibition). Note that the duration of the inhibitions is shorter in the medial prefrontal (mPF) circuits, whereas the appearance of all three responses is delayed when compared to the sensorimotor (SM) circuits, as a higher latency is observed. (EE: early excitation [SM: n = 70; mPF: n = 54]; INH: inhibition [SM: n = 72; mPF: n = 67]; LE: late excitation [SM: n = 68; mPF: n = 77]). Each bar represents the mean ± SEM of n rats. *$p < 0.05$, two-tailed unpaired Student's *t* test.

4.1.2. Effect of cannabinoids on spontaneous and cortically-evoked activity in *substantia nigra pars reticulata* neurons: Involvement of the CB₁ receptor

We further explored the effect of the synthetic CB₁/CB₂-receptor full agonist WIN, and the natural cannabinoid Δ^9-THC, a CB₁/CB₂-partial agonist, on the spontaneous and cortically-evoked activity of SNr neurons identified as receiving input from the MC or the ACC. To demonstrate the contribution of the CB₁ receptor on these effects the synthetic, CB₁-selective antagonist, AM251 was used to block the effects induced by cannabinoid drugs. Cannabinoid drugs doses used in this study were carefully selected to minimize modifications on the firing activity of SNr neurons that could affect the analysis of the cortically-evoked responses.

4.1.2.1. Effect of WIN 55,212-2 on spontaneous and cortically-evoked activity of *substantia nigra pars reticulata* neurons by CB₁ receptor activation

Administration of WIN (125 µg/kg, i.v.) was not able to modify most of the studied parameters associated with the spontaneous activity of these neurons in either of the two recorded functional territories. Despite that, differences were observed in the CV, where neurons from the lateral SNr became more regular after WIN administration (Annex 4.I). Additionally, administration of the CB₁ receptor antagonist AM251 (2 mg/kg i.v.) did not modify the spontaneous activity of SNr neurons (Annex 4.II).

Regarding the cortically-evoked activity, systemic administration of WIN modulated cortico-nigral information transmission through the hyperdirect pathway in the SM and mPF BG circuits differently. While WIN was not able to significantly affect the amplitude of the hyperdirect pathway in the SM circuits, it reduced this response in the mPF circuits (Figure 4.2A, B, C, top). On the other hand, transmission through the direct pathway was significantly diminished in both circuits, as a consequence of WIN administration; this is shown by a reduction in the duration of the inhibitory component of the response (Figure 4.2A, B, C, middle). Transmission through the indirect pathway was also reduced in both

circuits after WIN injection, as seen by a reduction in the amplitude of this response (Figure 4.2A, B, C, bottom). Effects induced by WIN on cortico-nigral transmission through both BG circuits, were effectively blocked by previous administration of AM251. Moreover, AM251 did not modify the cortico-nigral information transfer by itself in either of the two circuits (Figure 4.3).

Figure 4.2: Effect of systemic administration of WIN 55,212-2 (125 μg/kg, i.v.) on cortico-nigral information transmission through the sensorimotor (SM) and medial prefrontal (mPF) basal ganglia circuits. **A.** Top: raster plot and peristimulus time histogram showing a representative example of a triphasic response evoked in a *substantia nigra pars reticulata* (SNr) neuron by stimulation of the motor cortex in basal condition. Bottom: after WIN 55,212-2 injection, the inhibitory and late excitatory components disappeared, without affecting the early excitation. Arrows indicate the stimulation artefact. Dashed lines indicate the threshold for excitatory responses. **C.** Top: raster plot and peristimulus time histogram showing a representative example of a triphasic response evoked in a SNr neuron by stimulation of the anterior cingulate cortex under basal conditions. Bottom: WIN 55,212-2 injection was able to reduce transmission through all three pathways. Arrows indicate the stimulation artefact. Dashed lines indicate the threshold for excitatory responses. **B.** Bar graphs showing the mean effect of WIN 55,212-2 (125 μg/kg, i.v.) on cortically-evoked responses in SNr neurons (amplitude of early [EE; SM: n = 5 | mPF: n = 8] and late [LE; SM: n = 5 | mPF: n = 7] excitations and duration of inhibition (INH; SM: n = 5| mPF: n = 11]) in SM and mPF circuits. Each bar represents the mean ± SEM of n rats. Each dot represents the value from one neuron before and after drug administration. *$p < 0.05$, two-tailed paired Student's *t* test.

Figure 4.3: Blockade of WIN 55,212-2-induced effect on cortico-nigral information transmission in sensorimotor (SM) and medial prefrontal (mPF) basal ganglia circuits by pre-treatment with the selective CB₁ antagonist AM251 (2 mg/kg, i.v.). **A.** Top: raster plot and peristimulus time histogram showing a representative example of a triphasic response evoked in a *substantia nigra pars reticulata* (SNr) neuron by stimulation of the motor cortex under basal conditions. AM251 administration did not modify the characteristics of the three components of the cortically-evoked response (middle) but blocked the effects induced by WIN 55,212-2 (bottom). Arrows indicate the stimulation artefact. Dashed lines indicate the threshold for excitatory responses. **C.** Top: raster plot and peristimulus time histogram showing a representative example of a triphasic response evoked in a SNr neuron by stimulation of the anterior cingulate cortex under basal conditions. Administration of AM251 did not modify the characteristics of the cortically-evoked triphasic response (middle) but blocked the effects mediated by WIN 55,212-2 (bottom). Arrows indicate the stimulation artefact. Dashed lines indicate the threshold for excitatory responses. **B.** Bar graphs showing the mean effect of AM251 (2 mg/kg, i.v.) and WIN 55,212-2 (125 μg/kg, i.v.) on cortically-evoked responses in SNr neurons (amplitude of early [EE; SM: n = 7 | mPF: n = 6] and late [LE; SM: n = 6| mPF: n = 6] excitations and duration of inhibition [INH; SM: n = 8| mPF: n = 7]) in SM and mPF circuits. Each bar represents the mean ± SEM of n rats. Each dot represents the value from one neuron before and after drug administration.

4.1.2.2. Effect of Δ⁹-tetrahydrocannabinol on spontaneous and cortically-evoked activity of *substantia nigra pars reticulata* neurons by CB₁ receptor activation

Δ⁹-THC (0.5 mg/kg, i.v.) administration at the dose used in this study was not able to change the spontaneous FR in either functional territory of the SNr (Annex 4.III). Similar to the effect of WIN, Δ⁹-THC affected the burst firing of SNr neurons inducing a decrease in the burst duration of lateral SNr neurons, and reducing the intraburst frequency in medial SNr neurons. Furthermore, administration of the CB₁ receptor antagonist AM251 (2 mg/kg, i.v.) did not change the spontaneous activity of SNr neurons (Annex 4.IV).

Cortically-evoked activity in SNr neurons was affected after administration of Δ⁹-THC. Transmission through the hyperdirect pathway was significantly reduced in both circuits after administration of the drug, as it reduced the amplitude of this response. The effect of Δ⁹-THC on this pathway was significantly smaller in the SM circuits than in the mPF circuits, completely abolishing hyperdirect pathway transmission through the mPF circuits (Figure 4.4A, B, C, top). Moreover, Δ⁹-THC administration was shown to significantly reduce transmission through the direct pathway in both circuits since it reduced the duration of the inhibitory response (Figure 4.4A, B, C, middle). A disruption in information transmission was also observed through the indirect pathway in both circuits, as seen by a reduction in the amplitude of the LE after Δ⁹-THC administration (Figure 4.4A, B, C, bottom). In line with the results obtained with WIN, the effects induced by Δ⁹-THC administration on cortico-nigral transmission through the SM and mPF BG circuits were blocked by previous administration of AM251. As we have previously described, in these experiments AM251 was not able to alter cortically-evoked responses in SNr neurons by itself (Figure 4.5).
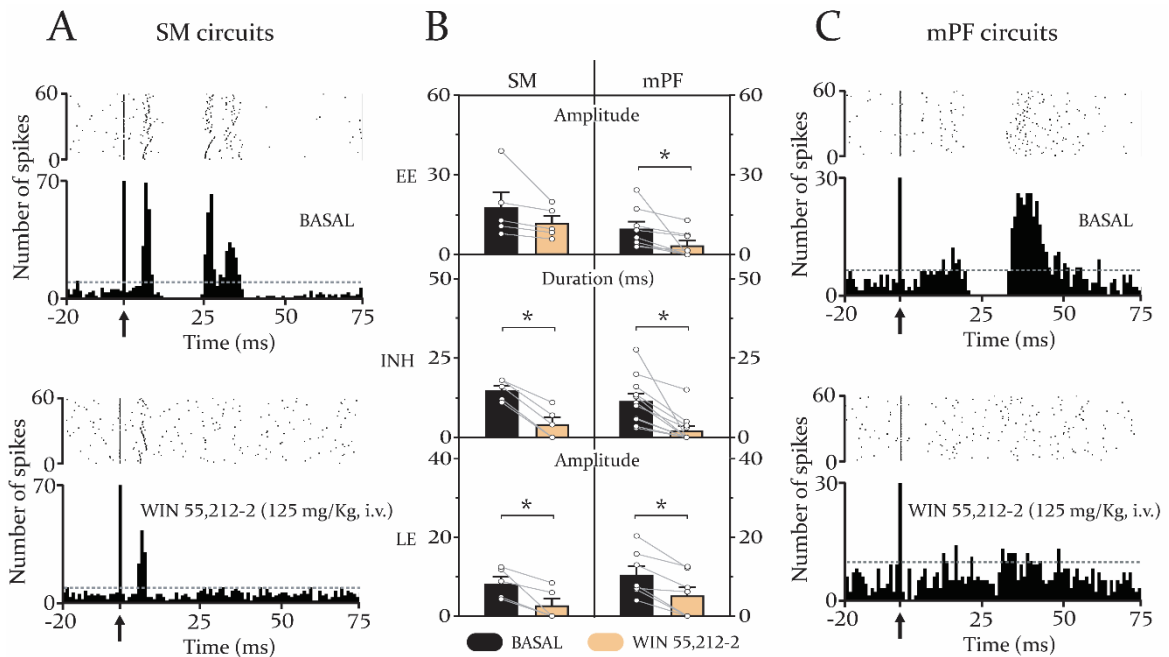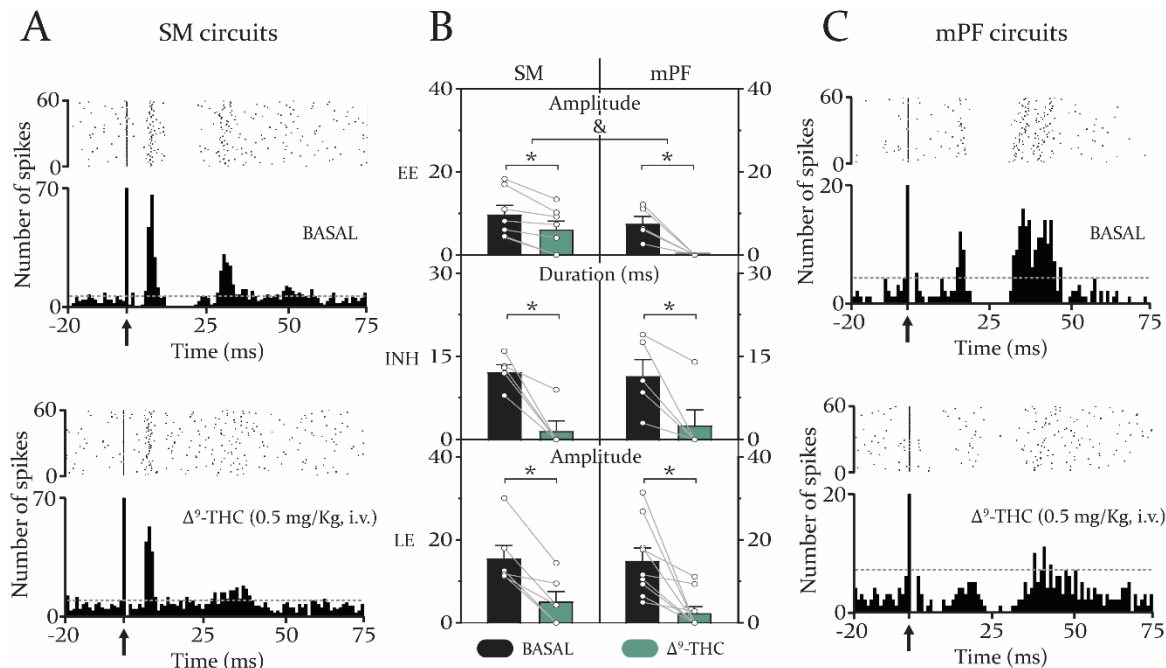
Figure 4.4: Effect of systemic administration of Δ⁹-THC (0.5 mg/kg, i.v.) on cortico-nigral information transmission in the sensorimotor (SM) and medial prefrontal (mPF) basal ganglia circuits. **A.** Top: raster plot and peristimulus time histogram showing a representative example of a triphasic response evoked in a *substantia nigra pars reticulata* (SNr) neuron by stimulation of the motor cortex under basal conditions. Bottom: after Δ⁹-THC injection, the inhibitory and late excitatory components disappeared, with the early excitation diminished. Arrows indicate the stimulation artefact. Dashed lines indicate the threshold for excitatory responses. **C.** Top: raster plot and peristimulus time histogram showing a representative example of a triphasic response evoked in a SNr neuron by stimulation of the anterior cingulate cortex under basal conditions. Bottom: in this circuit, Δ⁹-THC injection was able to reduce transmission through all three pathways. Arrows indicate the stimulation artefact. Dashed lines indicate the threshold for excitatory responses. **B.** Bar graphs showing the mean effect of Δ⁹-THC (0.5 mg/kg, i.v.) on cortically-evoked responses in SNr neurons (amplitude of early [EE; SM: n = 7 | mPF: n = 5] and late [LE; SM: n = 6 | mPF: n = 9] excitations and duration of inhibition [I; SM: n = 5 | mPF: n = 5]) in SM and mPF circuits. Each bar represents the mean ± SEM of n rats. Each dot represents the value from one neuron before and after drug administratio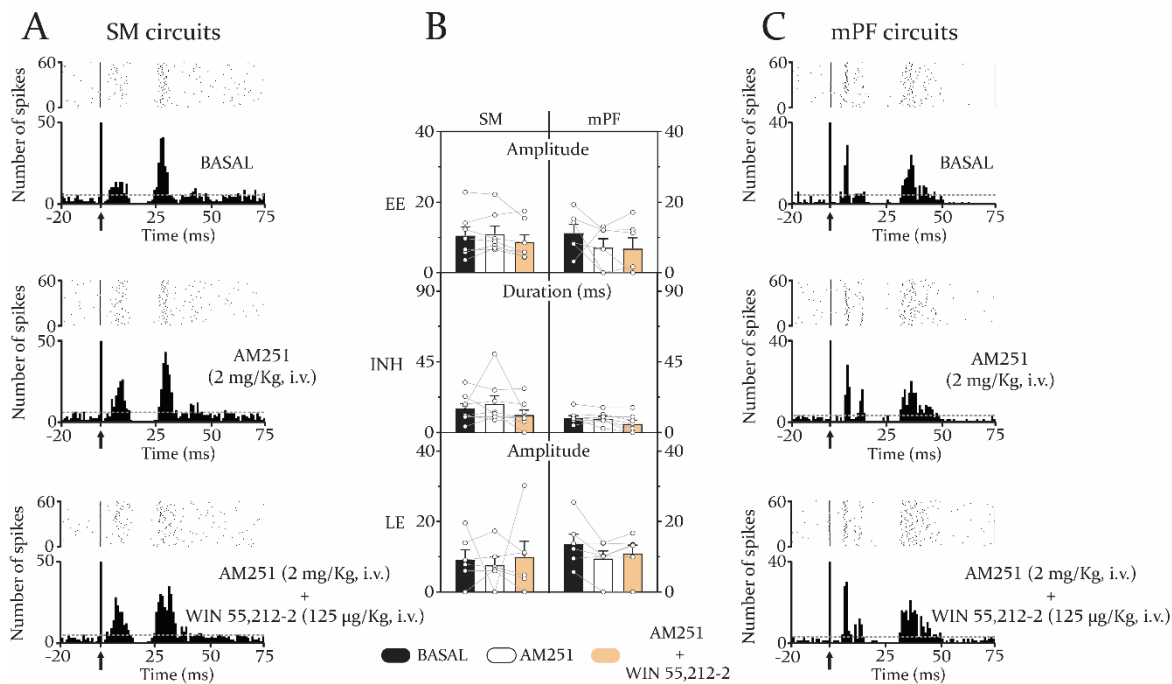n. *$p < 0.05$, two-tailed paired Student's *t* test. &$p < 0.05$, interaction (Circuit × Drug) repeated-measures two-way ANOVA.

Figure 4.5: Blockade of Δ^9-THC-induced effects on cortico-nigral information transmission in sensorimotor (SM) and medial prefrontal (mPF) basal ganglia circuits by pre-treatment with the selective CB$_1$ antagonist AM251 (2 mg/kg, i.v.). **A.** Top: raster plot and peristimulus time histogram showing a representative example of a triphasic response evoked in a *substantia nigra pars reticulata* (SNr) neuron by stimulation of the motor cortex under basal conditions. AM251 administration did not modify the characteristics of the three components of the cortically-evoked response (middle) but blocked the effects induced by Δ^9-THC (bottom). Arrows indicate the stimulation artefact. Dashed lines indicate the threshold for excitatory responses. **C.** Top: raster plot and peristimulus time histogram showing a representative example of a triphasic response evoked in a SNr neuron by stimulation of the anterior cingulate cortex under basal conditions. AM251 administration did not modify the characteristics of the cortically-evoked triphasic response (middle) but blocked the effects induced by Δ^9-THC (bottom). Arrows indicate the stimulation artefact. Dashed lines indicate the threshold for excitatory responses. **B.** Bar graphs showing the mean effect of AM251 (2 mg/kg, i.v.) and Δ^9-THC (0.5 mg/kg, i.v.) on cortically-evoked responses in SNr neurons (amplitude of early [EE; SM: n = 3 | mPF: n = 6] and late [LE; SM: n = 3 | mPF: n = 11] excitations and duration of inhibition [INH; SM: n = 5 | mPF: n = 11]) in SM and mPF circuits. Each bar represents the mean ± SEM of n rats. Each dot represents the value from one neuron before and after drug administration.

Annex 4.I: Effect of WIN 55,212-2 (125 µg/kg, i.v.) on the firing properties of neurons from the lateral and medial subdivisions of the *substantia nigra pars reticulata* (SNr).

Lateral SNr	Before WIN (n = 7)	After WIN
Firing rate (Hz)	24.4 ± 3.6	27.8 ± 4.0
Coefficient of variation (%)	38.7 ± 4.4	33.1 ± 3.9*
Burst firing neurons / recorded neurons	1 / 7	1 / 7
Neurons exhibiting burst firing pattern (%)	14.3	14.3
Number of bursts	25.0	1
Duration of burst (ms)	0.3	0.04
Nº spikes/burst	10.2	3
Recurrence of burst (nº burst/min)	8.3	0.3
Intraburst frequency (Hz)	36.0	82.9

Medial SNr	Before WIN (n = 17)	After WIN
Firing rate (Hz)	21.0 ± 2.1	24.2 ± 2.5
Coefficient of variation (%)	55.1 ± 7.3	58.4 ± 8.0
Burst firing neurons / recorded neurons	14 / 17	13 / 17
Neurons exhibiting burst firing pattern (%)	82.4	76.5
Number of bursts	33.2 ± 12.3	27.4 ± 13.4
Duration of burst (ms)	0.3 ± 0.1	2.2 ± 1.1
Nº spikes/burst	11.3 ± 2.0	41.6 ± 15.2
Recurrence of burst (nº burst/min)	13.3 ± 4.9	13.7 ± 6.7
Intraburst frequency (Hz)	48.6 ± 6.4	45.9 ± 9.3

Each value represents the mean ± SEM of (n) recorded rats. *$p<0.05$ *vs.* WIN (coefficient of variation: two-tailed paired Student's *t* test)

Annex 4.II: Effect of AM251 (2 mg/kg, i.v) and WIN 55,212-2 (125 μg/kg, i.v.) on the firing properties of neurons from the lateral and medial subdivisions of the *substantia nigra pars reticulata* (SNr).

Lateral SNr	Before AM (n = 9)	After AM	After AM+WIN
Firing rate (Hz)	21.8 ± 3.7	21.0 ± 3.5	20.7 ± 3.8
Coefficient of variation (%)	53.4 ± 7.9	50.6 ± 4.4	48.4 ± 4.4
Burst firing neurons/ recorded neurons	5 / 9	5 / 9	6 / 9
Neurons exhibiting burst firing pattern (%)	55.6	55.6	66.7
Number of bursts	4.3 ± 1.9	3.7 ± 1.3	4.0 ± 2.3
Duration of burst (ms)	0.7 ± 0.3	0.8 ± 0.4	1.0 ± 0.7
Nº spikes/burst	27.7 ± 13.2	17.4 ± 4.1	14.1 ± 4.8
Recurrence of burst (nº burst/min)	1.7 ± 0.8	1.8 ± 0.6	1.9 ± 1.2
Intraburst frequency (spikes/s)	30.4 ± 7.6	30.7 ± 9.5	53.3 ± 16.5

Medial SNr	Before AM (n = 11)	After AM	After AM+WIN
Firing rate (Hz)	23.6 ± 3.2	22.5 ± 285	23.5 ± 3.4
Coefficient of variation (%)	43.5 ± 5.7	45.4 ± 4.9	41.8 ± 3.0
Burst firing neurons/ recorded neurons	8 / 11	6 / 11	7 / 11
Neurons exhibiting burst firing pattern (%)	72.7	54.5	63.6
Number of bursts	10.9 ± 6.7	6.3 ± 2.6	4.6 ± 1.7
Duration of burst (ms)	0.3 ± 0.1	0.6 ± 0.2	0.6 ± 0.2
Nº spikes/burst	13.7 ± 5.6	14.2 ± 4.5	26.9 ± 10.1
Recurrence of burst (nº burst/min)	4.7 ± 3.0	3.2 ± 1.3	2.3 ± 0.8
Intraburst frequency (Hz)	36.2 ± 9.0	28.8 ± 8.8	40.4 ± 17.3

Each value represents the mean ± SEM of (n) recorded rats.

Annex 4.III: Effect of Δ⁹-THC (0.5 mg/kg) on the firing properties of neurons from the lateral and medial subdivisions of the *substantia nigra pars reticulata* (SNr).

Lateral SNr	**Before Δ⁹-THC** (n = 11)	**After Δ⁹-THC**
Firing rate (Hz)	25.3 ± 2.3	25.1 ± 3.1
Coefficient of variation (%)	53.2 ± 7.0	51.4 ± 8.7
Burst firing neurons / recorded neurons	8 / 11	3 / 11
Neurons exhibiting burst firing pattern (%)	80.0	30.0
Number of bursts	16.5 ± 9.4	13.2 ± 12.7
Duration of burst (ms)	0.5 ± 0.2	0.2 ± 0.2*
Nº spikes/burst	20.6 ± 6.8	8.0 ± 6.6
Recurrence of burst (nº burst/min)	6.5 ± 3.8	6.6 ± 6.3
Intraburst frequency (Hz)	51.2 ± 5.9	23.4 ± 14.3

Medial SNr	**Before Δ⁹-THC** (n = 15)	**After Δ⁹-THC**
Firing rate (Hz)	24.6 ± 2.2	23.7 ± 2.6
Coefficient of variation (%)	46.9 ± 4.9	45.1 ± 5.6
Burst firing neurons / recorded neurons	12 / 15	9 / 15
Neurons exhibiting burst firing pattern (%)	80.0	60.0
Number of bursts	15.7 ± 5.1	12.3 ± 5.4
Duration of burst (ms)	0.7 ± 0.1	1.5 ± 0.9
Nº spikes/burst	25.1 ± 4.4	20.8 ± 6.6
Recurrence of burst (nº burst/min)	6.3 ± 2.0	5.2 ± 2.2
Intraburst frequency (Hz)	42.0 ± 5.0	25.3 ± 6.6*

Each value represents the mean ± SEM of (n) recorded rats. *$p<0.05$ *vs.* Δ⁹-THC (Duration of bursts: Wilcoxon matched-pairs signed rank test; Intraburst frequency: two-tailed paired Student's *t* test).

Annex 4.IV: Effect of AM251 (2 mg/kg, i.v) and Δ⁹-THC (0.5 mg/kg) on the firing properties of neurons from the lateral and medial subdivisions of the *substantia nigra pars reticulata* (SNr).

Lateral SNr	Before AM (n = 5)	After AM	After AM + Δ⁹-THC
Firing rate (Hz)	22.6 ± 4.0	24.7 ± 2.9	23.9 ± 3
Coefficient of variation (%)	43.5 ± 4.7	41.8 ± 5.8	44.2 ± 7.9
Burst firing neurons/ recorded neurons	0 / 5	0 / 5	1 / 5
Neurons exhibiting burst firing pattern (%)	0.00	0.00	20.0
Number of bursts	n.d	n.d	2.0
Duration of burst (ms)	n.d	n.d	0.5
Nº spikes/burst	n.d	n.d	20.5
Recurrence of burst (nº burst/min)	n.d	n.d	1.0
Intraburst frequency (Hz)	n.d	n.d	42.3

Medial SNr	Before AM (n = 14)	After AM	After AM + Δ⁹-THC
Firing rate (Hz)	24.9 ± 3.7	24.3 ± 3.8	22.43 ± 2.4
Coefficient of variation (%)	46.4 ± 4.4	47.4 ± 7.0	41.0 ± 4.5
Burst firing neurons/ recorded neurons	8 / 14	8 / 14	7 / 14
Neurons exhibiting burst firing pattern (%)	57.1	57.1	50.0
Number of bursts	15.2 ± 5.6	11.5 ± 5.5	7.7 ± 3.3
Duration of burst (ms)	0.7 ± 0.4	0.9 ± 0.4	1.0 ± 0.4
Nº spikes/burst	14.8 ± 3.7	23.9 ± 9.6	12.9 ± 4.2
Recurrence of burst (nº burst/min)	8.2 ± 2.8	5.8 ± 2.7	3.9 ± 1.6
Intraburst frequency (Hz)	38.9 ± 9.0	37.7 ± 9.5	24.9 ± 7.3

Each value represents the mean ± SEM of (n) recorded rats.

4.2. STUDY II: Impact of dopaminergic denervation on cortico-nigral transmission through the sensorimotor and medial prefrontal basal ganglia circuits and CB$_1$ receptor function

In this study, animals were tested in the cylinder test for motor asymmetry 4 – 5 weeks after 6-OHDA stereotaxic injection into the right MFB. All 6-OHDA-lesioned rats used in this study showed biased use of the ipsilateral forelimb above 70%, thus being considered to have severe damage of the DA system (Figure 4.6A). After electrophysiological recordings were performed, TH immunostaining was used to confirm DA denervation. All animals in the 6-OHDA-lesioned group showed a reduction above 90% in TH$^+$ density in the striatum of the lesioned hemisphere (Figure 4.6B).

As in the Study I, all recorded cells exhibited the typical electrophysiological characteristics of GABAergic SNr neurons, including a narrow spike waveform and a relatively high FR with a regular pattern of discharge. To ensure the belonging of the recorded cells to their corresponding BG circuits, only those with a FR above 7 Hz and responding to cortical stimulation within the latency ranges stablished (Annex 4.V and Annex 4.VI), were included in the analyses. Neurons meeting these criteria were recorded from 114 animals, among which 49 were in the sham group (SM: n = 17 | mPF: n = 28 | SM & mPF: n = 4), and 65 in the 6-OHDA-lesioned group (SM: n = 24 | mPF: n = 29 | SM & mPF: n = 12).
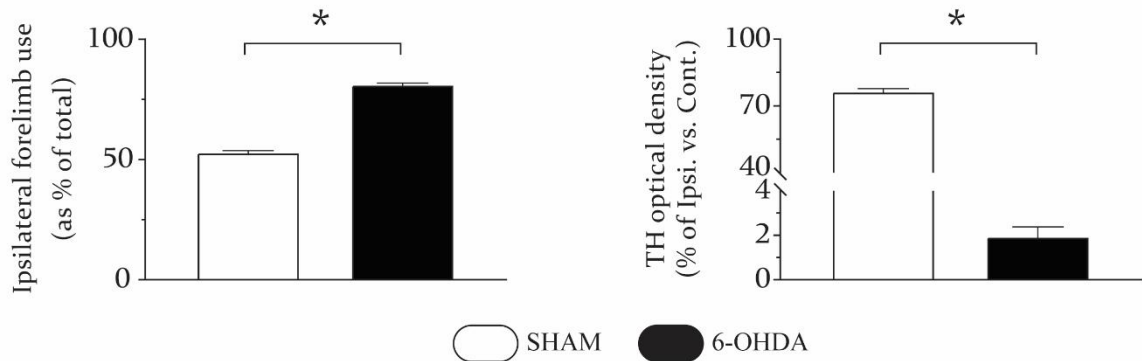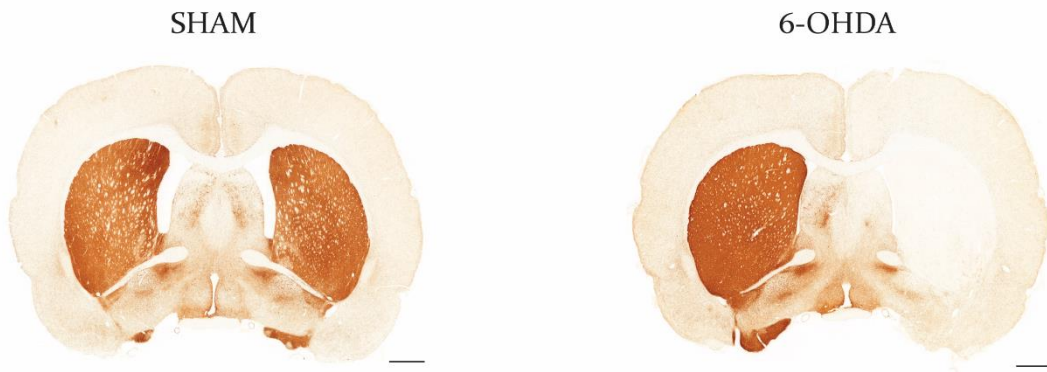
Figure 4.6: Motor asymmetry and dopaminergic denervation in sham and 6-OHDA-lesioned rats. **A.** Left: Mean percentage of ipsilateral forelimb use shows that 6-OHDA-lesioned rats use more the forelimb ipsilateral to the lesioned hemisphere, indicating an important degree of motor asymmetry, and suggesting severe dopaminergic denervation. Right: mean percentage of variation in TH optical density (OD), referring to the change in the hemisphere ipsilateral to the lesion vs. the contralateral hemisphere. 6-OHDA-lesioned animals show a severe dopaminergic denervation. **B.** Representative brain slices showing TH immunostaining for both sham and 6-OHDA-lesioned rats. Note the severe striatal dopaminergic denervation in 6-OHDA-lesioned rats, after infusion of the toxin in the MFB. Slice scale bars are set to 1 mm. *$p < 0.05$, two-tailed unpaired Student's *t*-test.

4.2.1. Spontaneous and cortically-evoked activity of *substantia nigra pars reticulata* neurons after dopaminergic denervation

Lateral and medial SNr neurons were differently affected by DA denervation. The FR of neurons from the medial SNr was reduced in 6-OHDA-lesioned animals, while neurons from the lateral SNr were not affected, in comparison to sham rats. Moreover, lateral and medial SNr neurons presented a higher CV in lesioned animals. In addition, firing pattern analysis revealed that the number of neurons with bursts was increased in both SNr functional territories after DA denervation. In line with this, further burst firing analysis showed alterations in neurons from the lateral and medial SNr in 6-OHDA-lesioned animals. In the lateral SNr of 6-OHDA-lesioned animals, neurons displayed a greater number of bursts than neurons from sham rats. In the case of the medial SNr of these animals, neurons showed the same alterations that those in the lateral SNr, adding a decreased duration of burst, and number of spikes per burst (Table 4.2).

As in Study I, cortical stimulation of the MC or ACC evoked characteristic triphasic responses in SNr neurons that consisted of an EE, followed by an INH and a LE, from the activation of the different pathways that constitute these circuits. Different patterns of response can be observed in both SNr functional territories, yielding triphasic, biphasic or monophasic cortically-evoked responses. These patterns of response observed in the lateral SNr were altered after DA denervation: the proportion of neurons displaying triphasic and biphasic (i.e. INH + LE) responses was reduced, in favour of more monophasic (i.e. EE) responses, in the 6-OHDA-lesioned group. DA loss also changed patterns of response in neurons from the medial SNr, showing a greater amount of monophasic (i.e. INH) responses (Figure 4.7A). Overall, lateral SNr neurons displayed fewer INHs and LEs, while neurons from the medial SNr displayed only fewer LEs after DA loss (Figure 4.7B).

Table 4.2: Firing properties of neurons from the lateral and the medial *substantia nigra pars reticulata* (SNr) in sham and 6-OHDA-lesioned animals

Lateral SNr	Sham (n = 21)	6-OHDA (n = 36)
Firing rate (Hz)	21.2 ± 1.8	19.0 ± 1.2
Coefficient of variation (%)	43.6 ± 2.4	70.3 ± 4.6*
Burst firing neurons / recorded neurons	51 / 98	91 / 115
Neurons exhibiting burst firing pattern (%)	52.0	79.1*
Number of bursts	12.8 ± 2.5	45.9 ± 7.2*
Duration of burst (ms)	0.5 ± 0.1	0.6 ± 0.1
Nº spikes/burst	14.6 ± 1.8	13.3 ± 1.8
Recurrence of burst (nº burst/min)	5.1 ± 1.0	18.4 ± 2.9*
Intraburst frequency (Hz)	36.1 ± 2.6	35.5 ±1.9

Medial SNr	Sham (n = 32)	6-OHDA (n = 41)
Firing rate (Hz)	24.8 ± 1.3	19.4 ± 1.0*
Coefficient of variation (%)	49.0 ± 2.4	102.5 ± 5.9*
Burst firing neurons / recorded neurons	126 / 187	144 / 160
Neurons exhibiting burst firing pattern (%)	67.4	89.6*
Number of bursts	24.0 ± 3.9	87.3 ± 7.6*
Duration of burst (ms)	0.6 ± 0.1	0.3 ± 0.1*
Nº spikes/burst	18.4 ± 2.2	11.1 ± 0.5*
Recurrence of burst (nº burst/min)	9.6 ± 1.6	34.9 ± 3.0*
Intraburst frequency (Hz)	46.2 ± 2.7	49.5 ± 2.9

Each value represents the mean ± S.E.M. of (n) recorded rats. *$p<0.05$ *vs.* 6-OHDA (Firing rate, coefficient of variation and response parameters: two-tailed unpaired Student's *t*-test; neurons exhibiting burst firing pattern: Fisher's exact test; burst parameters: Mann-Whitney rank sum test).

A
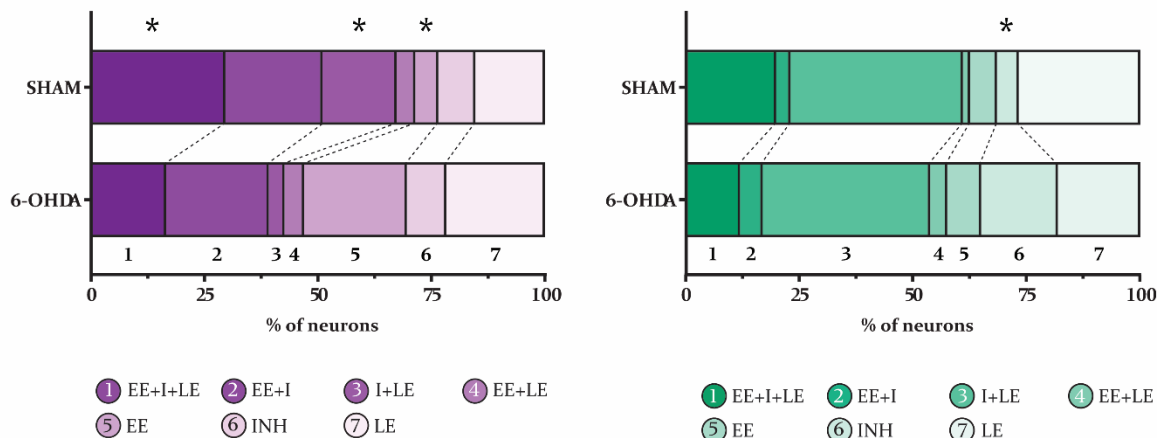
B
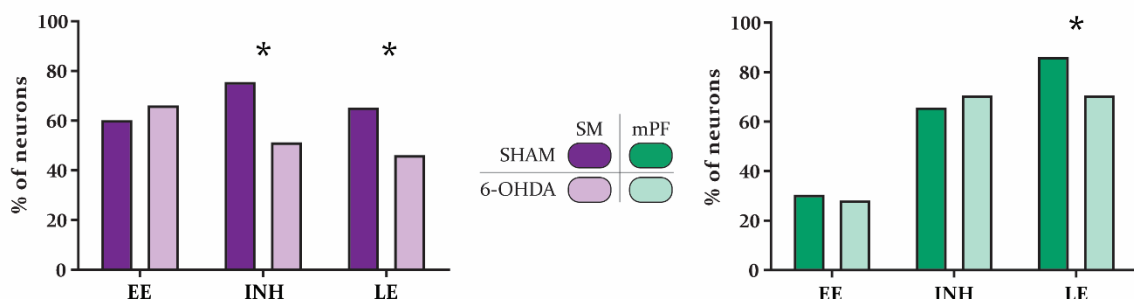
Figure 4.7: Patterns of response evoked in *substantia nigra pars reticulata* (SNr) neurons by cortical stimulation of the motor cortex and anterior cingulate cortex, in sham and 6-OHDA-lesioned animals. **A.** Percentage of occurrence of the different patterns of responses evoked in SNr cells by cortical stimulation. From left (darker colour) to right (lighter colour): EE+I+LE; EE+I; I+LE; EE+LE; EE; I; LE. Note that triphasic (EE+I+LE) and biphasic responses (I+LE) are less common in lateral SNr neurons from 6-OHDA-lesioned animals, while monophasic early excitations (EE) are more common. Regarding medial SNr neurons, monophasic inhibition (INH) responses are more common in the DA-denervated animal. **B.** Percentage of SNr neurons displaying early or late excitation, or inhibition after cortical stimulation. Note that the occurrence of inhibitions is reduced in lateral SNr neurons in DA-denervated animals, and the late excitation occurrence is diminished in neurons from both SNr functional territories. *$p < 0.05$, Fisher's exact test.

DA denervation changed the electrophysiological characteristics of the cortically-evoked responses in neurons from both functional territories of the SNr. In the SM circuits, the EE had a greater duration in 6-OHDA-lesioned animals than in sham rats. On the other hand, DA loss also affected the EE in the mPF circuits increasing its latency. In addition, the latency of the INH was higher in both circuits after DA denervation (Table 4.3).

Table 4.3: Electrophysiological characteristics of the cortically-evoked responses in neurons from the lateral and medial functional territories of the *substantia nigra pars reticulata* (SNr) in sham and 6-OHDA-lesioned rats

SM circuits	Sham (n = 21)	6-OHDA (n = 36)
Early excitation	*n = 19*	*n = 27*
Duration (ms)	5.3 ± 0.4	8.3 ± 1.0*
Latency (ms)	5.5 ± 0.4	5.7 ± 0.3
Amplitude	14.4 ± 1.3	13.2 ± 0.8
Inhibition	*n = 20*	*n = 29*
Duration (ms)	19.8 ± 2.1	27.6 ± 4.6
Latency (ms)	12.1 ± 0.4	14.0 ± 0.4*
Late excitation	*n = 21*	*n = 29*
Duration (ms)	6.0 ± 0.5	7.5 ± 0.7
Latency (ms)	27.1 ± 0.6	27.7 ± 0.7
Amplitude	17.9 ± 2.5	13.7 ± 1.5

mPF circuits	Sham (n = 32)	6-OHDA (n = 41)
Early excitation	*n = 30*	*n = 28*
Duration (ms)	7.2 ± 0.7	6.4 ± 1.0
Latency (ms)	8.5 ± 0.6	13.7 ± 0.5*
Amplitude	8.2 ± 0.5	7.9 ± 0.8
Inhibition	*n = 32*	*n = 38*
Duration (ms)	11.5 ± 0.8	13.0 ± 1.7
Latency (ms)	18.8 ± 0.4	20.8 ± 0.4*
Late excitation	*n = 32*	*n = 38*
Duration (ms)	11.2 ± 0.8	11.3 ± 0.9
Latency (ms)	33.4 ± 0.4	33.5 ± 0.5
Amplitude	15.4 ± 1.0	13.8 ± 0.8

Each value represents the mean ± S.E.M. of (n) recorded rats. *$p<0.05$ *vs.* 6-OHDA (two-tailed unpaired Student's *t*-test).

4.2.2. Effect of cannabinoids on spontaneous and cortically-evoked activity in *substantia nigra pars reticulata* neurons: Dopaminergic denervation influence

Next, we investigated the influence of the DA system on the cannabinoid modulation of BG circuits. For this, we studied the spontaneous activity of SNr neurons receiving input from the MC or ACC, and the cortico-nigral transmission through the SM and mPF BG circuits. We used the synthetic CB$_1$/CB$_2$-receptor full agonist WIN, and the synthetic CB$_1$-selective antagonist AM251 to evaluate the endocannabinoid system function under DA denervation. As in the Study I, we used drug doses known not to alter the firing activity of SNr neurons substantially, so the analysis of the cortically-evoked responses was not affected.

4.2.2.1. Effect of WIN 55,212-2 on spontaneous and cortically-evoked responses of lateral *substantia nigra pars reticulata* neurons

The effect of the synthetic cannabinoid agonist WIN (125 µg/kg, i.v.) on the spontaneous and cortically-evoked activity of lateral SNr neurons from sham and 6-OHDA-lesioned rats was investigated. At the administered dose, WIN did not modify the FR, the number of neurons with burst activity, or any of the analysed burst-related parameters in the lateral SNr from sham and 6-OHDA-lesioned animals, although some changes were observed regarding the regularity of these neurons in 6-OHDA-lesioned animals (Annex 4.VII).

As shown in Study I, the EE was not altered after systemic administration of WIN in sham rats (Figure 4.8A, B, top), but diminished cortico-nigral transmission through the indirect pathway, as shown by a reduction in the amplitude of the LE (Figure 4.8A, B, bottom). In contrast to what was found in Study I, no statistically significant decrease was observed in transmission through the direct pathway (Figure 4.8A, B, middle). In the SM circuits, 6-OHDA lesions modified the effect of WIN on cortico-nigral transmission, being the EE decreased after drug administration (Figure 4.8B, C, top). However, cortico-nigral information transfer through the trans-striatal pathways (i.e. direct and indirect pathways) was not affected after WIN administration in 6-OHDA-lesioned animals (Figure 4.8B, C,

middle/bottom). The effects observed in sham rats were blocked by the previous administration of the CB$_1$-selective antagonist AM251 (2 mg/kg, i.v.) (Figure 4.9). Moreover, AM251 alone did not modify cortico-nigral information transfer (Figure 4.9), or the spontaneous activity of lateral SNr neurons (Annex 4.VIII).

Figure 4.8: Effect of systemic administration of WIN 55,212-2 (125 μg/kg, i.v.) on cortico-nigral information transmission through the sensorimotor basal ganglia circuits in sham and 6-OHDA-lesioned animals. **A.** Top: raster plot and peristimulus time histogram showing a representative example of a triphasic response evoked in a neuron from the lateral *substantia nigra pars reticulata* (SNr) in a sham rat by stimulation of the motor cortex (MC) in basal condition. Bottom: after WIN 55,212-2 injection, the inhibitory and late excitatory components disappeared, with the early excitation still present. Arrows indicate cortical stimulus application. Dashed lines indicate the threshold for excitatory responses. **C.** Top: raster plot and peristimulus time histogram showing a representative example of a triphasic response evoked in a neuron from the lateral SNr in a 6-OHDA-lesioned animal by stimulation of the MC under basal conditions. Bottom: After WIN 55,212-2 injection only a decrease in transmission through the early excitation was observed in 6-OHDA-lesioned animals. Arrows indicate cortical stimulus application. Dashed lines indicate the threshold for excitatory responses. **B.** Bar graphs showing the mean effect of WIN 55,212-2 (125 μg/kg, i.v.), on cortically-evoked responses in lateral SNr neurons (amplitude of early (EE: sham: n=5 | 6-OHDA: n=6) and late (LE: sham: n=5 | 6-OHDA: n=6) excitations and duration of inhibition (INH: sham: n=6 | 6-OHDA: n=6)) in the SM circuits. Each bar represents the mean ± S.E.M. of n rats. Each dot represents the value from one neuron before and after drug administration. *$p < 0.05$ before vs. after WIN, repeated measures two-way ANOVA (Drug × Lesion).

A
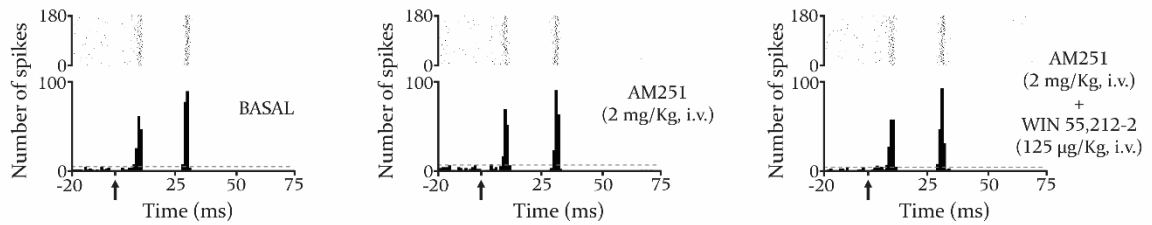
B

Figure 4.9: Blockade of WIN 55,212-2-induced effects on cortico-nigral information transmission in sensorimotor basal ganglia circuits in sham animals by the previous administration of the CB_1 selective antagonist AM251 (2 mg/kg, i.v.). **A.** Left: raster plot and peristimulus time histogram showing a representative example of a triphasic response evoked in a lateral *substantia nigra pars reticulata* (SNr) neuron by stimulation of the motor cortex in a sham rat under basal conditions. AM251 administration did not modify the characteristics of the three components of the cortically-evoked response (middle) but blocked the effects induced by WIN 55,212-2 (right). Arrows indicate cortical stimulus application. Dashed lines indicate threshold for excitatory responses. **B.** Bar graphs showing the mean effect of AM251 (2 mg/kg, i.v.) and WIN 55,212-2 (125 μg/kg, i.v.) on cortically-evoked responses in lateral SNr neurons (amplitude of early (EE: n = 4) and late (LE: n = 4) excitations and duration of inhibition (INH: n = 4)) in SM circuits. Each bar represents the mean ± S.E.M. of n rats. Each dot represents the value from one neuron before and after drug administration.

4.2.2.2. Effect of WIN 55,212-2 on spontaneous and cortically-evoked responses of medial *substantia nigra pars reticulata* neurons

We also explored the effect of WIN (125 µg/kg, i.v.) on the spontaneous and cortically-evoked activity of medial SNr neurons from sham and 6-OHDA-lesioned animals. At the administered dose, WIN did not modify the neuronal FR, regularity or the number of neurons displaying burst activity in medial SNr neurons. On the other hand, WIN induced a decrease in the intraburst frequency, as well as in the number of bursts and burst recurrence. This seemed to depend on DA transmission as it was only observed in sham animals (Annex 4.IX).

As in Study I, WIN administration impaired all cortically-evoked responses, reducing the amplitude of the EE and LE and the duration of the INH (Figure 4.10A, B). As in SM circuits, DA denervation induced changes in the way WIN modulates transmission through the mPF circuits. The administration of WIN reduced the amplitude of the EE but had no effect on cortical information transfer through the direct and indirect pathways (Figure 4.10B, C). These effects were blocked by previous administration of the CB$_1$-selective antagonist AM251 (2 mg/kg, i.v.) in both sham and 6-OHDA-lesioned animals (Figure 4.11). Moreover, AM251 alone did not have any effect on cortico-nigral information transfer (Figure 4.11), or the spontaneous activity of medial SNr neurons (Annex 4.X).
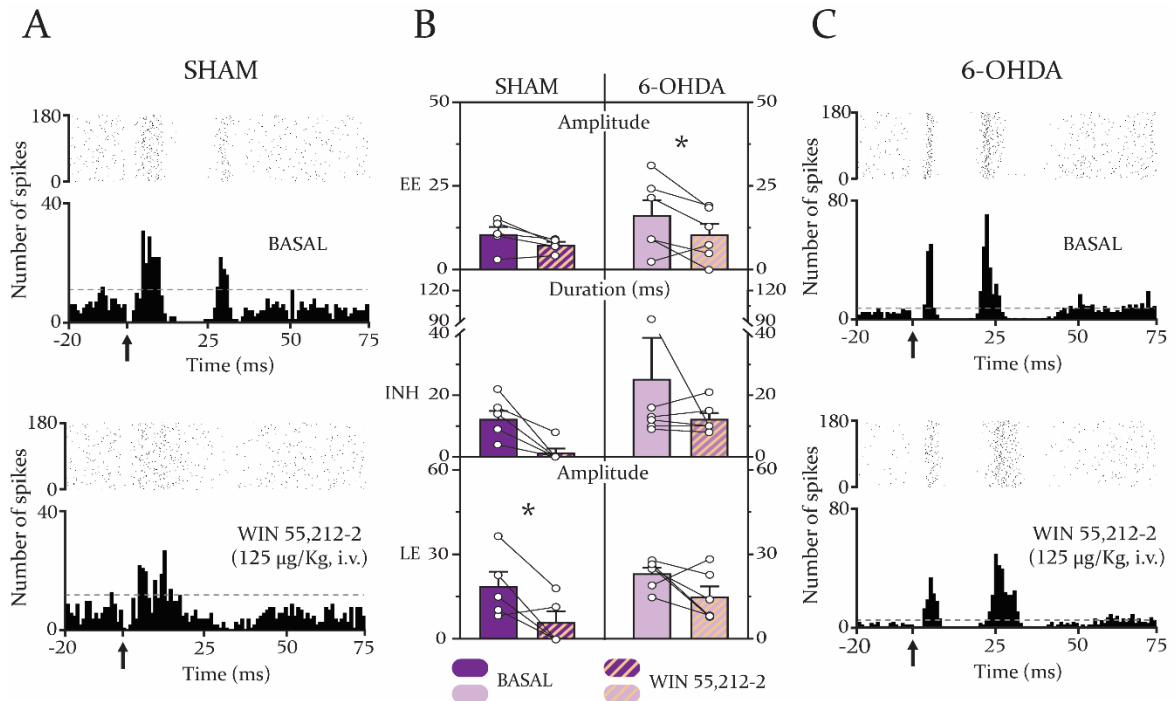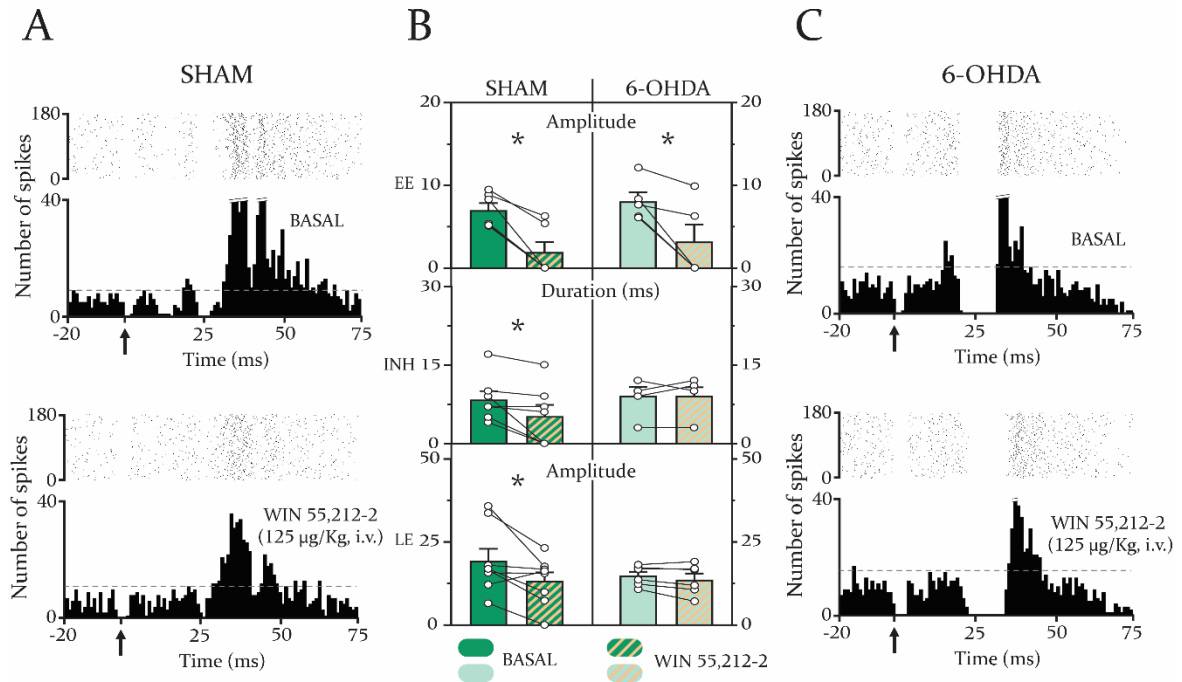
Figure 4.10: Effect of systemic administration of WIN 55,212-2 (125 µg/kg, i.v.) on cortico-nigral information transmission in medial prefrontal basal ganglia circuits in sham and 6-OHDA-lesioned animals. **A.** Top: raster plot and peristimulus time histogram showing a representative example of a triphasic response evoked in a medial *substantia nigra pars reticulata* (SNr) neuron from a sham rat after stimulation of the anterior cingulate cortex (ACC) under basal conditions. Bottom: WIN 55,212-2 injection was able to reduce transmission through the three pathways. Arrows indicate cortical stimulus application. Dashed lines indicate the threshold for excitatory responses. **C.** Top: raster plot and peristimulus time histogram showing a representative example of a triphasic response evoked in a medial SNr neuron from a 6-OHDA-lesioned animal after stimulation of the ACC under basal conditions. Bottom: after WIN 55,212-2 injection, only reduced transmission through the early excitation in 6-OHDA-lesioned animals was observed. Arrows indicate cortical stimulus application. Dashed lines indicate the threshold for excitatory responses. **B.** Bar graphs showing the mean effect of WIN 55,212-2 (125 µg/kg, i.v.) on cortically-evoked responses in medial SNr neurons (amplitude of early (EE: sham: n = 6 | 6-OHDA: n = 5) and late (LE: sham: n = 8 | 6-OHDA: n = 6) excitations and the duration of inhibition (INH: sham: n = 7 | 6-OHDA: n = 5)) in mPF circuits. Each bar represents the mean ± the S.E.M. of n rats. Each dot represents the value from one neuron before and after drug administration. *$p < 0.05$ before vs. after WIN, repeated-measures two-way ANOVA (Drug x Lesion).
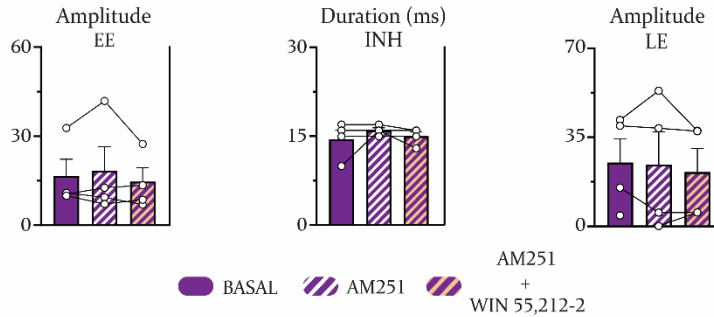
Figure 4.11: Blockade of WIN 55,212-2-induced effects on cortico-nigral information transmission in medial prefrontal basal ganglia circuits in sham and 6-OHDA-lesioned animals by the previous administration of the CB$_1$ selective antagonist AM251 (2 mg/kg, i.v.). **A.** Top: raster plot and peristimulus time histogram showing a representative example of a triphasic response evoked in a medial *substantia nigra pars reticulata* (SNr) neuron by stimulation of the anterior cingulate cortex (ACC) in a sham rat under basal conditions. AM251 administration did not modify the characteristics of the three components of the cortically-evoked response (middle) but blocked the effects induced by WIN 55,212-2 (bottom). Arrows indicate cortical stimulus application. Dashed lines indicate threshold for excitatory responses. **C.** Top: raster plot and peristimulus time histogram showing a representative example of a triphasic response evoked in a medial SNr neuron by stimulation of the ACC in a 6-OHDA-lesioned rat under basal conditions. AM251 administration did not modify the characteristics of the three components of the cortically-evoked response (middle) but blocked the effects induced by WIN 55,212-2 (bottom). Arrows indicate cortical stimulus application. Dashed lines indicate threshold for excitatory responses. **B.** Bar graphs showing the mean effect of AM251 (2 mg/kg, i.v.) and WIN 55,212-2 (125 µg/kg, i.v.) on cortically-evoked responses in medial SNr neurons (amplitude of early (EE: sham: n = 5 | 6-OHDA: n = 5) and late (LE: sham: n = 5 | 6-OHDA: n = 5) excitations and duration of inhibition (INH: sham: n = 5 | 6-OHDA: n = 6) in mPF circuits. Each bar represents the mean ± S.E.M. of n rats. Each dot represents the value from one neuron before and after drug administration.

4.2.2.3. CB$_1$ receptor localization in the sensorimotor and medial prefrontal functional territories of the basal ganglia nuclei in sham and 6-OHDA-lesioned rats

Finally, CB$_1$ immunostaining was measured in all BG structures relevant for transmission through the SM and mPF BG circuits. The study of the mean OD obtained from all the slices in which these structures were present, and the comparison between the divisions related to the SM and mPF circuits for every nucleus revealed some differences in CB$_1$ receptor presence. In the striatum of sham animals, CB$_1$-positive labelling in the dorsolateral division related to the SM circuits was higher than in the dorsomedial division related to the mPF circuits. This difference was also statistically significant in 6-OHDA-lesioned animals. On the other hand, no statistically significant changes were found in the CB$_1$ receptor immunostaining between sham (n = 5) and 6-OHDA-lesioned (n = 5) rats, in any of the analysed divisions of the BG nuclei (Figure 4.12B).
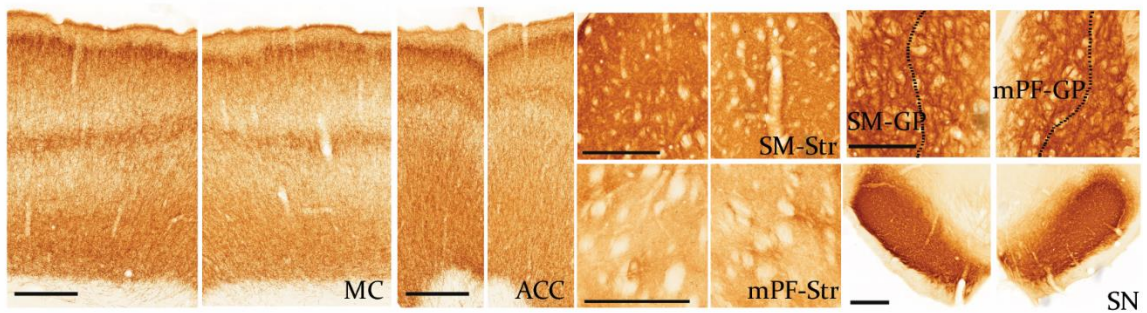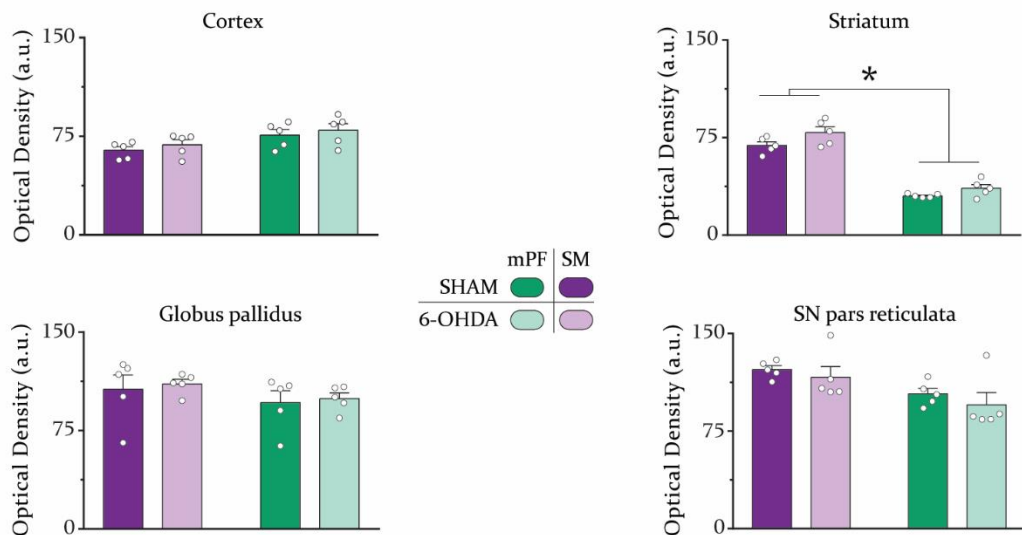
Figure 4.12: CB₁ receptor immunoreactivity in the sensorimotor (SM) and medial prefrontal (mPF) functional territories of the basal ganglia in cortex, striatum (Str), *globus pallidus* (GP) and *substantia nigra* (SN) from sham and 6-OHDA-lesioned rats. **A.** Brain microphotographs of coronal sections showing the CB₁ receptor immunohistochemistry. The first four panels show (from left to right) the distribution of the CB₁ receptor in the motor cortex (MC) and anterior cingulate cortex (ACC). The next four panels show the sensorimotor territory (Top: dorsolateral striatum; SM-Str) and the medial prefrontal territory (Bottom: dorsomedial striatum; mPF-Str). The last four panels show the GP (Top) divided in its sensorimotor (SM-GP) and medial prefrontal territory (mPF-GP), and the SN (Bottom). Studied areas are shown in pairs, being the pictures on the left from the lesioned hemisphere. **B.** Bar graphs showing the mean CB₁ receptor optical density (OD) in the SM and mPF territories of the studied brain areas in sham and 6-OHDA-lesioned animals. Note that there is significantly less CB₁ receptor immunoreactivity in the mPF territories of the Str in both sham and 6-OHDA-lesioned animals compared to SM territories. Scale bars are set to 500 μm. Each bar represents the mean ± the S.E.M. Each dot represents the averaged value from one rat. *$p < 0.05$ SM vs. mPF, repeated-measures two-way ANOVA (Territory × Lesion).

Annex 4.V: Firing properties and electrophysiological characteristics of triphasic responses in lateral *substantia nigra pars reticulata* (SNr) neurons from the sensorimotor (SM) circuits of the basal ganglia in sham and 6-OHDA-lesioned rats

SM circuits	Sham (n= 17)	6-OHDA (n=16)
Firing rate (Hz)	19.0 ± 1.9	17.2 ± 1.4
Coefficient of variation (%)	39.6 ± 2.3	56.6 ± 6.2*
Burst firing neurons / recorded neurons	11 / 29	9 / 19
Neurons exhibiting burst firing pattern (%)	37.9	47.4
Number of bursts	9.1 ± 3.8	20.1 ± 7.4
Duration of burst (ms)	0.6 ± 0.1	0.6 ± 0.2
Nº spikes/burst	15.0 ± 3.7	13.7 ± 2.3
Recurrence of burst (nº burst/min)	3.7 ± 1.5	8.0 ± 3.0
Intraburst frequency (Hz)	27.3 ± 2.7	28.0 ± 2.8
Early excitation		
Duration (ms)	4.5 ± 0.3	5.4 ± 0.4
Latency (ms)	5.6 ± 0.5	5.1 ± 0.4
	Min: 2 - Max: 12	*Min: 2 - Max: 9*
Amplitude	12.1 ± 1.7	14.1 ± 1.9
Inhibition		
Duration (ms)	13.6 ± 0.8	11.8 ± 0.8
Latency (ms)	12.9 ± 0.7	13.1 ± 0.6
	Min: 7 - Max: 21	*Min: 7 - Max: 18*
Late excitation		
Duration (ms)	5.1 ± 0.5	6.2 ± 0.6
Latency (ms)	28.0 ± 0.6	27.1 ± 1.1
	Min: 15 - Max: 37	*Min: 19 - Max: 37*
Amplitude	20.0 ± 3.2	18.6 ± 2.5

Each value represents the mean ± S.E.M. of (n) recorded rats. *$p<0.05$ *vs.* 6-OHDA (two-tailed unpaired Student's t-test)

Annex 4.VI: Firing properties and electrophysiological characteristics of triphasic responses in medial *substantia nigra pars reticulata* (SNr) neurons from the medial prefrontal (mPF) circuits of the basal ganglia in sham and 6-OHDA-lesioned rats

mPF circuits	Sham (n= 28)	6-OHDA (n=16)
Firing rate (Hz)	24.4 ± 1.8	21.7 ± 3.1
Coefficient of variation (%)	44.6 ± 2.4	95.1 ± 12.0*
Burst firing neurons / recorded neurons	27 / 37	16 / 19
Neurons exhibiting burst firing pattern (%)	73.0	84.2
Number of bursts	18.6 ± 5.6	76.4 ± 16.9*
Duration of burst (ms)	0.5 ± 0.1	0.3 ± 0.1
Nº spikes/burst	15.2 ± 2.2	10.6 ± 0.9
Recurrence of burst (nº burst/min)	7.5 ± 2.2	30.6 ± 6.7*
Intraburst frequency (Hz)	42.8 ± 3.6	52.0 ± 8.3
Early excitation		
Duration (ms)	5.5 ± 0.5	4.9 ± 0.6
Latency (ms)	8.6 ± 0.7	13.6 ± 0.7*
	Min: 2 - Max: 18	*Min: 8 - Max: 18*
Amplitude	7.3 ± 0.5	6.4 ± 0.7
Inhibition		
Duration (ms)	11.0 ± 1.0	9.8 ± 0.8
Latency (ms)	18.3 ± 0.5	20.8 ± 0.6*
	Min: 13 - Max: 24	*Min: 16 - Max: 26*
Late excitation		
Duration (ms)	13.3 ± 1.4	11.2 ± 1.8
Latency (ms)	32.9 ± 0.8	34.0 ± 0.9
	Min: 26 - Max: 47	*Min: 27 – Max: 44*
Amplitude	18.5 ± 1.6	16.5 ± 1.4

Each value represents the mean ± S.E.M. of (n) recorded rats. *$p<0.05$ *vs.* 6-OHDA (Coefficient of variation and response parameters: two-tailed unpaired Student's t-test; burst parameters: Mann-Whitney rank sum test).

Annex 4.VII: Effect of WIN 55,212-2 (125 µg/kg, i.v.) on the firing properties of lateral *substantia nigra pars reticulata* neurons from sham and 6-OHDA-lesioned rats

Sham	Before WIN (n = 6)	After WIN
Firing rate (Hz)	21.6 ± 4.1	23.3 ± 3.2
Coefficient of variation (%)	40.7 ± 6.2	33.2 ± 3.43
Burst firing neurons / recorded neurons	3 / 6	1 / 6
Neurons exhibiting burst firing pattern (%)	50.0	16.7
Number of bursts	4.7 ± 3.7	0.7
Duration of burst (ms)	1.3 ± 0.2	0.5
Nº spikes/burst	28.9 ± 3.5	15.8
Recurrence of burst (nº burst/min)	1.9 ± 1.5	0.3
Intraburst frequency (Hz)	23.7 ± 2.5	12.4

6-OHDA	Before WIN (n = 7)	After WIN
Firing rate (Hz)	21.0 ± 2.5	20.0 ± 3.2
Coefficient of variation (%)	71.0 ± 12.0	58.1 ± 10.6*
Burst firing neurons / recorded neurons	5 / 7	4 / 7
Neurons exhibiting burst firing pattern (%)	71.4	57.1
Number of bursts	41.8 ± 13.9	20.6 ± 16.0
Duration of burst (ms)	1.2 ± 0.8	0.5 ± 0.3
Nº spikes/burst	20.0 ± 8.3	9.5 ± 3.3
Recurrence of burst (nº burst/min)	16.7 ± 6.9	10.3 ± 8.0
Intraburst frequency (Hz)	29.6 ± 5.7	25.9 ± 9.7

Each value represents the mean ± SEM of (n) recorded rats. *$p<0.05$ before vs. after WIN (repeated-measures two-way ANOVA (Drug x Lesion)).

Annex 4.VIII: Effect of AM251 (2 mg/kg, i.v) and WIN 55,212-2 (125 μg/kg, i.v.) on the firing properties of lateral *substantia nigra pars reticulata* neurons from sham and 6-OHDA-lesioned rats

Sham	Before AM (n = 4)	After AM	After AM+WIN
Firing rate (Hz)	19.8 ± 0.2	17.0 ± 1.6	16.7 ± 1.3
Coefficient of variation (%)	37.1 ± 7.4	38.8 ± 8.8	38.6 ± 8.3
Burst firing neurons/ recorded neurons	1 / 4	1 / 4	1 / 4
Neurons exhibiting burst firing pattern (%)	25.0	25.0	25.0
Number of bursts	11	9	4
Duration of burst (ms)	0.5	0.5	1.1
Nº spikes/burst	16.9	11.9	23
Recurrence of burst (nº burst/min)	4.4	4.5	2.0
Intraburst frequency (spikes/s)	40.3	25.7	22.5

Each value represents the mean ± SEM of (n) recorded rats.

Annex 4.IX: Effect of WIN 55,212-2 (125 µg/kg, i.v.) on the firing properties of medial *substantia nigra pars reticulata* neurons from sham and 6-OHDA-lesioned rats

Sham	Before WIN (n = 8)	After WIN
Firing rate (Hz)	22.0 ± 1.6	22.3 ± 1.7
Coefficient of variation (%)	39.1 ± 4.1	31.7 ± 2.2
Burst firing neurons / recorded neurons	6 / 8	2 / 8
Neurons exhibiting burst firing pattern (%)	75.0	25.0
Number of bursts	20.7 ± 13.5	6.7 ± 6.1*
Duration of burst (ms)	0.3 ± 0.1	0.1 ± 0.1
Nº spikes/burst	11.7 ± 1.7	4.1 ± 2.6
Recurrence of burst (nº burst/min)	8.3 ± 5.4	3.3 ± 3.1*
Intraburst frequency (Hz)	42.7 ± 6.2	13.4 ± 9.2*

6-OHDA	Before WIN (n = 5)	After WIN
Firing rate (Hz)	33.1 ± 8.4	28.8 ± 9.6
Coefficient of variation (%)	76.9 ± 19.7$^{\$}$	68.9 ± 16.0$^{\$}$
Burst firing neurons / recorded neurons	4 / 5	4 / 5
Neurons exhibiting burst firing pattern (%)	80.0	80.0
Number of bursts	70.3 ± 45.2	45.5 ± 28.8
Duration of burst (ms)	0.2 ± 0.1	1.1 ± 0.7
Nº spikes/burst	11.3 ± 3.2	18.7 ± 4.6
Recurrence of burst (nº burst/min)	28.1 ± 18.1	22.8 ± 14.4
Intraburst frequency (Hz)	74.6 ± 25.9	60.7 ± 31.9

Each value represents the mean ± SEM of (n) recorded rats. *$p<0.05$ before vs. after WIN; $^{\$}p<0.05$ Sham vs. 6-OHDA (Coefficient of variation and intraburst frequency: repeated-measures two-way ANOVA (Drug x Lesion); Number of bursts and burst recurrence: Wilcoxon matched-pairs signed rank test).

Annex 4.X: Effect of AM251 (2 mg/kg, i.v) and WIN 55,212-2 (125 µg/kg, i.v.) on the firing properties of medial *substantia nigra pars reticulata* neurons from sham and 6-OHDA-lesioned rats

Sham	Before AM (n = 9)	After AM	After AM+WIN
Firing rate (Hz)	22.0 ± 3.3	20.8 ± 3.2	20.8 ± 2.7
Coefficient of variation (%)	43.5 ± 4.8	41.3 ± 4.6	41.0 ± 5.4
Burst firing neurons/ recorded neurons	3 / 5	3 / 5	3 / 5
Neurons exhibiting burst firing pattern (%)	60.0	60.0	60.0
Number of bursts	14 ± 9.8	6.3 ± 3.9	5.3 ± 3.4
Duration of burst (ms)	0.2 ± 0.1	0.2 ± 0.1	0.3 ± 0.1
Nº spikes/burst	6.8 ± 2.4	7.3 ± 3.3	8.1 ± 2.8
Recurrence of burst (nº burst/min)	5.6 ± 3.9	3.1 ± 2.0	2.6 ± 1.7
Intraburst frequency (spikes/s)	34.4 ± 13.3	35.5 ± 12.3	27.3 ± 11.4

6-OHDA	Before AM (n = 11)	After AM	After AM+WIN
Firing rate (Hz)	16.2 ± 2.2	12.2 ± 1.1	11.9 ± 1.1
Coefficient of variation (%)	92.5 ± 23.8	89.5 ± 21.8	91.4 ± 20.7
Burst firing neurons/ recorded neurons	5 / 6	5 / 6	5 / 6
Neurons exhibiting burst firing pattern (%)	83.3	83.3	83.3
Number of bursts	47.3 ± 28.7	37.3 ± 17.2	37.3 ± 17.5
Duration of burst (ms)	0.3 ± 0.1	0.3 ± 0.1	0.2 ± 0.1
Nº spikes/burst	10.1 ± 2.5	8.1 ± 2.0	5.5 ± 1.8
Recurrence of burst (nº burst/min)	18.9 ± 11.5	18.7 ± 8.6	18.7 ± 8.7
Intraburst frequency (Hz)	32.3 ± 8.7	24.7 ± 6.0	26.7 ± 5.9

Each value represents the mean ± SEM of (n) recorded rats.

4.3.   STUDY III: Cannabinoid modulation of cortico-striatal networks

To study cortico-striatal functional relationships, spontaneously active neurons ($\geq$ 0.03 Hz) displaying consistent low-latency (< 20 ms) responses to cortical stimulation were recorded during cortical SWA (spectral dominant frequency < 1.6 Hz). These criteria ensured the functional connection between the cortex and the striatal functional territory. Therefore, allowing us to establish relationships between cortical SWA, and spontaneous neuron activity. Cortical and striatal recordings meeting these criteria were obtained from 42 animals, among which 21 were recorded in the MC/dorsolateral striatum, and the other 21 in the ACC/dorsomedial striatum. One LFP from the dorsolateral and another from the dorsomedial striatum were excluded from the analysis due to the non-optimal condition of the recording. Putative MSNs were identified in terms of their spike waveform and low FR (<1 Hz). Posterior morphological identification of juxtacellularly labelled neurons would confirm a MSN was recorded by the presence of single neurons labelled with dense spiny dendrites. Further molecular identification using preproenkephalin somatic expression would confirm the involvement of the recorded MSNs to the direct or indirect pathway. (Figure 4.13).
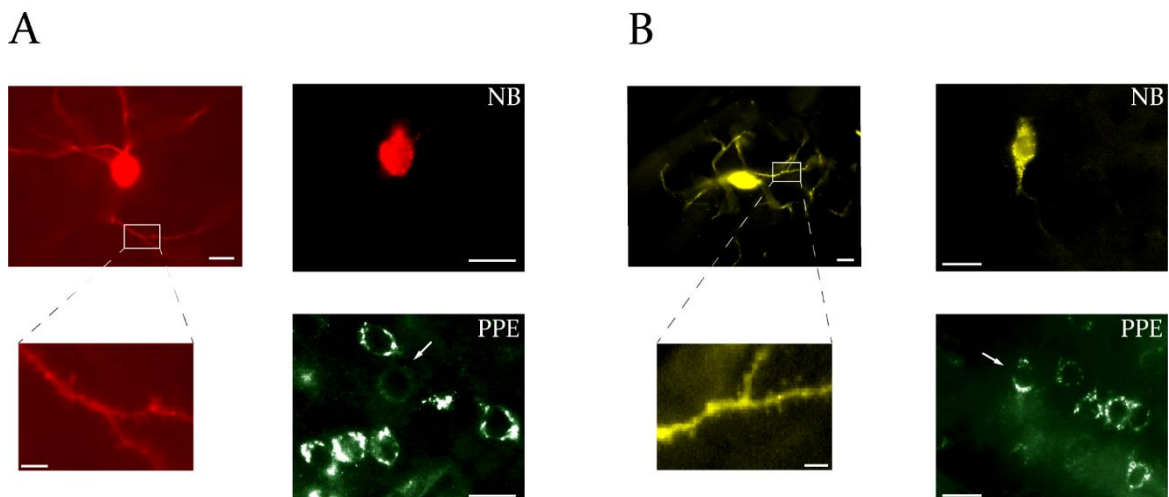
Figure 4.13: Fluorescence micrographs of neurobiotin (NB)-labelled medium spiny neurons (MSN; Top) from the direct (**A**) and indirect (**B**) pathways as determined by their preproenkephalin (PPE) expression (PPE$^-$ and PPE$^+$, respectively) (**A,B.** Bottom right). Arrows indicate the position of the NB-labelled neuron. Note their densely spiny dendrites (**A**, **B**. Bottom left) characteristic of MSNs. Scale bars are set to 20 μm and 5 μm for the dendritic spine zoom-in.

4.3.1. Spontaneous, cortically-evoked and oscillatory activity in sensorimotor and medial prefrontal cortico-striatal networks

As summarized in Table 4.4, putative MSNs from the dorsolateral and dorsomedial striatum, included in the SM and mPF functional territories of the striatum, respectively, could not be differentiated by their spontaneous firing activity. These neurons showed no differences in their FR, CV or index of pauses when grouped by striatal territory, preproenkephalin expression or sex of the rat. The firing of these neurons was relatively irregular and generally phase-locked to SWA (0.4 - 1.6 Hz) (Figure 4.14). The mean firing phase of these neurons to cortical SWA was not different between functional territories. Moreover, phase vector lengths to cortical slow oscillations were smaller in neurons from the dorsolateral striatum, suggesting more variability in phase firing than those in the dorsomedial striatum. No additional differences were found in the firing phase angle or vector lengths, for cortical SWA as per functional territory, preproenkephalin expression or sex of the rat. Regarding the responses evoked after MC or ACC stimulation in putative MSNs from the dorsolateral or dorsomedial striatum, responses from neurons located in the dorsolateral striatum had lower latencies, as well as an increased amplitude, than those in the dorsomedial striatum. Moreover, indirect-pathway MSNs showed a higher duration in their responses than direct-pathway MSNs.

Table 4.4: Spontaneous, phase-locked and cortically-evoked firing properties of putative medium spiny neurons from the dorsolateral (DLS) or dorsomedial (DMS) striatum

	Striatal territory		Sex	Pathway
	DLS n = 23	**DMS** n = 24	**Male** (n = 40) **Female** (n = 7)	**dMSN** (n = 8) **iMSN** (n = 8)
Firing rate (Hz)	0.2 ± 0.02	0.3 ± 0.07	0.2 ± 0.03 0.5 ± 0.2	0.1 ± 0.03 0.2 ± 0.03
Coefficient of variation (%)	141.5 ± 9.3	151.8 ± 8.4	144.1 ± 6.7 161.9 ± 17.7	161.5 ± 15.0 163.1 ± 13.4
Index of pauses (s)	17.1 ± 0.8	17.7 ± 1.4	18.0 ± 0.9 14.2 ± 2.2	17.9 ± 2.3 16.9 ± 2.6
ECoG phase-locked neurons (%)	91.3 (21/23)	95.8 (23/24)	92.5 (37/40) 100 (7/7)	75 (6/8) 100 (8/8)
ECoG Phase (°)	353.4 ± 0.1	357.5 ± 0.1	354.9 ± 0.1 359.2 ± 0.2	19.2 ± 0.3 352.4 ± 0.2
ECoG vector length	0.6 ± 0.04	0.7 ± 0.03*	0.7 ± 0.03 0.8 ± 0.03	0.6 ± 0.08 0.7 ± 0.05
Duration (ms)	10.4 ± 0.8	12.8 ± 1.3	10.9 ± 0.7 15.6 ± 3.2	8.6 ± 1.5 15.4 ± 2.8[&]
Latency (ms)	6.4 ± 0.5	8.5 ± 0.7*	7.7 ± 0.5 6.3 ± 1.0	8 ± 1.6 7.9 ± 0.7
Amplitude	180.1 ± 15.5	132.0 ± 11.7*	159.1 ± 11.2 135.3 ± 23.5	126.1 ± 14.1 156.4 ± 27.7

Each value represents the mean ± S.E.M. of (n) recorded neurons. *$p<0.05$ *vs.* DLS; [&]$p<0.05$ *vs.* dMSN (Mann-Whitney rank sum test). dMSN: direct-pathway medium spiny neurons; iMSN: indirect-pathway medium spiny neurons.
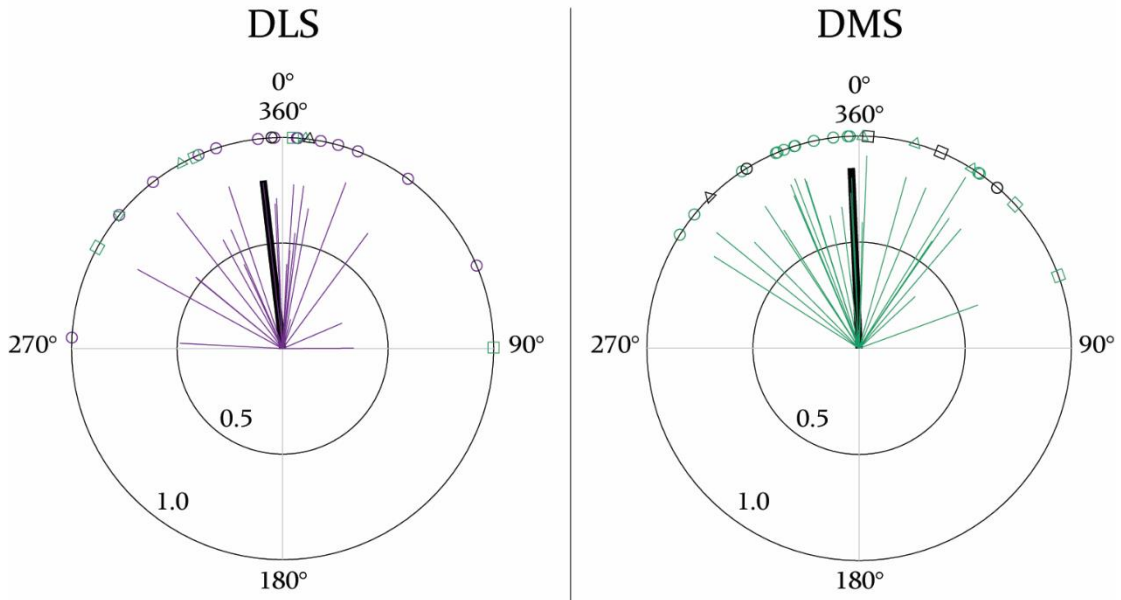
Figure 4.14: Circular plots of the preferred firing angles of putative medium spiny neurons from the dorsolateral (DLS, purple) and dorsomedial (DMS, green) striatum to cortical slow oscillations (0.4 – 1.6 Hz). The black line indicates the mean firing phase angle of that group of neurons. Thin lines indicate the mean firing phase angle for individual neurons, also shown in the outer circle of the plot. Lengths of lines show the vector length; large vectors would indicate less variability in neuron(s) firing around the mean phase angle for that neuron/group. Labelled medium spiny neurons from the direct pathway are represented as squares, while those from the indirect pathway are triangles. Circles represent unlabelled putative medium spiny neurons from the DLS or DMS. Neurons recorded from males are represented in colour, while those from females are shown in black. Only neurons with more than 10 spikes in the analysed period are shown, regardless of being significantly or non-significantly phase-locked to slow oscillations. [MC: n=23 | ACC: n=24].

Regarding the oscillatory activity recorded in both cortices and functional territories of the striatum, differences were found between SM and mPF networks, as well as between sexes. Signals recorded from the MC and the ACC were similar in terms of their dominant frequency (Figure 4.15A). Contribution of the δ band frequency to the signal from the MC is lower than that from ACC. On the other hand, the contribution of the rest of the studied frequency bands (i.e., θ, α, β and γ) to the MC oscillatory activity is higher in comparison to ACC. Regarding sex differences, females displayed smaller dominant frequencies and δ band frequency contribution to their ECoG signals. Moreover, higher contribution of β and γ band frequencies was found in recordings from females (Annex 4.XI). Local oscillatory activity recorded in the dorsolateral and dorsomedial striatum was similar in terms of their dominant frequency and contribution of the studied frequency bands to the signal (Figure 4.15B), although differences in striatal recordings between male and female rats were found. Female

rats showed smaller dominant frequencies than males, as well as less δ band frequencies contributing to their striatal oscillatory activity. Additionally, female rats had more α, β and γ band frequencies contributing to their LFP signal (Annex 4.XII).

The coherence spectra of ECoG – LFP pairs was calculated to study the relationship between the cortical oscillatory activity in MC and ACC and the local oscillatory activity from the dorsolateral and dorsomedial striatum. The dominant frequency in the coherence spectra in SM and mPF networks was found in the δ band, in line with the important contribution of this frequency band to the ECoG – LFP coherence of these cortico-striatal networks. Even so, there seems to be lesser coherence in the δ band in the SM network than in the mPF network. In addition, β and γ frequency bands contribute importantly to the coherence in both SM and mPF cortico-striatal networks, being the γ frequency band more prominent in the SM network. The smaller coherence found in these networks correspond to the θ and α frequency bands, where no differences between networks were found (Figure 4.15C). Again, the sex of the rat was an important source of variation. Coherence in the θ and α bands are higher in female rather than male rats, while the coherence at the γ frequency band was reduced (Annex 4.XIII).
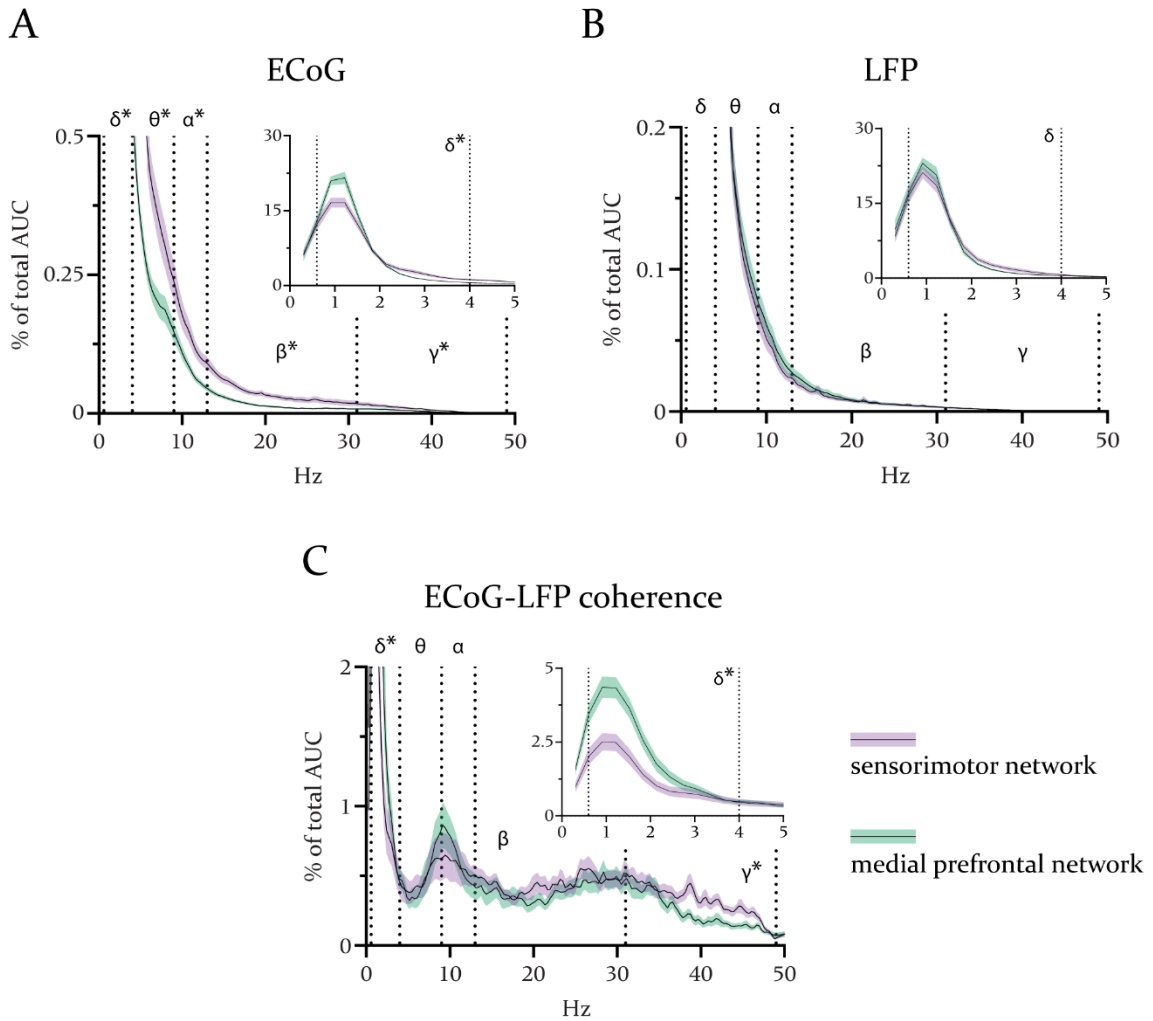
Figure 4.15: Normalized power spectra from motor cortex (MC) and anterior cingulate cortex (ACC) electrocorticograms (ECoG) (**A**), dorsolateral striatum (DLS) and dorsomedial striatum (DMS) local field potentials (LFP) (**B**) and the normalized coherence spectra for ECoG – LFP pairs (**C**). Note that frequencies in the δ band are higher in the medial prefrontal cortico striatal networks (i.e., ECoG and coherence spectra). Moreover, in the ACC the θ, α, β and γ bands contribute less to its ECoG signal, while only less γ band contribution is found in the coherence spectra from the medial prefrontal cortico striatal networks. Dotted lines illustrate frequency band delimitation. Data are expressed as the percentage of the total area under the curve (AUC) of a given spectrum. Blunt black lines indicate the mean, while the coloured shadows represent the S.E.M of n recordings [ECoGs: MC: n=23 | ACC: n=24 // LFPs: DLS: n=22 | DMS: n=23 // Coherence: MC-DLS: n=22 | ACC-DMS: n=23]. *$p<0.05$ vs. MC (Mann-Whitney rank sum test).

4.3.2. Effect of cannabinoids on spontaneous, cortically-evoked and oscillatory activity of sensorimotor and medial prefrontal cortico-striatal networks

The effect of the synthetic CB_1/CB_2-receptor full agonist WIN was used to study the impact of cannabinoids on spontaneous, evoked and oscillatory activity of the SM and mPF cortico-striatal networks. To explore the contribution of the CB1 receptor on these effects, the CB_1-selective antagonist AM251 was used to reverse the effects induced by WIN. In need of more experiments to clarify the role of sex, or pathway-specific effects exerted by cannabinoids, the data herein presented correspond to males and both putative MSNs and identified MSNs.

4.3.2.1. Effect of cannabinoids on spontaneous, cortically-evoked and oscillatory activity of the sensorimotor cortico-striatal network

The effect of the synthetic cannabinoid agonist WIN (125 μg/kg, i.v.) on the spontaneous, evoked and oscillatory activity of the SM cortico-striatal network was investigated. The administered dose of WIN almost completely silenced putative MSNs from the dorsolateral striatum, an effect that was not entirely reversed by the administration of AM251 (2 mg/kg, i.v.) (Annex 4.XIV). This effect on spontaneous activity interfered with regularity (i.e., CV and index of pauses) and phase-lock analyses, which could not be performed. Regarding the cortically-evoked responses in putative MSNs from the dorsolateral striatum, the administration of WIN, as well as the posterior administration of AM251, had no effect on the latency or the duration of these responses. However, administration of WIN was able to increase the amplitude, an effect that was reversed by the subsequent administration of AM251 (Figure 4.16).
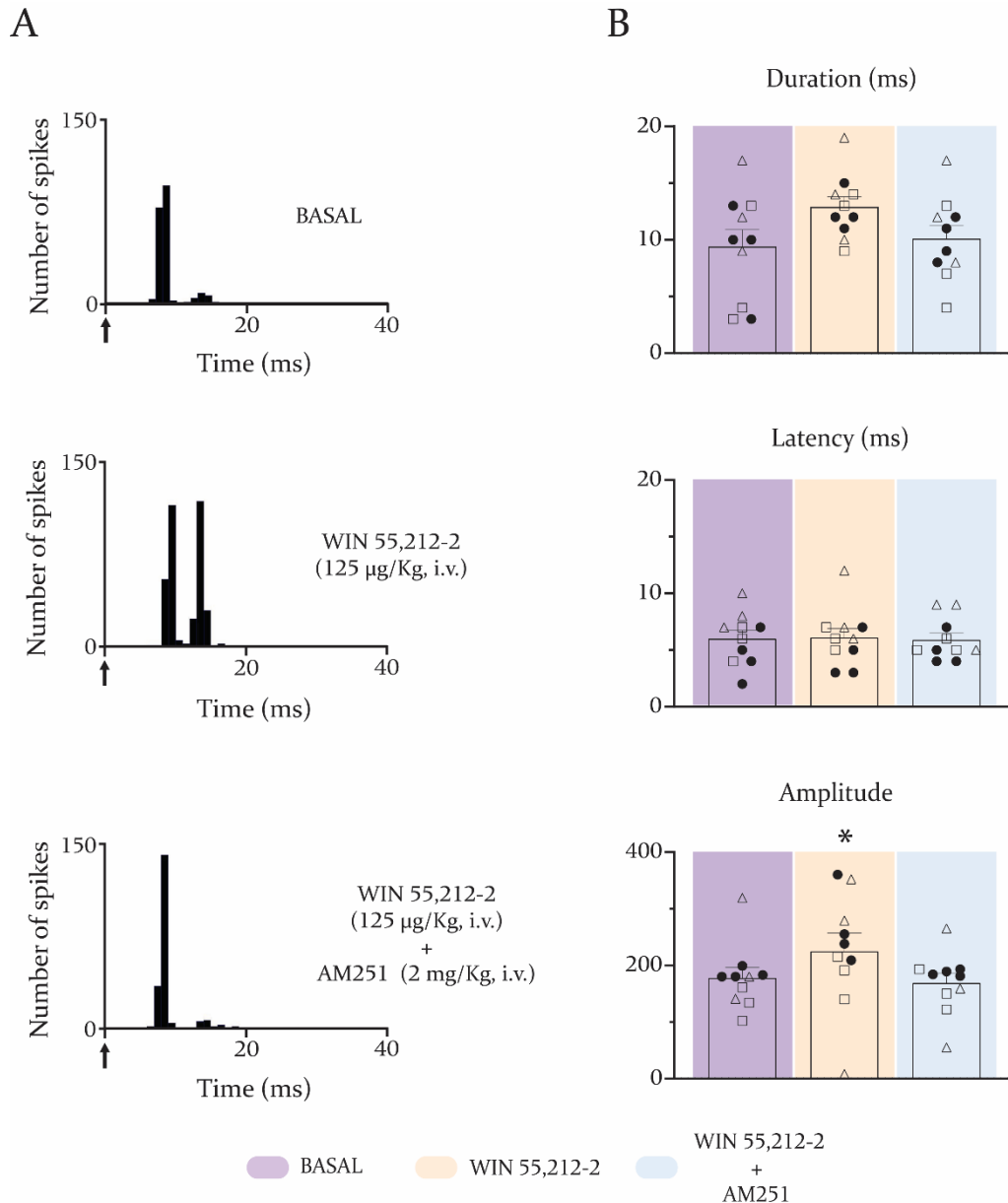
Figure 4.16: Effect of systemic administration of WIN 55,212-2 (125 µg/kg, i.v.) on the cortically-evoked responses of putative medium spiny neurons from the dorsolateral striatum, and its reversal by the administration of the CB_1 selective antagonist AM251 (2 mg/kg, i.v.). **A.** Top: peristimulus time histogram showing a representative example of response evoked in a putative medium spiny neurons of the dorsolateral striatum after motor cortex (MC) electrical stimulation. Middle: after WIN 55,212-2 administration the number of spikes constituting the response increased. Bottom: reversal of the effects caused by WIN 55,212-2 back to basal levels after the administration of the CB_1 antagonist AM251. Arrows indicate cortical stimulus application. **B.** Bar graphs showing the mean effect of WIN 55,212-2 and AM251 on cortically-evoked responses in putative medium spiny neurons from the dorsolateral striatum. Each bar represents the mean ± S.E.M. of n = 10 neurons. Each symbol represents the value from one neuron. Squares indicate direct-pathway MSNs and triangles indicate indirect-pathway MSNs. Black dots represent unlabelled putative medium spiny neurons. *$p<0.05$ vs. BASAL (Friedman test).

Cannabinoid administration induced changes in the oscillatory activity of the SM cortico-striatal network. The dose of AM251 administered after WIN reduced the δ band frequencies contributing to MC ECoG signal. Moreover, after AM251 administration frequencies in the θ, β and γ band increased (Figure 4.17A). The local oscillatory activity recorded in the dorsolateral striatum was also affected by cannabinoids. Administration of WIN only was able to induce a decrease in the γ band frequencies contributing to the LFP signal. Like in MC, AM251 administration reduced δ band contribution to the LFP signal, although without inducing any significant changes in other frequency bands (Figure 4.17B). The only effect exerted by cannabinoids on the coherence between MC ECoGs and dorsolateral striatum LFPs was that of AM251, after whose administration, increased the coherence between MC and dorsolateral striatum in the β frequency band (Figure 4.17C).
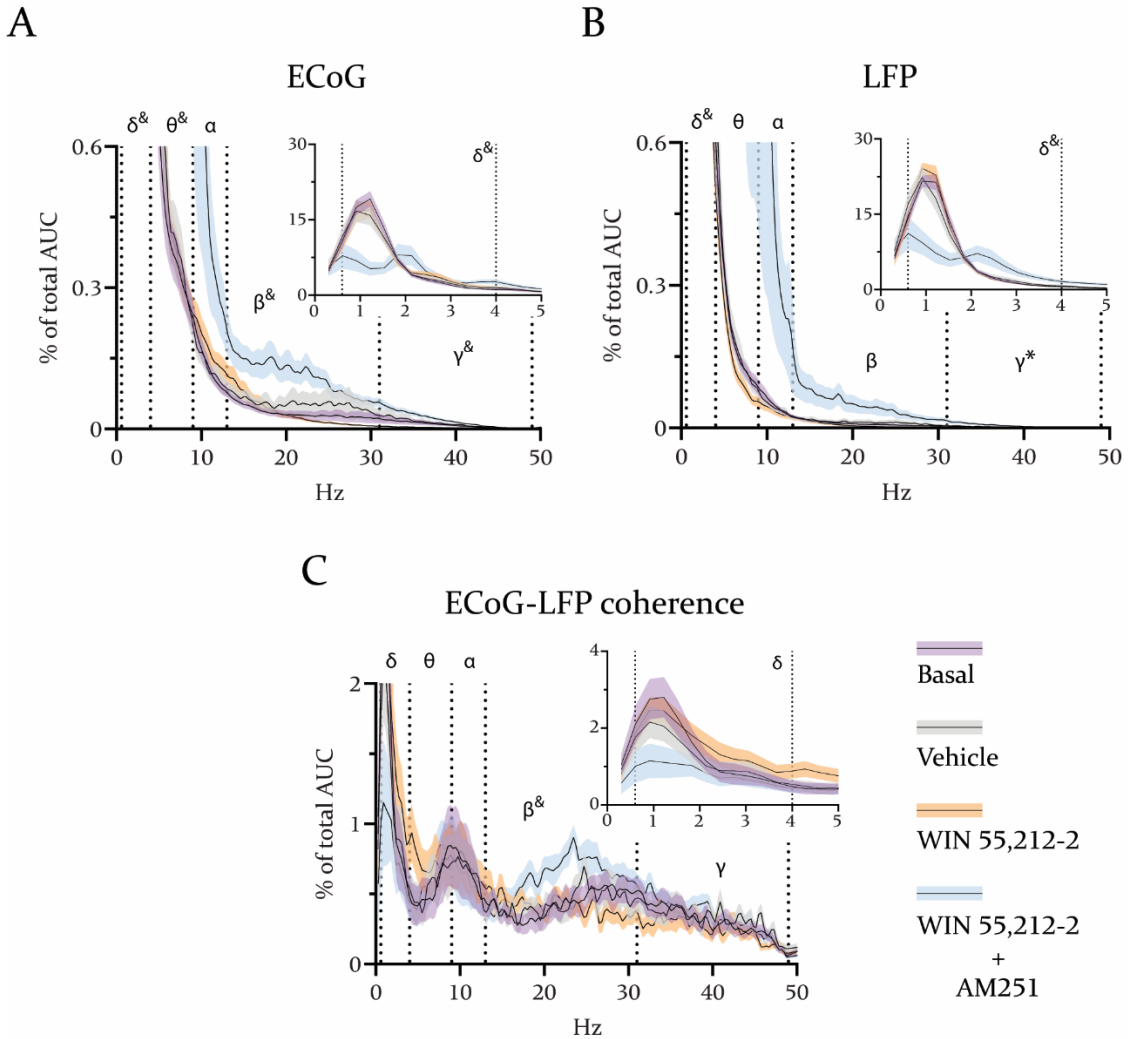
Figure 4.17: Normalized power spectra from motor cortex (MC) electrocorticograms (ECoG) (**A**), dorsolateral striatum local field potentials (LFP) (**B**) and the normalized coherence spectra for ECoG – LFP pairs (**C**) showing the effect of WIN 55,212-2 (125 µg/kg, i.v.) and AM251 (2 mg/kg, i.v.) systemic administration on the sensorimotor cortico-striatal network. WIN 55,212-2 administration could only induce a decrease in the γ frequency band of LFPs in the dorsolateral striatum. Note the decrease in the δ band after AM251 (2 mg/kg, i.v.) administration in signals from both the MC and the dorsolateral striatum. AM251 also had significant effects on MC oscillatory activity in the θ, β and γ frequency bands, enhancing them. Additionally, AM251 administration increased the MC- dorsolateral striatum coherence in the β band. Data are expressed as the percentage of the total area under the curve (AUC) of a given spectrum. Blunt black lines indicate the mean, while the coloured shadows represent the S.E.M of n = 10 recordings. *$p<0.05$ Basal vs. WIN 55,212-2; &$p<0.05$ Basal vs. AM251 (Friedman test).

4.3.2.2. Effect of cannabinoids on spontaneous, cortically-evoked and oscillatory activity of the medial prefrontal cortico-striatal network

We also explored the effect of WIN (125 µg/kg, i.v.) on the spontaneous, evoked and oscillatory activity in the mPF cortico-striatal network. As in the dorsolateral striatum, putative MSNs from the dorsomedial striatum were almost entirely silenced after the administered dose of WIN. Such an effect was not reversed by the administration of AM251 (2 mg/kg, i.v.) (Annex 4.XIV). As happened with neurons from the SM cortico-striatal network, this effect upon spontaneous activity made impossible to perform regularity and phase-lock analyses. Cortically-evoked responses in putative MSNs from the dorsomedial striatum experienced no change in their latency, duration or amplitude, after the administration of WIN or the subsequent AM251 administration (Figure 4.18).

The administration of cannabinoids affected the oscillatory activity of the mPF cortico-striatal network. Administration of WIN increased the θ and β frequency bands, while reducing the contribution of γ band frequencies to the signal. Moreover, posterior administration of AM251 reduced the contribution of δ band frequencies to the ACC ECoG signal, as well as in the MC. Additionally, AM251 increased the contribution of all the other studied frequency bands (i.e., θ, α, β and γ) (Figure 4.19A). Local oscillatory activity recorded in the dorsomedial striatum also experienced changes after the administration of cannabinoid drugs. Regarding the effect induced by WIN, it caused a reduction in the θ and γ frequency band contribution to the LFP signal. Moreover, AM251 administration decreased δ band contribution, while increasing the rest of the studied frequency bands (Figure 4.19B). Administration of cannabinoids also affected the coherence between ACC and dorsomedial striatum. The administered dose of WIN caused an increase in coherence between ACC and dorsomedial striatum in the θ and α frequency bands. Additionally, AM251 changed the frequency at which ACC and dorsomedial striatum displayed more coherence, increasing the dominant frequency of the coherence spectra. Moreover, its administration decreased the coherence at the δ frequency band, while increasing the coherences between these signals in the θ, β and γ frequency bands (Figure 4.19C).
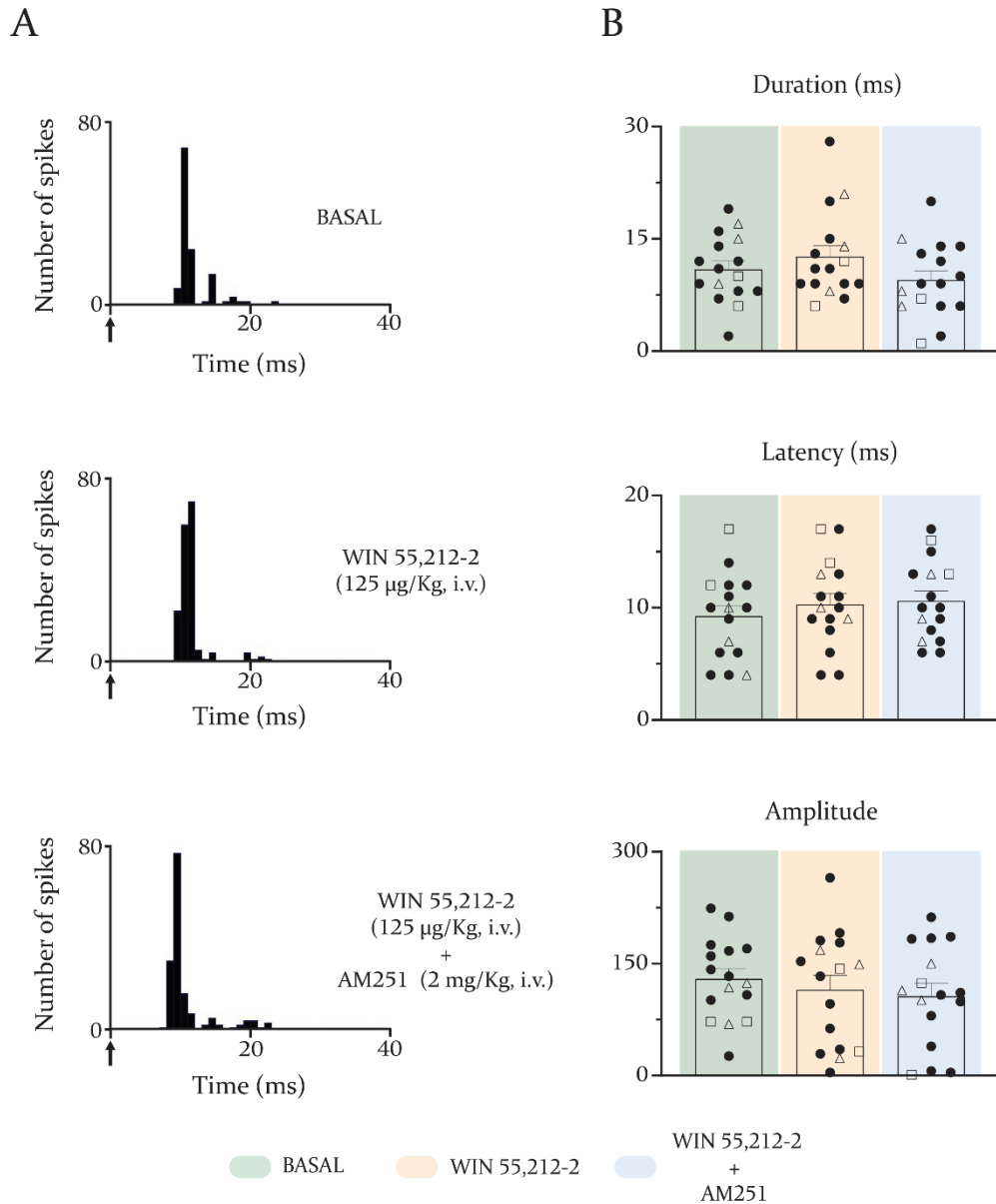
Figure 4.18: Effect of systemic administration of WIN 55,212-2 (125 µg/kg, i.v.) and AM251 (2 mg/kg, i.v.) on the cortically-evoked responses of putative medium spiny neurons from the dorsomedial striatum. **A.** Top: peristimulus time histogram showing a representative example of the response evoked in putative medium spiny neurons from the dorsomedial striatum after anterior cingulate cortex (ACC) electrical stimulation. Middle: after WIN 55,212-2 administration. Bottom: after the administration of the CB_1 antagonist AM251. Note that none of this cannabinoids had any substantial effect on the electrophysiological parameters of this response. Arrows indicate cortical stimulus application. **B.** Bar graphs showing the mean effect of WIN 55,212-2 and AM251 on cortically-evoked responses in putative medium spiny neurons from the dorsomedial striatum. Each bar represents the mean ± S.E.M. of n = 16 neurons. Each symbol represents the value from one neuron. Squares indicate direct-pathway MSNs and triangles indicate indirect-pathway MSNs. Black dots represent unlabelled putative medium spiny neurons.
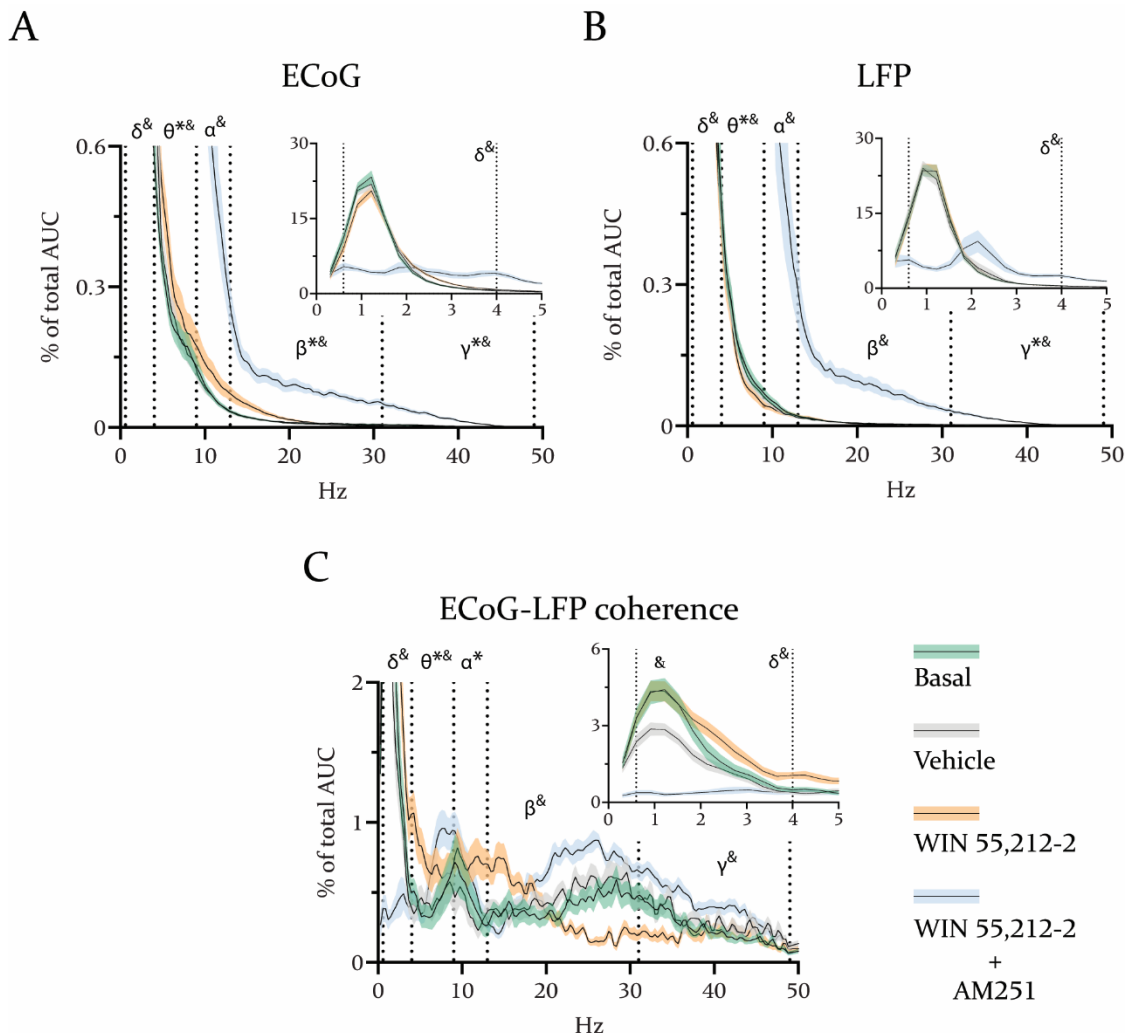
Figure 4.19: Normalized power spectra from anterior cingulate cortex (ACC) electrocorticograms (ECoG) (**A**), dorsomedial striatum local field potentials (LFP) (**B**) and the normalized coherence spectra for ECoG – LFP pairs (**C**) showing the effect of WIN 55,212-2 (125 µg/kg, i.v.) and AM251 (2 mg/kg, i.v.) systemic administration on the medial prefrontal cortico-striatal network. Administration of WIN 55,212-2 increased θ and β frequency bands, while decreasing the γ band in signals from the ACC. In a similar way, it decreased the γ band in LFPs from the dorsomedial striatum. Additionally, it also decreased the θ frequency band. Moreover, WIN 55,212-2 increased coherence in the θ and α frequency bands of the spectrum. AM251 administration decreased cortical and striatal oscillations in the δ frequency band. On the other hand, it increased θ, α, β and γ frequency bands in signals from both ACC and dorsomedial striatum. This same effect of AM251 was observed in the coherence, with the exception of the α frequency band, in which it caused no effect. Data are expressed as the percentage of the total area under the curve (AUC) of a given spectrum. Blunt black lines indicate the mean, while the coloured shadows represent the S.E.M of n recordings [ECoGs: n = 16 // LFPs & Coherence: n = 15]. *$p<0.05$ Basal vs. WIN 55,212-2; &$p<0.05$ Basal vs. AM251 (Friedman test).

Annex 4.XI: Frequency description of the electrocorticogram (ECoG) from the motor cortex (MC) or anterior cingulate cortex (ACC).

ECoG	Cortical area		Sex
	MC (n = 23)	ACC (n = 24)	Male (n = 40) Female (n = 7)
Dominant frequency (Hz)	0.9 ± 0.06	0.8 ± 0.05	0.9 ± 0.04 0.6 ± 0.04[&]
δ [0.6 – 4 Hz] (% of total AUC)	68.9 ± 1.9	74.6 ± 2.5*	74.6 ± 1.4 56.2 ± 2.4[&]
θ [4 – 9 Hz] (% of total AUC)	6.8 ± 0.7	3.6 ± 0.3*	5.0 ± 0.4 6.1 ± 1.6
α [9 – 13 Hz] (% of total AUC)	1.7 ± 0.2	1.0 ± 0.1*	1.2 ± 0.1 2.0 ± 0.6
β [13 – 31 Hz] (% of total AUC)	2.0 ± 0.3	0.9 ± 0.1*	1.3 ± 0.2 2.1 ± 0.5[&]
γ [31 – 49 Hz] (% of total AUC)	0.4 ± 0.08	0.2 ± 0.04*	0.3 ± 0.05 0.5 ± 0.07[&]

Each value represents the mean ± S.E.M. of (n) recordings. *$p<0.05$ *vs.* MC; [&]$p<0.05$ *vs.* Male (Mann-Whitney rank sum test).

Annex 4.XII: Frequency description of the local field potential (LFP) from the dorsolateral (DLS) or dorsomedial (DMS) striatum.

LFP	Striatal territory		Sex
	DLS (n = 22)	DMS (n = 23)	Male (n = 38) Female (n = 7)
Dominant frequency (Hz)	0.9 ± 0.07	0.8 ± 0.05	0.9 ± 0.05 0.5 ± 0.06$^{\&}$
δ [0.6 – 4 Hz] (% of total AUC)	70.7 ± 2.6	68.8 ± 3.6	74.3 ± 1.7 44.6 ± 2.7$^{\&}$
θ [4 – 9 Hz] (% of total AUC)	2.7 ± 0.3	2.5 ± 0.2	2.5 ± 0.2 3.1 ± 0.5
α [9 – 13 Hz] (% of total AUC)	0.5 ± 0.06	0.6 ± 0.07	0.5 ± 0.04 0.9 ± 0.2$^{\&}$
β [13 – 31 Hz] (% of total AUC)	0.5 ± 0.07	0.5 ± 0.09	0.4 ± 0.05 0.9 ± 0.2$^{\&}$
γ [31 – 49 Hz] (% of total AUC)	0.05 ± 0.01	0.06 ± 0.01	0.05 ± 0.01 0.08 ± 0.01$^{\&}$

Each value represents the mean ± S.E.M. of (n) recordings. $^{\&}$*p*<0.05 *vs.* Male (Mann-Whitney rank sum test).

Annex 4.XIII: Frequency description of the coherence between the electrocorticogram (ECoG) of the motor cortex (MC) and anterior cingulate cortex (ACC) and the local field potential (LFP) from the dorsolateral (DLS) and dorsomedial (DMS) striatum, respectively.

ECoG – LFP Coherence	ECoG – LFP pairs		Sex
	MC/DLS (n = 22)	**ACC/DMS** (n = 23)	**Male** (n = 38) **Female** (n = 7)
Dominant frequency (Hz)	3.3 ± 1.6	0.9 ± 0.04	2.3 ± 0.94 0.7 ± 0.04
δ [0.6 – 4 Hz] (% of total AUC)	13.4 ± 1.8	21.6 ± 1.9*	17.4 ± 1.7 18.8 ± 2.4
θ [4 – 9 Hz] (% of total AUC)	7.3 ± 1.5	7.5 ± 1.4	6.2 ± 1.0 13.5 ± 2.7&
α [9 – 13 Hz] (% of total AUC)	6.9 ± 1.4	7.4 ± 1.2	5.8 ± 0.9 14.4 ± 2.1&
β [13 – 31 Hz] (% of total AUC)	25.82 ± 2.3	22.9 ± 2.3	25.4 ± 1.7 18.4 ± 3.9
γ [31 – 49 Hz] (% of total AUC)	18.7 ± 2.0	13.3 ± 1.6*	17.1 ± 1.4 9.4 ± 2.7&

Each value represents the mean ± S.E.M. of (n) recordings. *$p<0.05$ *vs.* MC/DLS; &$p<0.05$ *vs.* Male (Mann-Whitney rank sum test).

Annex 4.XIV: Effect of WIN 55,212-2 (125 μg/kg, i.v.) and AM251 (2 mg/kg, i.v) on the firing rate of putative medium spiny neurons (pMSNs) from the dorsolateral striatum (DLS) and dorsomedial striatum (DMS).

Firing rate (Hz)	DLS pMSNs n = 10	DMS pMSNs n = 16
Basal	0.2 ± 0.03	0.1 ± 0.03
Vehicle	0.2 ± 0.04	0.1 ± 0.03
WIN	0.04 ± 0.02*	0.02 ± 0.01*
WIN + AM	0.1 ± 0.1	0.01 ± 0.01*

Each value represents the mean ± S.E.M. of (n) recordings. *$p<0.05$ *vs.* Basal (Friedman test).

5. DISCUSSION

5. DISCUSSION

5.1. Study I: CB₁ receptor control of cortico-nigral transmission through the sensorimotor and medial prefrontal basal ganglia circuits

This study presents results showing differences in the spontaneous and cortically-evoked activity of SNr neurons from different functional territories, as well as evidence on how cortico-nigral transmission through the SM and mPF BG circuits is differently modulated by cannabinoid drugs through CB₁ receptor activation. While cannabinoid agonists equally affected cortico-nigral transmission through the direct and the indirect pathways of both circuits, the impact of these drugs upon the hyperdirect pathway was different.

5.1.1. Spontaneous and cortically-evoked activity differential characteristics of neurons from the lateral and medial territories of the substantia nigra pars reticulata

Results from this study show that rats recorded in the medial SNr are more likely to have neurons presenting burst firing than those recorded in the lateral SNr. These animals also display neurons with a greater number of bursts, duration of the burst and recurrence of bursts. SNr neuronal burst activity is mainly related to NMDA receptor activation by glutamate release from subthalamic terminals (Ding et al., 2013; Ibáñez-Sandoval et al., 2007; Shen & Johnson, 2006). This may be due to differences in the glutamatergic input that these two territories receive, either a higher glutamatergic innervation or greater presence of NMDA receptors in the medial SNr would account for these results.

The latency of the responses recorded in the medial SNr resulted to be higher than those recorded in the lateral SNr. This might be due to the distance that cortical information has to travel until reaching the SNr. In the mPF circuits, cortical projections reach more caudal tiers of the dorsomedial striatum, whereas in the case of the SM circuits, the MC projections are restricted to more rostral areas of the dorsolateral striatum (McGeorge & Faull, 1989). Thus, the MC would be closer to its targets than the ACC, resulting in lower latencies in the responses evoked in the SNr after MC stimulation. Besides that, electrical particularities of these circuits or additional modulatory synapses may be influencing information transmission. The inhibitory response, related to the transmission through the direct pathway, had more duration in the SM than in the mPF circuits. This could be explained as a consequence of a higher activation of the SM circuits since binding experiments showed higher amounts of AMPA receptors in the dorsolateral striatum, in comparison to the dorsomedial striatum (Nicolle & Baxter, 2003).

5.1.2. Cannabinoids reduce cortico-nigral transmission through the SM and mPF BG circuits

Our results show that the systemic administration of CB_1 receptor agonists (i.e., WIN and Δ^9-THC) disrupt cortical information transmission through the trans-subthalamic hyperdirect pathway, as well as through the trans-striatal direct and indirect pathways. These data are in line with previous *in vivo* and *in vitro* electrophysiological studies demonstrating that cannabinoid agonists inhibit GABAergic and glutamatergic neurotransmission. Specifically, cannabinoids reduce cortico-striatal and subthalamo-nigral glutamatergic neurotransmissions (Gerdeman & Lovinger, 2001; Sañudo-Peña & Walker, 1997; Szabo et al., 2000), as well as striato-pallidal and striato-nigral GABAergic signalling (Miller & Walker, 1996; Wallmichrath & Szabo, 2002a, 2002b). Moreover, recent reports show that CB_1 receptor activation decreased transmission through the direct and indirect pathways of the SM circuits after sensory stimulation (Báez-Cordero et al., 2020). However, the administered cannabinoid drugs exerted a differential modulation of cortico-nigral information transmission through the SM and mPF BG circuits. While CB_1 receptor agonists equally

impaired transmission through the trans-striatal pathways of the SM and mPF BG circuits, the hyperdirect pathway from the mPF BG circuits seemed to be more sensitive to the administration of these drugs. These observations could be explained by the heterogeneous presence of the CB_1 receptor within the BG. Although CB_1 receptor expression has been detected in the STN, no topographical variations in the expression between its motor and limbic/associative areas were demonstrated (Mailleux & Vanderhaeghen, 1992). Previous electrophysiological studies show that CB_1 receptor agonists have different effects on STN neurons from motor and limbic/associative territories of the STN (Morera-Herreras et al., 2010). Therefore, differences in the sensitivity of the hyperdirect pathway to CB_1 receptor agonists may underlie differences in cortical CB_1 receptor expression between mPF and SM cortical areas. In line with this, high CB_1 receptor expression levels are found in territories of the striatum related with the SM circuit (i.e., dorsolateral striatum), receiving afferents from motor cortical areas with relatively low CB_1 receptor expression. On the other hand, striatal territories related with the mPF circuits (i.e., dorsomedial striatum) show low CB_1 receptor expression levels, and receive afferents from mPF cortical areas where the CB_1 receptor is relatively highly expressed (Heng et al., 2011; Van Waes et al., 2012). Data presented in this study fits the hypothesis proposed by Van Waes et al., (2012) where, based in this CB_1 receptor distribution, cannabinoid agonists would principally inhibit striatal GABA release from the dorsolateral striatum, while preferentially inhibiting cortical glutamate release from mPF cortical areas. Therefore, as shown in this study, both cannabinoid agonists would be more efficient inhibiting striatal GABA release in the SM circuits, thus impairing cortico-nigral transmission through the trans-striatal pathways. Additionally, in the mPF circuits, these drugs would principally inhibit glutamate release from cortex, leading to a disruption in cortico-nigral information transfer through the three pathways that constitute these circuits.

Regarding the cannabinoid drugs tested, although both WIN and Δ^9-THC activate CB_1 receptors, their pharmacological profiles are different. The synthetic compound WIN is a potent CB_1/CB_2 full agonist. However, Δ^9-THC is a CB_1/CB_2 partial agonist that also targets GPR55 and GPR18 receptors, although it seems to exert its effects principally via CB_1 receptors (Pertwee, 2006). In fact, all the effects we observed seem to be mediated by the

CB$_1$ receptor since they were blocked by previous administration of AM251 a selective CB$_1$ antagonist, and GPR55/GPR18 agonist. Moreover, the administration of AM251 at the tested dose did not have any effect on the triphasic responses, indicating no tonic endocannabinoid control over these circuits. Administration of Δ^9-THC seemed to have a stronger effect than WIN administration on cortico-nigral transmission through the BG circuits, especially on the transmission through the hyperdirect pathway. Both agonists show to have similar affinities for the CB$_1$ receptor, with binding affinity values that range from 15.3 to 41 nM for the Δ^9-THC, and from 24 to 62.3 nM for the WIN (Breivogel et al., 2001; Brents et al., 2011; Felder et al., 1995; Showalter et al., 1996; Wiley et al., 1998). Moreover, GTPγS binding experiments show that both agonists are similarly effective, or Δ^9-THC more effective, inducing CB$_1$ receptor G coupling (EC50: 81-167 nM for the Δ^9-THC and 170 nM for the WIN) (Breivogel et al., 2001; Brents et al., 2011). This, together with the higher dose of Δ^9-THC that was used in comparison to that of WIN (0.5 mg/kg *vs.* 125 µg/kg), could explain the apparently stronger effect observed on cortico-nigral information transmission through the hyperdirect pathway after the administration of Δ^9-THC.

5.1.3. *Conclusion*

In this study, results show differences in cortico-nigral transmission through the SM and mPF BG circuits, as well as in SNr spontaneous activity between functional territories. These changes fit with a hypothetical different presence of the glutamatergic system within the BG nuclei. Moreover, the CB$_1$ receptor would act hindering cortico-nigral transmission through the SM and mPF BG circuits, although differently affecting the hyperdirect pathway depending on the circuits. The relative sensitivity of this pathway might account for the different CB$_1$ receptor distribution along the SM and mPF BG circuits.

5.2. Study II: Impact of dopaminergic denervation on cortico-nigral transmission through the sensorimotor and medial prefrontal basal ganglia circuits and CB$_1$ receptor function

This study shows that 6-OHDA-induced DA denervation differently affected spontaneous and cortically-evoked activity in SNr neurons from different functional territories. Moreover, results herein suggest that DA denervation alters the way cannabinoids modulate cortico-nigral transmission through the SM and mPF BG circuits, regardless of CB$_1$ receptor expression. In both circuits, WIN lost its ability to affect transmission through the trans-striatal pathways (i.e., direct and indirect pathways), while it increased hyperdirect pathway sensitivity to cannabinoids in the SM circuits.

5.2.1. Dopaminergic denervation changes the spontaneous and cortically-evoked activity of substantia nigra pars reticulata neurons from the lateral and medial territories

Neurons from the lateral and medial SNr in DA-denervated animals principally exhibit alterations in their spontaneous activity, displaying a more irregular firing pattern followed by more burst firing neurons and alterations in burst-related parameters. In addition to this, FR of medial SNr neurons is decreased in 6-OHDA-lesioned animals, as noted by other groups after injection of 6-OHDA in the MFB (Wang et al., 2010). On the other hand, there is much more evidence supporting the hyperactive SNr neuronal discharge pattern after DA depletion, without changes in the FR of lateral SNr neurons (Aristieta et al., 2016; Maurice, Deltheil, et al., 2015; Meissner et al., 2006; Murer et al., 1997; Tseng et al., 2000; Vegas-Suárez et al., 2020). Several studies suggest that there might be a mediolateral gradient in the SNr regarding its DA content, with less DA in the lateral SNr and more DA in the medial SNr (Ciliax et al., 1995; Cragg et al., 1997; Rice et al., 1994, 1997; Weiss-Wunder & Chesselet, 1990). This would be in accordance with the greater impact DA denervation has on the FR and discharge pattern of medial SNr neurons. Altogether, this suggests that medial

SNr neurons are more reliant on DA for their normal function than those in the lateral SNr. Since D_1 and D_2 receptors in the SNr are located mainly in axons and terminals (Levey et al., 1993; Yung et al., 1995), DA denervation effects on the spontaneous activity of SNr neurons likely involve indirect mechanisms. A hypothetical predominant D_2 receptor involvement in glutamate release (Ibañez-Sandoval et al., 2006), or a decreased D_1-mediated facilitation of GABA release (Chuhma et al., 2011), would promote the hyperactive pattern observed in SNr neurons (Ibáñez-Sandoval et al., 2007). Moreover, several studies show STN hyperactivity in 6-OHDA-lesioned animals (Aristieta et al., 2012; Hassani et al., 1996; Magill et al., 2001; Vila et al., 2000), which would explain the increased irregularity and burst firing pattern observed in both SNr territories, as an increased glutamate release would be expected. In contrast to earlier works, there is evidence for the co-expression of D_1/D_5 receptors in SNr neurons with a direct role on the physiology of SNr neurons (Zhou et al., 2009). This would not only explain the increased irregularity and burst firing observed in neurons from both SNr territories, but also the decreased FR observed in neurons from the medial part of this nucleus after DA denervation.

Regarding transmission through the SM circuits there is an increase in transmission through the hyperdirect trans-subthalamic pathway, reflected by a greater mean duration and more neurons displaying monophasic EEs in 6-OHDA-lesioned animals. Moreover, less neurons displayed triphasic responses, together with less neurons displaying INHs and LEs after DA denervation. These data differ at least in part from that in other studies, although these heterogeneous results may depend on methodological differences like the DA interruption method (6-OHDA lesion or pharmacological blockade) (Degos et al., 2005; Sano & Nambu, 2019). Moreover, another source of variation could be the degree of DA denervation, and time after the 6-OHDA injection (Willard et al., 2019). The effect of acute pharmacological blockade of DA transmission on circuit functionality assessed by systemic neuroleptic injection, showed a decreased direct pathway transmission and a reinforced transmission through the indirect pathway, without any changes in the hyperdirect pathway (Degos et al., 2005). In awake mice, DA denervation after 6-OHDA injection into the MFB, resulted in EEs and LEs being more prevalent and INHs less prevalent after DA denervation (Sano & Nambu, 2019). However, predominant transmission through the hyperdirect

pathway of the SM circuits described in this study, is consistent with the extensively described overactive state of the STN under low DA conditions that has been related to PD motor features (Benabid et al., 1994; Bergman et al., 1994; Hassani et al., 1996; Steigerwald et al., 2008).

Regarding the mPF circuits, we observed an increase in neurons showing monophasic inhibitory responses, as well as a decreased number in neurons showing LEs. To our knowledge, this study shows the first demonstration that DA denervation alters the cortically-evoked responses in medial SNr neurons, leading to a predominant information transfer though the direct pathway, together with a loss of efficacy in transmission through the indirect pathway. Spontaneous and cortically-evoked activity alterations in medial SNr neurons, suggest abnormal functionality inside associative and limbic territories of the BG after DA denervation. Behavioural studies performed in similar PD models show cognitive dysfunctions, such as apathy (Anderson et al., 2020; Carvalho et al., 2013; Furlanetti et al., 2015) or depression-like behaviours (Winter et al., 2007; Zhang et al., 2011), that are linked to the BG and are present in PD patients (Tremblay et al., 2015). Thus, the observed alterations in the mPF circuits after DA denervation might help understand the neurobiological components behind these motivational symptoms in PD patients.

Although, in principle, data presented in this study are not in line with studies showing hyperactivity in direct and indirect pathway MSNs in animal models and PD patients (Fieblinger et al., 2014; Singh et al., 2016; Suarez et al., 2016), other factors could influence the output of the circuits seen in SNr neurons after cortical stimulation. Some studies point out alterations during hypodopaminergic states such as dendritic atrophy, spine pruning and reduced cortico-striatal glutamatergic synapses in direct-pathway MSN, indirect-pathway MSN or both MSNs that could be reducing cortical input on these neurons (Fieblinger et al., 2014; Gagnon et al., 2017; Graves & Surmeier, 2019; Suarez et al., 2016). Moreover, functional studies show a decreased cortico-striatal connectivity in direct-pathway MSNs, and increased in indirect-pathway MSNs in a 6-OHDA model similar to ours, in line with the classical model of BG function in hypodopaminergic states (Escande et al., 2016; Mallet et al., 2006). Overall, this evidence would support the reduced percentage of

neurons displaying INHs (i.e., direct pathway activation) that we observe in the SM circuits of 6-OHDA-lesioned animals. However, the reduced transmission through the indirect pathway of the SM circuits in lesioned animals is contradictory. Being the indirect pathway a polysynaptic pathway, interpretation of the effects of DA denervation grows in complexity, especially if we consider the impact of the DA loss in pallidal and subthalamic function (Aristieta et al., 2012; Chan et al., 2011; Magill et al., 2001; Miguelez et al., 2012). Moreover, one characteristic of the BG nuclei is the high synaptic convergence in its output nuclei. DA denervation increases the time window at which indirect-pathway MSNs respond to stimulation of the MC (Mallet et al., 2006). This variability in indirect-pathway MSNs response time after cortical stimulation could interfere with the summation of multiple inputs on neurons in downstream nuclei, therefore failing to engage neuronal activity efficiently, and provoke full transmission through the indirect pathway, reaching the SNr.

Most of the studies discussed above address how BG physiology is altered in hypodopaminergic states with special emphasis on the SM territories, but few have addressed this same topic on the mPF territories of the BG nuclei. Some studies manifest substantial differences between SM and mPF territories. For instance, sensory- and limbic-related cortical areas preferentially innervate direct-pathway MSNs, whilst motor-related areas innervate indirect-pathway MSNs (Wall et al., 2013). Moreover, functional studies have shown different forms of plasticity taking place under different conditions in SM and mPF territories of the striatum, besides differences in components from key striatal neurotransmitter systems (Arbuthnott & Wickens, 2007; Atwood et al., 2014; Braz et al., 2017; Herkenham, Lynn, de Costa, et al., 1991). Together, this evidence calls for caution in extrapolating traits typically related with components from the SM circuits, into components from the mPF circuits. These differences could affect the way mPF circuits behaves, not only under physiological conditions, but also in pathological states, therefore stepping aside from what is expected from BG physiology under low DA conditions.

Overall, our results indicate that DA denervation lead to deficits in cortical information selection through the segregated anatomo-functional cortico-BG loops, although compensatory changes induced by DA denervation should not be ruled out. The

abnormal information selectivity affecting motor, cognitive and motivational domains could be the neurophysiological impetus to the development of the motor and non-motor symptoms observed in PD, and it can be due to reduced anatomical and functional connectivity in cortico-BG networks, as demonstrated in PD patients and more evident for SM connections (Sharman et al., 2013).

5.2.2. Cannabinoid modulation of cortico-nigral transmission through the SM and mPF basal ganglia circuits is affected after dopaminergic denervation

Cannabinoid modulation of cortical information transmission through the SM or mPF BG circuits is changed in 6-OHDA-lesioned animals. In agreement with study I, administration of WIN in sham rats caused a reduction in the information transmission through the indirect pathway, without affecting the hyperdirect pathway in the SM circuits. Regarding the mPF circuits, administration of WIN in sham rats decreased information transmission through the three pathways (i.e., hyperdirect, direct and indirect pathways). However, no statistically significant reduction in transmission through the direct pathway was observed in the SM circuits in this study, contrary to the observations made in study I. This could be due to the extreme value present in the 6-OHDA dataset, which would increase data dispersion, and make the statistical test uncertain whether to reject the null hypothesis or not. Supporting this, data obtained here and in study I before and after WIN administration are similar, both mean and dispersion values (Before WIN: 12.3 ± 2.6 *vs.* 15.0 ± 1.5; After WIN: 3.5 ± 2.3 *vs.* 4.4 ± 2.1).

After DA denervation, the hyperdirect pathway in the SM circuits became sensitive to WIN administration. In line with this, administration of WIN in 6-OHDA-lesioned rats reduces FR of STN neurons, while increases it in control animals (Morera-Herreras et al., 2011), therefore this could explain the reduced transmission through the hyperdirect pathway after WIN administration in the SM circuits of 6-OHDA-lesioned animals. In the mPF circuits, this pathway remains sensitive to WIN in the 6-OHDA group. However, after DA denervation trans-striatal pathways in both circuits became insensitive to WIN administration.

A possible explanation for these findings could be CB_1 receptor expression alteration induced by DA denervation. For this reason, we decided to perform immunohistochemical assays to determine the precise territory-specific potential changes in CB_1 receptor for each of the nuclei involved in the BG circuits. In sham animals, sub-territorial analysis of the immunolabelling revealed predominant CB_1 expression in the dorsolateral areas of the striatum compared to medial/ventral regions. These data is consistent with previous work suggesting that CB_1 receptors located in these striatal regions could regulate principally information processing through the SM circuits, or at least to a greater extent than in the mPF circuits. (Hohmann & Herkenham, 1999; Mailleux & Vanderhaeghen, 1992; Marsicano & Lutz, 1999; Matsuda et al., 1993; Van Waes et al., 2012; Zimmer et al., 1999). In the SM areas of the striatum, and given the preferential location of CB_1 receptors on terminals (Irving et al., 2000), extensive location of the CB_1 receptor in the dorsolateral striatum likely comes from MSNs axon collaterals. Therefore, contributions from striatal afferents to CB_1 immunostaining in this region is probably minimal. Although the CB_1 receptor is expressed in cortical areas projecting to SM territories of the striatum, this expression is modest, and located principally in non-pyramidal neurons (Heng et al., 2011; Mailleux & Vanderhaeghen, 1992). Moreover, midbrain DA neurons and thalamic neurons show negligible levels of CB_1 expression (Herkenham, Lynn, de Costa, et al., 1991; Mailleux & Vanderhaeghen, 1992). This is in line with the sparse CB_1 presence in mPF territories of the striatum (i.e., dorsomedial striatum), where the expression of this receptor is minimal (Hohmann & Herkenham, 2000; Van Waes et al., 2012). In this case, afferences from mPF cortical areas, and to some extent hippocampus and amygdala where CB_1 receptor is highly expressed would be contributing to the sparse CB_1 immunostaining in this territory (Herkenham, Lynn, de Costa, et al., 1991; Mailleux & Vanderhaeghen, 1992; Voorn et al., 2004). Overall, contribution to CB_1 immunostaining from striatal interneurons is probably low since they represent $< 3\%$ of the total number of striatal neurons, even though some of them express CB_1 receptor (Hohmann & Herkenham, 2000; Martín et al., 2008; Oorschot et al., 2002).

Additionally, we did not find any topographical difference in CB_1 receptor expression under conditions of low DA, although the higher CB_1 expression in the striatal SM territory in comparison to the mPF territory was preserved in 6-OHDA-lesioned animals. In

agreement with our observations, using the unilateral-MFB 6-OHDA rat model, no changes in CB_1 receptor binding in the BG have been described, measured by $[^3H]$-WIN-55,212-2 autoradiography 7-10 weeks after the lesion (Romero et al., 2000), by immunohistochemistry at different post-lesion time points (Walsh et al., 2010), or by mRNA *in situ* hybridization histochemistry (Zeng et al., 1999). More recently, similar results have been reported in MPTP parkinsonian monkeys (Rojo-Bustamante et al., 2018). Data coming from PD patients *post mortem* brain tissue are inconclusive, showing increased (Lastres-Becker et al., 2001) or no changes (Farkas et al., 2012) in CB_1 receptor binding or decreased receptor expression measured through mRNA (Hurley et al., 2003).

Taking into account these results, we can conclude that, in our experimental conditions, CB_1 receptor expression in the BG nuclei is not affected by DA denervation, suggesting that the loss of cannabinoid modulation on cortico-BG circuits could be due to a mechanism related to an alteration in CB_1 receptor functionality. In this sense, current evidence also shows some discrepancies, describing increased activation of GTP-binding proteins in PD patients treated with L-DOPA and MPTP marmosets (Lastres-Becker et al., 2001), as well as no changes in 6-OHDA-lesioned rats (Romero et al., 2000). In our experimental model, and according to the observed results, we hypothesize that after 4-5 weeks of inducing DA denervation by unilateral-MFB 6-OHDA injection, CB_1 receptor hyposensitivity to cannabinoid drugs occurs within the cortico-BG circuits, explaining the lack of modulation in these networks.

5.2.3. *Conclusion*

Results gathered in this study show hyperactive SNr neurons in lateral and medial territories of this nucleus, consistent with the known hyperactive state of the STN in 6-OHDA PD models, although other mechanisms might be involved. Several alterations through the SM and mPF BG circuits are observed because of DA denervation. Although some concur with the classical model of the BG circuits in low DA conditions, results herein challenge this view and suggest that complex changes take place along the BG circuits after DA denervation, affecting the final output of these circuits. After 6-OHDA lesion

cannabinoids lose their ability to decrease cortical information processing through the direct and indirect pathways of the SM and mPF BG circuit, although they gain control over the hyperdirect pathway of the SM circuits. These changes in cannabinoid modulation of the BG circuits were not related with changes in CB_1 receptor expression in the BG nuclei, suggesting changes in CB_1 receptor functionality.

5.3.   Study III: Cannabinoid modulation of cortico-striatal networks

This study brings to light differences in the cortically-evoked responses of putative MSNs and the oscillatory activity of SM and mPF cortico-striatal networks. CB_1 receptor activation only affects cortico-striatal connectivity between MC and the dorsolateral striatum, while having no effects on cortico-striatal connectivity between ACC and the dorsomedial striatum. Moreover, the effects of cannabinoids on cortical and local SWA suggest a differential modulation of CB_1 receptor agonists on the studied frequency bands, together with the ability of CB_1 receptor antagonists to change brain state in anaesthetized rats.

5.3.1. Spontaneous, cortically-evoked and oscillatory activity differential characteristics of SM and mPF cortico-striatal networks

In this study spontaneously active putative MSNs displayed a low FR during SWA, similar to that observed in other studies with rodents under anaesthesia, were MSNs from different striatal functional territories (i.e., dorsolateral or dorsomedial) or pathways (i.e., direct or indirect) were undistinguishable in terms of their spontaneous activity (Alegre-Cortés et al., 2021; Huerta-Ocampo et al., 2014; Mallet et al., 2005; Sharott et al., 2012, 2017). The firing of MSNs in the dorsolateral and dorsomedial striatum is generally phase-locked to cortical SWA and no difference was found regarding the phase angle between direct and indirect-pathway MSNs, in agreement with previous data (Huerta-Ocampo et al., 2014; Sharott et al., 2012, 2017). However, putative MSNs in the dorsolateral striatum present a reduced vector length, suggesting a more variable phase firing in relation to cortical SWA.

Regarding the cortically-evoked responses in putative MSNs after cortical stimulation, neurons in the dorsolateral striatum show responses with smaller latencies and higher amplitudes after MC stimulation, than those putative MSNs in the dorsomedial striatum after ACC stimulation. Higher amplitude of cortically-evoked responses from putative MSNs in the dorsolateral striatum could reflect higher amounts of AMPA receptors

in this striatal territory (Nicolle & Baxter, 2003). As shown in study I and II, responses in the SM BG circuits have lower latencies than those form mPF BG circuits. In this case, the distance that cortical projections have to travel until reaching the striatum could underlie differences between dorsolateral and dorsomedial functional territories of the striatum in the latencies observed in putative MSNs. However, latencies in our study were shorter than those reported in other studies. This discrepancy is likely due to differences in the way latency was calculated in each study (Mallet et al., 2005, 2006; Sharott et al., 2012).

Additionally, indirect-pathway MSNs show higher duration in cortically-evoked responses than direct-pathway MSNs. Given the way response duration is conceived in this study, this higher duration could be differently interpreted regarding neuronal physiology. Increased inter-stimulation variability in latency after cortical stimulation could be translated into an increased duration. However, this hypothesis seems unlikely given the less inter-stimulation variability reported for indirect-pathway MSNs in comparison to direct-pathway MSNs (Mallet et al., 2006). Moreover, an increased ability for indirect-pathway MSNs to fire more than one spike per stimulation could also explain the observed increase in duration, although normally MSNs fire one single spike per stimulation trial (Sharott et al., 2012). However, in line with this hypothesis, *in vitro* studies have shown a higher FR in indirect-pathway MSNs after cortical stimulation than direct-pathway MSNs, together with higher neurotransmitter release probability and smaller firing threshold (Cepeda et al., 2008; Flores-Barrera et al., 2010; Kreitzer & Malenka, 2007; Maurice, Liberge, et al., 2015). On the other hand, *in vivo* recordings show that direct-pathway MSNs are more readily activated after cortical stimulation (Escande et al., 2016). It is worth mentioning that the observed differences in cortically-evoked responses might be influenced by striatal interneurons differently modulating striatal functional territories and MSN subpopulations (Fino et al., 2018; Garas et al., 2016). On top of this, the reduced sample size, and the possible participation of other factors in this particular result (i.e., striatal territory or sex) calls for caution when interpreting these results.

In line with previous reports in anaesthetized animals, cortical and local oscillations during SWA show a dominant frequency in the δ band around 1 Hz, together with a predominant contribution of this frequency band to the activity of SM and mPF cortico-striatal networks (Alegre-Cortés et al., 2021; Garas et al., 2016; Mallet et al., 2005, 2006; Sharott et al., 2017). Despite this, δ frequency band contribution to the ACC ECoG signal was higher than its contribution to the MC signal, together with a higher contribution of the rest of the studied frequency bands (i.e., θ, α, β and γ) to the MC ECoG signal. During slow-wave sleep in humans, slow oscillations are likely generated in fronto-central cortical regions, expanding from there (Massimini et al., 2004). Moreover, a similar observation has been made in ketamine-anaesthetized rats (Ruiz-Mejias et al., 2011). Therefore, this could explain the higher presence of δ frequency oscillations in fronto-central cortical structures such as the ACC of the rat, where this SWA would originate. In line with this, coherence in the mPF cortico-striatal network is greater than that in the SM cortico-striatal network in the δ frequency band.

Additionally, females show smaller dominant frequencies than males in both cortical and striatal power spectra, which might reflect a higher sensibility to the anaesthetic regime. In fact, some studies report different pharmacokinetics in female rats after intraperitoneal administration of anaesthetic agents, leading to increased anaesthetic concentrations (Mansouri et al., 2019; Saland & Kabbaj, 2018). Contrary to this hypothesis is the decreased δ frequency band in females. This decrease would argue against an increased effect of anaesthesia in females. However, this would not be explainable by changes in the contribution of other frequency bands, but might account for the range of frequencies defining δ band in this work (i.e., 0.6 – 4 Hz). Therefore, this decrease is likely to be due to increases in the AUC below 0.6 Hz, which would support the idea of a higher sensibility of females to the anaesthetic regime used. Anyway, differences reported herein regarding the effects of sex on cortical and local oscillations should be taken with caution given the reduced sample size, together with the possible effect of other factors (i.e., direct-indirect pathway MSNs or striatal territory).

5.3.2. Cannabinoids alter spontaneous, cortically-evoked and oscillatory activity in SM and mPF cortico-striatal networks

Cannabinoids were able to modulate spontaneous activity of putative MSNs in the dorsolateral and dorsomedial striatum. After administration of WIN putative MSNs in both striatal functional territories were silenced, without producing any changes in cortical SWA (i.e., δ frequency band) to which these neurons were phase-locked to. Functional CB_1 receptors are present at cortico-striatal synapses, modulating cortical input onto MSNs. A possible explanation to the inhibition of WIN on spontaneous firing would be the obstruction of cortico-striatal transmission by activation of the CB_1 receptor in cortico-striatal terminals, thus decreasing glutamate release and 'disconnecting' striatal circuits from cortical activity dynamics (Gerdeman & Lovinger, 2001; Kreitzer & Malenka, 2007). Moreover, subsequent administration of the CB_1-selective antagonist AM251 was not able to reverse the effect of WIN on spontaneous activity. At first glance, this suggests a non-CB_1-dependent mechanism to the effect of WIN. However, administration of AM251 induced changes in cortical oscillatory activity, decreasing the δ frequency band and increasing the contribution of higher frequency bands (i.e., θ, α, β and γ), thus recreating a state of 'cortical activation' that has been proven to silence MSNs by fast-spiking interneuron feed-forward inhibition (Magill et al., 2006; Mallet et al., 2005). This way, the effect of AM251 on cortical activity would mask the exact participation of the CB_1 receptor in the effects exerted by WIN, leaving the role of the CB_1 receptor on the spontaneous activity of putative MSNs yet to be determined. Data in this study suggest that WIN and AM251 administration might have a similar effect on the spontaneous activity of putative MSNs in anaesthetized rats by inducing different changes in cortico-striatal network dynamics. In this scenario, while WIN administration might hypothetically disrupt connection between cortex and striatum, AM251 would disrupt cortical SWA, producing in both cases the silencing of putative MSNs observed in this study. In line with this, other studies evidence the deep changes striatal activity suffers in relationship to cortical oscillatory activity (i.e., SWA, 'cortical activation' state) (Magill et al., 2006; Mallet et al., 2005; Sharott et al., 2012, 2017; Zold et al., 2012).

Furthermore, administration of WIN was able to differently modulate cortically-evoked responses in dorsolateral and dorsomedial putative MSNs. The expected result was a decrease in cortically-evoked responses, especially in neurons from the dorsomedial striatum, since mPF cortico-striatal terminals express a higher amount of CB_1 receptors in comparison to MC (Heng et al., 2011). However, administration of WIN was able to increase the cortically-evoked response in putative MSNs from the dorsolateral striatum after MC stimulation, in a CB_1-dependent manner. On the other hand, neither of the cannabinoid drugs used (i.e., WIN and AM251) had any effect on the cortically-evoked response of putative MSNs in the dorsomedial striatum after ACC stimulation. Most of the CB_1 receptor expression detected in cortex is found in interneurons, rather than in pyramidal projection neurons (Bodor et al., 2005; Mailleux & Vanderhaeghen, 1992; Marsicano & Lutz, 1999). Therefore is possible that the low dose of WIN used in this study, together with the high intensity of cortical stimulation procedures, may have overridden a hypothetical CB_1-receptor-mediated decrease in glutamate neurotransmission from cortico-striatal terminals. Moreover, cortically-evoked responses of putative MSNs in the dorsomedial striatum after ACC stimulation, where CB_1 receptor expression is higher, was unchanged after WIN administration (Heng et al., 2011; Mailleux & Vanderhaeghen, 1992). Therefore, disinhibition of pyramidal projecting neurons in cortex after activation of CB_1 receptors at GABAergic interneuron-pyramidal neuron synapses is not likely to explain our results (Bodor et al., 2005). This is also consistent with the subtle effect WIN had on cortical oscillations in SM and mPF cortico-striatal networks in this study, suggesting mild changes in the activity pattern of cortical neurons. In a similar experimental setting, fast-spiking interneurons demonstrated to inhibit MSNs spontaneous and cortically-evoked activity, showing to control MSN activity (Mallet et al., 2005). Moreover, fast-spiking interneurons and MSNs show similar CB_1 receptor expression (Hohmann & Herkenham, 2000; Martín et al., 2008). Therefore, CB_1 receptor activation might be obstructing GABA release at fast-spiking interneuron-MSN synapses, ultimately disinhibiting MSNs. In support of this hypothesis, fast-spiking interneurons in the *nucleus accumbens* provide an inhibitory input to MSNs that is reduced upon CB_1 receptor activation (Wright et al., 2017). Moreover, in this same study, authors also find that inhibitory input provided by collaterals from other MSNs is not affected by the activation of the CB_1 receptor (Wright et al., 2017). In additional support of

this hypothesis, a similar mechanism has been described *in vitro* in the dorsolateral striatum, where CB$_1$ receptor reduces fast-spiking interneuron-MSN neurotransmission (Narushima et al., 2006). In agreement with data in this study, this phenomenon might be more relevant in the dorsolateral striatum, where parvalbumin-expressing interneurons (i.e., fast-spiking interneurons) are more abundant (Fino et al., 2018; Gerfen et al., 1985). However, the participation of collaterals from other MSNs in the dorsolateral striatum should not be ruled out, given the high CB$_1$ receptor expression in this area in comparison to the *nucleus accumbens* (Herkenham, Lynn, Johnson, et al., 1991; Julian et al., 2003; Mailleux & Vanderhaeghen, 1992).

Most of the studies addressing the effect of cannabinoids on cortical or local oscillations have been made in awake animals and humans (Cortes-Briones et al., 2015; Hernandez & Cheer, 2012; Kucewicz et al., 2011; Liao et al., 2020; Ohiorhenuan et al., 2014; Robbe et al., 2006; Sales-Carbonell et al., 2013; Skosnik et al., 2018). In this study, while WIN administration was not able to induce any changes in the cortical oscillatory activity of the MC, oscillatory activity in the ACC was affected after cannabinoid drug administration, in line with the higher CB$_1$ receptor expression found in mPF cortex (Heng et al., 2011). Administration of WIN induced an increase in θ and β frequency bands and reduced γ band in the ACC ECoG. Some studies show a decrease in the θ and γ frequency band in the mPF cortex after administration of CB$_1$ receptor agonists in animals and humans (Cortes-Briones et al., 2015; Ilan et al., 2004; Kucewicz et al., 2011; Nelong et al., 2019). Moreover, alterations in θ, β and γ frequency bands have been related with perceptual abnormalities observed in psychosis and working memory impairments, altered states known to be caused by cannabis intoxication (Ilan et al., 2004; Javitt et al., 2018; Nottage et al., 2015; Skosnik et al., 2016; Wilkinson et al., 2014). Differences between results in this study and others might stem mainly from differences in the arousal state of the animals, since rats in this study were deeply anaesthetized.

WIN administration induced little changes in the SM cortico-striatal network, just reducing the γ band frequency contribution to the LFP signal from the dorsolateral striatum. Similarly, administration of WIN also reduced this frequency band in the dorsomedial

striatum LFP. In the ventral striatum, γ band has been reported to follow a dorsoventral gradient and is related with reward and movement, among other functions (Berke et al., 2004; van der Meer et al., 2010). This band is particularly increased before movement initiation (Masimore et al., 2005; van der Meer & Redish, 2009). The effect of WIN on reducing γ striatal oscillations might lay the origin for the motor impairments cannabis users experience (Boggs et al., 2018; Schreiner & Dunn, 2012). In addition to changes in the γ band in the dorsomedial striatum, WIN administration decreased θ oscillations in this territory. It has been proposed that some frequency bands in the striatal LFP –specially the θ band–, might be 'contaminated' by signal from other nucleus (Lalla et al., 2017). In this work, authors propose the hippocampus to be a source of θ contamination in striatal LFPs. In line with this, administration of CB$_1$ receptor agonists induced a θ band decrease in the hippocampus (Robbe et al., 2006). Therefore, the decreased θ band observed in this study might underlie changes in hippocampal synchrony.

In order to establish a relationship between the observed changes in SM and mPF cortico-striatal networks and CB$_1$ receptor activation, AM251 was administered. However, although some effects were 'reverted' after the administration of this CB$_1$ receptor antagonist, other changes were in the same direction that those observed after WIN administration. Moreover, in both of the cortico-striatal networks studied a similar effect was observed: AM251 administration reduced δ band contribution to cortical and local activity, together with a decrease in cortico-striatal coherence at this band, and generally provoked an increase in higher frequency bands (i.e., θ, α, β and γ) in cortical and local activity, as well as in coherence. This pattern of SWA decreased, together with an increase in higher frequency bands has been observed after the transition from cortical SWA to 'cortical activation', induced by a sensory stimulus on an anaesthetized rat (Magill et al., 2006). Therefore, is not possible to draw any conclusions about CB$_1$ receptor involvement in the changes induced by WIN nor the effect endocannabinoids might have on the oscillatory activity. Nevertheless, is clear that the administration of WIN, followed by AM251 administration, changed the functional state of the network towards a state resembling that of an awake animal. This shift from SWA to cortical activation is accomplished after sensory stimulus, normally nociceptive. Therefore, one possibility is that AM251 administration increases nociception,

causing the shift from SWA to cortical activation. In line with this, the CB_1 receptor is a proposed target for nociception, and its blockade by AM251, increases nociceptive response (Guindon et al., 2007; Woodhams et al., 2015). Moreover, CB_1 receptor knock-out mice spent more time awake, suggesting that CB_1 receptor blockade might induce aroused states (Silvani et al., 2014).

5.3.3. Conclusion

In summary, data from this study, show differences in cortically-evoked responses between putative MSNs from the dorsolateral and dorsomedial striatum. Moreover, CB_1 receptor activation differently affected cortico-striatal transmission selectively enhancing cortical input onto putative MSNs from the dorsolateral striatum, with no effect on cortico-striatal transmission onto dorsomedial striatum putative MSNs. This observation relate with CB1 receptor expression in the striatum, but could also suggest the participation of striatal fast-spiking interneurons, placing them at a central spot in the regulation of cortico-striatal information transmission mediated by cannabinoids. Consistent with CB_1 receptor expression, in this study, ACC SWA was more sensible than MC to CB_1 receptor drugs, which also altered frequency bands related with functions affected after cannabis use. Moreover, the CB_1 receptor agonist silenced putative MSNs in both territories in a way that was not reversed by CB_1 receptor antagonism, and that might be related with effects of the antagonist on brain state.

6. CONCLUSIONS

6. CONCLUSIONS

The results obtained in the aforementioned studies lead us to the following conclusions:

1. In control animals, spontaneous activity of lateral and medial SNr neurons is different, especially in those neurons exhibiting burst firing pattern.

2. The electrophysiological characteristics of the responses from the SM and mPF BG circuits indicate that cortical information processing through these circuits takes place differently, showing shorter latencies in the three pathways, and longer duration in the direct pathway of the SM BG circuits.

3. CB_1 receptor differently modulates cortical information transmission through the SM or mPF BG circuits. Cortico-nigral transmission through the direct and indirect pathways in both circuits is reduced upon activation of this receptor. However, transmission through the hyperdirect pathway is only impaired in the mPF circuits, while showing reduced sensitivity to CB_1 receptor activation in the SM BG circuits.

4. DA denervation induced by unilateral 6-OHDA injection in the MFB produces electrophysiological changes in the spontaneous activity of lateral and medial SNr neurons, displaying more irregular and burst firing patterns, suggesting that DA denervation induces hyperactivity in these neuronal populations.

5. DA denervation leads to deficits in cortical information selection through the SM and mPF BG circuits, specially affecting the SM circuits. The hyperdirect and direct pathways show electrophysiological alterations in both BG circuits. In the SM BG circuits cortico-nigral transmission is enhanced through the hyperdirect

pathway, while in the mPF BG circuits this transmission is enhanced through the direct pathway.

6. CB_1-mediated modulation of cortico-nigral transmission through the direct and indirect pathways of the SM and mPF BG circuits is lost after DA denervation, while CB_1 receptor agonism gains control over the transmission through the hyperdirect pathway of the SM BG circuits.

7. CB_1 receptor expression in the BG nuclei is not affected after DA denervation, suggesting that the loss of cannabinoid modulation on cortico-nigral transmission through both BG circuits might reflect an alteration in CB_1 receptor functionality after DA denervation.

8. In control rats, putative MSNs from the dorsolateral and dorsomedial striatum respond differently to cortical stimulation. Moreover, during states of slow cortical oscillatory activity the mPF cortico-striatal network is more synchronized in the δ band.

9. Activation of the CB_1 receptor selectively enhances responses to cortical stimulation in putative MSNs from the dorsolateral striatum, with no effects on the cortically-evoked response of putative MSNs from the dorsomedial striatum. This suggests that CB_1 receptor activation disinhibit putative MSNs by acting on a circuit component involved in cortico-striatal transmission, especially in the dorsolateral striatum.

10. Systemic CB_1 receptor activation induces changes in slow cortical oscillatory activity in the SM and mPF cortico-striatal networks, especially in the latter, altering θ, β and γ frequency bands. On the other hand, CB_1 receptor antagonism alters nearly all frequency bands in both cortico-striatal networks.

In summary, the present results indicate that cortical information transfer through the SM and mPF BG circuits is differently processed. Moreover, CB_1 receptor activation impairs information transmission through both BG circuits, differently affecting the transmission through the hyperdirect pathway. DA denervation induced by 6-OHDA modifies cortico-nigral transmission through both BG circuits, especially affecting the SM circuits. Moreover, DA denervation differently affects the modulatory role of CB_1 receptor on cortico-nigral transmission through these circuits, in a way that suggests changes in CB_1 receptor functionality. Further assessment on the role of CB_1 receptor activation in the SM and mPF BG circuits reveals to especifically affect cortico-striatal transmission onto the dorsolateral striatum.

Overall, these findings contribute to the better understanding of the CB_1 receptor-mediated modulation of cortico-BG information processing in physiological condition and in pathologies where DA neurotransmission is compromised, such as PD. Moreover, the present data indicate that the endocannabinoid system may represent a promising target in the development of new therapies for several pathologies related with cortico-BG transmission dysfunctionallity.

7. BIBLIOGRAPHY

7. Bibliography

Aarsland, D., Marsh, L., & Schrag, A. (2009). Neuropsychiatric symptoms in Parkinson's disease. *Movement Disorders*, *24*(15), 2175–2186. https://doi.org/10.1002/mds.22589

Abdi, A., Mallet, N., Mohamed, F. Y., Sharott, A., Dodson, P. D., Nakamura, K. C., Suri, S., Avery, S. V., Larvin, J. T., Garas, F. N., Garas, S. N., Vinciati, F., Morin, S., Bezard, E., Baufreton, J., & Magill, P. J. (2015). Prototypic and arkypallidal neurons in the dopamine-intact external globus pallidus. *Journal of Neuroscience*, *35*(17), 6667–6688. https://doi.org/10.1523/JNEUROSCI.4662-14.2015

Afsharpour, S. (1985a). Light microscopic analysis of golgi-impregnated rat subthalamic neurons. *Journal of Comparative Neurology*, *236*(1), 1–13. https://doi.org/10.1002/cne.902360102

Afsharpour, S. (1985b). Topographical projections of the cerebral cortex to the subthalamic nucleus. *The Journal of Comparative Neurology*, *236*(1), 14–28. https://doi.org/10.1002/cne.902360103

Aguado, T., Monory, K., Palazuelos, J., Stella, N., Cravatt, B., Lutz, B., Marsicano, G., Kokaia, Z., Guzmán, M., & Galve-Roperh, I. (2005). The endocannabinoid system drives neural progenitor proliferation. *The FASEB Journal*, *19*(12), 1704–1706. https://doi.org/10.1096/fj.05-3995fje

Alam, Z. I., Daniel, S. E., Lees, A. J., Marsden, D. C., Jenner, P., & Halliwell, B. (1997). A generalised increase in protein carbonyls in the brain in Parkinson's but not incidental Lewy body disease. *Journal of Neurochemistry*, *69*(3), 1326–1329. https://doi.org/10.1046/j.1471-4159.1997.69031326.x

Alam, Z. I., Jenner, A., Daniel, S. E., Lees, A. J., Cairns, N., Marsden, C. D., Jenner, P., & Halliwell, B. (1997). Oxidative DNA damage in the parkinsonian brain: An apparent selective increase in 8-hydroxyguanine levels in substantia nigra. *Journal of Neurochemistry*, *69*(3), 1196–1203. https://doi.org/10.1046/j.1471-4159.1997.69031196.x

7. Bibliography

Albin, R. L., Young, A. B., & Penney, J. B. (1989). The functional anatomy of basal ganglia disorders. *Trends in Neurosciences, 12*(10), 366–375. https://doi.org/10.1016/0166-2236(89)90074-X

Alegre-Cortés, J., Sáez, M., Montanari, R., & Reig, R. (2021). Medium spiny neurons activity reveals the discrete segregation of mouse dorsal striatum. *ELife, 10*, e60580. https://doi.org/10.7554/eLife.60580

Alexander, G. E., DeLong, M. R., & Strick, P. L. (1986). Parallel organization of functionally segregated circuits linking basal ganglia and cortex. *Annual Review of Neuroscience, VOL. 9*(1), 357–381. https://doi.org/10.1146/annurev.ne.09.030186.002041

Aliane, V., Pérez, S., Nieoullon, A., Deniau, J.-M., & Kemel, M.-L. (2009). Cocaine-induced stereotypy is linked to an imbalance between the medial prefrontal and sensorimotor circuits of the basal ganglia. *European Journal of Neuroscience, 30*(7), 1269–1279. https://doi.org/10.1111/j.1460-9568.2009.06907.x

Ambrosi, G., Cerri, S., & Blandini, F. (2014). A further update on the role of excitotoxicity in the pathogenesis of Parkinson's disease. *Journal of Neural Transmission, 121*(8), 849–859. https://doi.org/10.1007/s00702-013-1149-z

Anderson, C., Sheppard, D., & Dorval, A. D. (2020). Parkinsonism and subthalamic deep brain stimulation dysregulate behavioral motivation in a rodent model. *Brain Research, 1736*, 146776. https://doi.org/10.1016/j.brainres.2020.146776

Aoki, S., Smith, J. B., Li, H., Yan, X., Igarashi, M., Coulon, P., Wickens, J. R., Ruigrok, T. J. H., & Jin, X. (2019). An open cortico-basal ganglia loop allows limbic control over motor output via the nigrothalamic pathway. *ELife, 8*, e49995. https://doi.org/10.7554/eLife.49995

Arbuthnott, G. W., & Wickens, J. (2007). Space, time and dopamine. *Trends in Neurosciences, 30*(2), 62–69. https://doi.org/10.1016/j.tins.2006.12.003

Aristieta, A., Azkona, G., Sagarduy, A., Miguelez, C., Ruiz-Ortega, J. Á., Sanchez-Pernaute, R., & Ugedo, L. (2012). The role of the subthalamic nucleus in L-DOPA induced dyskinesia in 6-hydroxydopamine lesioned rats. *PLoS ONE, 7*(8), e42652. https://doi.org/10.1371/journal.pone.0042652

Aristieta, A., Ruiz-Ortega, J. A., Miguelez, C., Morera-Herreras, T., & Ugedo, L. (2016). Chronic L-DOPA administration increases the firing rate but does not reverse enhanced slow frequency oscillatory activity and synchronization in substantia nigra pars reticulata neurons from 6-hydroxydopamine-lesioned rats. *Neurobiology of Disease*, *89*, 88–100. https://doi.org/10.1016/j.nbd.2016.02.003

Ascherio, A., & Schwarzschild, M. A. (2016). The epidemiology of Parkinson's disease: Risk factors and prevention. *The Lancet Neurology*, *15*(12), 1257–1272. https://doi.org/10.1016/S1474-4422(16)30230-7

Assous, M., Faust, T. W., Assini, R., Shah, F., Sidibe, Y., & Tepper, J. M. (2018). Identification and Characterization of a Novel Spontaneously Active Bursty GABAergic Interneuron in the Mouse Striatum. *Journal of Neuroscience*, *38*(25), 5688–5699. https://doi.org/10.1523/JNEUROSCI.3354-17.2018

Atwood, B. K., Kupferschmidt, D. A., & Lovinger, D. M. (2014). Opioids induce dissociable forms of long-term depression of excitatory inputs to the dorsal striatum. *Nature Neuroscience*, *17*(4), 540–548. https://doi.org/10.1038/nn.3652

Auclair, N., Otani, S., Soubrie, P., & Crepel, F. (2000). Cannabinoids modulate synaptic strength and plasticity at glutamatergic synapses of rat prefrontal cortex pyramidal neurons. *Journal of Neurophysiology*, *83*(6), 3287–3293. https://doi.org/10.1152/jn.2000.83.6.3287

Báez-Cordero, A. S., Pimentel-Farfan, A. K., Peña-Rangel, T., & Rueda-Orozco, P. E. (2020). Unbalanced Inhibitory/excitatory responses in the substantia nigra pars reticulata underlie cannabinoid-related slowness of movements. *The Journal of Neuroscience*, *40*(30), 5769–5784. https://doi.org/10.1523/JNEUROSCI.0045-20.2020

Ball, N., Teo, W. P., Chandra, S., & Chapman, J. (2019). Parkinson's disease and the environment. *Frontiers in Neurology*, *10*. https://doi.org/10.3389/fneur.2019.00218

Balleine, B. W., & O'Doherty, J. P. (2010). Human and rodent homologies in action control: Corticostriatal determinants of goal-directed and habitual action. *Neuropsychopharmacology*, *35*(1), 48–69. https://doi.org/10.1038/npp.2009.131

Belin, D., & Everitt, B. J. (2008). Cocaine Seeking Habits Depend upon Dopamine-Dependent Serial Connectivity Linking the Ventral with the Dorsal Striatum. *Neuron*, *57*(3), 432–441. https://doi.org/10.1016/j.neuron.2007.12.019

7. Bibliography

Benabid, A. L., Pollak, P., Gross, C., Hoffmann, D., Benazzouz, A., Gao, D. M., Laurent, A., Gentil, M., & Perret, J. (1994). Acute and long-term effects of subthalamic nucleus stimulation of Parkinson's disease. *Stereotactic and Functional Neurosurgery*, *62*(1–4), 76–84. https://doi.org/10.1159/000098600

Bénard, G., Massa, F., Puente, N., Lourenço, J., Bellocchio, L., Soria-Gómez, E., Matias, I., Delamarre, A., Metna-Laurent, M., Cannich, A., Hebert-Chatelain, E., Mulle, C., Ortega-Gutiérrez, S., Martín-Fontecha, M., Klugmann, M., Guggenhuber, S., Lutz, B., Gertsch, J., Chaouloff, F., … Marsicano, G. (2012). Mitochondrial CB 1 receptors regulate neuronal energy metabolism. *Nature Neuroscience*, *15*(4), 558–564. https://doi.org/10.1038/nn.3053

Benito, C., Tolón, R. M., Pazos, M. R., Núñez, E., Castillo, A. I., & Romero, J. (2008). Cannabinoid CB2 receptors in human brain inflammation. *British Journal of Pharmacology*, *153*(2), 277–285. https://doi.org/10.1038/sj.bjp.0707505

Berendse, H. W., Graaf, Y. G., & Groenewegen, H. J. (1992). Topographical organization and relationship with ventral striatal compartments of prefrontal corticostriatal projections in the rat. *Journal of Comparative Neurology*, *316*(3), 314–347. https://doi.org/10.1002/cne.903160305

Berendse, H. W., & Groenewegen, H. J. (1991). The Connections of the Medial Part of the Subthalamic Nucleus in the Rat: Evidence for a Parallel Organization. In G. Bernardi, M. B. Carpenter, G. Di Chiara, M. Morelli, & P. Stanzione (Eds.), *The Basal Ganglia III* (pp. 89–98). Springer New York. https://doi.org/10.1007/978-1-4684-5871-8_10

Berens, P. (2009). CircStat: A MATLAB Toolbox for Circular Statistics. *Journal of Statistical Software*, *31*(10), 1–21. https://doi.org/10.18637/jss.v031.i10

Bergman, H., Wichmann, T., Karmon, B., & DeLong, M. R. (1994). The primate subthalamic nucleus. II. Neuronal activity in the MPTP model of parkinsonism. *Journal of Neurophysiology*, *72*(2), 507–520. https://doi.org/10.1152/jn.1994.72.2.507

Berke, J. D., Okatan, M., Skurski, J., & Eichenbaum, H. B. (2004). Oscillatory entrainment of striatal neurons in freely moving rats. *Neuron*, *43*(6), 883–896. https://doi.org/10.1016/j.neuron.2004.08.035

Bevan, M. D., Booth, P. A. C., Eaton, S. A., & Bolam, J. P. (1998). Selective innervation of neostriatal interneurons by a subclass of neuron in the globus pallidus of the rat.

Journal of Neuroscience, *18*(22), 9438–9452. https://doi.org/10.1523/JNEUROSCI.18-22-09438.1998

Beyeler, A., Kadiri, N., Navailles, S., Boujema, M. B., Gonon, F., Moine, C. L., Gross, C., & De Deurwaerdère, P. (2010). Stimulation of serotonin2C receptors elicits abnormal oral movements by acting on pathways other than the sensorimotor one in the rat basal ganglia. *Neuroscience*, *169*(1), 158–170. https://doi.org/10.1016/j.neuroscience.2010.04.061

Bhattacharyya, S., Falkenberg, I., Martin-Santos, R., Atakan, Z., Crippa, J. A., Giampietro, V., Brammer, M., & McGuire, P. (2015). Cannabinoid Modulation of Functional Connectivity within Regions Processing Attentional Salience. *Neuropsychopharmacology*, *40*(6), 1343–1352. https://doi.org/10.1038/npp.2014.258

Birkmayer, W., & Hornykiewicz, O. (1961). [The L-3,4-dioxyphenylalanine (DOPA)-effect in Parkinson-akinesia]. *Wiener Klinische Wochenschrift*, *73*, 787–788.

Blanco-Hinojo, L., Pujol, J., Harrison, B. J., Macià, D., Batalla, A., Nogué, S., Torrens, M., Farré, M., Deus, J., & Martín-Santos, R. (2017). Attenuated frontal and sensory inputs to the basal ganglia in cannabis users. *Addiction Biology*, *22*(4), 1036–1047. https://doi.org/10.1111/adb.12370

Blázquez, C., Chiarlone, A., Bellocchio, L., Resel, E., Pruunsild, P., García-Rincón, D., Sendtner, M., Timmusk, T., Lutz, B., Galve-Roperh, I., & Guzmán, M. (2015). The CB1 cannabinoid receptor signals striatal neuroprotection via a PI3K/Akt/mTORC1/BDNF pathway. *Cell Death and Differentiation*, *22*(10), 1618–1629. https://doi.org/10.1038/cdd.2015.11

Bloem, B. R., Hausdorff, J. M., Visser, J. E., & Giladi, N. (2004). Falls and freezing of gait in Parkinson's disease: A review of two interconnected, episodic phenomena. *Movement Disorders: Official Journal of the Movement Disorder Society*, *19*(8), 871–884. https://doi.org/10.1002/mds.20115

Bodor, Á. L., Katona, I., Nyíri, G., Mackie, K., Ledent, C., Hájos, N., & Freund, T. F. (2005). Endocannabinoid signaling in rat somatosensory cortex: Laminar differences and involvement of specific interneuron types. *Journal of Neuroscience*, *25*(29), 6845–6856. https://doi.org/10.1523/JNEUROSCI.0442-05.2005

7. Bibliography

Boggs, D. L., Cortes-Briones, J. A., Surti, T., Luddy, C., Ranganathan, M., Cahill, J. D., Sewell, A. R., D'Souza, D. C., & Skosnik, P. D. (2018). The dose-dependent psychomotor effects of intravenous delta-9-tetrahydrocannabinol (Δ9-THC) in humans. *Journal of Psychopharmacology*, *32*(12), 1308–1318. https://doi.org/10.1177/0269881118799953

Boraud, T., Bezard, E., Guehl, D., Bioulac, B., & Gross, C. (1998). Effects of L-DOPA on neuronal activity of the globus pallidus externalis (GPe) and globus pallidus internalis (GPi) in the MPTP-treated monkey. *Brain Research*, *787*(1), 157–160. https://doi.org/10.1016/S0006-8993(97)01563-1

Braak, H., Del Tredici, K., Rüb, U., De Vos, R. A. I., Jansen Steur, E. N. H., & Braak, E. (2003). Staging of brain pathology related to sporadic Parkinson's disease. *Neurobiology of Aging*, *24*(2), 197–211. https://doi.org/10.1016/S0197-4580(02)00065-9

Braak, H., Ghebremedhin, E., Rüb, U., Bratzke, H., & Del Tredici, K. (2004). Stages in the development of Parkinson's disease-related pathology. *Cell and Tissue Research*, *318*(1), 121–134. https://doi.org/10.1007/s00441-004-0956-9

Braz, B. Y., Belforte, J. E., Murer, M. G., & Galiñanes, G. L. (2017). Properties of the corticostriatal long term depression induced by medial prefrontal cortex high frequency stimulation in vivo. *Neuropharmacology*, *121*, 278–286. https://doi.org/10.1016/j.neuropharm.2017.05.001

Breivogel, C. S., Griffin, G., Di Marzo, V., & Martin, B. R. (2001). Evidence for a new G protein-coupled cannabinoid receptor in mouse brain. *Molecular Pharmacology*, *60*(1), 155–163. https://doi.org/10.1124/mol.60.1.155

Brents, L. K., Reichard, E. E., Zimmerman, S. M., Moran, J. H., Fantegrossi, W. E., & Prather, P. L. (2011). Phase I Hydroxylated Metabolites of the K2 Synthetic Cannabinoid JWH-018 Retain In Vitro and In Vivo Cannabinoid 1 Receptor Affinity and Activity. *PLOS ONE*, *6*(7), e21917. https://doi.org/10.1371/journal.pone.0021917

Brown, P., Oliviero, A., Mazzone, P., Insola, A., Tonali, P., & Lazzaro, V. D. (2001). Dopamine dependency of oscillations between subthalamic nucleus and pallidum in Parkinson's disease. *Journal of Neuroscience*, *21*(3), 1033–1038. https://doi.org/10.1523/JNEUROSCI.21-03-01033.2001

Brown, P., & Williams, D. (2005). Basal ganglia local field potential activity: Character and functional significance in the human. *Clinical Neurophysiology, 116*(11), 2510–2519. https://doi.org/10.1016/j.clinph.2005.05.009

Canteras, N. S., Shammah-Lagnado, S. J., Silva, B. A., & Ricardo, J. A. (1990). Afferent connections of the subthalamic nucleus: A combined retrograde and anterograde horseradish peroxidase study in the rat. *Brain Research, 513*(1), 43–59. https://doi.org/10.1016/0006-8993(90)91087-w

Carroll, C. B., Zeissler, M. L., Hanemann, C. O., & Zajicek, J. P. (2012). Δ9-tetrahydrocannabinol (Δ9-THC) exerts a direct neuroprotective effect in a human cell culture model of Parkinson's disease. *Neuropathology and Applied Neurobiology, 38*(6), 535–547. https://doi.org/10.1111/j.1365-2990.2011.01248.x

Carvalho, A. F., & Van Bockstaele, E. J. (2012). Cannabinoid modulation of noradrenergic circuits: Implications for psychiatric disorders. *Progress in Neuro-Psychopharmacology and Biological Psychiatry, 38*(1), 59–67. https://doi.org/10.1016/j.pnpbp.2012.01.008

Carvalho, M. M., Campos, F. L., Coimbra, B., Pêgo, J. M., Rodrigues, C., Lima, R., Rodrigues, A. J., Sousa, N., & Salgado, A. J. (2013). Behavioral characterization of the 6-hydroxidopamine model of Parkinson's disease and pharmacological rescuing of non-motor deficits. *Molecular Neurodegeneration, 8*(1), 14. https://doi.org/10.1186/1750-1326-8-14

Casteels, C., Lauwers, E., Baitar, A., Bormans, G., Baekelandt, V., & Van Laere, K. (2010). In vivo type 1 cannabinoid receptor mapping in the 6-hydroxydopamine lesion rat model of Parkinson's disease. *Brain Research, 1316*, 153–162. https://doi.org/10.1016/j.brainres.2009.12.026

Cebrián, C., Parent, A., & Prensa, L. (2005). Patterns of axonal branching of neurons of the substantia nigra pars reticulata and pars lateralis in the rat. *The Journal of Comparative Neurology, 492*(3), 349–369. https://doi.org/10.1002/cne.20741

Ceccarini, J., Casteels, C., Ahmad, R., Crabbé, M., Van de Vliet, L., Vanhaute, H., Vandenbulcke, M., Vandenberghe, W., & Van Laere, K. (2019). Regional changes in the type 1 cannabinoid receptor are associated with cognitive dysfunction in Parkinson's disease. *European Journal of Nuclear Medicine and Molecular Imaging, 46*(11), 2348–2357. https://doi.org/10.1007/s00259-019-04445-x

7. Bibliography

Cepeda, C., André, V. M., Yamazaki, I., Wu, N., Kleiman-Weiner, M., & Levine, M. S. (2008). Differential electrophysiological properties of dopamine D1 and D2 receptor-containing striatal medium-sized spiny neurons. *European Journal of Neuroscience, 27*(3), 671–682. https://doi.org/10.1111/j.1460-9568.2008.06038.x

Cerri, S., Levandis, G., Ambrosi, G., Montepeloso, E., Antoninetti, G. F., Franco, R., Lanciego, J. L., Baqi, Y., Müller, C. E., Pinna, A., Blandini, F., & Armentero, M. T. (2014). Neuroprotective potential of adenosine A2A and cannabinoid CB1 receptor antagonists in an animal model of Parkinson disease. *Journal of Neuropathology and Experimental Neurology, 73*(5), 414–424. https://doi.org/10.1097/NEN.0000000000000064

Chan, C. S., Glajch, K. E., Gertler, T. S., Guzman, J. N., Mercer, J. N., Lewis, A. S., Goldberg, A. B., Tkatch, T., Shigemoto, R., Fleming, S. M., Chetkovich, D. M., Osten, P., Kita, H., & Surmeier, D. J. (2011). HCN channelopathy in external globus pallidus neurons in models of Parkinson's disease. *Nature Neuroscience, 14*(1), 85–92. https://doi.org/10.1038/nn.2692

Chang, H. T., Kita, H., & Kitai, S. T. (1983). The fine structure of the rat subthalamic nucleus: An electron microscopic study. *The Journal of Comparative Neurology, 221*(1), 113–123. https://doi.org/10.1002/cne.902210110

Charcot, J. M. (1892). *Oeuvres complètes de J.M. Charcot. T.1-*.

Chaves-Kirsten, G. P., Mazucanti, C. H. Y., Real, C. C., Souza, B. M., Britto, L. R. G., & Torrão, A. S. (2013). Temporal Changes of CB1 Cannabinoid Receptor in the Basal Ganglia as a Possible Structure-Specific Plasticity Process in 6-OHDA Lesioned Rats. *PLoS ONE, 8*(10), e76874. https://doi.org/10.1371/journal.pone.0076874

Cheer, J. F., Marsden, C. A., Kendall, D. A., & Mason, R. (2000). Lack of response suppression follows repeated ventral tegmental cannabinoid administration: An in vitro electrophysiological study. *Neuroscience, 99*(4), 661–667. https://doi.org/10.1016/S0306-4522(00)00241-4

Cheer, J. F., Wassum, K. M., Heien, M. L. A. V., Phillips, P. E. M., & Wightman, R. M. (2004). Cannabinoids Enhance Subsecond Dopamine Release in the Nucleus Accumbens of Awake Rats. *Journal of Neuroscience, 24*(18), 4393–4400. https://doi.org/10.1523/JNEUROSCI.0529-04.2004

Cheramy, A., Leviel, V., & Glowinski, J. (1981). Dendritic release of dopamine in the substantia nigra. *Nature*, *289*(5798), 537–542. https://doi.org/10.1038/289537a0

Chevalier, G., & Deniau, J. M. (1990). Disinhibition as a basic process in the expression of striatal functions. *Trends in Neurosciences*, *13*(7), 277–280. https://doi.org/10.1016/0166-2236(90)90109-n

Chiu, C. Q., Puente, N., Grandes, P., & Castillo, P. E. (2010). Dopaminergic modulation of endocannabinoid-mediated plasticity at GABAergic synapses in the prefrontal cortex. *Journal of Neuroscience*, *30*(21), 7236–7248. https://doi.org/10.1523/JNEUROSCI.0736-10.2010

Chu, J., & Anderson, S. A. (2015). Development of Cortical Interneurons. *Neuropsychopharmacology*, *40*(1), 16–23. https://doi.org/10.1038/npp.2014.171

Chuhma, N., Tanaka, K. F., Hen, R., & Rayport, S. (2011). Functional Connectome of the Striatal Medium Spiny Neuron. *Journal of Neuroscience*, *31*(4), 1183–1192. https://doi.org/10.1523/JNEUROSCI.3833-10.2011

Chung, Y. C., Bok, E., Huh, S. H., Park, J.-Y., Yoon, S.-H., Kim, S. R., Kim, Y.-S., Maeng, S., Hyun Park, S., & Jin, B. K. (2011). Cannabinoid Receptor Type 1 Protects Nigrostriatal Dopaminergic Neurons against MPTP Neurotoxicity by Inhibiting Microglial Activation. *The Journal of Immunology*, *187*(12), 6508–6517. https://doi.org/10.4049/jimmunol.1102435

Chung, Y. C., Shin, W. H., Baek, J. Y., Cho, E. J., Baik, H. H., Kim, S. R., Won, S. Y., & Jin, B. K. (2016). CB2 receptor activation prevents glial-derived neurotoxic mediator production, BBB leakage and peripheral immune cell infiltration and rescues dopamine neurons in the MPTP model of Parkinson's disease. *Experimental and Molecular Medicine*, *48*(1), e205–e205. https://doi.org/10.1038/emm.2015.100

Ciliax, B. J., Heilman, C., Demchyshyn, L. L., Pristupa, Z. B., Ince, E., Hersch, S. M., Niznik, H. B., & Levey, A. I. (1995). The dopamine transporter: Immunochemical characterization and localization in brain. *Journal of Neuroscience*, *15*(3), 1714–1723. https://doi.org/10.1523/JNEUROSCI.15-03-01714.1995

Concannon, R. M., Okine, B. N., Finn, D. P., & Dowd, E. (2015). Differential upregulation of the cannabinoid CB2 receptor in neurotoxic and inflammation-driven rat models of

Parkinson's disease. *Experimental Neurology, 269*, 133–141. https://doi.org/10.1016/j.expneurol.2015.04.007

Cools, R., Barker, R. A., Sahakian, B. J., & Robbins, T. W. (2001). Enhanced or impaired cognitive function in Parkinson's disease as a function of dopaminergic medication and task demands. *Cerebral Cortex (New York, N.Y.: 1991), 11*(12), 1136–1143. https://doi.org/10.1093/cercor/11.12.1136

Cortes-Briones, J., Skosnik, P. D., Mathalon, D., Cahill, J., Pittman, B., Williams, A., Sewell, R. A., Ranganathan, M., Roach, B., Ford, J., & D'Souza, D. C. (2015). Δ9-THC Disrupts Gamma (γ)-Band Neural Oscillations in Humans. *Neuropsychopharmacology, 40*(9), 2124–2134. https://doi.org/10.1038/npp.2015.53

Corvaja, N., Doucet, G., & Bolam, J. P. (1993). Ultrastructure and synaptic targets of the raphe-nigral projection in the rat. *Neuroscience, 55*(2), 417–427. https://doi.org/10.1016/0306-4522(93)90510-m

Coupland, K. G., Mellick, G. D., Silburn, P. A., Mather, K., Armstrong, N. J., Sachdev, P. S., Brodaty, H., Huang, Y., Halliday, G. M., Hallupp, M., Kim, W. S., Dobson-Stone, C., & Kwok, J. B. J. (2014). DNA methylation of the MAPT gene in Parkinson's disease cohorts and modulation by vitamin E In Vitro. *Movement Disorders: Official Journal of the Movement Disorder Society, 29*(13), 1606–1614. https://doi.org/10.1002/mds.25784

Cragg, S. J., Rice, M. E., & Greenfield, S. A. (1997). Heterogeneity of electrically evoked dopamine release and reuptake in substantia nigra, ventral tegmental area, and striatum. *Journal of Neurophysiology, 77*(2), 863–873. https://doi.org/10.1152/jn.1997.77.2.863

Cui, G., Jun, S. B., Jin, X., Pham, M. D., Vogel, S. S., Lovinger, D. M., & Costa, R. M. (2013). Concurrent activation of striatal direct and indirect pathways during action initiation. *Nature, 494*(7436), 238–242. https://doi.org/10.1038/nature11846

Damier, P., Hirsch, E. C., Agid, Y., & Graybiel, A. M. (1999). The substantia nigra of the human brain: II. Patterns of loss of dopamine-containing neurons in Parkinson's disease. *Brain, 122*(8), 1437–1448. https://doi.org/10.1093/brain/122.8.1437

De Fonseca, F. R., Gorriti, M. A., Fernández-Ruiz, J. J., Palomo, T., & Ramos, J. A. (1994). Downregulation of rat brain cannabinoid binding sites after chronic Δ9-

tetrahydrocannabinol treatment. *Pharmacology, Biochemistry and Behavior, 47*(1), 33–40. https://doi.org/10.1016/0091-3057(94)90108-2

Defelipe, J., López-Cruz, P. L., Benavides-Piccione, R., Bielza, C., Larrañaga, P., Anderson, S., Burkhalter, A., Cauli, B., Fairén, A., Feldmeyer, D., Fishell, G., Fitzpatrick, D., Freund, T. F., González-Burgos, G., Hestrin, S., Hill, S., Hof, P. R., Huang, J., Jones, E. G., … Ascoli, G. A. (2013). New insights into the classification and nomenclature of cortical GABAergic interneurons. *Nature Reviews Neuroscience, 14*(3), 202–216. https://doi.org/10.1038/nrn3444

Degos, B., Deniau, J. M., Thierry, A. M., Glowinski, J., Pezard, L., & Maurice, N. (2005). Neuroleptic-induced catalepsy: Electrophysiological mechanisms of functional recovery induced by high-frequency stimulation of the subthalamic nucleus. *Journal of Neuroscience, 25*(33), 7687–7696. https://doi.org/10.1523/JNEUROSCI.1056-05.2005

Del Rey, N. L.-G., Quiroga-Varela, A., Garbayo, E., Carballo-Carbajal, I., Fernández-Santiago, R., Monje, M. H. G., Trigo-Damas, I., Blanco-Prieto, M. J., & Blesa, J. (2018). Advances in Parkinson's Disease: 200 Years Later. *Frontiers in Neuroanatomy, 12*. https://doi.org/10.3389/fnana.2018.00113

DeLong, M. R. (1990). Primate models of movement disorders of basal ganglia origin. *Trends in Neurosciences, 13*(7), 281–285. https://doi.org/10.1016/0166-2236(90)90110-V

Deniau, J. M., Kitai, S. T., Donoghue, J. P., & Grofova, I. (1982). Neuronal interactions in the substantia nigra pars reticulata through axon collaterals of the projection neurons. An electrophysiological and morphological study. *Experimental Brain Research, 47*(1), 105–113. https://doi.org/10.1007/BF00235891

Deniau, J. M., Mailly, P., Maurice, N., & Charpier, S. (2007). The pars reticulata of the substantia nigra: A window to basal ganglia output. *Progress in Brain Research, 160*, 151–172. https://doi.org/10.1016/S0079-6123(06)60009-5

Deniau, J. M., Menetrey, A., & Charpier, S. (1996). The lamellar organization of the rat substantia nigra pars reticulata: Segregated patterns of striatal afferents and relationship to the topography of corticostriatal projections. *Neuroscience, 73*(3), 761–781. https://doi.org/10.1016/0306-4522(96)00088-7

7. Bibliography

Deniau, J. M., Menetrey, A., & Thierry, A. M. (1994). Indirect nucleus accumbens input to the prefrontal cortex via the substantia nigra pars reticulata: A combined anatomical and electrophysiological study in the rat. *Neuroscience*, *61*(3), 533–545. https://doi.org/10.1016/0306-4522(94)90432-4

Devane, W. A., Dysarz, F. A., Johnson, M. R., Melvin, L. S., & Howlett, A. C. (1988). Determination and characterization of a cannabinoid receptor in rat brain. *Molecular Pharmacology*, *34*(5), 605–613.

Devane, W. A., Hanuš, L., Breuer, A., Pertwee, R. G., Stevenson, L. A., Griffin, G., Gibson, D., Mandelbaum, A., Etinger, A., & Mechoulam, R. (1992). Isolation and structure of a brain constituent that binds to the cannabinoid receptor. *Science, 258*(5090), 1946–1949. https://doi.org/10.1126/science.1470919

Dexter, D. T., Holley, A. E., Flitter, W. D., Slater, T. F., Wells, F. R., Daniel, S. E., Lees, A. J., Jenner, P., & Marsden, C. D. (1994). Increased levels of lipid hydroperoxides in the parkinsonian substantia nigra: An HPLC and ESR study. *Movement Disorders*, *9*(1), 92–97. https://doi.org/10.1002/mds.870090115

Di Marzo, V., Bisogno, T., Melck, D., Ross, R., Brockie, H., Stevenson, L., Pertwee, R., & De Petrocellis, L. (1998). Interactions between synthetic vanilloids and the endogenous cannabinoid system. *FEBS Letters*, *436*(3), 449–454. https://doi.org/10.1016/S0014-5793(98)01175-2

Di Marzo, V., Lastres-Becker, I., Bisogno, T., De Petrocellis, L., Milone, A., Davis, J. B., & Fernandez-Ruiz, J. J. (2001). Hypolocomotor effects in rats of capsaicin and two long chain capsaicin homologues. *European Journal of Pharmacology*, *420*(2–3), 123–131. https://doi.org/10.1016/S0014-2999(01)01012-3

Dijkstra, A. A., Voorn, P., Berendse, H. W., Groenewegen, H. J., Netherlands Brain Bank, Rozemuller, A. J. M., & van de Berg, W. D. J. (2014). Stage-dependent nigral neuronal loss in incidental Lewy body and Parkinson's disease. *Movement Disorders: Official Journal of the Movement Disorder Society*, *29*(10), 1244–1251. https://doi.org/10.1002/mds.25952

Ding, S., Li, L., & Zhou, F. M. (2013). Presynaptic Serotonergic gating of the subthalamonigral glutamatergic projection. *Journal of Neuroscience*, *33*(11), 4875–4885. https://doi.org/10.1523/JNEUROSCI.4111-12.2013

Dodson, P. D., Larvin, J. T., Duffell, J. M., Garas, F. N., Doig, N. M., Kessaris, N., Duguid, I. C., Bogacz, R., Butt, S. J. B., & Magill, P. J. (2015). Distinct developmental origins manifest in the specialized encoding of movement by adult neurons of the external globus pallidus. *Neuron*, *86*(2), 501–513. https://doi.org/10.1016/j.neuron.2015.03.007

Egerton, A., Brett, R. R., & Pratt, J. A. (2005). Acute Δ9-tetrahydrocannabinol-induced deficits in reversal learning: Neural correlates of affective inflexibility. *Neuropsychopharmacology*, *30*(10), 1895–1905. https://doi.org/10.1038/sj.npp.1300715

Ehringer, H., & Hornykiewicz, O. (1998). Distribution of noradrenaline and dopamine (3-hydroxytyramine) in the human brain and their behavior in diseases of the extrapyramidal system. *Parkinsonism and Related Disorders*, *4*(2), 53–57. https://doi.org/10.1016/S1353-8020(98)00012-1

Engler, B., Freiman, I., Urbanski, M., & Szabo, B. (2006). Effects of exogenous and endogenous cannabinoids on GABAergic neurotransmission between the caudate-putamen and the globus pallidus in the mouse. *Journal of Pharmacology and Experimental Therapeutics*, *316*(2), 608–617. https://doi.org/10.1124/jpet.105.092718

Escande, M. V., Taravini, I. R. E., Zold, C. L., Belforte, J. E., & Murer, M. G. (2016). Loss of homeostasis in the direct pathway in a mouse model of asymptomatic parkinson's disease. *Journal of Neuroscience*, *36*(21), 5686–5698. https://doi.org/10.1523/JNEUROSCI.0492-15.2016

Fahn, S. (2008). The history of dopamine and levodopa in the treatment of Parkinson's disease. *Movement Disorders*, *23*(S3), S497–S508. https://doi.org/10.1002/mds.22028

Farkas, S., Nagy, K., Jia, Z., Harkany, T., Palkovits, M., Donohou, S. R., Pike, V. W., Halldin, C., Máthé, D., Csiba, L., & Gulyás, B. (2012). The decrease of dopamine D_2/D_3 receptor densities in the putamen and nucleus caudatus goes parallel with maintained levels of CB_1 cannabinoid receptors in Parkinson's disease: A preliminary autoradiographic study with the selective dopamine D_2/D_3 antagonist [³H]raclopride and the novel CB_1 inverse agonist [¹²⁵I]SD7015. *Brain Research Bulletin*, *87*(6), 504–510. https://doi.org/10.1016/j.brainresbull.2012.02.012

7. Bibliography

Faust, T. W., Assous, M., Shah, F., Tepper, J. M., & Koós, T. (2015). Novel fast adapting interneurons mediate cholinergic-induced fast GABAA inhibitory postsynaptic currents in striatal spiny neurons. *The European Journal of Neuroscience*, *42*(2), 1764–1774. https://doi.org/10.1111/ejn.12915

Fearnley, J. M., & Lees, A. J. (1991). Ageing and Parkinson's disease: Substantia nigra regional selectivity. *Brain: A Journal of Neurology*, *114 (Pt 5)*(5), 2283–2301. https://doi.org/10.1093/brain/114.5.2283

Felder, C. C., Joyce, K. E., Briley, E. M., Mansouri, J., Mackie, K., Blond, O., Lai, Y., Ma, A. L., & Mitchell, R. L. (1995). Comparison of the pharmacology and signal transduction of the human cannabinoid CB1 and CB2 receptors. *Molecular Pharmacology*, *48*(3), 443–450.

Fénelon, G., & Alves, G. (2010). Epidemiology of psychosis in Parkinson's disease. *Journal of the Neurological Sciences*, *289*(1), 12–17. https://doi.org/10.1016/j.jns.2009.08.014

Fernández-Ruiz, J., Moreno-Martet, M., Rodríguez-Cueto, C., Palomo-Garo, C., Gõmez-Cañas, M., Valdeolivas, S., Guaza, C., Romero, J., Guzmán, M., Mechoulam, R., & Ramos, J. A. (2011). Prospects for cannabinoid therapies in basal ganglia disorders. *British Journal of Pharmacology*, *163*(7), 1365–1378. https://doi.org/10.1111/j.1476-5381.2011.01365.x

Fernández-Ruiz, J., Romero, J., Velasco, G., Tolón, R. M., Ramos, J. A., & Guzmán, M. (2007). Cannabinoid CB2 receptor: A new target for controlling neural cell survival? *Trends in Pharmacological Sciences*, *28*(1), 39–45. https://doi.org/10.1016/j.tips.2006.11.001

Fieblinger, T., Graves, S. M., Sebel, L. E., Alcacer, C., Plotkin, J. L., Gertler, T. S., Chan, C. S., Heiman, M., Greengard, P., Cenci, M. A., & Surmeier, D. J. (2014). Cell type-specific plasticity of striatal projection neurons in parkinsonism and L-DOPA-induced dyskinesia. *Nature Communications*, *5*(1), 5316. https://doi.org/10.1038/ncomms6316

Filbey, F., & Yezhuvath, U. (2013). Functional connectivity in inhibitory control networks and severity of cannabis use disorder. *American Journal of Drug and Alcohol Abuse*, *39*(6), 382–391. https://doi.org/10.3109/00952990.2013.841710

Filion, M., & Tremblay, L. (1991). Abnormal spontaneous activity of globus pallidus neurons in monkeys with MPTP-induced parkinsonism. *Brain Research*, *547*(1), 142–151.

Filion, M., Tremblay, L., & Be´dard, P. J. (1991). Effects of dopamine agonists on the spontaneous activity of globus pallidus neurons in monkeys with MPTP-induced parkinsonism. *Brain Research*, *547*(1), 145–149. https://doi.org/10.1016/0006-8993(91)90586-K

Fino, E., Vandecasteele, M., Perez, S., Saudou, F., & Venance, L. (2018). Region-specific and state-dependent action of striatal GABAergic interneurons. *Nature Communications*, *9*(1), 3339. https://doi.org/10.1038/s41467-018-05847-5

Fitzgerald, M. L., Shobin, E., & Pickel, V. M. (2012). Cannabinoid modulation of the dopaminergic circuitry: Implications for limbic and striatal output. *Progress in Neuro-Psychopharmacology and Biological Psychiatry*, *38*(1), 21–29. https://doi.org/10.1016/j.pnpbp.2011.12.004

Flores-Barrera, E., Vizcarra-Chacón, B. J., Tapia, D., Bargas, J., & Galarraga, E. (2010). Different Corticostriatal Integration in Spiny Projection Neurons from Direct and Indirect Pathways. *Frontiers in Systems Neuroscience*, *4*. https://doi.org/10.3389/fnsys.2010.00015

Frank, M. J., Seeberger, L. C., & O'Reilly, R. C. (2004). By carrot or by stick: Cognitive reinforcement learning in Parkinsonism. *Science*, *306*(5703), 1940–1943. https://doi.org/10.1126/science.1102941

Freiman, I., & Szabo, B. (2005). Cannabinoids depress excitatory neurotransmission between the subthalamic nucleus and the globus pallidus. *Neuroscience*, *133*(1), 305–313. https://doi.org/10.1016/j.neuroscience.2005.01.058

Fujiyama, F., Nakano, T., Matsuda, W., Furuta, T., Udagawa, J., & Kaneko, T. (2016). A single-neuron tracing study of arkypallidal and prototypic neurons in healthy rats. *Brain Structure & Function*, *221*(9), 4733–4740. https://doi.org/10.1007/s00429-015-1152-2

Furlanetti, L. L., Coenen, V. A., Aranda, I. A., & Döbrössy, M. D. (2015). Chronic deep brain stimulation of the medial forebrain bundle reverses depressive-like behavior in a hemiparkinsonian rodent model. *Experimental Brain Research*, *233*(11), 3073–3085. https://doi.org/10.1007/s00221-015-4375-9

Gagnon, D., Petryszyn, S., Sanchez, M. G., Bories, C., Beaulieu, J. M., De Koninck, Y., Parent, A., & Parent, M. (2017). Striatal Neurons Expressing D1 and D2 Receptors are

Morphologically Distinct and Differently Affected by Dopamine Denervation in Mice. *Scientific Reports*, *7*(1), 41432. https://doi.org/10.1038/srep41432

Galiègue, S., Mary, S., Marchand, J., Dussossoy, D., Carrière, D., Carayon, P., Bouaboula, M., Shire, D., LE Fur, G., & Casellas, P. (1995). Expression of Central and Peripheral Cannabinoid Receptors in Human Immune Tissues and Leukocyte Subpopulations. *European Journal of Biochemistry*, *232*(1), 54–61. https://doi.org/10.1111/j.1432-1033.1995.tb20780.x

Gaoni, Y., & Mechoulam, R. (1964). Isolation, Structure, and Partial Synthesis of an Active Constituent of Hashish. *Journal of the American Chemical Society*, *86*(8), 1646–1647. https://doi.org/10.1021/ja01062a046

Garas, F. N., Shah, R. S., Kormann, E., Doig, N. M., Vinciati, F., Nakamura, K. C., Dorst, M. C., Smith, Y., Magill, P. J., & Sharott, A. (2016). Secretagogin expression delineates functionally-specialized populations of striatal parvalbumin-containing interneurons. *ELife*, *5*, e16088. https://doi.org/10.7554/eLife.16088

Gérard, C. M., Mollereau, C., Vassart, G., & Parmentier, M. (1991). Molecular cloning of a human cannabinoid receptor which is also expressed in testis. *Biochemical Journal*, *279*(1), 129–134. https://doi.org/10.1042/bj2790129

Gerdeman, G., & Lovinger, D. M. (2001). CB1 cannabinoid receptor inhibits synaptic release of glutamate in rat dorsolateral striatum. *Journal of Neurophysiology*, *85*(1), 468–471. https://doi.org/10.1152/jn.2001.85.1.468

Gerfen, C. R., Baimbridge, K. G., & Miller, J. J. (1985). The neostriatal mosaic: Compartmental distribution of calcium-binding protein and parvalbumin in the basal ganglia of the rat and monkey. *Proceedings of the National Academy of Sciences*, *82*(24), 8780–8784. https://doi.org/10.1073/pnas.82.24.8780

Gerfen, C. R., Economo, M. N., & Chandrashekar, J. (2018). Long distance projections of cortical pyramidal neurons. *Journal of Neuroscience Research*, *96*(9), 1467–1475. https://doi.org/10.1002/jnr.23978

Gerfen, C. R., Engber, T. M., Mahan, L. C., Susel, Z., Chase, T. N., Monsma, F. J., & Sibley, D. R. (1990). D1 and D2 dopamine receptor-regulated gene expression of striatonigral and striatopallidal neurons. *Science*, *250*(4986), 1429–1432. https://doi.org/10.1126/science.2147780

Gerfen, C. R., & Young, W. (1988). Distribution of striatonigral and striatopallidal peptidergic neurons in both patch and matrix compartments: An in situ hybridization histochemistry and fluorescent retrograde tracing study. *Brain Research*, *460*(1), 161–167. https://doi.org/10.1016/0006-8993(88)91217-6

Gomez, O., Sanchez-Rodriguez, A., Le, M., Sanchez-Caro, C., Molina-Holgado, F., & Molina-Holgado, E. (2011). Cannabinoid receptor agonists modulate oligodendrocyte differentiation by activating PI3K/Akt and the mammalian target of rapamycin (mTOR) pathways. *British Journal of Pharmacology*, *163*(7), 1520–1532. https://doi.org/10.1111/j.1476-5381.2011.01414.x

Gong, J. P., Onaivi, E. S., Ishiguro, H., Liu, Q. R., Tagliaferro, P. A., Brusco, A., & Uhl, G. R. (2006). Cannabinoid CB2 receptors: Immunohistochemical localization in rat brain. *Brain Research*, *1071*(1), 10–23. https://doi.org/10.1016/j.brainres.2005.11.035

González-Hernández, T., & Rodríguez, M. (2000). Compartmental organization and chemical profile of dopaminergic and GABAergic neurons in the substantia nigra of the rat. *Journal of Comparative Neurology*, *421*(1), 107–135. https://doi.org/10.1002/(SICI)1096-9861(20000522)421:1<107::AID-CNE7>3.0.CO;2-F

Gouty-Colomer, L.-A., Michel, F. J., Baude, A., Lopez-Pauchet, C., Dufour, A., Cossart, R., & Hammond, C. (2018). Mouse subthalamic nucleus neurons with local axon collaterals. *Journal of Comparative Neurology*, *526*(2), 275–284. https://doi.org/10.1002/cne.24334

Graves, S. M., & Surmeier, D. J. (2019). Delayed Spine Pruning of Direct Pathway Spiny Projection Neurons in a Mouse Model of Parkinson's Disease. *Frontiers in Cellular Neuroscience*, *13*. https://doi.org/10.3389/fncel.2019.00032

Graybiel, A. M., & Ragsdale, C. W. (1978). Histochemically distinct compartments in the striatum of human, monkeys, and cat demonstrated by acetylthiocholinesterase staining. *Proceedings of the National Academy of Sciences of the United States of America*, *75*(11), 5723–5726. https://doi.org/10.1073/pnas.75.11.5723

Gremel, C. M., & Costa, R. M. (2013). Orbitofrontal and striatal circuits dynamically encode the shift between goal-directed and habitual actions. *Nature Communications*, *4*(May), 1–12. https://doi.org/10.1038/ncomms3264

7. Bibliography

Grimaldi, P., Orlando, P., Di Siena, S., Lolicato, F., Petrosino, S., Bisogno, T., Geremia, R., De Petrocellis, L., & Di Marzo, V. (2009). The endocannabinoid system and pivotal role of the CB2 receptor in mouse spermatogenesis. *Proceedings of the National Academy of Sciences of the United States of America*, *106*(27), 11131–11136. https://doi.org/10.1073/pnas.0812789106

Groenewegen, H. J., & Berendse, H. W. (1990). Connections of the subthalamic nucleus with ventral striatopallidal parts of the basal ganglia in the rat. *The Journal of Comparative Neurology*, *294*(4), 607–622. https://doi.org/10.1002/cne.902940408

Groenewegen, H. J., Berendse, H. W., & Haber, S. N. (1993). Organization of the output of the ventral striatopallidal system in the rat: Ventral pallidal efferents. *Neuroscience*, *57*(1), 113–142. https://doi.org/10.1016/0306-4522(93)90115-v

Groenewegen, H. J., Mulder, A. B., Beijer, A. V. J., Wright, C. I., Lopes Da Silva, F. H., & Pennartz, C. M. A. (1999). Hippocampal and amygdaloid interactions in the nucleus accumbens. *Psychobiology*, *27*(2), 149–164. https://doi.org/10.3758/BF03332111

Grofová, I. (1975). The identification of striatal and pallidal neurons projecting to substantia nigra. An experimental study by means of retrograde axonal transport of horseradish peroxidase. *Brain Research*, *91*(2), 286–291. https://doi.org/10.1016/0006-8993(75)90550-8

Gu, M., Owen, A. D., Toffa, S. E. K., Cooper, J. M., Dexter, D. T., Jenner, P., Marsden, C. D., & Schapira, A. H. V. (1998). Mitochondrial function, GSH and iron in neurodegeneration and Lewy body diseases. *Journal of the Neurological Sciences*, *158*(1), 24–29. https://doi.org/10.1016/S0022-510X(98)00095-1

Guindon, J., Desroches, J., & Beaulieu, P. (2007). The antinociceptive effects of intraplantar injections of 2-arachidonoyl glycerol are mediated by cannabinoid CB2 receptors. *British Journal of Pharmacology*, *150*(6), 693–701. https://doi.org/10.1038/sj.bjp.0706990

Haj-Dahmane, S., & Shen, R.-Y. (2011). Modulation of the serotonin system by endocannabinoid signaling. *Neuropharmacology*, *61*(3), 414–420. https://doi.org/10.1016/j.neuropharm.2011.02.016

Halliday, G. M., Blumbergs, P. C., Cotton, R. G., Blessing, W. W., & Geffen, L. B. (1990). Loss of brainstem serotonin- and substance P-containing neurons in Parkinson's disease. *Brain Research*, *510*(1), 104–107. https://doi.org/10.1016/0006-8993(90)90733-r

Hassani, O. K., Mouroux, M., & Féger, J. (1996). Increased subthalamic neuronal activity after nigral dopaminergic lesion independent of disinhibition via the globus pallidus. *Neuroscience*, *72*(1), 105–115. https://doi.org/10.1016/0306-4522(95)00535-8

Hattori, T., Fibiger, H. C., & McGeer, P. L. (1975). Demonstration of a pallido-nigral projection innervating dopaminergic neurons. *The Journal of Comparative Neurology*, *162*(4), 487–504. https://doi.org/10.1002/cne.901620406

Hauber, W. (1998). Involvement of basal ganglia transmitter systems in movement initiation. *Progress in Neurobiology*, *56*(5), 507–540. Scopus. https://doi.org/10.1016/S0301-0082(98)00041-0

Heilbronner, S. R., Rodriguez-Romaguera, J., Quirk, G. J., Groenewegen, H. J., & Haber, S. N. (2016). Circuit-Based Corticostriatal Homologies Between Rat and Primate. *Biological Psychiatry*, *80*(7), 509–521. https://doi.org/10.1016/j.biopsych.2016.05.012

Heng, L., Beverley, J. A., Steiner, H., & Tseng, K. Y. (2011). Differential developmental trajectories for CB1 cannabinoid receptor expression in limbic/associative and sensorimotor cortical areas. *Synapse*, *65*(4), 278–286. https://doi.org/10.1002/syn.20844

Herkenham, M., Lynn, A. B., de Costa, B. R., & Richfield, E. K. (1991). Neuronal localization of cannabinoid receptors in the basal ganglia of the rat. *Brain Research*, *547*(2), 267–274. https://doi.org/10.1016/0006-8993(91)90970-7

Herkenham, M., Lynn, A. B., Johnson, M. R., Melvin, L. S., De Costa, B. R., & Rice, K. C. (1991). Characterization and localization of cannabinoid receptors in rat brain: A quantitative in vitro autoradiographic study. *Journal of Neuroscience*, *11*(2), 563–583. https://doi.org/10.1523/jneurosci.11-02-00563.1991

Herkenham, M., & Pert, C. B. (1981). Mosaic distribution of opiate receptors, parafascicular projections and acetylcholinesterase in rat striatum. *Nature*, *291*(5814), 415–418. https://doi.org/10.1038/291415a0

7. Bibliography

Hernandez, G., & Cheer, J. F. (2012). Effect of CB1 receptor blockade on food-reinforced responding and associated nucleus accumbens neuronal activity in rats. *Journal of Neuroscience, 32*(33), 11467–11477. https://doi.org/10.1523/JNEUROSCI.1833-12.2012

Herrán, E., Requejo, C., Ruiz-Ortega, J. A., Aristieta, A., Igartua, M., Bengoetxea, H., Ugedo, L., Pedraz, J. L., Lafuente, J. V., & Hernández, R. M. (2014). Increased antiparkinson efficacy of the combined administration of VEGF- and GDNF-loaded nanospheres in a partial lesion model of Parkinson's disease. *International Journal of Nanomedicine, 9*(1), 2677–2687. https://doi.org/10.2147/IJN.S61940

Higley, M. J., Gittis, A. H., Oldenburg, I. A., Balthasar, N., Seal, R. P., Edwards, R. H., Lowell, B. B., Kreitzer, A. C., & Sabatini, B. L. (2011). Cholinergic interneurons mediate fast VGluT3-dependent glutamatergic transmission in the striatum. *PLOS ONE, 6*(4), e19155. https://doi.org/10.1371/journal.pone.0019155

Hikida, T., Kimura, K., Wada, N., Funabiki, K., & Nakanishi, S. (2010). Distinct Roles of Synaptic Transmission in Direct and Indirect Striatal Pathways to Reward and Aversive Behavior. *Neuron, 66*(6), 896–907. https://doi.org/10.1016/j.neuron.2010.05.011

Hikida, T., Yawata, S., Yamaguchi, T., Danjo, T., Sasaoka, T., Wang, Y., & Nakanishi, S. (2013). Pathway-specific modulation of nucleus accumbens in reward and aversive behavior via selective transmitter receptors. *Proceedings of the National Academy of Sciences of the United States of America, 110*(1), 342–347. https://doi.org/10.1073/pnas.1220358110

Hill, M. N., Froese, L. M., Morrish, A. C., Sun, J. C., & Floresco, S. B. (2006). Alterations in behavioral flexibility by cannabinoid CB1 receptor agonists and antagonists. *Psychopharmacology, 187*(2), 245–259. https://doi.org/10.1007/s00213-006-0421-4

Hoffman, A. F., & Lupica, C. R. (2001). Direct actions of cannabinoids on synaptic transmission in the nucleus accumbens: A comparison with opioids. *Journal of Neurophysiology, 85*(1), 72–83. https://doi.org/10.1152/jn.2001.85.1.72

Hohmann, A. G., & Herkenham, M. (1999). Localization of central cannabinoid CB1 receptor messenger RNA in neuronal subpopulations of rat dorsal root ganglia: A double-label in situ hybridization study. *Neuroscience, 90*(3), 923–931. https://doi.org/10.1016/S0306-4522(98)00524-7

Hohmann, A. G., & Herkenham, M. (2000). Localization of cannabinoid CB1 receptor mRNA in neuronal subpopulations of rat striatum: A double-label in situ hybridization study. *Synapse*, *37*(1), 71–80. https://doi.org/10.1002/(SICI)1098-2396(200007)37:1<71::AID-SYN8>3.0.CO;2-K

Holdorff, B. (2019). Centenary of Tretiakoff's thesis on the morphology of Parkinson's disease, evolved on the grounds of encephalitis lethargica pathology. *Journal of the History of the Neurosciences*, *28*(4), 387–398. https://doi.org/10.1080/0964704X.2019.1622361

Hornykiewicz, O., & Kish, S. J. (1987). Biochemical pathophysiology of Parkinson's disease. *Advances in Neurology, 45*, 19–34.

Huerta-Ocampo, I., Mena-Segovia, J., & Bolam, J. P. (2014). Convergence of cortical and thalamic input to direct and indirect pathway medium spiny neurons in the striatum. *Brain Structure & Function*, *219*(5), 1787–1800. https://doi.org/10.1007/s00429-013-0601-z

Hurley, M. J., Mash, D. C., & Jenner, P. (2003). Expression of cannabinoid CB1 receptor mRNA in basal ganglia of normal and parkinsonian human brain. *Journal of Neural Transmission*, *110*(11), 1279–1288. https://doi.org/10.1007/s00702-003-0033-7

Hutchison, W. D., Lozano, A. M., Davis, K. D., Saint-Cyr, J. A., Lang, A. E., & Dostrovsky, J. O. (1994). Differential neuronal activity in segments of globus pallidus in Parkinson's disease patients. *NeuroReport*, *5*(12), 1533–1537.

Hutchison, W. D., Lozano, A. M., Tasker, R. R., Lang, A. E., & Dostrovsky, J. O. (1997). Identification and characterization of neurons with tremor-frequency activity in human globus pallidus. *Experimental Brain Research*, *113*(3), 557–563. https://doi.org/10.1007/pl00005606

Iacono, D., Geraci-Erck, M., Rabin, M. L., Adler, C. H., Serrano, G., Beach, T. G., & Kurlan, R. (2015). Parkinson disease and incidental Lewy body disease: Just a question of time? *Neurology*, *85*(19), 1670–1679. https://doi.org/10.1212/WNL.0000000000002102

Ibáñez-Sandoval, O., Carrillo-Reid, L., Galarraga, E., Tapia, D., Mendoza, E., Gomora, J. C., Aceves, J., & Bargas, J. (2007). Bursting in substantia nigra pars reticulata neurons in vitro: Possible relevance for Parkinson disease. *Journal of Neurophysiology*, *98*(4), 2311–2323. https://doi.org/10.1152/jn.00620.2007

7. Bibliography

Ibañez-Sandoval, O., Hernández, A., Florán, B., Galarraga, E., Tapia, D., Valdiosera, R., Erlij, D., Aceves, J., & Bargas, J. (2006). Control of the subthalamic innervation of substantia nigra pars reticulata by D1 and D2 dopamine receptors. *Journal of Neurophysiology*, *95*(3), 1800–1811. https://doi.org/10.1152/jn.01074.2005

Ibáñez-Sandoval, O., Tecuapetla, F., Unal, B., Shah, F., Koós, T., & Tepper, J. M. (2010). Electrophysiological and morphological characteristics and synaptic connectivity of tyrosine hydroxylase-expressing neurons in adult mouse striatum. *The Journal of Neuroscience: The Official Journal of the Society for Neuroscience*, *30*(20), 6999–7016. https://doi.org/10.1523/JNEUROSCI.5996-09.2010

Ibáñez-Sandoval, O., Tecuapetla, F., Unal, B., Shah, F., Koós, T., & Tepper, J. M. (2011). A novel functionally distinct subtype of striatal neuropeptide Y interneuron. *The Journal of Neuroscience: The Official Journal of the Society for Neuroscience*, *31*(46), 16757–16769. https://doi.org/10.1523/JNEUROSCI.2628-11.2011

Ilan, A. B., Smith, M. E., & Gevins, A. (2004). Effects of marijuana on neurophysiological signals of working and episodic memory. *Psychopharmacology*, *176*(2), 214–222. https://doi.org/10.1007/s00213-004-1868-9

Irving, A. J., Coutts, A. A., Harvey, J., Rae, M. G., Mackie, K., Bewick, G. S., & Pertwee, R. G. (2000). Functional expression of cell surface cannabinoid CB1 receptors on presynaptic inhibitory terminals in cultured rat hippocampal neurons. *Neuroscience*, *98*(2), 253–262. https://doi.org/10.1016/S0306-4522(00)00120-2

Janssen, M. L. F., Temel, Y., Delaville, C., Zwartjes, D. G. M., Heida, T., De Deurwaerdère, P., Visser-Vandewalle, V., & Benazzouz, A. (2017). Cortico-subthalamic inputs from the motor, limbic, and associative areas in normal and dopamine-depleted rats are not fully segregated. *Brain Structure and Function*, *222*(6), 2473–2485. https://doi.org/10.1007/s00429-016-1351-5

Javed, H., Azimullah, S., Haque, M. E., & Ojha, S. K. (2016). Cannabinoid type 2 (CB2) receptors activation protects against oxidative stress and neuroinflammation associated dopaminergic neurodegeneration in rotenone model of parkinson's disease. *Frontiers in Neuroscience*, *10*(AUG), 321. https://doi.org/10.3389/fnins.2016.00321

Javitt, D. C., Lee, M., Kantrowitz, J. T., & Martinez, A. (2018). Mismatch negativity as a biomarker of theta band oscillatory dysfunction in schizophrenia. *Schizophrenia Research*, *191*, 51–60. https://doi.org/10.1016/j.schres.2017.06.023

Jin, X., Tecuapetla, F., & Costa, R. M. (2014). Basal ganglia subcircuits distinctively encode the parsing and concatenation of action sequences. *Nature Neuroscience, 17*(3), 423–430. https://doi.org/10.1038/nn.3632

Joel, D., & Weiner, I. (2000). The connections of the dopaminergic system with the striatum in rats and primates: An analysis with respect to the functional and compartmental organization of the striatum. *Neuroscience, 96*(3), 451–474. https://doi.org/10.1016/S0306-4522(99)00575-8

Jomova, K., Vondrakova, D., Lawson, M., & Valko, M. (2010). Metals, oxidative stress and neurodegenerative disorders. *Molecular and Cellular Biochemistry, 345*(1–2), 91–104. https://doi.org/10.1007/s11010-010-0563-x

Jordt, S.-E., Bautista, D. M., Chuang, H.-H., McKemy, D. D., Zygmunt, P. M., Högestätt, E. D., Meng, I. D., & Julius, D. (2004). Mustard oils and cannabinoids excite sensory nerve fibres through the TRP channel ANKTM1. *Nature, 427*(6971), 260–265. https://doi.org/10.1038/nature02282

Joyeux, M., Arnaud, C., Godin-Ribuot, D., Demenge, P., Lamontagne, D., & Ribuot, C. (2002). Endocannabinoids are implicated in the infarct size-reducing effect conferred by heat stress preconditioning in isolated rat hearts. *Cardiovascular Research, 55*(3), 619–625. https://doi.org/10.1016/s0008-6363(02)00268-7

Julian, M. D., Martin, A. B., Cuellar, B., Rodriguez De Fonseca, F., Navarro, M., Moratalla, R., & Garcia-Segura, L. M. (2003). Neuroanatomical relationship between type 1 cannabinoid receptors and dopaminergic systems in the rat basal ganglia. *Neuroscience, 119*(1), 309–318. https://doi.org/10.1016/S0306-4522(03)00070-8

Kageyama, T., Nakamura, M., Matsuo, A., Yamasaki, Y., Takakura, Y., Hashida, M., Kanai, Y., Naito, M., Tsuruo, T., Minato, N., & Shimohama, S. (2000). The 4F2hc/LAT1 complex transports L-DOPA across the blood-brain barrier. *Brain Research, 879*(1–2), 115–121. https://doi.org/10.1016/S0006-8993(00)02758-X

7. Bibliography

Kaur, K., Gill, J. S., Bansal, P. K., & Deshmukh, R. (2017). Neuroinflammation—A major cause for striatal dopaminergic degeneration in Parkinson's disease. *Journal of the Neurological Sciences*, *381*, 308–314. https://doi.org/10.1016/j.jns.2017.08.3251

Kawaguchi, Y., Wilson, C. J., Augood, S. J., & Emson, P. C. (1995). Striatal interneurones: Chemical, physiological and morphological characterization. *Trends in Neurosciences*, *18*(12), 527–535. https://doi.org/10.1016/0166-2236(95)98374-8

Kha, H. T., Finkelstein, D. I., Tomas, D., Drago, J., Pow, D. V., & Horne, M. K. (2001). Projections from the substantia nigra pars reticulata to the motor thalamus of the rat: Single axon reconstructions and immunohistochemical study. *The Journal of Comparative Neurology*, *440*(1), 20–30. https://doi.org/10.1002/cne.1367

Khaspekov, L. G., Verca, M. S. B., Frumkina, L. E., Hermann, H., Marsicano, G., & Lutz, B. (2004). Involvement of brain-derived neurotrophic factor in cannabinoid receptor-dependent protection against excitotoxicity. *European Journal of Neuroscience*, *19*(7), 1691–1698. https://doi.org/10.1111/j.1460-9568.2004.03285.x

Kim, J., Inoue, K., Ishii, J., Vanti, W. B., Voronov, S. V., Murchison, E., Hannon, G., & Abeliovich, A. (2007). A microRNA feedback circuit in midbrain dopamine neurons. *Science*, *317*(5842), 1220–1224. https://doi.org/10.1126/science.1140481

Kish, S. J., Shannak, K., & Hornykiewicz, O. (1988). Uneven pattern of dopamine loss in the striatum of patients with idiopathic Parkinson's disease. Pathophysiologic and clinical implications. *The New England Journal of Medicine*, *318*(14), 876–880. https://doi.org/10.1056/NEJM198804073181402

Kita, H. (1994). Physiology of Two Disynaptic Pathways from the Sensori-Motor Cortex to the Basal Ganglia Output Nuclei. In G. Percheron, J. S. McKenzie, & J. Féger (Eds.), *The Basal Ganglia IV: New Ideas and Data on Structure and Function* (pp. 263–276). Springer US. https://doi.org/10.1007/978-1-4613-0485-2_28

Kita, H. (2007). Globus pallidus external segment. *Progress in Brain Research*, *160*, 111–133. https://doi.org/10.1016/S0079-6123(06)60007-1

Kita, H., Chang, H. T., & Kitai, S. T. (1983). The morphology of intracellularly labeled rat subthalamic neurons: A light microscopic analysis. *Journal of Comparative Neurology*, *215*(3), 245–257. https://doi.org/10.1002/cne.902150302

Kita, H., & Kitai, S. T. (1987). Efferent projections of the subthalamic nucleus in the rat: Light and electron microscopic analysis with the PHA-L method. *The Journal of Comparative Neurology, 260*(3), 435–452. https://doi.org/10.1002/cne.902600309

Koketsu, D., Chiken, S., Hisatsune, T., Miyachi, S., & Nambu, A. (2021). Elimination of the cortico-subthalamic hyperdirect pathway induces motor hyperactivity in mice. *Journal of Neuroscience.* https://doi.org/10.1523/JNEUROSCI.1330-20.2021

Kolomiets, B. P., Deniau, J. M., Glowinski, J., & Thierry, A. M. (2003). Basal ganglia and processing of cortical information: Functional interactions between trans-striatal and trans-subthalamic circuits in the substantia nigra pars reticulata. *Neuroscience, 117*(4), 931–938.

Koshimizu, Y., Fujiyama, F., Nakamura, K. C., Furuta, T., & Kaneko, T. (2013). Quantitative analysis of axon bouton distribution of subthalamic nucleus neurons in the rat by single neuron visualization with a viral vector. *Journal of Comparative Neurology, 521*(9), 2125–2146. https://doi.org/10.1002/cne.23277

Kravitz, A. V., Freeze, B. S., Parker, P. R. L., Kay, K., Thwin, M. T., Deisseroth, K., & Kreitzer, A. C. (2010). Regulation of parkinsonian motor behaviours by optogenetic control of basal ganglia circuitry. *Nature, 466*(7306), 622–626. https://doi.org/10.1038/nature09159

Kravitz, A. V., Tye, L. D., & Kreitzer, A. C. (2012). Distinct roles for direct and indirect pathway striatal neurons in reinforcement. *Nature Neuroscience, 15*(6), 816–818. https://doi.org/10.1038/nn.3100

Kreitzer, A. C., & Malenka, R. C. (2007). Endocannabinoid-mediated rescue of striatal LTD and motor deficits in Parkinson's disease models. *Nature, 445*(7128), 643–647. https://doi.org/10.1038/nature05506

Kucewicz, M. T., Tricklebank, M. D., Bogacz, R., & Jones, M. W. (2011). Dysfunctional prefrontal cortical network activity and interactions following cannabinoid receptor activation. *Journal of Neuroscience, 31*(43), 15560–15568. https://doi.org/10.1523/JNEUROSCI.2970-11.2011

Kühn, A. A., Tsui, A., Aziz, T., Ray, N., Brücke, C., Kupsch, A., Schneider, G.-H., & Brown, P. (2009). Pathological synchronisation in the subthalamic nucleus of patients with

Parkinson's disease relates to both bradykinesia and rigidity. *Experimental Neurology, 215*(2), 380–387. https://doi.org/10.1016/j.expneurol.2008.11.008

Lalla, L., Rueda Orozco, P. E., Jurado-Parras, M.-T., Brovelli, A., & Robbe, D. (2017). Local or Not Local: Investigating the Nature of Striatal Theta Oscillations in Behaving Rats. *ENeuro, 4*(5). https://doi.org/10.1523/ENEURO.0128-17.2017

Lanciego, J. L., Barroso-Chinea, P., Rico, A. J., Conte-Perales, L., Callén, L., Roda, E., Gómez-Bautista, V., López, I. P., Lluis, C., Labandeira-García, J. L., & Franco, R. (2011). Expression of the mRNA coding the cannabinoid receptor 2 in the pallidal complex of Macaca fascicularis. *Journal of Psychopharmacology, 25*(1), 97–104. https://doi.org/10.1177/0269881110367732

Lang, A. E., & Espay, A. J. (2018). Disease Modification in Parkinson's Disease: Current Approaches, Challenges, and Future Considerations. *Movement Disorders: Official Journal of the Movement Disorder Society, 33*(5), 660–677. https://doi.org/10.1002/mds.27360

Lang, A. E., & Lozano, A. M. (1998). Parkinson's disease. Second of two parts. *The New England Journal of Medicine, 339*(16), 1130–1143. https://doi.org/10.1056/NEJM199810153391607

Lange, K. W., Robbins, T. W., Marsden, C. D., James, M., Owen, A. M., & Paul, G. M. (1992). L-dopa withdrawal in Parkinson's disease selectively impairs cognitive performance in tests sensitive to frontal lobe dysfunction. *Psychopharmacology, 107*(2–3), 394–404. https://doi.org/10.1007/BF02245167

Lastres-Becker, I., Cebeira, M., De Ceballos, M. L., Zeng, B. Y., Jenner, P., Ramos, J. A., & Fernández-Ruiz, J. J. (2001). Increased cannabinoid CB1 receptor binding and activation of GTP-binding proteins in the basal ganglia of patients with Parkinson's syndrome and of MPTP-treated marmosets. *European Journal of Neuroscience, 14*(11), 1827–1832. https://doi.org/10.1046/j.0953-816X.2001.01812.x

Lastres-Becker, I., Molina-Holgado, F., Ramos, J. A., Mechoulam, R., & Fernández-Ruiz, J. (2005). Cannabinoids provide neuroprotection against 6-hydroxydopamine toxicity in vivo and in vitro: Relevance to Parkinson's disease. *Neurobiology of Disease, 19*(1–2), 96–107. https://doi.org/10.1016/j.nbd.2004.11.009

Lee, A., & Gilbert, R. M. (2016). Epidemiology of Parkinson Disease. *Neurologic Clinics, 34*(4), 955–965. https://doi.org/10.1016/j.ncl.2016.06.012

Lee, T., Kaneko, T., Taki, K., & Mizuno, N. (1997). Preprodynorphin-, preproenkephalin-, and preprotachykinin-expressing neurons in the rat neostriatum: An analysis by immunocytochemistry and retrograde tracing. *Journal of Comparative Neurology, 386*(2), 229–244. https://doi.org/10.1002/(SICI)1096-9861(19970922)386:2<229::AID-CNE5>3.0.CO;2-3

Legendy, C. R., & Salcman, M. (1985). Bursts and recurrences of bursts in the spike trains of spontaneously active striate cortex neurons. *Journal of Neurophysiology, 53*(4), 926–939. https://doi.org/10.1152/jn.1985.53.4.926

Levey, A. I., Hersch, S. M., Rye, D. B., Sunahara, R. K., Niznik, H. B., Kitt, C. A., Price, D. L., Maggio, R., Brann, M. R., & Ciliax, B. J. (1993). Localization of D1 and D2 dopamine receptors in brain with subtype-specific antibodies. *Proceedings of the National Academy of Sciences of the United States of America, 90*(19), 8861–8865. https://doi.org/10.1073/pnas.90.19.8861

Levy, R., Hutchison, W. D., Lozano, A. M., & Dostrovsky, J. O. (2002). Synchronized Neuronal Discharge in the Basal Ganglia of Parkinsonian Patients Is Limited to Oscillatory Activity. *Journal of Neuroscience, 22*(7), 2855–2861. https://doi.org/10.1523/JNEUROSCI.22-07-02855.2002

Lewis, S. J. G., Dove, A., Robbins, T. W., Barker, R. A., & Owen, A. M. (2004). Striatal contributions to working memory: A functional magnetic resonance imaging study in humans. *The European Journal of Neuroscience, 19*(3), 755–760. https://doi.org/10.1111/j.1460-9568.2004.03108.x

Lewis, S. J. G., Slabosz, A., Robbins, T. W., Barker, R. A., & Owen, A. M. (2005). Dopaminergic basis for deficits in working memory but not attentional set-shifting in Parkinson's disease. *Neuropsychologia, 43*(6), 823–832. https://doi.org/10.1016/j.neuropsychologia.2004.10.001

Lewy, FH. (1912). Paralysis agitans. 1. Pathologische Anatomie. In *Handbuch der Neurologie, Dritter Band, Spezielle Neurologie I* (pp. 920–933). Berlin: Julius Springer.

Liao, W.-T., Chang, C.-L., & Hsiao, Y.-T. (2020). Activation of cannabinoid type 1 receptors decreases the synchronization of local field potential oscillations in the hippocampus

and entorhinal cortex and prolongs the interresponse time during a differential-reinforcement-of-low-rate task. *European Journal of Neuroscience, 52*(10), 4249–4266. https://doi.org/10.1111/ejn.14856

Linkert, M., Rueden, C. T., Allan, C., Burel, J. M., Moore, W., Patterson, A., Loranger, B., Moore, J., Neves, C., MacDonald, D., Tarkowska, A., Sticco, C., Hill, E., Rossner, M., Eliceiri, K. W., & Swedlow, J. R. (2010). Metadata matters: Access to image data in the real world. *Journal of Cell Biology, 189*(5), 777–782. https://doi.org/10.1083/jcb.201004104

Lisboa, S. F., Reis, D. G., Da Silva, A. L., Corrêa, F. M. A., Guimarães, F. S., & Resstel, L. B. M. (2010). Cannabinoid CB1 receptors in the medial prefrontal cortex modulate the expression of contextual fear conditioning. *International Journal of Neuropsychopharmacology, 13*(9), 1163–1173. https://doi.org/10.1017/S1461145710000684

Liu, H., Song, Z., Liao, D., Zhang, T., Liu, F., Zhuang, K., Luo, K., & Yang, L. (2015). Neuroprotective Effects of Trans-Caryophyllene Against Kainic Acid Induced Seizure Activity and Oxidative Stress in Mice. *Neurochemical Research, 40*(1), 118–123. https://doi.org/10.1007/s11064-014-1474-0

Lonskaya, I., Hebron, M. L., Algarzae, N. K., Desforges, N., & Moussa, C. E.-H. (2013). Decreased parkin solubility is associated with impairment of autophagy in the nigrostriatum of sporadic Parkinson's disease. *Neuroscience, 232*, 90–105. https://doi.org/10.1016/j.neuroscience.2012.12.018

Louis, E. D. (2016). Diagnosis and Management of Tremor. *Continuum (Minneapolis, Minn.), 22*(4 Movement Disorders), 1143–1158. https://doi.org/10.1212/CON.0000000000000346

Lovinger, D. M., & Mathur, B. N. (2016). Endocannabinoid Signaling in the Striatum. In *Handbook of Behavioral Neuroscience* (Vol. 24, pp. 197–215). Elsevier B.V.

Lupica, C. R., & Riegel, A. C. (2005). Endocannabinoid release from midbrain dopamine neurons: A potential substrate for cannabinoid receptor antagonist treatment of addiction. *Neuropharmacology, 48*(8), 1105–1116. https://doi.org/10.1016/j.neuropharm.2005.03.016

Mackovski, N., Liao, J., Weng, R., Wei, X., Wang, R., Chen, Z., Liu, X., Yu, Y., Meyer, B. J., Xia, Y., Deng, C., Huang, X.-F., & Wang, Q. (2016). Reversal effect of simvastatin on the decrease in cannabinoid receptor 1 density in 6-hydroxydopamine lesioned rat brains. *Life Sciences*, *155*, 123–132. https://doi.org/10.1016/j.lfs.2016.05.005

Magill, P. J., Bolam, J. P., & Bevan, M. D. (2001). Dopamine regulates the impact of the cerebral cortex on the subthalamic nucleus-globus pallidus network. *Neuroscience*, *106*(2), 313–330. https://doi.org/10.1016/S0306-4522(01)00281-0

Magill, P. J., Pogosyan, A., Sharott, A., Csicsvari, J., Bolam, J. P., & Brown, P. (2006). Changes in functional connectivity within the rat striatopallidal axis during global brain activation in vivo. *The Journal of Neuroscience: The Official Journal of the Society for Neuroscience*, *26*(23), 6318–6329. https://doi.org/10.1523/JNEUROSCI.0620-06.2006

Mailleux, P., & Vanderhaeghen, J. J. (1992). Distribution of neuronal cannabinoid receptor in the adult rat brain: A comparative receptor binding radioautography and in situ hybridization histochemistry. *Neuroscience*, *48*(3), 655–668. https://doi.org/10.1016/0306-4522(92)90409-U

Mailleux, P., & Vanderhaeghen, J. J. (1993). Dopaminergic regulation of cannabinoid receptor mRNA levels in the rat caudate-putamen: An in situ hybridization study. *Journal of Neurochemistry*, *61*(5), 1705–1712.

Malek, N., Popiolek-Barczyk, K., Mika, J., Przewlocka, B., & Starowicz, K. (2015). Anandamide, acting via CB2 receptors, alleviates LPS-induced neuroinflammation in rat primary microglial cultures. *Neural Plasticity*, *2015*, 130639. https://doi.org/10.1155/2015/130639

Mallet, N., Ballion, B., Le Moine, C., & Gonon, F. (2006). Cortical inputs and GABA interneurons imbalance projection neurons in the striatum of parkinsonian rats. *Journal of Neuroscience*, *26*(14), 3875–3884. https://doi.org/10.1523/JNEUROSCI.4439-05.2006

Mallet, N., Le Moine, C., Charpier, S., & Gonon, F. (2005). Feedforward inhibition of projection neurons by fast-spiking GABA interneurons in the rat striatum in vivo. *Journal of Neuroscience*, *25*(15), 3857–3869. https://doi.org/10.1523/JNEUROSCI.5027-04.2005

7. Bibliography

Mallet, N., Micklem, B. R., Henny, P., Brown, M. T., Williams, C., Bolam, J. P., Nakamura, K. C., & Magill, P. J. (2012). Dichotomous Organization of the External Globus Pallidus. *Neuron*, *74*(6), 1075–1086. https://doi.org/10.1016/J.NEURON.2012.04.027

Mansouri, M. T., Fidler, J. A., Meng, Q. C., Eckenhoff, R. G., & García, P. S. (2019). Sex effects on behavioral markers of emergence from propofol and isoflurane anesthesia in rats. *Behavioural Brain Research*, *367*, 59–67. https://doi.org/10.1016/j.bbr.2019.03.029

Marín, O. (2012). Interneuron dysfunction in psychiatric disorders. *Nature Reviews Neuroscience*, *13*(2), 107–120. https://doi.org/10.1038/nrn3155

Markham, A. (2016). Pimavanserin: First Global Approval. *Drugs*, *76*(10), 1053–1057. https://doi.org/10.1007/s40265-016-0597-9

Marsden, C. D., & Parkes, J. D. (1977). Success and problems of long-term levodopa therapy in Parkinson's disease. *Lancet (London, England)*, *1*(8007), 345–349. https://doi.org/10.1016/s0140-6736(77)91146-1

Marsicano, G., Goodenough, S., Monory, K., Hermann, H., Eder, M., Cannich, A., Azad, S. C., Cascio, M. G., Ortega-Gutiérrez, S., Van der Stelt, M., López-Rodríguez, M. L., Casanova, E., Schütz, G., Zieglgänsberger, W., Di Marzo, V., Behl, C., & Lutz, B. (2003). CB1 cannabinoid receptors and on-demand defense against excitotoxicity. *Science*, *302*(5642), 84–88. https://doi.org/10.1126/science.1088208

Marsicano, G., & Lutz, B. (1999). Expression of the cannabinoid receptor CB1 in distinct neuronal subpopulations in the adult mouse forebrain. *European Journal of Neuroscience*, *11*(12), 4213–4225. https://doi.org/10.1046/j.1460-9568.1999.00847.x

Marsicano, G., Moosmann, B., Hermann, H., Lutz, B., & Behl, C. (2002). Neuroprotective properties of cannabinoids against oxidative stress: Role of the cannabinoid receptor CB1. *Journal of Neurochemistry*, *80*(3), 448–456. https://doi.org/10.1046/j.0022-3042.2001.00716.x

Martín, A. B., Fernandez-Espejo, E., Ferrer, B., Gorriti, M. A., Bilbao, A., Navarro, M., Rodriguez De Fonseca, F., & Moratalla, R. (2008). Expression and function of CB1 receptor in the rat striatum: Localization and effects on D1 and D2 dopamine receptor-mediated motor behaviors. *Neuropsychopharmacology*, *33*(7), 1667–1679. https://doi.org/10.1038/sj.npp.1301558

Martínez-Fernández, R., Rodríguez-Rojas, R., del Álamo, M., Hernández-Fernández, F., Pineda-Pardo, J. A., Dileone, M., Alonso-Frech, F., Foffani, G., Obeso, I., Gasca-Salas, C., de Luis-Pastor, E., Vela, L., & Obeso, J. A. (2018). Focused ultrasound subthalamotomy in patients with asymmetric Parkinson's disease: A pilot study. *The Lancet Neurology*, *17*(1), 54–63. https://doi.org/10.1016/S1474-4422(17)30403-9

Martínez-Murillo, R., Villalba, R., Montero-Caballero, M. I., & Rodrigo, J. (1989). Cholinergic somata and terminals in the rat substantia nigra: An immunocytochemical study with optical and electron microscopic techniques. *The Journal of Comparative Neurology*, *281*(3), 397–415. https://doi.org/10.1002/cne.902810306

Masimore, B., Schmitzer-Torbert, N. C., Kakalios, J., & David Redish, A. (2005). Transient striatal γ local field potentials signal movement initiation in rats. *NeuroReport*, *16*(18), 2021–2024.

Mason, S. T., & Fibiger, H. C. (1979). Regional topography within noradrenergic locus coeruleus as revealed by retrograde transport of horseradish peroxidase. *The Journal of Comparative Neurology*, *187*(4), 703–724. https://doi.org/10.1002/cne.901870405

Massimini, M., Huber, R., Ferrarelli, F., Hill, S., & Tononi, G. (2004). The Sleep Slow Oscillation as a Traveling Wave. *Journal of Neuroscience*, *24*(31), 6862–6870. https://doi.org/10.1523/JNEUROSCI.1318-04.2004

Mateo, Y., Johnson, K. A., Covey, D. P., Atwood, B. K., Wang, H. L., Zhang, S., Gildish, I., Cachope, R., Bellocchio, L., Guzmán, M., Morales, M., Cheer, J. F., & Lovinger, D. M. (2017). Endocannabinoid Actions on Cortical Terminals Orchestrate Local Modulation of Dopamine Release in the Nucleus Accumbens. *Neuron*, *96*(5), 1112-1126.e5. https://doi.org/10.1016/j.neuron.2017.11.012

Mathur, B. N., Tanahira, C., Tamamaki, N., & Lovinger, D. M. (2013). Voltage drives diverse endocannabinoid signals to mediate striatal microcircuit-specific plasticity. *Nature Neuroscience*, *16*(9), 1275–1283. https://doi.org/10.1038/nn.3478

Matsuda, L. A., Bonner, T. I., & Lolait, S. J. (1993). Localization of cannabinoid receptor mRNA in rat brain. *Journal of Comparative Neurology*, *327*(4), 535–550. https://doi.org/10.1002/cne.903270406

Maurice, N., Deltheil, T., Melon, C., Degos, B., Mourre, C., Amalric, M., & Goff, L. K. L. (2015). Bee venom alleviates motor deficits and modulates the transfer of cortical

information through the basal ganglia in rat models of Parkinson's disease. *PLoS ONE, 10*(11). https://doi.org/10.1371/journal.pone.0142838

Maurice, N., Deniau, J. M., Glowinski, J., & Thierry, A. M. (1999). Relationships between the prefrontal cortex and the basal ganglia in the rat: Physiology of the cortico-nigral circuits. *Journal of Neuroscience, 19*(11), 4674–4681. https://doi.org/10.1523/jneurosci.19-11-04674.1999

Maurice, N., Liberge, M., Jaouen, F., Ztaou, S., Hanini, M., Camon, J., Deisseroth, K., Amalric, M., Kerkerian-Le Goff, L., & Beurrier, C. (2015). Striatal Cholinergic Interneurons Control Motor Behavior and Basal Ganglia Function in Experimental Parkinsonism. *Cell Reports, 13*(4), 657–666. https://doi.org/10.1016/j.celrep.2015.09.034

McFarland, N. R., & Haber, S. N. (2002). Thalamic relay nuclei of the basal ganglia form both reciprocal and nonreciprocal cortical connections, linking multiple frontal cortical areas. *Journal of Neuroscience, 22*(18), 8117–8132. https://doi.org/10.1523/jneurosci.22-18-08117.2002

McGeer, P. L., Itagaki, S., Boyes, B. E., & McGeer, E. G. (1988). Reactive microglia are positive for HLA-DR in the substantia nigra of Parkinson's and Alzheimer's disease brains. *Neurology, 38*(8), 1285–1291. https://doi.org/10.1212/wnl.38.8.1285

McGeorge, A. J., & Faull, R. L. M. (1989). The organization of the projection from the cerebral cortex to the striatum in the rat. *Neuroscience, 29*(3), 503–537. https://doi.org/10.1016/0306-4522(89)90128-0

McGregor, M. M., & Nelson, A. B. (2019). Circuit Mechanisms of Parkinson's Disease. *Neuron, 101*(6), 1042–1056. https://doi.org/10.1016/j.neuron.2019.03.004

McHugh, D., Page, J., Dunn, E., & Bradshaw, H. B. (2012). Δ9-Tetrahydrocannabinol and N-arachidonyl glycine are full agonists at GPR18 receptors and induce migration in human endometrial HEC-1B cells. *British Journal of Pharmacology, 165*(8), 2414–2424. https://doi.org/10.1111/j.1476-5381.2011.01497.x

Mclaughlin, P. J., Delevan, C. E., Carnicom, S., Robinson, J. K., & Brener, J. (2000). Fine motor control in rats is disrupted by delta-9-tetrahydrocannabinol. *Pharmacology, Biochemistry, and Behavior, 66*(4), 803–809. https://doi.org/10.1016/s0091-3057(00)00281-1

McMillan, P. J., White, S. S., Franklin, A., Greenup, J. L., Leverenz, J. B., Raskind, M. A., & Szot, P. (2011). Differential response of the central noradrenergic nervous system to the loss of locus coeruleus neurons in Parkinson's disease and Alzheimer's disease. *Brain Research*, *1373*, 240–252. https://doi.org/10.1016/j.brainres.2010.12.015

McNaught, K. S., & Jenner, P. (2001). Proteasomal function is impaired in substantia nigra in Parkinson's disease. *Neuroscience Letters*, *297*(3), 191–194. https://doi.org/10.1016/s0304-3940(00)01701-8

Meissner, W., Ravenscroft, P., Reese, R., Harnack, D., Morgenstern, R., Kupsch, A., Klitgaard, H., Bioulac, B., Gross, C. E., Bezard, E., & Boraud, T. (2006). Increased slow oscillatory activity in substantia nigra pars reticulata triggers abnormal involuntary movements in the 6-OHDA-lesioned rat in the presence of excessive extracelullar striatal dopamine. *Neurobiology of Disease*, *22*(3), 586–598. https://doi.org/10.1016/j.nbd.2006.01.009

Miguelez, C., Morin, S., Martinez, A., Goillandeau, M., Bezard, E., Bioulac, B., & Baufreton, J. (2012). Altered pallido-pallidal synaptic transmission leads to aberrant firing of globus pallidus neurons in a rat model of Parkinson's disease. *Journal of Physiology*, *590*(22), 5861–5875. https://doi.org/10.1113/jphysiol.2012.241331

Miller, A. S., Sañudo-Peña, M. C., & Walker, J. M. (1998). Ipsilateral turning behavior induced by unilateral microinjections of a cannabinoid into the rat subthalamic nucleus. *Brain Research*, *793*(1), 7–11. https://doi.org/10.1016/S0006-8993(97)01475-3

Miller, A. S., & Walker, J. M. (1995). Effects of a cannabinoid on spontaneous and evoked neuronal activity in the substantia nigra pars reticulata. *European Journal of Pharmacology*, *279*(2–3), 179–185. https://doi.org/10.1016/0014-2999(95)00151-A

Miller, A. S., & Walker, J. M. (1996). Electrophysiological effects of a cannabinoid on neural activity in the globus pallidus. *European Journal of Pharmacology*, *304*(1–3), 29–35. https://doi.org/10.1016/0014-2999(96)00111-2

Miller, W. C., & DeLong, M. R. (1987). Altered Tonic Activity of Neurons in the Globus Pallidus and Subthalamic Nucleus in the Primate MPTP Model of Parkinsonism. In M. B. Carpenter & A. Jayaraman (Eds.), *The Basal Ganglia II* (pp. 415–427). Springer US. https://doi.org/10.1007/978-1-4684-5347-8_29

7. Bibliography

Mink, J. W. (2003). The basal ganglia and involuntary movements: Impaired inhibition of competing motor patterns. *Archives of Neurology*, *60*(10), 1365–1368. Scopus. https://doi.org/10.1001/archneur.60.10.1365

Molina-Holgado, F., Molina-Holgado, E., Guaza, C., & Rothwell, N. J. (2002). Role of CB1 and CB2 receptors in the inhibitory effects of cannabinoids on lipopolysaccharide-induced nitric oxide release in astrocyte cultures. *Journal of Neuroscience Research*, *67*(6), 829–836. https://doi.org/10.1002/jnr.10165

Morales, M., & Root, D. H. (2014). Glutamate neurons within the midbrain dopamine regions. *Neuroscience*, *282*, 60–68. https://doi.org/10.1016/j.neuroscience.2014.05.032

Morera-Herreras, T., Ruiz-Ortega, J. A., Gómez-Urquijo, S., & Ugedo, L. (2008). Involvement of subthalamic nucleus in the stimulatory effect of Δ9-tetrahydrocannabinol on dopaminergic neurons. *Neuroscience*, *151*(3), 817–823. https://doi.org/10.1016/j.neuroscience.2007.11.016

Morera-Herreras, T., Ruiz-Ortega, J. Á., Linazasoro, G., & Ugedo, L. (2011). Nigrostriatal denervation changes the effect of cannabinoids on subthalamic neuronal activity in rats. *Psychopharmacology*, *214*(2), 379–389. https://doi.org/10.1007/s00213-010-2043-0

Morera-Herreras, T., Ruiz-Ortega, J. A., & Ugedo, L. (2010). Two opposite effects of Δ9-tetrahydrocannabinol on subthalamic nucleus neuron activity: Involvement of GABAergic and glutamatergic neurotransmission. *Synapse*, *64*(1), 20–29. https://doi.org/10.1002/syn.20701

Müller, M. L. T. M., & Bohnen, N. I. (2013). Cholinergic dysfunction in Parkinson's disease. *Current Neurology and Neuroscience Reports*, *13*(9), 377. https://doi.org/10.1007/s11910-013-0377-9

Munro, S., Thomas, K. L., & Abu-Shaar, M. (1993). Molecular characterization of a peripheral receptor for cannabinoids. *Nature*, *365*(6441), 61–65. https://doi.org/10.1038/365061a0

Murer, M. G., Riquelme, L. A., Tseng, K. Y., & Pazo, J. H. (1997). Substantia nigra pars reticulata single unit activity in normal and 60HDA-lesioned rats: Effects of

intrastriatal apomorphine and subthalamic lesions. *Synapse*, *27*(4), 278–293. https://doi.org/10.1002/(SICI)1098-2396(199712)27:4<278::AID-SYN2>3.0.CO;2-9

Naito, A., & Kita, H. (1994). The cortico-nigral projection in the rat: An anterograde tracing study with biotinylated dextran amine. *Brain Research*, *637*(1–2), 317–322. Scopus. https://doi.org/10.1016/0006-8993(94)91252-1

Nakanishi, S., Hikida, T., & Yawata, S. (2014). Distinct dopaminergic control of the direct and indirect pathways in reward-based and avoidance learning behaviors. *Neuroscience*, *282*, 49–59. https://doi.org/10.1016/j.neuroscience.2014.04.026

Nalls, M. A., Pankratz, N., Lill, C. M., Do, C. B., Hernandez, D. G., Saad, M., Destefano, A. L., Kara, E., Bras, J., Sharma, M., Schulte, C., Keller, M. F., Arepalli, S., Letson, C., Edsall, C., Stefansson, H., Liu, X., Pliner, H., Lee, J. H., … Ansorge, O. (2014). Large-scale meta-analysis of genome-wide association data identifies six new risk loci for Parkinson's disease. *Nature Genetics*, *46*(9), 989–993. https://doi.org/10.1038/ng.3043

Nambu, A., Tokuno, H., & Takada, M. (2002). Functional significance of the cortico–subthalamo–pallidal 'hyperdirect' pathway. *Neuroscience Research*, *43*(2), 111–117. https://doi.org/10.1016/S0168-0102(02)00027-5

Narushima, M., Uchigashima, M., Hashimoto, K., Watanabe, M., & Kano, M. (2006). Depolarization-induced suppression of inhibition mediated by endocannabinoids at synapses from fast-spiking interneurons to medium spiny neurons in the striatum. *European Journal of Neuroscience*, *24*(8), 2246–2252. https://doi.org/10.1111/j.1460-9568.2006.05119.x

Navarrete, F., García-Gutiérrez, M. S., Aracil-Fernández, A., Lanciego, J. L., & Manzanares, J. (2018). Cannabinoid CB1 and CB2 Receptors, and Monoacylglycerol Lipase Gene Expression Alterations in the Basal Ganglia of Patients with Parkinson's Disease. *Neurotherapeutics*, *15*(2), 1–11. https://doi.org/10.1007/s13311-018-0603-x

Nelong, T. F., Jenkins, B. W., Perreault, M. L., & Khokhar, J. Y. (2019). Extended Attenuation of Corticostriatal Power and Coherence after Acute Exposure to Vapourized Δ9-Tetrahydrocannabinol in Rats. *Canadian Journal of Addiction*, *10*(3), 60–66. https://doi.org/10.1097/CXA.0000000000000063

7. Bibliography

Nicolle, M. M., & Baxter, M. G. (2003). Glutamate receptor binding in the frontal cortex and dorsal striatum of aged rats with impaired attentional set-shifting. *European Journal of Neuroscience*, *18*(12), 3335–3342. https://doi.org/10.1111/j.1460-9568.2003.03077.x

Nonomura, S., Nishizawa, K., Sakai, Y., Kawaguchi, Y., Kato, S., Uchigashima, M., Watanabe, M., Yamanaka, K., Enomoto, K., Chiken, S., Sano, H., Soma, S., Yoshida, J., Samejima, K., Ogawa, M., Kobayashi, K., Nambu, A., Isomura, Y., & Kimura, M. (2018). Monitoring and Updating of Action Selection for Goal-Directed Behavior through the Striatal Direct and Indirect Pathways. *Neuron*, *99*(6), 1302-1314.e5. https://doi.org/10.1016/j.neuron.2018.08.002

Nottage, J. F., Stone, J., Murray, R. M., Sumich, A., Bramon-Bosch, E., Ffytche, D., & Morrison, P. D. (2015). Delta-9-tetrahydrocannabinol, neural oscillations above 20 Hz and induced acute psychosis. *Psychopharmacology*, *232*(3), 519–528. https://doi.org/10.1007/s00213-014-3684-1

Obeso, J. A., Rodriguez-Oroz, M. C., Goetz, C. G., Marin, C., Kordower, J. H., Rodriguez, M., Hirsch, E. C., Farrer, M., Schapira, A. H. V., & Halliday, G. (2010). Missing pieces in the Parkinson's disease puzzle. *Nature Medicine*, *16*(6), 653–661. https://doi.org/10.1038/nm.2165

Ofek, O., Karsak, M., Leclerc, N., Fogel, M., Frenkel, B., Wright, K., Tam, J., Attar-Namdar, M., Kram, V., Shohami, E., Mechoulam, R., Zimmer, A., & Bab, I. (2006). Peripheral cannabinoid receptor, CB2, regulates bone mass. *Proceedings of the National Academy of Sciences of the United States of America*, *103*(3), 696–701. https://doi.org/10.1073/pnas.0504187103

Ohiorhenuan, I. E., Mechler, F., Purpura, K. P., Schmid, A. M., Hu, Q., & Victor, J. D. (2014). Cannabinoid Neuromodulation in the Adult Early Visual Cortex. *PLOS ONE*, *9*(2), e87362. https://doi.org/10.1371/journal.pone.0087362

Ojha, S., Javed, H., Azimullah, S., & Haque, M. E. (2016). β-Caryophyllene, a phytocannabinoid attenuates oxidative stress, neuroinflammation, glial activation, and salvages dopaminergic neurons in a rat model of Parkinson disease. *Molecular and Cellular Biochemistry*, *418*(1–2), 59–70. https://doi.org/10.1007/s11010-016-2733-y

Olanow, C. W. (2008). Levodopa/dopamine replacement strategies in Parkinson's disease—Future directions. *Movement Disorders*, *23*(S3), S613–S622. https://doi.org/10.1002/mds.22061

Oorschot, D. E., Tunstall, M. J., & Wickens, J. R. (2002). Local Connectivity Between Striatal Spiny Projection Neurons: A Re-Evaluation. In L. F. B. Nicholson & R. L. M. Faull (Eds.), *The Basal Ganglia VII* (pp. 421–434). Springer US. https://doi.org/10.1007/978-1-4615-0715-4_42

O'Sullivan, S. E. (2016). An update on PPAR activation by cannabinoids. *British Journal of Pharmacology*, *173*(12), 1899–1910. https://doi.org/10.1111/bph.13497

O'Sullivan, S. E., & Kendall, D. A. (2010). Cannabinoid activation of peroxisome proliferator-activated receptors: Potential for modulation of inflammatory disease. *Immunobiology*, *215*(8), 611–616. https://doi.org/10.1016/j.imbio.2009.09.007

Ouchi, Y., Yoshikawa, E., Sekine, Y., Futatsubashi, M., Kanno, T., Ogusu, T., & Torizuka, T. (2005). Microglial activation and dopamine terminal loss in early Parkinson's disease. *Annals of Neurology*, *57*(2), 168–175. https://doi.org/10.1002/ana.20338

Pagano, G., Rengo, G., Pasqualetti, G., Femminella, G. D., Monzani, F., Ferrara, N., & Tagliati, M. (2015). Cholinesterase inhibitors for Parkinson's disease: A systematic review and meta-analysis. *Journal of Neurology, Neurosurgery and Psychiatry*, *86*(7), 767–773. https://doi.org/10.1136/jnnp-2014-308764

Pan, M. K., Kuo, S. H., Tai, C. H., Liou, J. Y., Pei, J. C., Chang, C. Y., Wang, Y. M., Liu, W. C., Wang, T. R., Lai, W. S., & Kuo, C. C. (2016). Neuronal firing patterns outweigh circuitry oscillations in parkinsonian motor control. *Journal of Clinical Investigation*, *126*(12), 4516–4526. https://doi.org/10.1172/JCI88170

Pandya, D. N., Seltzer, B., Petrides, M., & Cipolloni, P. B. (2014). *Cerebral cortex: Architecture, connections, and the dual origin concept*. Oxford University Press.

Parent, A., & Hazrati, L. N. (1995). Functional anatomy of the basal ganglia. II. The place of subthalamic nucleus and external pallidium in basal ganglia circuitry. *Brain Research Reviews*, *20*(1), 128–154. https://doi.org/10.1016/0165-0173(94)00008-D

7. Bibliography

Park, G., Tan, J., Garcia, G., Kang, Y., Salvesen, G., & Zhang, Z. (2016). Regulation of histone acetylation by autophagy in Parkinson disease. *Journal of Biological Chemistry*, *291*(7), 3531–3540. https://doi.org/10.1074/jbc.M115.675488

Parkinson, J. (2002). An essay on the shaking palsy. 1817. *The Journal of Neuropsychiatry and Clinical Neurosciences*, *14*(2), 223–236; discussion 222. https://doi.org/10.1176/jnp.14.2.223

Paxinos, G., & Watson, C. (2006). *The Rat Brain in Stereotaxic Coordinates: Hard Cover Edition*. Elsevier.

Pennartz, C. M. A., Berke, J. D., Graybiel, A. M., Ito, R., Lansink, C. S., Van Der Meer, M., Redish, A. D., Smith, K. S., & Voorn, P. (2009). Corticostriatal interactions during learning, memory processing, and decision making. *Journal of Neuroscience*, *29*(41), 12831–12838. https://doi.org/10.1523/JNEUROSCI.3177-09.2009

Perkins, M. N., & Stone, T. W. (1983). Neuronal responses to 5-hydroxytryptamine and dorsal raphe stimulation within the globus pallidus of the rat. *Experimental Neurology*, *79*(1), 118–129. https://doi.org/10.1016/0014-4886(83)90383-7

Pertwee, R. G. (2001). Cannabinoids and the gastrointestinal tract. *Gut*, *48*(6), 859–867. https://doi.org/10.1136/gut.48.6.859

Pertwee, R. G. (2006). The pharmacology of cannabinoid receptors and their ligands: An overview. *International Journal of Obesity*, *30*, S13–S18. https://doi.org/10.1038/sj.ijo.0803272

Phillips, J. G., Bradshaw, J. L., Iansek, R., & Chiu, E. (1993). *Motor functions of the basal ganglia*. 7.

Pinault, D. (2005). A new stabilizing craniotomy–duratomy technique for single-cell anatomo-electrophysiological exploration of living intact brain networks. *Journal of Neuroscience Methods*, *141*(2), 231–242. https://doi.org/10.1016/J.JNEUMETH.2004.06.015

Piomelli, D. (2003). The molecular logic of endocannabinoid signalling. *Nature Reviews Neuroscience*, *4*(11), 873–884. https://doi.org/10.1038/nrn1247

Pistis, M., Ferraro, L., Pira, L., Flore, G., Tanganelli, S., Gessa, G. L., & Devoto, P. (2002). Δ9-Tetrahydrocannabinol decreases extracellular GABA and increases extracellular glutamate and dopamine levels in the rat prefrontal cortex: An in vivo microdialysis study. *Brain Research*, *948*(1), 155–158. https://doi.org/10.1016/S0006-8993(02)03055-X

Poewe, W., Seppi, K., Tanner, C. M., Halliday, G. M., Brundin, P., Volkmann, J., Schrag, A.-E., & Lang, A. E. (2017). Parkinson disease. *Nature Reviews Disease Primers*, *3*(1), 1–21. https://doi.org/10.1038/nrdp.2017.13

Polissidis, A., Chouliara, O., Galanopoulos, A., Naxakis, G., Papahatjis, D., Papadopoulou-Daifoti, Z., & Antoniou, K. (2014). Cannabinoids negatively modulate striatal glutamate and dopamine release and behavioural output of acute D-amphetamine. *Behavioural Brain Research*, *270*, 261–269. https://doi.org/10.1016/j.bbr.2014.05.029

Pontone, G. M., Williams, J. R., Anderson, K. E., Chase, G., Goldstein, S. A., Grill, S., Hirsch, E. S., Lehmann, S., Little, J. T., Margolis, R. L., Rabins, P. V., Weiss, H. D., & Marsh, L. (2009). Prevalence of anxiety disorders and anxiety subtypes in patients with Parkinson's disease. *Movement Disorders*, *24*(9), 1333–1338. https://doi.org/10.1002/mds.22611

Postuma, R. B., Berg, D., Stern, M., Poewe, W., Olanow, C. W., Oertel, W., Obeso, J., Marek, K., Litvan, I., Lang, A. E., Halliday, G., Goetz, C. G., Gasser, T., Dubois, B., Chan, P., Bloem, B. R., Adler, C. H., & Deuschl, G. (2015). MDS clinical diagnostic criteria for Parkinson's disease. *Movement Disorders: Official Journal of the Movement Disorder Society*, *30*(12), 1591–1601. https://doi.org/10.1002/mds.26424

Price, D. A., Martinez, A. A., Seillier, A., Koek, W., Acosta, Y., Fernandez, E., Strong, R., Lutz, B., Marsicano, G., Roberts, J. L., & Giuffrida, A. (2009). WIN55,212-2, a cannabinoid receptor agonist, protects against nigrostriatal cell loss in the 1-methyl-4-phenyl-1,2,3,6-tetrahydropyridine mouse model of Parkinson's disease. *European Journal of Neuroscience*, *29*(11), 2177–2186. https://doi.org/10.1111/j.1460-9568.2009.06764.x

Qin, N., Neeper, M. P., Liu, Y., Hutchinson, T. L., Lubin, M. L., & Flores, C. M. (2008). TRPV2 is activated by cannabidiol and mediates CGRP release in cultured rat dorsal root ganglion neurons. *The Journal of Neuroscience: The Official Journal of the Society for Neuroscience*, *28*(24), 6231–6238. https://doi.org/10.1523/JNEUROSCI.0504-08.2008

7. Bibliography

Rajakumar, N., Elisevich, K., & Flumerfelt, B. A. (1994). Parvalbumin-containing GABAergic neurons in the basal ganglia output system of the rat. *Journal of Comparative Neurology, 350*(2), 324–336. https://doi.org/10.1002/cne.903500214

Rajakumar, N., Rushlow, W., Naus, C. C. G., Elisevich, K., & Flumerfelt, B. A. (1994). Neurochemical compartmentalization of the globus pallidus in the rat: An immunocytochemical study of calcium-binding proteins. *Journal of Comparative Neurology, 346*(3), 337–348. https://doi.org/10.1002/cne.903460303

Ramaekers, J. G., Moeller, M. R., van Ruitenbeek, P., Theunissen, E. L., Schneider, E., & Kauert, G. (2006). Cognition and motor control as a function of Δ9-THC concentration in serum and oral fluid: Limits of impairment. *Drug and Alcohol Dependence, 85*(2), 114–122. https://doi.org/10.1016/j.drugalcdep.2006.03.015

Ramsey, C. P., & Tansey, M. G. (2014). A survey from 2012 of evidence for the role of neuroinflammation in neurotoxin animal models of Parkinson's disease and potential molecular targets. *Experimental Neurology, 256*, 126–132. https://doi.org/10.1016/j.expneurol.2013.05.014

Reijnders, J. S. A. M., Ehrt, U., Weber, W. E. J., Aarsland, D., & Leentjens, A. F. G. (2008). A systematic review of prevalence studies of depression in Parkinson's disease. *Movement Disorders, 23*(2), 183–189. https://doi.org/10.1002/mds.21803

Rice, M. E., Cragg, S. J., & Greenfield, S. A. (1997). Characteristics of electrically evoked somatodendritic dopamine release in substantia nigra and ventral tegmental area in vitro. *Journal of Neurophysiology, 77*(2), 853–862. https://doi.org/10.1152/jn.1997.77.2.853

Rice, M. E., Richards, C. D., Nedergaard, S., Hounsgaard, J., Nicholson, C., & Greenfield, S. A. (1994). Direct monitoring of dopamine and 5-HT release in substantia nigra and ventral tegmental area in vitro. *Experimental Brain Research, 100*(3), 395–406. https://doi.org/10.1007/bf02738400

Robbe, D., Montgomery, S. M., Thome, A., Rueda-Orozco, P. E., McNaughton, B. L., & Buzsaki, G. (2006). Cannabinoids reveal importance of spike timing coordination in hippocampal function. *Nature Neuroscience, 9*(12), 1526–1533. https://doi.org/10.1038/nn1801

Robbins, T. W., & Cools, R. (2014). Cognitive deficits in Parkinson's disease: A cognitive neuroscience perspective: Cognitive Neuroscience Of Parkinson's disease. *Movement Disorders*, *29*(5), 597–607. https://doi.org/10.1002/mds.25853

Roche, R., Hoareau, L., Bes-Houtmann, S., Gonthier, M. P., Laborde, C., Baron, J. F., Haffaf, Y., Cesari, M., & Festy, F. (2006). Presence of the cannabinoid receptors, CB1 and CB2, in human omental and subcutaneous adipocytes. *Histochemistry and Cell Biology*, *126*(2), 177–187. https://doi.org/10.1007/s00418-005-0127-4

Rojo-Bustamante, E., Abellanas, M. A., Clavero, P., Thiolat, M. L., Li, Q., Luquin, M. R., Bezard, E., & Aymerich, M. S. (2018). The expression of cannabinoid type 1 receptor and 2-arachidonoyl glycerol synthesizing/degrading enzymes is altered in basal ganglia during the active phase of levodopa-induced dyskinesia. *Neurobiology of Disease*, *118*, 64–75. https://doi.org/10.1016/j.nbd.2018.06.019

Romero, J., Berrendero, F., Pérez-Rosado, A., Manzanares, J., Rojo, A., Fernández-Ruiz, J. J., De Yebenes, J. G., & Ramos, J. A. (1999). Unilateral 6-hydroxydopamine lesions of nigrostriatal dopaminergic neurons increased CB1 receptor mRNA levels in the caudate-putamen. *Life Sciences*, *66*(6), 485–494. https://doi.org/10.1016/S0024-3205(99)00618-9

Romero, J., de Miguel, R., García-Palomero, E., Fernández-Ruiz, J. J., & Ramos, J. A. (1995). Time-course of the effects of anandamide, the putative endogenous cannabinoid receptor ligand, on extrapyramidal function. *Brain Research*, *694*(1–2), 223–232. https://doi.org/10.1016/0006-8993(95)00835-e

Romero, J., García, L., Cebeira, M., Zadrozny, D., Fernández-Ruiz, J. J., & Ramos, J. A. (1995). The endogenous cannabinoid receptor ligand, anandamide, inhibits the motor behavior: Role of nigrostriatal dopaminergic neurons. *Life Sciences*, *56*(23–24), 2033–2040. https://doi.org/10.1016/0024-3205(95)00186-a

Rommelfanger, K. S., & Wichmann, T. (2010). Extrastriatal Dopaminergic Circuits of the Basal Ganglia. *Frontiers in Neuroanatomy*, *4*. https://doi.org/10.3389/fnana.2010.00139

Rosales, M. G., Flores, G., Hernández, S., Martínez-Fong, D., & Aceves, J. (1994). Activation of subthalamic neurons produces NMDA receptor-mediated dendritic dopamine release in substantia nigra pars reticulata: A microdialysis study in the rat. *Brain Research*, *645*(1), 335–337. https://doi.org/10.1016/0006-8993(94)91669-1

7. Bibliography

Ruiz-Mejias, M., Ciria-Suarez, L., Mattia, M., & Sanchez-Vives, M. V. (2011). Slow and fast rhythms generated in the cerebral cortex of the anesthetized mouse. *Journal of Neurophysiology*, *106*(6), 2910–2921. https://doi.org/10.1152/jn.00440.2011

Sadek, A. R., Magill, P. J., & Bolam, J. P. (2007). A single-cell analysis of intrinsic connectivity in the rat globus pallidus. *Journal of Neuroscience*, *27*(24), 6352–6362. https://doi.org/10.1523/JNEUROSCI.0953-07.2007

Saggu, H., Cooksey, J., Dexter, D., Wells, F. R., Lees, A., Jenner, P., & Marsden, C. D. (1989). A selective increase in particulate superoxide dismutase activity in parkinsonian substantia nigra. *Journal of Neurochemistry*, *53*(3), 692–697. https://doi.org/10.1111/j.1471-4159.1989.tb11759.x

Saland, S. K., & Kabbaj, M. (2018). Sex Differences in the Pharmacokinetics of Low-dose Ketamine in Plasma and Brain of Male and Female Rats. *Journal of Pharmacology and Experimental Therapeutics*, *367*(3), 393–404. https://doi.org/10.1124/jpet.118.251652

Sales-Carbonell, C., Rueda-Orozco, P. E., Soria-Gómez, E., Buzsáki, G., Marsicano, G., & Robbe, D. (2013). Striatal GABAergic and cortical glutamatergic neurons mediate contrasting effects of cannabinoids on cortical network synchrony. *Proceedings of the National Academy of Sciences*, *110*(2), 719–724. https://doi.org/10.1073/pnas.1217144110

Sano, H., & Nambu, A. (2019). The effects of zonisamide on L-DOPA–induced dyskinesia in Parkinson's disease model mice. *Neurochemistry International*, *124*, 171–180. https://doi.org/10.1016/j.neuint.2019.01.011

Sañudo-Peña, M. C., Force, M., Tsou, K., Miller, A. S., & Walker, J. M. (1998). Effects of intrastriatal cannabinoids on rotational behavior in rats: Interactions with the dopaminergic system. *Synapse*, *30*(2), 221–226. https://doi.org/10.1002/(SICI)1098-2396(199810)30:2<221::AID-SYN12>3.0.CO;2-4

Sañudo-Peña, M. C., Tsou, K., & Walker, J. M. (1999). Motor actions of cannabinoids in the basal ganglia output nuclei. *Life Sciences*, *65*(6–7), 703–713. https://doi.org/10.1016/S0024-3205(99)00293-3

Sañudo-Peña, M. C., & Walker, J. M. (1997). Role of the subthalamic nucleus in cannabinoid actions in the substantia nigra of the rat. *Journal of Neurophysiology*, *77*(3), 1635–1638. https://doi.org/10.1152/jn.1997.77.3.1635

Sañudo-Peña, M. C., & Walker, J. M. (1998). Effects of intrapallidal cannabinoids on rotational behavior in rats: Interactions with the dopaminergic system. *Synapse*, *28*(1), 27–32. https://doi.org/10.1002/(SICI)1098-2396(199801)28:1<27::AID-SYN4>3.0.CO;2-E

Saunders, A., Huang, K. W., & Sabatini, B. L. (2016). Globus Pallidus Externus Neurons Expressing parvalbumin Interconnect the Subthalamic Nucleus and Striatal Interneurons. *PLOS ONE*, *11*(2), e0149798. https://doi.org/10.1371/journal.pone.0149798

Sawada, M., Kato, K., Kunieda, T., Mikuni, N., Miyamoto, S., Onoe, H., Isa, T., & Nishimura, Y. (2015). Function of the nucleus accumbens in motor control during recovery after spinal cord injury. *Science*, *350*(6256), 98–101. https://doi.org/10.1126/science.aab3825

Schapira, A. H., & Jenner, P. (2011). Etiology and pathogenesis of Parkinson's disease. *Movement Disorders*, *26*(6), 1049–1055. https://doi.org/10.1002/mds.23732

Schapira, A. H., Mann, V. M., Cooper, J. M., Dexter, D., Daniel, S. E., Jenner, P., Clark, J. B., & Marsden, C. D. (1990). Anatomic and disease specificity of NADH CoQ1 reductase (complex I) deficiency in Parkinson's disease. *Journal of Neurochemistry*, *55*(6), 2142–2145. https://doi.org/10.1111/j.1471-4159.1990.tb05809.x

Schindelin, J., Arganda-Carreras, I., Frise, E., Kaynig, V., Longair, M., Pietzsch, T., Preibisch, S., Rueden, C., Saalfeld, S., Schmid, B., Tinevez, J. Y., White, D. J., Hartenstein, V., Eliceiri, K., Tomancak, P., & Cardona, A. (2012). Fiji: An open-source platform for biological-image analysis. *Nature Methods*, *9*(7), 676–682. https://doi.org/10.1038/nmeth.2019

Schreiner, A. M., & Dunn, M. E. (2012). Residual effects of cannabis use on neurocognitive performance after prolonged abstinence: A meta-analysis. *Experimental and Clinical Psychopharmacology*, *20*(5), 420–429. https://doi.org/10.1037/a0029117

Seirafi, M., Kozlov, G., & Gehring, K. (2015). Parkin structure and function. *The Febs Journal*, *282*(11), 2076–2088. https://doi.org/10.1111/febs.13249

Sethi, K. (2008). Levodopa unresponsive symptoms in Parkinson disease. *Movement Disorders*, *23*(S3), S521–S533. https://doi.org/10.1002/mds.22049

7. Bibliography

Sharman, M., Valabregue, R., Perlbarg, V., Marrakchi-Kacem, L., Vidailhet, M., Benali, H., Brice, A., & Lehéricy, S. (2013). Parkinson's disease patients show reduced cortical-subcortical sensorimotor connectivity. *Movement Disorders*, *28*(4), 447–454. https://doi.org/10.1002/mds.25255

Sharott, A., Doig, N. M., Mallet, N., & Magill, P. J. (2012). Relationships between the firing of identified striatal interneurons and spontaneous and driven cortical activities in vivo. *Journal of Neuroscience*, *32*(38), 13221–13236. https://doi.org/10.1523/JNEUROSCI.2440-12.2012

Sharott, A., Vinciati, F., Nakamura, K. C., & Magill, P. J. (2017). A population of indirect pathway striatal projection neurons is selectively entrained to parkinsonian beta oscillations. *Journal of Neuroscience*, *37*(41), 9977–9998. https://doi.org/10.1523/JNEUROSCI.0658-17.2017

Shen, K. Z., & Johnson, S. W. (2006). Subthalamic stimulation evokes complex EPSCs in the rat substantia nigra pars reticulata in vitro. *Journal of Physiology*, *573*(3), 697–709. https://doi.org/10.1113/jphysiol.2006.110031

Shepherd, G. M. G. (2013). Corticostriatal connectivity and its role in disease. *Nature Reviews Neuroscience*, *14*(4), 278–291. https://doi.org/10.1038/nrn3469

Showalter, V. M., Compton, D. R., Martin, B. R., & Abood, M. E. (1996). Evaluation of binding in a transfected cell line expressing a peripheral cannabinoid receptor (CB2): Identification of cannabinoid receptor subtype selective ligands. *The Journal of Pharmacology and Experimental Therapeutics*, *278*(3), 989–999.

Sidló, Z., Reggio, P. H., & Rice, M. E. (2008). Inhibition of striatal dopamine release by CB1 receptor activation requires nonsynaptic communication involving GABA, H2O2, and KATP channels. *Neurochemistry International*, *52*(1–2), 80–88. https://doi.org/10.1016/j.neuint.2007.07.014

Silvani, A., Berteotti, C., Bastianini, S., Martire, V. L., Mazza, R., Pagotto, U., Quarta, C., & Zoccoli, G. (2014). Multiple Sleep Alterations in Mice Lacking Cannabinoid Type 1 Receptors. *PLOS ONE*, *9*(2), e89432. https://doi.org/10.1371/journal.pone.0089432

Singh, A., Mewes, K., Gross, R. E., DeLong, M. R., Obeso, J. A., & Papa, S. M. (2016). Human striatal recordings reveal abnormal discharge of projection neurons in Parkinson's

disease. *Proceedings of the National Academy of Sciences of the United States of America, 113*(34), 9629–9634. https://doi.org/10.1073/pnas.1606792113

Skosnik, P. D., Cortes-Briones, J. A., & Hajós, M. (2016). It's all in the rhythm: The role of cannabinoids in neural oscillations and psychosis. *Biological Psychiatry, 79*(7), 568–577. https://doi.org/10.1016/j.biopsych.2015.12.011

Skosnik, P. D., Hajós, M., Cortes-Briones, J. A., Edwards, C. R., Pittman, B. P., Hoffmann, W. E., Sewell, A. R., D'Souza, D. C., & Ranganathan, M. (2018). Cannabinoid receptor-mediated disruption of sensory gating and neural oscillations: A translational study in rats and humans. *Neuropharmacology, 135*, 412–423. https://doi.org/10.1016/j.neuropharm.2018.03.036

Smith, I. D., & Grace, A. A. (1992). Role of the subthalamic nucleus in the regulation of nigral dopamine neuron activity. *Synapse, 12*(4), 287–303. https://doi.org/10.1002/syn.890120406

Smith, S. R., Terminelli, C., & Denhardt, G. (2000). Effects of cannabinoid receptor agonist and antagonist ligands on production of inflammatory cytokines and anti-inflammatory interleukin-10 in endotoxemic mice. *Journal of Pharmacology and Experimental Therapeutics, 293*(1), 136–150.

Smith, Y., & Bolam, J. P. (1989). Neurons of the substantia nigra reticulata receive a dense GABA-containing input from the globus pallidus in the rat. *Brain Research, 493*(1), 160–167. https://doi.org/10.1016/0006-8993(89)91011-1

Soares, J., Kliem, M. A., Betarbet, R., Greenamyre, J. T., Yamamoto, B., & Wichmann, T. (2004). Role of external pallidal segment in primate parkinsonism: Comparison of the effects of 1-methyl-4-phenyl-1,2,3,6-tetrahydropyridine-induced parkinsionism and lesions of the external pallidal segment. *Journal of Neuroscience, 24*(29), 6417–6426. https://doi.org/10.1523/JNEUROSCI.0836-04.2004

Souilhac, J., Poncelet, M., Rinaldi-Carmona, M., Le Fur, G., & Soubrié, P. (1995). Intrastriatal injection of cannabinoid receptor agonists induced turning behavior in mice. *Pharmacology, Biochemistry, and Behavior, 51*(1), 3–7. https://doi.org/10.1016/0091-3057(94)00396-z

7. Bibliography

Starr, P. A., Vitek, J. L., & Bakay, R. A. E. (1998). Ablative surgery and deep brain stimulation for Parkinson's disease. *Neurosurgery*, *43*(5), 989–1013. https://doi.org/10.1097/00006123-199811000-00001

Steigerwald, F., Pötter, M., Herzog, J., Pinsker, M., Kopper, F., Mehdorn, H., Deuschl, G., & Volkmann, J. (2008). Neuronal activity of the human subthalamic nucleus in the parkinsonian and nonparkinsonian state. *Journal of Neurophysiology*, *100*(5), 2515–2524. https://doi.org/10.1152/jn.90574.2008

Steinbusch, H. W. M. (1981). Distribution of serotonin-immunoreactivity in the central nervous system of the rat-Cell bodies and terminals. *Neuroscience*, *6*(4), 557–618. https://doi.org/10.1016/0306-4522(81)90146-9

Steinbusch, H. W. M., Niewenhuys, R., Verhofstad, A. A. J., & Van Der Kooy, D. (1981). The nucleus raphe dorsalis of the rat and its projection upon the caudatoputamen. A combined cytoarchitectonic, immunohistochemical and retrograde transport study. *Journal de Physiologie*, *77*(2–3), 157–174.

Storr, M., Gaffal, E., Saur, D., Schusdziarra, V., & Allescher, H. D. (2002). Effect of cannabinoids on neural transmission in rat gastric fundus. *Canadian Journal of Physiology and Pharmacology*, *80*(1), 67–76. https://doi.org/10.1139/y02-005

Suarez, L. M., Solis, O., Aguado, C., Lujan, R., & Moratalla, R. (2016). L-DOPA Oppositely Regulates Synaptic Strength and Spine Morphology in D1 and D2 Striatal Projection Neurons in Dyskinesia. *Cerebral Cortex*, *26*(11), 4253–4264. https://doi.org/10.1093/cercor/bhw263

Sun, S., Hu, F., Wu, J., & Zhang, S. (2017). Cannabidiol attenuates OGD/R-induced damage by enhancing mitochondrial bioenergetics and modulating glucose metabolism via pentose-phosphate pathway in hippocampal neurons. *Redox Biology*, *11*, 577–585. https://doi.org/10.1016/j.redox.2016.12.029

Surmeier, D. J. (2018). Determinants of dopaminergic neuron loss in Parkinson's disease. *FEBS Journal*, *285*(19), 3657–3668. https://doi.org/10.1111/febs.14607

Surmeier, D. J., Halliday, G. M., & Simuni, T. (2017). Calcium, mitochondrial dysfunction and slowing the progression of Parkinson's disease. *Experimental Neurology*, *298*, 202–209. https://doi.org/10.1016/j.expneurol.2017.08.001

Sylantyev, S., Jensen, T. P., Ross, R. A., & Rusakov, D. A. (2013). Cannabinoid- and lysophosphatidylinositol-sensitive receptor GPR55 boosts neurotransmitter release at central synapses. *Proceedings of the National Academy of Sciences of the United States of America*, *110*(13), 5193–5198. https://doi.org/10.1073/pnas.1211204110

Szabo, B., Dörner, L., Pfreundtner, C., Nörenberg, W., & Starke, K. (1998). Inhibition of GABAergic inhibitory postsynaptic currents by cannabinoids in rat corpus striatum. *Neuroscience*, *85*(2), 395–403. https://doi.org/10.1016/S0306-4522(97)00597-6

Szabo, B., & Schlicker, E. (2005). Effects of cannabinoids on neurotransmission. In *Handbook of Experimental Pharmacology* (Vol. 168, pp. 327–365). Springer, Berlin, Heidelberg.

Szabo, B., Siemes, S., & Wallmichrath, I. (2002). Inhibition of GABAergic neurotransmission in the ventral tegmental area by cannabinoids. *European Journal of Neuroscience*, *15*(12), 2057–2061. Scopus. https://doi.org/10.1046/j.1460-9568.2002.02041.x

Szabo, B., Wallmichrath, I., Mathonia, P., & Pfreundtner, C. (2000). Cannabinoids inhibit excitatory neurotransmission in the substantia nigra pars reticulata. *Neuroscience*, *97*(1), 89–97. https://doi.org/10.1016/S0306-4522(00)00036-1

Teismann, P., & Schulz, J. B. (2004). Cellular pathology of Parkinson's disease: Astrocytes, microglia and inflammation. *Cell and Tissue Research*, *318*(1), 149–161. https://doi.org/10.1007/s00441-004-0944-0

Tepper, J. M., Martin, L. P., & Anderson, D. R. (1995). GABA(A) receptor-mediated inhibition of rat substantia nigra dopaminergic neurons by pars reticulata projection neurons. *Journal of Neuroscience*, *15*(4), 3092–3103. https://doi.org/10.1523/JNEUROSCI.15-04-03092.1995

Tofaris, G. K., Layfield, R., & Spillantini, M. G. (2001). α-Synuclein metabolism and aggregation is linked to ubiquitin-independent degradation by the proteasome. *FEBS Letters*, *509*(1), 22–26. https://doi.org/10.1016/S0014-5793(01)03115-5

Toulorge, D., Schapira, A. H. V., & Hajj, R. (2016). Molecular changes in the postmortem parkinsonian brain. *Journal of Neurochemistry*, *139 Suppl*, 27–58. https://doi.org/10.1111/jnc.13696

7. Bibliography

Tremblay, L., Worbe, Y., Thobois, S., Sgambato-Faure, V., & Féger, J. (2015). Selective dysfunction of basal ganglia subterritories: From movement to behavioral disorders. *Movement Disorders*, *30*(9), 1155–1170. https://doi.org/10.1002/mds.26199

Trettel, J., & Levine, E. S. (2002). Cannabinoids Depress Inhibitory Synaptic Inputs Received by Layer 2/3 Pyramidal Neurons of the Neocortex. *Journal of Neurophysiology*, *88*(1), 534–539. https://doi.org/10.1152/jn.2002.88.1.534

Trettel, J., & Levine, E. S. (2003). Endocannabinoids mediate rapid retrograde signaling at interneuron → pyramidal neuron synapses of the neocortex. *Journal of Neurophysiology*, *89*(4), 2334–2338. https://doi.org/10.1152/jn.01037.2002

Tseng, K. Y., Riquelme, L. A., Belforte, J. E., Pazo, J. H., & Murer, M. G. (2000). Substantia nigra pars reticulata units in 6-hydroxydopamine-lesioned rats: Responses to striatal D2 dopamine receptor stimulation and subthalamic lesions. *European Journal of Neuroscience*, *12*(1), 247–256. https://doi.org/10.1046/j.1460-9568.2000.00910.x

Tysnes, O.-B., & Storstein, A. (2017). Epidemiology of Parkinson's disease. *Journal of Neural Transmission*, *124*(8), 901–905. https://doi.org/10.1007/s00702-017-1686-y

Uchigashima, M., Narushima, M., Fukaya, M., Katona, I., Kano, M., & Watanabe, M. (2007). Subcellular arrangement of molecules for 2-arachidonoyl-glycerol-mediated retrograde signaling and its physiological contribution to synaptic modulation in the striatum. *Journal of Neuroscience*, *27*(14), 3663–3676. https://doi.org/10.1523/JNEUROSCI.0448-07.2007

Van Den Eeden, S. K., Tanner, C. M., Bernstein, A. L., Fross, R. D., Leimpeter, A., Bloch, D. A., & Nelson, L. M. (2003). Incidence of Parkinson's disease: Variation by age, gender, and race/ethnicity. *American Journal of Epidemiology*, *157*(11), 1015–1022. https://doi.org/10.1093/aje/kwg068

Van Der Brug, M. P., Singleton, A., Gasser, T., & Lewis, P. A. (2015). Parkinson's disease: From human genetics to clinical trials. *Science Translational Medicine*, *7*(305), 205ps20. https://doi.org/10.1126/scitranslmed.aaa8280

Van Der Kooy, D., & Hattori, T. (1980). Single subthalamic nucleus neurons project to both the globus pallidus and substantia nigra in rat. *Journal of Comparative Neurology*, *192*(4), 751–768. https://doi.org/10.1002/cne.901920409

van der Meer, M. A. A., Kalenscher, T., Lansink, C. S., Pennartz, C. M. A., Berke, J. D., & Redish, A. D. (2010). Integrating early results on ventral striatal gamma oscillations in the rat. *Frontiers in Neuroscience*, *4*(SEP). https://doi.org/10.3389/fnins.2010.00300

van der Meer, M. A. A., & Redish, A. D. (2009). Low and high gamma oscillations in rat ventral striatum have distinct relationships to behavior, reward, and spiking activity on a learned spatial decision task. *Frontiers in Integrative Neuroscience*, *3*(JUN). https://doi.org/10.3389/neuro.07.009.2009

Van Der Stelt, M., Veldhuis, W. B., Bär, P. R., Veldink, G. A., Vliegenthart, J. F. G., & Nicolay, K. (2001). Neuroprotection by Δ9-tetrahydrocannabinol, the main active compound in marijuana, against ouabain-induced in vivo excitotoxicity. *Journal of Neuroscience*, *21*(17), 6475–6479. https://doi.org/10.1523/jneurosci.21-17-06475.2001

Van der Werf, Y. D., Witter, M. P., & Groenewegen, H. J. (2002). The intralaminar and midline nuclei of the thalamus. Anatomical and functional evidence for participation in processes of arousal and awareness. *Brain Research Reviews*, *39*(2), 107–140. https://doi.org/10.1016/S0165-0173(02)00181-9

Van Laere, K., Casteels, C., Lunskens, S., Goffin, K., Grachev, I. D., Bormans, G., & Vandenberghe, W. (2012). Regional changes in type 1 cannabinoid receptor availability in Parkinson's disease in vivo. *Neurobiology of Aging*, *33*(3), 620.e1-620.e8. https://doi.org/10.1016/j.neurobiolaging.2011.02.009

Van Sickle, M. D., Duncan, M., Kingsley, P. J., Mouihate, A., Urbani, P., Mackie, K., Stella, N., Makriyannis, A., Piomelli, D., Davison, J. S., Marnett, L. J., Di Marzo, V., Pittman, Q. J., Patel, K. D., & Sharkey, K. A. (2005). Identification and functional characterization of brainstem cannabinoid CB2 receptors. *Science*, *310*(5746), 329–332. https://doi.org/10.1126/science.1115740

Van Waes, V., Beverley, J. A., Siman, H., Tseng, K. Y., & Steiner, H. (2012). CB1 Cannabinoid Receptor Expression in the Striatum: Association with Corticostriatal Circuits and Developmental Regulation. *Frontiers in Pharmacology*, *3*, 21. https://doi.org/10.3389/fphar.2012.00021

Vegas-Suárez, S., Pisanò, C. A., Requejo, C., Bengoetxea, H., Lafuente, J. V., Morari, M., Miguelez, C., & Ugedo, L. (2020). 6-Hydroxydopamine lesion and levodopa

treatment modify the effect of buspirone in the substantia nigra pars reticulata. *British Journal of Pharmacology*, *177*(17), 3957–3974. https://doi.org/10.1111/bph.15145

Vila, M., Périer, C., Féger, J., Yelnik, J., Faucheux, B., Ruberg, M., Raisman-Vozari, R., Agid, Y., & Hirsch, E. C. (2000). Evolution of changes in neuronal activity in the subthalamic nucleus of rats with unilateral lesion of the substantia nigra assessed by metabolic and electrophysiological measurements. *European Journal of Neuroscience*, *12*(1), 337–344. https://doi.org/10.1046/j.1460-9568.2000.00901.x

Voorn, P., Vanderschuren, L. J. M. J., Groenewegen, H. J., Robbins, T. W., & Pennartz, C. M. A. (2004). Putting a spin on the dorsal-ventral divide of the striatum. *Trends in Neurosciences*, *27*(8), 468–474. https://doi.org/10.1016/j.tins.2004.06.006

Vrechi, T. A., Crunfli, F., Costa, A. P., & Torrão, A. S. (2018). Cannabinoid Receptor Type 1 Agonist ACEA Protects Neurons from Death and Attenuates Endoplasmic Reticulum Stress-Related Apoptotic Pathway Signaling. *Neurotoxicity Research*, *33*(4), 846–855. https://doi.org/10.1007/s12640-017-9839-1

Wall, N. R., DeLaParra, M., Callaway, E. M., & Kreitzer, A. C. (2013). Differential innervation of direct- and indirect-pathway striatal projection neurons. *Neuron*, *79*(2), 347–360. https://doi.org/10.1016/j.neuron.2013.05.014

Wallmichrath, I., & Szabo, B. (2002a). Cannabinoids inhibit striatonigral GABAergic neurotransmission in the mouse. *Neuroscience*, *113*(3), 671–682. https://doi.org/10.1016/S0306-4522(02)00109-4

Wallmichrath, I., & Szabo, B. (2002b). Analysis of the effect of cannabinoids on GABAergic neurotransmission in the substantia nigra pars reticulata. *Naunyn-Schmiedeberg's Archives of Pharmacology*, *365*(4), 326–334. https://doi.org/10.1007/s00210-001-0520-z

Walsh, S., Mnich, K., Mackie, K., Gorman, A. M., Finn, D. P., & Dowd, E. (2010). Loss of cannabinoid CB1 receptor expression in the 6-hydroxydopamine-induced nigrostriatal terminal lesion model of Parkinson's disease in the rat. *Brain Research Bulletin*, *81*(6), 543–548. https://doi.org/10.1016/j.brainresbull.2010.01.009

Walter, L., Franklin, A., Witting, A., Wade, C., Xie, Y., Kunos, G., Mackie, K., & Stella, N. (2003). Nonpsychotropic cannabinoid receptors regulate microglial cell migration.

Journal of Neuroscience, *23*(4), 1398–1405. https://doi.org/10.1523/jneurosci.23-04-01398.2003

Wang, Y., Zhang, Q. J., Liu, J., Ali, U., Gui, Z. H., Hui, Y. P., Chen, L., & Wang, T. (2010). Changes in firing rate and pattern of GABAergic neurons in subregions of the substantia nigra pars reticulata in rat models of Parkinson's disease. *Brain Research*, *1324*, 54–63. https://doi.org/10.1016/j.brainres.2010.02.008

Weintraub, D., Koester, J., Potenza, M. N., Siderowf, A. D., Stacy, M., Voon, V., Whetteckey, J., Wunderlich, G. R., & Lang, A. E. (2010). Impulse control disorders in Parkinson disease: A cross-sectional study of 3090 patients. *Archives of Neurology, 67*(5). https://doi.org/10.1001/archneurol.2010.65

Weiss-Wunder, L. T., & Chesselet, M.-F. (1990). Heterogeneous distribution of cytochrome oxidase activity in the rat substantia nigra: Correlation with tyrosine hydroxylase and dynorphin immunoreactivities. *Brain Research*, *529*(1), 269–276. https://doi.org/10.1016/0006-8993(90)90837-2

Wickens, A. P., & Pertwee, R. G. (1993). Δ9-tetrahydrocannabinol and anandamide enhance the ability of muscimol to induce catalepsy in the globus pallidus of rats. *European Journal of Pharmacology*, *250*(1), 205–208. https://doi.org/10.1016/0014-2999(93)90646-Y

Wiley, J. L., Compton, D. R., Dai, D., Lainton, J. A., Phillips, M., Huffman, J. W., & Martin, B. R. (1998). Structure-activity relationships of indole- and pyrrole-derived cannabinoids. *The Journal of Pharmacology and Experimental Therapeutics*, *285*(3), 995–1004.

Wilkinson, S. T., Radhakrishnan, R., & D'Souza, D. C. (2014). Impact of Cannabis Use on the Development of Psychotic Disorders. *Current Addiction Reports*, *1*(2), 115–128. https://doi.org/10.1007/s40429-014-0018-7

Willard, A. M., Isett, B. R., Whalen, T. C., Mastro, K. J., Ki, C. S., Mao, X., & Gittis, A. H. (2019). State transitions in the substantia nigra reticulata predict the onset of motor deficits in models of progressive dopamine depletion in mice. *ELife, 8*. https://doi.org/10.7554/eLife.42746

Winter, C., von Rumohr, A., Mundt, A., Petrus, D., Klein, J., Lee, T., Morgenstern, R., Kupsch, A., & Juckel, G. (2007). Lesions of dopaminergic neurons in the substantia nigra pars

compacta and in the ventral tegmental area enhance depressive-like behavior in rats. *Behavioural Brain Research*, *184*(2), 133–141. https://doi.org/10.1016/j.bbr.2007.07.002

Woodhams, S. G., Sagar, D. R., Burston, J. J., & Chapman, V. (2015). The Role of the Endocannabinoid System in Pain. In H.-G. Schaible (Ed.), *Pain Control* (pp. 119–143). Springer Berlin Heidelberg. https://doi.org/10.1007/978-3-662-46450-2_7

Wright, C. I., Beijer, A. V. J., & Groenewegen, H. J. (1996). Basal amygdaloid complex afferents to the rat nucleus accumbens are compartmentally organized. *Journal of Neuroscience*, *16*(5), 1877–1893. https://doi.org/10.1523/jneurosci.16-05-01877.1996

Wright, W. J., Schlüter, O. M., & Dong, Y. (2017). A Feedforward Inhibitory Circuit Mediated by CB1-Expressing Fast-Spiking Interneurons in the Nucleus Accumbens. *Neuropsychopharmacology*, *42*(5), 1146–1156. https://doi.org/10.1038/npp.2016.275

Yang, L., Rozenfeld, R., Wu, D., Devi, L. A., Zhang, Z., & Cederbaum, A. (2014). Cannabidiol protects liver from binge alcohol-induced steatosis by mechanisms including inhibition of oxidative stress and increase in autophagy. *Free Radical Biology and Medicine*, *68*, 260–267. https://doi.org/10.1016/j.freeradbiomed.2013.12.026

Yanovsky, Y., Mades, S., & Misgeld, U. (2003). Retrograde signaling changes the venue of postsynaptic inhibition in rat substantia nigra. *Neuroscience*, *122*(2), 317–328. https://doi.org/10.1016/s0306-4522(03)00607-9

Yawata, S., Yamaguchi, T., Danjo, T., Hikida, T., & Nakanishi, S. (2012). Pathway-specific control of reward learning and its flexibility via selective dopamine receptors in the nucleus accumbens. *Proceedings of the National Academy of Sciences of the United States of America*, *109*(31), 12764–12769. https://doi.org/10.1073/pnas.1210797109

Yuan, X.-S., Wang, L., Dong, H., Qu, W.-M., Yang, S.-R., Cherasse, Y., Lazarus, M., Schiffmann, S. N., d'Exaerde, A. de K., Li, R.-X., & Huang, Z.-L. (2017). Striatal adenosine A2A receptor neurons control active-period sleep via parvalbumin neurons in external globus pallidus. *ELife*, *6*. https://doi.org/10.7554/eLife.29055

Yung, K. K. L., Bolam, J. P., Smith, A. D., Hersch, S. M., Ciliax, B. J., & Levey, A. I. (1995). Immunocytochemical localization of D1 and D2 dopamine receptors in the basal ganglia of the rat: Light and electron microscopy. *Neuroscience*, *65*(3), 709–730. https://doi.org/10.1016/0306-4522(94)00536-E

Zeissler, M. L., Eastwood, J., McCorry, K., Hanemann, O. O., Zajicek, J. P., & Carroll, C. B. (2016). Delta-9-tetrahydrocannabinol protects against MPP+ toxicity in SH-SY5Y cells by restoring proteins involved in mitochondrial biogenesis. *Oncotarget*, *7*(29), 46603–46614. https://doi.org/10.18632/oncotarget.10314

Zeng, B. Y., Dass, B., Owen, A., Rose, S., Cannizzaro, C., Tel, B. C., & Jenner, P. (1999). Chronic L-DOPA treatment increases striatal cannabinoid CB1 receptor mRNA expression in 6-hydroxydopamine-lesioned rats. *Neuroscience Letters*, *276*(2), 71–74. https://doi.org/10.1016/S0304-3940(99)00762-4

Zhang, J., Culp, M. L., Craver, J. G., & Darley-Usmar, V. (2018). Mitochondrial function and autophagy: Integrating proteotoxic, redox, and metabolic stress in Parkinson's disease. *Journal of Neurochemistry*, *144*(6), 691–709. https://doi.org/10.1111/jnc.14308

Zhang, X., Egeland, M., & Svenningsson, P. (2011). Antidepressant-like properties of sarizotan in experimental Parkinsonism. *Psychopharmacology*, *218*(4), 621–634. https://doi.org/10.1007/s00213-011-2356-7

Zhou, F. M. (2016). The Substantia Nigra Pars Reticulata. In *Handbook of Behavioral Neuroscience* (Vol. 24, pp. 293–316). Elsevier B.V.

Zhou, F.-W., Jin, Y., Matta, S. G., Xu, M., & Zhou, F.-M. (2009). An Ultra-Short Dopamine Pathway Regulates Basal Ganglia Output. *Journal of Neuroscience*, *29*(33), 10424–10435. https://doi.org/10.1523/JNEUROSCI.4402-08.2009

Zimmer, A., Steiner, H., Bonner, T. I., Zimmer, A. M., & Kitai, S. T. (1999). Altered gene expression in striatal projection neurons in CB1 cannabinoid receptor knockout mice. *Proceedings of the National Academy of Sciences of the United States of America*, *96*(10), 5786–5790. https://doi.org/10.1073/pnas.96.10.5786

Zold, C. L., Escande, M. V., Pomata, P. E., Riquelme, L. A., & Murer, M. G. (2012). Striatal NMDA receptors gate cortico-pallidal synchronization in a rat model of Parkinson's disease. *Neurobiology of Disease*, *47*(1), 38–48. https://doi.org/10.1016/j.nbd.2012.03.022

Zoratti, C., Kipmen-Korgun, D., Osibow, K., Malli, R., & Graier, W. F. (2003). Anandamide initiates Ca(2+) signaling via CB2 receptor linked to phospholipase C in calf pulmonary endothelial cells. *British Journal of Pharmacology*, *140*(8), 1351–1362. https://doi.org/10.1038/sj.bjp.0705529

8. APPENDIX – THESIS PUBLICATIONS

Cannabinoids differentially modulate cortical information transmission
through the sensorimotor or medial prefrontal basal ganglia circuits

8. APPENDIX – Study I

RESEARCH PAPER

Cannabinoids differentially modulate cortical information transmission through the sensorimotor or medial prefrontal basal ganglia circuits

Mario Antonazzo[1,2]* | Amaia Gutierrez-Ceballos[1,2]* | Irati Bustinza[1,2] | Luisa Ugedo[1,2] | Teresa Morera-Herreras[1,2]

[1]Department of Pharmacology, Faculty of Medicine and Nursing, University of the Basque Country (UPV/EHU), Leioa, Spain

[2]Neurodegenerative Diseases Group, Biocruces Health Research Institute, Barakaldo, Spain

Correspondence
Teresa Morera-Herreras, Department of Pharmacology, Faculty of Medicine and Nursing, University of the Basque Country (UPV/EHU), Barrio Sarriena s/n, 48940 Leioa, Spain.
Email: teresa.morera@ehu.eus

Background and Purpose: In the sensorimotor (SM) and medial prefrontal (mPF) basal ganglia (BG) circuits, the cortical information is transferred to the *substantia nigra pars reticulata* (SNr) through the hyperdirect trans-subthalamic pathway and through the direct and indirect trans-striatal pathways. The cannabinoid CB_1 receptor, which is highly expressed in both BG circuits, may participate in the regulation of motor and motivational behaviours. Here, we investigated the modulation of cortico-nigral information transmission through the BG circuits by cannabinoids.

Experimental Approach: We used single-unit recordings of SNr neurons along with simultaneous electrical stimulation of motor or mPF cortex in anaesthetized rats.

Key Results: Cortical stimulation elicited a triphasic response in the SNr neurons from both SM and mPF-BG circuits, which consisted of an early excitation (hyperdirect transmission pathway), an inhibition (direct transmission pathway), and a late excitation (indirect transmission pathway). In the SM circuit, after Δ^9-tetrahydrocannabinol or WIN 55,212-2 administration, the inhibition and the late excitation were decreased or completely lost, whereas the early excitation response remained unaltered. However, cannabinoid administration dramatically decreased all the responses in the mPF circuit. The CB_1 receptor antagonist AM251 (2 mg·kg^{-1}, i.v.) did not modify the triphasic response, but blocked the effects induced by cannabinoid agonists.

Conclusions and Implications: CB_1 receptor activation modulates the SM information transmission through the trans-striatal pathways and profoundly decreases the cortico-BG transmission through the mPF circuit. These results may be relevant for elucidating the involvement of the cannabinoid system in motor performance and in decision making or goal-directed behaviour.

*These authors participated equally in this work.

- -

207

8. APPENDIX – Study I

Cannabinoids differentially modulate cortical information transmission
through the sensorimotor or medial prefrontal basal ganglia circuits

1 | INTRODUCTION

The basal ganglia (BG), which consist of the striatum, the external and internal *globus pallidus*, the subthalamic nucleus (STN), and the *substantia nigra pars reticulata* (SNr), are a highly organized network of subcortical nuclei that connects the cortex with the thalamus, creating the cortico-BG-thalamo-cortical loop circuits. In these complex circuits, cortical information is transferred to the output structures of the BG, SNr, and internal *globus pallidus* (equivalent to the entopeduncular nucleus in rodents) through three different pathways: (a) the hyperdirect trans-subthalamic pathway, (b) the direct trans-striatal pathway, and (c) the indirect trans-striatal pathway (Maurice, Deniau, Glowinski, & Thierry, 1999). Moreover, different anatomo-functional BG circuits can be distinguished according to the origin of cortical information they process. In rodents, the main distinction can be made between medial prefrontal (mPF) and sensorimotor (SM) BG circuits. While the SM circuits are important for appropriate motor functions, the mPF circuits play an important role in decision making, goal-directed behaviour, emotions, motivation, and cognition (G. E. Alexander, DeLong, & Strick, 1986; Haber, 2003; Parent & Hazrati, 1995). Abnormal functionality of these circuits has been described in motor and behavioural disorders and cognitive deficits (for review, see Tremblay, Worbe, Thobois, Sgambato-Faure, & Féger, 2015), and it has been related to the mechanism of action of some drugs, such as cannabinoids that also affect motor and cognitive functions. The use of cannabis is associated with deficits in working memory and decision making (related to mPF circuitry functionality; Grant, Gonzalez, Carey, Natarajan, & Wolfson, 2003; Schreiner & Dunn, 2012; Solowij & Battisti, 2008), as well as with alterations in sensory perception or impaired SM gating (related to dysfunctional processing in SM circuits; Broyd et al., 2013; Edwards, Skosnik, Steinmetz, O'Donnell, & Hetrick, 2009).

Cannabinoids regulate the strength of excitatory and inhibitory synaptic transmission in the mPF and SM-BG circuits via the activation of CB_1 receptors, which are located pre-synaptically in the mPF and motor cortex (Freund, Katona, & Piomelli, 2003; Harkany, Mackie, & Doherty, 2008) and on glutamatergic corticostriatal projections (for review, see Morera-Herreras et al., 2016). The cortical expression of the CB_1 receptor is heterogenic, being higher in the mPF cortex than in the motor cortex (Heng, Beverley, Steiner, & Tseng, 2011). Similarly, striatal CB_1 receptor expression shows regional variations, displaying minimal levels in ventromedial areas and displaying the highest expression in dorso and ventrolateral territories (Julian et al., 2003; Mailleux & Vanderhaeghen, 1992; Van Waes, Beverley, Siman, Tseng, & Steiner, 2012). According to these observations, Van Waes et al. (2012) found an inverse relationship between cortical and striatal CB_1 receptor expression in the SM and the mPF circuits. In the SM circuits, there is a high striatal and low cortical CB_1 expression, and in contrast, in the mPF circuits, CB1 expression is low in striatum and high in the cortical region. CB_1 receptors have also been observed in striatal projections to the *globus pallidus* and the SNr and on subthalamonigral

and subthalamopallidal terminals (for review, see Morera-Herreras et al., 2016). Therefore, the effect of cannabinoids may vary depending on the cortico-BG pathway they affect more. In addition, we have previously shown, by using in vivo recording techniques, that systemic cannabinoid agonist administration inhibits subthalamic neurons recorded in the area related to the motor circuits but stimulates neurons located in associative/limbic territories (Morera-Herreras, Ruiz-Ortega, Taupignon, et al., 2010; Morera-Herreras, Ruiz-Ortega, & Ugedo, 2010). In mice, the cannabinoid receptor agonist **WIN 55,212-2** induces long-term depression (a form of plasticity that is key to motor learning and habit formation; Jin & Costa, 2015) in the *nucleus accumbens* but does not induce long-term depression in the dorsolateral striatum (Zhang, Feng, & Chergui, 2015). Moreover, in healthy humans, **Δ⁹-tetrahydrocannabinol** (Δ⁹-THC) modulates dopamine transmission in the limbic striatum but not in other striatal subdivisions (Bossong et al., 2015). Nevertheless, at present, the specific cannabinoid regulation of cortico-BG transmission through cortical-BG circuits is unknown.

The present study further investigated the modulatory role of the CB_1 receptor on cortical information transfer in both circuits. For this purpose, the effect of pharmacological agents targeting the CB_1 receptor on the transmission of SM and mPF cortical information to SNr neurons was studied by performing extracellular single-unit recordings in anaesthetized rats. Our results show that cannabinoids activating the CB_1 receptor hamper the SM information transfer through the trans-striatal pathways and dramatically reduce the cortico-BG transmission through the mPF circuit.

What is already known

- Different anatomo-functional basal ganglia (BG) circuits exist according to the cortical information they process.
- The cannabinoid CB_1 receptor is expressed and modulates BG nuclei activity.

What this study adds

- CB_1 receptors modulate cortical information transmission through the sensorimotor and medial prefrontal circuits of the BG.
- CB_1 receptors differentially modulate the cortical information transfer through both circuits.

What is the clinical significance

- The sensorimotor and medial prefrontal circuits are known to function abnormally in several disorders.
- Understanding the CB_1 receptor-mediated modulation of the BG may contribute to the development of therapies based on cannabinoids.

Cannabinoids differentially modulate cortical information transmission
through the sensorimotor or medial prefrontal basal ganglia circuits

8. APPENDIX – Study I

2 | METHODS

2.1 | Animals

Male Sprague–Dawley rats (250–325 g, RRID:RGD_70508) were housed in groups of four under standard laboratory conditions (22 ± 1°C, 55 ± 5% relative humidity, and 12:12 hr light/dark cycle) with food and water provided ad libitum. Every effort was made to minimize animal suffering and to use the minimum number of animals per group and experiment. Animal studies are reported in compliance with the ARRIVE guidelines (Kilkenny et al., 2010) and with the recommendations made by the *British Journal of Pharmacology*. The experimental protocols were reviewed and approved by the Local Ethical Committee for Animal Research of the University of the Basque Country (UPV/EHU, CEEA, Ref. ES48/054000/6069). All of the experiments were performed in accordance with the European Community Council Directive on "The Protection of Animals Used for Scientific Purposes" (2010/63/EU) and with Spanish Law (RD 53/2013) for the care and use of laboratory animals. A total of 177 animals were used in the present study for the characterization of the spontaneous and cortically-evoked activity of SNr neurons, 87 for recording in the SM circuits, and 90 for recording in the mPF circuits. For the pharmacological studies, cannabinoid drugs were administered to 32 of the 87 rats for recording in the SM, and in 57 of the 90 rats for recording in the mPF.

2.2 | Electrophysiological procedures

The electrophysiological procedures are schematically illustrated in Figure 1. The animals were anaesthetized with chloral hydrate (420 mg·kg^{-1} [i.p.] for induction, followed by continuous administration [i.p.] of chloral hydrate at a rate of 115.5 mg·kg^{-1}·hr^{-1} using a peristaltic pump to keep a steady level of anaesthesia). For additional drug administration, the right jugular vein was cannulated. The animal body temperature was maintained at ~37°C for the entire experiment with a heating pad connected to a rectal probe. The rat was placed in a stereotaxic frame with its head secured in a horizontal orientation. The skull was exposed, and two 3-mm burr holes were drilled over the right SNr and the ipsilateral motor or mPF cortex.

Single-unit extracellular recordings were made by an Omegadot single glass micropipette, pulled with an electrode puller (Narishige Scientific Instrument Lab., PE-2, Japan), broken back to a tip diameter of 1–2.5 μm under a light microscope and filled with 2% pontamine sky blue in 0.5% sodium acetate. This electrode was lowered into the SM (5.8 mm posterior to Bregma, 2.5 mm lateral to midline, and 7–8 mm ventral to the dura mater) or mPF region (5.4 mm posterior to Bregma, 1.8 mm lateral to midline, and 7–8 mm ventral to the dura mater) of the SNr. The signal from the electrode was amplified with a high-input impedance amplifier and then monitored on an oscilloscope and on an audio-monitor. SNr neurons were identified as non-dopaminergic by their classically defined electrophysiological characteristics: thin spikes (width, <2 ms) and ability to present relatively high-frequency discharges without a decrease in spike amplitude (as described in Aristieta, Ruiz-Ortega, Miguelez, Morera-Herreras, & Ugedo, 2016). Neuronal spikes were digitized using computer software (CED micro 1401 interface and Spike2 software [version 7], Cambridge Electronic Design, UK). The basal firing rate (FR) was recorded for 5 min. Although multiple neurons were recorded in each animal in order to characterize the spontaneous and cortically evoked activity in both SM and mPF territories, only one SNr cell was pharmacologically studied per animal.

Firing parameters such as FR and coefficient of variation (CV) of SNr neurons were analysed offline using Spike2 software (version 7). Burst-related parameters such as the number of bursts, mean duration of burst, number of spikes per burst, recurrence of bursts, and intraburst frequency were analysed during time epochs of 150 s applying a Spike2 script ("surprise.s2 s"), based on the Poisson surprise algorithm.

2.2.1 | Stimulation procedures

The motor cortex (3.5 mm anterior to Bregma, 3.2 mm lateral to midline, and 1.6 mm ventral to the dura mater) or the mPF cortex (2.9 mm anterior to Bregma, 0.6 mm lateral to midline, and 1.7 ventral to the dura mater) ipsilateral to the recording site was stimulated at 1 Hz (pulse width, 600 μs; intensity, 1 mA) using coaxial stainless-steel electrodes (diameter, 250 μm; tip diameter, 100 μm; tip-to-barrel distance, 300 μm; Cibertec S.A.).

As described previously (Maurice et al., 1999), cortical stimulation evokes characteristic triphasic responses in SNr cells consisting of a combination of an early excitation, inhibition, and/or late excitation. Peristimulus time histograms were generated from 180 stimulation trials using 1-ms bins. The criterion used to determine the existence of an excitatory response was set at an increase of twofold the SD, plus the mean of the number of spikes compared with the prestimulus frequency, for at least three consecutive bins. The amplitude of excitatory responses was quantified by calculating the difference between the mean number of spikes evoked within the time window of the excitation and the mean number of spikes occurring spontaneously before the stimulation. The duration of an inhibitory response corresponded to the time interval during which no spikes were observed, for at least three consecutive bins.

2.3 | Statistical analysis of data

The data and statistical analysis comply with the recommendations of the *British Journal of Pharmacology* on experimental design and analysis in pharmacology (Curtis et al., 2018). The experimental data, proceeding only from stimulation-responding neurons, was analysed using the computer program GraphPad Prism (v. 5.01, GraphPad Software, Inc; RRID:SCR_002798). As more than one neuron (one to three per rat) was recorded per animal in the characterization of the SM and mPF circuits, electrophysiological parameters such as FR, CV, burst-related parameters (i.e., number, duration, and spikes per burst, recurrence of burst, and intraburst frequency) and

Cannabinoids differentially modulate cortical information transmission
through the sensorimotor or medial prefrontal basal ganglia circuits
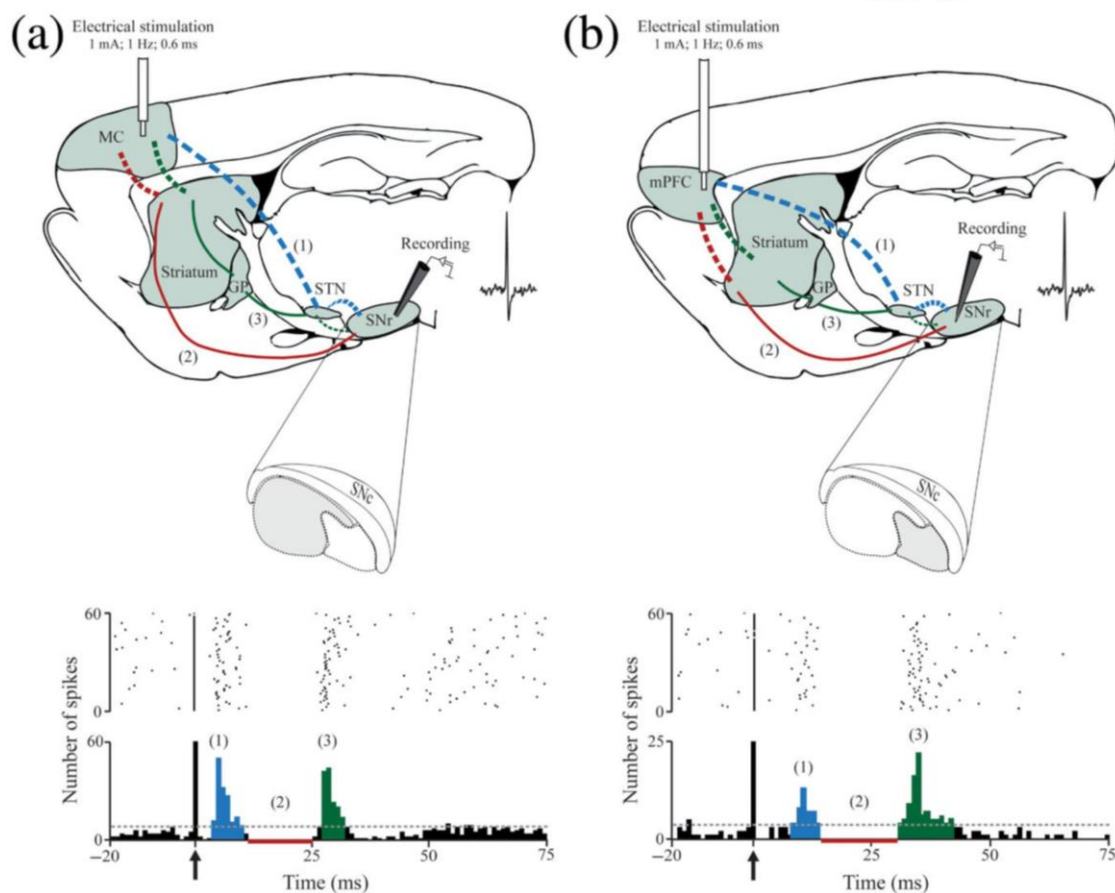
FIGURE 1 Illustration of the in vivo electrophysiological experiments in anaesthetized rats showing the SM and mPF circuits of the BG. (a) and (b) Top: schematic parasagittal sections of a rat brain showing the cortex and the BG nuclei (striatum, external *globus pallidus* [GP], STN and SNr. (a) Motor cortex (MC) or (b) mPF cortex (mPFC) was stimulated at 1 Hz (pulse width, 0.6 ms; intensity, 1 mA), and simultaneously, single-unit recordings were obtained in the corresponding anatomo-functional subdivisions of the SNr ([a] lateral part of the SNr [SM-SNr] or [b] medial part of the SNr [mPF-SNr]). Dashed lines represent glutamatergic projections and blunt line GABAergic projections. (a) and (b) Bottom: raster plot and peristimulus time histogram showing the characteristic cortically-evoked triphasic response in SNr neurons: (1)-blue: early excitation (activation of hyperdirect pathway [cortex-subthalamus-SNr]); (2)-red: inhibition (activation of direct pathway [cortex-striatum-SNr]), and (3)-green: late excitation (activation of indirect pathway [cortex-striatum-external GP-subthalamus-SNr]). Arrows indicate the time the stimulus was applied. SNc: *substantia nigra pars compacta*

parameters related to cortically-evoked responses (i.e., duration, latency, and amplitude of the responses) were averaged per animal, so that every animal had one value for each electrophysiological parameter. Averages from each rat FR, CV, and cortically-evoked related parameters were analysed by Student's two-tailed unpaired *t* test when looking for differences between SM and mPF circuits. To assess differences in the number of rats with burst firing neurons, Fisher's exact test was used. Parameters related to bursting activity were analysed using the Mann–Whitney rank sum test or, when necessary, Student's two-tailed unpaired *t* test. To assess the effects of the drugs (WIN 55,212-2 or Δ^9-THC), Student's two-tailed paired *t* test was used to compare the mean values of FR, CV, and parameters related to cortically-evoked responses, before and after

drug application (one neuron per animal). To study the effect of cannabinoid drugs on burst activity, Fisher's exact test was used to assess differences in the number of rats with burst firing, before and after drug administration. To analyse the burst-related parameters before and after drug application, Wilcoxon matched-pairs signed rank test was used and, when necessary, Student's two-tailed paired *t* test.

To determine the role of the CB$_1$ receptor in the effect of cannabinoid drugs the mean values of FR, CV, and cortically-evoked responses before AM251, post-AM251 and post-AM251 + WIN 55,212-2 or Δ^9-THC were compared using a repeated-measures one-way ANOVA (one cell per animal). To determine if there was any difference in the number of rats with burst firing, chi-squared

Cannabinoids differentially modulate cortical information transmission
through the sensorimotor or medial prefrontal basal ganglia circuits

8. APPENDIX – Study I

test was used. To assess whether these drugs were altering the burst-related parameters of these neurons or not, the Friedman test was used and, when necessary, a repeated-measures one-way ANOVA. To determine whether the drugs were affecting the SM or mPF circuits cortically-evoked responses differently, a repeated-measures two-way ANOVA was performed. The level of statistical significance was set at $P < 0.05$. Data are presented as group means ± SEM of n rats.

2.4 | Drugs

Δ^9-THC (CAS no. 1972-08-3) was a generous gift from GW Pharmaceuticals Ltd. (Salisbury, UK). WIN 55,212-2 (CAS no. 131543-23-2) and chloral hydrate (CAS no. 302-17-0) were obtained from Sigma (Madrid, Spain). AM251 (CAS no. 183232-66-8) was obtained from Tocris Bioscience (Spain). Δ^9-THC, WIN 55,212-2, and AM251 were diluted in 1:1:18 cremophor/ethanol/saline solution, and chloral hydrate was prepared in 0.9% saline. Drugs were freshly prepared immediately prior to use.

2.5 | Nomenclature of targets and ligands

Key protein targets and ligands in this article are hyperlinked to corresponding entries in http://www.guidetopharmacology.org, the common portal for data from the IUPHAR/BPS Guide to PHARMACOLOGY (Harding et al., 2018), and are permanently archived in the Concise Guide to PHARMACOLOGY 2017/18 (S. P. Alexander et al., 2017).

3 | RESULTS

3.1 | Firing properties and burst activity of SNr neurons

GABAergic neurons within the SNr display typical electrophysiological characteristics, that is, a narrow spike waveform and a relatively high firing rate with a regular pattern of discharge. To ensure the cells recorded cells belong to their corresponding nigral circuits (SM-SNr or mPF-SNr), only those responding to cortical stimulation were used in the analysis. Neurons meeting these criteria were recorded from a total of $n = 177$ animals, among which $n = 87$ were in the SM-SNr and $n = 90$ in the mPF-SNr. Their firing and burst activity properties are summarized in Table 1.

The firing pattern of the neurons from these two SNr territories was different. A larger percentage of mPF-SNr neurons exhibited bursting discharge in comparison to SM-SNr neurons. Consistently, the number and duration of bursts, as well as the recurrence of burst displayed by mPF-SNr neurons, was shown to be significantly higher than the number and duration of bursts, as well as the recurrence of burst, observed for the SM-SNr neurons.

TABLE 1 Firing properties of neurons from the SM and mPF subdivisions of the SNr

	SM-SNr (n = 87)	mPF-SNr (n = 90)
Firing rate (Hz)	25.2 ± 0.9	22.8 ± 0.9
Coefficient of variation (%)	47.0 ± 1.9	48.3 ± 2.2
Burst firing neurons/recorded neurons	39/87	74/90
Neurons exhibiting burst firing pattern (%)	44.8	82.2*
Number of bursts	12.4 ± 2.8	21.7 ± 3.0*
Duration of burst (ms)	0.6 ± 0.1	0.9 ± 0.1*
Number of spikes per burst	20.3 ± 3.5	23.2 ± 2.7
Recurrence of burst (number of burst·min^{-1})	4.1 ± 0.9	8.7 ± 1.2*
Intraburst frequency (spikes·s^{-1})	49.1 ± 2.8	45.5 ± 2.0

Note: Each value represents the mean ± SEM of n recorded rats.

*$P < 0.05$ versus SM-SNr (neurons exhibiting burst firing pattern: Fisher's exact test; burst parameters: Mann–Whitney rank sum test).

3.2 | Cortically-evoked responses of SNr neurons

According to previous publications (Aliane, Pérez, Nieoullon, Deniau, & Kemel, 2009; Kolomiets, Deniau, Glowinski, & Thierry, 2003; Maurice et al., 1999), cortical stimulation of the motor or mPF cortex evoked responses in the SNr neurons that consisted of an early excitation, followed by an inhibition and a late excitation, forming a characteristic triphasic response (bottom of Figure 1). The presence of the early excitation is attributable to the activation of the so-called "hyperdirect" cortico-subthalamo-nigral pathway. The activation of the "direct" cortico-striato-nigral pathway produces the observed inhibition, and the late excitation derives from the activation of the "indirect" cortico-striato-pallido-subthalamo-nigral pathway (Maurice et al., 1999). Different patterns of response were observed in both SNr territories, yielding triphasic, biphasic, and monophasic responses from the activation of the different pathways along the circuits. The percentage of occurrence of such patterns of responses in SM-SNr and mPF-SNr neurons is shown in Figure 2a.

Regarding the parameters analysed for each of the responses such as latency of appearance, duration of inhibition, and amplitude of the excitations, the major differences between the circuits were observed in the latency (Figure 2b). In the mPF circuit, the appearance of all three responses was significantly delayed in comparison to the SM circuit, as indicated by an increased latency (SM vs. mPF: 5.6 ± 0.4 vs. 8.5 ± 0.4 ms; 13.4 ± 0.3 vs. 21.2 ± 0.5 ms; 27.6 ± 0.7 vs. 34.5 ± 0.8 ms for early excitation, inhibition, and late excitation, respectively, $P < 0.05$, Student's two-tailed unpaired t test). Moreover, the duration of the inhibition was greater in the SM circuit than in the mPF circuit (SM vs. mPF; 15.0 ± 0.9 vs. 9.7 ± 0.6 ms, $P < 0.05$, Student's two-tailed unpaired t test).

8. APPENDIX – Study I

Cannabinoids differentially modulate cortical information transmission through the sensorimotor or medial prefrontal basal ganglia circuits
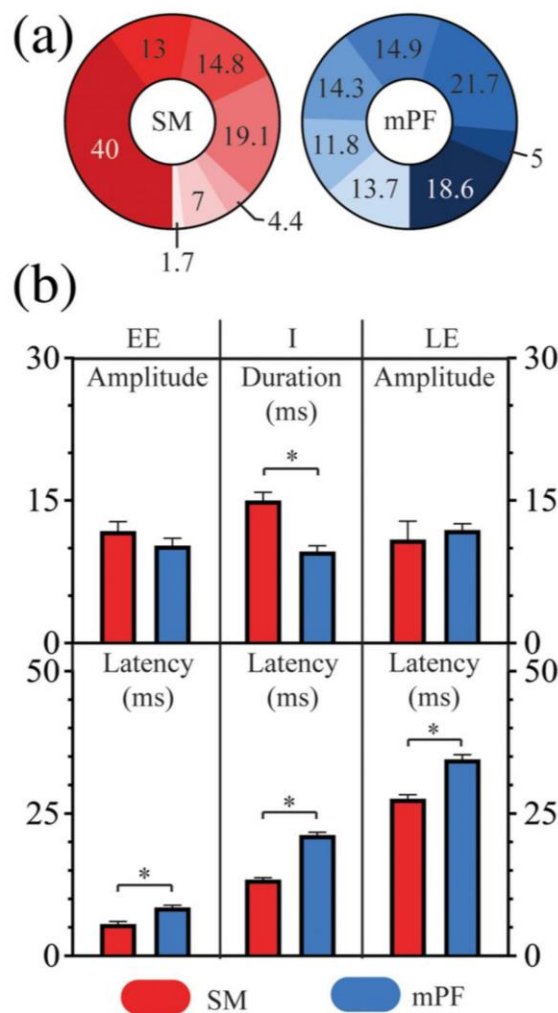
FIGURE 2 Patterns of responses evoked in the SNr neurons by cortical stimulation in SM- and mPF-BG circuits. (a) Percentage of occurrence of the different patterns of responses evoked in SNr cells by the cortical stimulation (EE: early excitation [SM: $n = 70$; mPF: $n = 54$]; I: inhibition [SM: $n = 72$; mPF: $n = 67$]; LE: late excitation [SM: $n = 68$; mPF: $n = 77$]). From darker to lighter colours: EE + I + LE; EE + I; I + LE; EE + LE; EE; I; LE. (b) Characteristics of the responses (latency, amplitude of excitations, and duration of the inhibition). Note that the duration of the inhibitions is shown to be shorter in the mPF circuit, whereas the appearance of all three responses is delayed when compared with the SM circuit, as a higher latency is observed. Each bar represents the mean ± SEM of n rats. *$P < 0.05$, Student's two-tailed unpaired t test

3.3 | Effects of cannabinoids on cortically-evoked activity in SNr neurons

We further explored the effect of the synthetic CB_1/**CB_2**-receptor full agonist, WIN 55,212-2, and the natural cannabinoid CB_1/CB_2-partial

agonist, Δ^9-THC, on cortically-evoked responses of SNr cells identified as receiving input from the mPF or motor cortex. The doses of the cannabinoid agonists used in this study were carefully selected to minimize any effects on the firing activity of SNr neurons, which could make the analysis of the cortically-evoked responses difficult.

3.3.1 | Effect of WIN 55,212-2 on cortically-evoked activity in SNr neurons

Systemic administration of WIN 55,212-2 (125 µg·kg^{-1}, i.v., SM: $n = 7$; mPF: $n = 17$) modulated the transmission of cortical information through the hyperdirect pathway in the SM and mPF circuits differently (Figure 3). In the SM circuit, WIN 55,212-2 did not alter the early excitation (basal amplitude: 18.0 ± 5.6; after WIN 55,212-2: 12.0 ± 2.6; $P > 0.05$, Student's paired t test). However, in the mPF circuit, WIN 55,212-2 significantly reduced the amplitude of this response, in 80% (eight of 10) of rats (basal amplitude: 9.9 ± 2.6; after WIN 55,212-2: 3.6 ± 1.7; $P < 0.05$, paired Student's two-tailed t test). Transmission through the direct pathway was significantly diminished in both circuits, as shown by a reduction in the duration of the inhibitory component of the response (Figure 3). Thus, in the SM circuit, 100% of the rats tested showed a reduced transmission through the direct pathway (basal duration: 15.0 ± 1.5; after WIN 55,212-2: 4.4 ± 2.1; $P < 0.05$, Student's two-tailed paired t test). A similar reduction of transmission occurred in the mPF circuit, where 85% (11 of 13) of rats exhibited a significant reduction in the duration of its inhibitory component, after administration of this cannabinoid agonist (basal duration: 11.8 ± 2.3; after WIN 55,212-2: 2.4 ± 1.4; $P < 0.05$, Student's two-tailed paired t test). Transmission through the "indirect" cortico-striato-pallido-subthalamo-nigral pathway was also reduced in both circuits after WIN 55,212-2 injection (Figure 3). In the case of the SM circuit, 83% (five of six) of the rats tested experienced a reduction in the late excitatory component of the response (basal amplitude: 8.5 ± 1.7; after WIN 55,212-2: 2.9 ± 1.8; $P < 0.05$, Student's two-tailed paired t test). In the same way, 64% (seven of 11) of rats showed a reduction in the amplitude of this response in mPF-SNr neurons (basal amplitude: 10.7 ± 2.2; after WIN 55,212-2: 5.5 ± 2.1; $P < 0.05$, Student's two-tailed paired t test). At the dose administered, WIN 55,212-2 did not modify rats SNr neuronal firing rate in either of the two regions studied (SM-SNr: 18 ± 9% over baseline; mPF-SNr: 17 ± 11% over baseline, $P > 0.05$, Student's two-tailed paired t test, Table S1).

In all of the rats tested, the effects induced by WIN 55,212-2 on the cortico-nigral transmission through these two BG circuits were effectively blocked by pretreatment with the selective CB_1 receptor antagonist AM251 (2 mg·kg^{-1}, i.v., SM: $n = 9$; mPF: $n = 11$; Figure 4). Moreover, AM251 did not modify the cortico-nigral information transfer by itself ($P > 0.05$, repeated-measures one-way ANOVA for early excitation, inhibition, and late excitation in both circuits; Figure 4). Additionally, no changes in the spontaneous activity of SNr cells were found after administration of AM251 in the rats tested (Table S2).
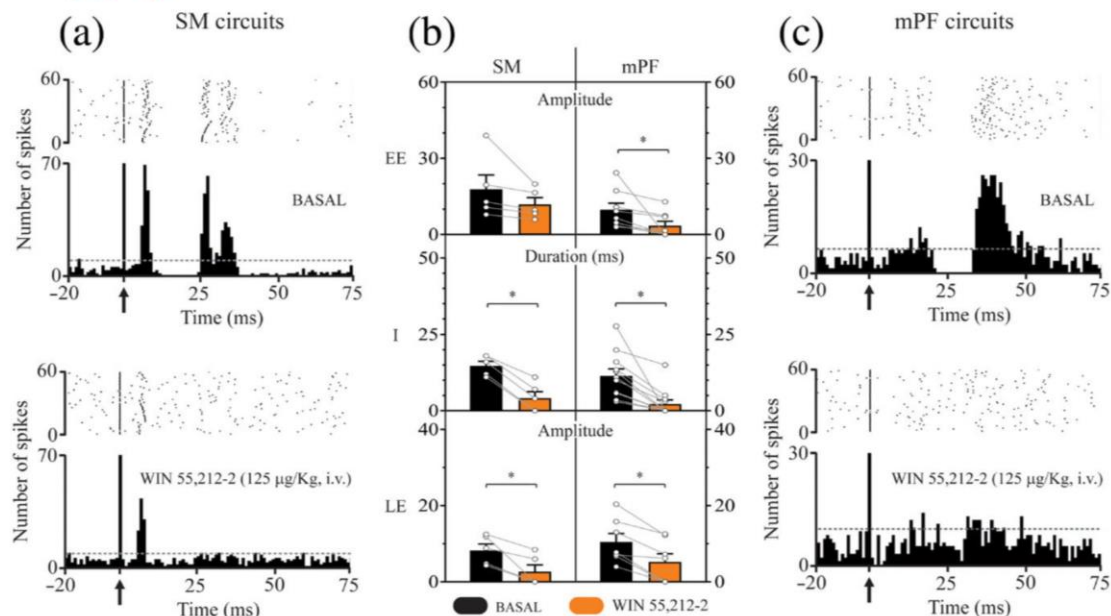
Cannabinoids differentially modulate cortical information transmission through the sensorimotor or medial prefrontal basal ganglia circuits

8. APPENDIX – Study I

FIGURE 3 Effect of systemic administration of WIN 55,212-2 (125 µg·kg^{-1}, i.v.) on cortico-nigral information transmission in SM and mPF BG circuits. (a) Top: raster plot and peristimulus time histogram showing a representative example of a triphasic response evoked in a SNr neuron by stimulation of the motor cortex in basal condition. Bottom: after WIN 55,212-2 injection, the inhibitory and late excitatory components disappeared, with the early excitation remaining unaltered. Arrows indicate a stimulation artefact. (c) Top: raster plot and peristimulus time histogram showing a representative example of a triphasic response evoked in a SNr neuron by stimulation of the mPF cortex under basal conditions. Bottom: in this circuit, WIN 55,212-2 injection was able to dramatically reduce transmission through all three pathways. Arrows indicate a stimulation artefact. (b) Bar graphs showing the mean effect of WIN 55,212-2 (125 µg·kg^{-1}, i.v.) on cortically-evoked responses in SNr neurons (amplitude of early [EE; SM: $n = 5$; mPF: $n = 8$] and late [LE; SM: $n = 5$; mPF: $n = 7$] excitations and duration of inhibition (I; SM: $n = 5$; mPF: $n = 11$]) in SM and mPF circuits. Each bar represents the mean ± SEM of n rats. Each dot represents the value from one neuron before and after drug administration. *$P < 0.05$, Student's two-tailed paired t test

3.3.2 | Effect of Δ⁹-THC on cortically-evoked activity in SNr neurons

I.v. administration of Δ⁹-THC (0.5 mg·kg^{-1}) profoundly affected the cortically-evoked activity of SNr neurons (Figure 5, SM: $n = 11$; mPF: $n = 15$). The transmission through the hyperdirect pathway appeared to be significantly reduced in both circuits after Δ⁹-THC administration. In the case of the SM circuit, a reduction in the amplitude of the early excitation was observed in 70% (seven of 10) of the rats tested (basal amplitude: 9.9 ± 2.2; after Δ⁹-THC: 6.3 ± 1.9; $P < 0.05$, Student's two-tailed paired t test), whereas the early excitation was completely abolished in 63% (five of eight) of the rats for the mPF circuit (basal amplitude: 7.7 ± 1.8; after Δ⁹-THC: 0 ± 0; $P < 0.05$, Student's two-tailed paired t test). The Δ⁹-THC effect on the information transmission through the hyperdirect pathway resulted in a significant difference between circuits, with changes caused in the early excitation being larger in the mPF circuit than in the SM circuit ($P < 0.05$, repeated-measures two-way ANOVA).

Moreover, i.v. administration of Δ⁹-THC was shown to significantly reduce transmission through the direct pathway in both circuits since a reduction in the duration of the inhibitory response was found

(Figure 5). In the SM circuit, a reduction in the inhibitory response was observed in 83% (five of six) of rats (basal duration: 12.5 ± 1.3; after Δ⁹-THC: 1.8 ± 1.8; $P < 0.05$, Student's two-tailed paired t test). The same pattern of response was seen in the mPF circuit, with 63% (five of eight) of rats displaying a reduction in the duration of the inhibitory component of the response (basal duration: 11.7 ± 2.9; after Δ⁹-THC: 2.8 ± 2.8; $P < 0.05$, Student's two-tailed paired t test). A disruption in information transmission was also observed through the indirect pathway in both circuits, as seen by a reduction in the amplitude of the late excitation after Δ⁹-THC administration (Figure 5). For the SM circuit, this reduction in the late excitation was observed in 67% (six of nine) of the rats tested (basal amplitude: 15.8 ± 3.0; after Δ⁹-THC: 5.4 ± 2.3; $P < 0.05$, Student's two-tailed paired t test). Similarly, in the mPF circuit, 82% (nine of 11) of rats showed a reduction in the late excitatory response (basal amplitude: 15.2 ± 3.0; after Δ⁹-THC: 2.6 ± 1.5; $P < 0.05$, Student's two-tailed paired t test). The dose of Δ⁹-THC used in this study was not able to change the spontaneous firing rate in either the SM-SNr or the mPF-SNr neurons of the rats tested (SM: 3 ± 12% over baseline; mPF: 0.3 ± 11% over baseline, $P > 0.05$, Student's two-tailed paired t test, Table S1).

FIGURE 4 Blockade of WIN 55,212-2-induced effects on cortico-nigral information transmission in SM and mPF BG circuits by pretreatment with the selective CB$_1$ antagonist AM251 (2 mg·kg^{-1}, i.v.). (a) Top: raster plot and peristimulus time histogram showing a representative example of a triphasic response evoked in a SNr neuron by stimulation of the motor cortex under basal conditions. AM251 administration did not modify the characteristics of the three components of the cortically-evoked response (middle) but blocked the effects induced by WIN 55,212-2 (bottom). Arrows indicate a stimulation artefact. (c) Top: raster plot and peristimulus time histogram showing a representative example of a triphasic response evoked in a SNr neuron by stimulation of the mPF cortex under basal conditions. As in an SM circuit, AM251 administration did not modify the characteristics of the cortically-evoked triphasic response (middle) but blocked the effects mediated by WIN 55,212-2 (bottom). Arrows indicate a stimulation artefact. (b) Bar graphs showing the mean effect of AM251 (2 mg·kg^{-1}, i.v.) and WIN 55,212-2 (125 µg·kg^{-1}, i.v.) on cortically-evoked responses in SNr neurons (amplitude of early [EE; SM: $n = 7$; mPF: $n = 6$] and late [LE; SM: $n = 6$; mPF: $n = 6$] excitations and duration of inhibition [I; SM: $n = 8$; mPF: $n = 7$]) in SM and mPF circuits. Each bar represents the mean ± SEM of n rats. Each dot represents the value from one neuron before and after drug administration

According to the results obtained with WIN 55,212-2, in all of the rats tested, the effects of Δ^9-THC administration on the cortico-nigral transmission through the SM- and mPF-BG circuits were blocked by pretreatment with AM251 (2 mg·kg^{-1}, i.v., SM: $n = 5$; mPF: $n = 14$; Figure 6). As we have previously demonstated, in these experiments, AM251 also did not alter the cortically-evoked responses ($P > 0.05$, repeated-measures one-way ANOVA for early excitation, inhibition, and late excitation in both circuits; Figure 6). Furthermore, AM251 did not change the spontaneous activity of the SNr neurons recorded (Table S2).

4 | DISCUSSION

In the present study, we analysed the role of the CB$_1$ receptor in cortico-nigral information transmission through the SM and mPF circuits of the BG. The results show that the activation of CB$_1$

receptors by the administration of the agonists, WIN 55,212-2 or Δ^9-THC, modulates them differently. While the cortico-nigral information transmission was almost completely abolished via direct and indirect trans-striatal pathways in both circuits, transmission via the trans-subthalamic pathway was only impaired in the mPF circuit, whereas that in the SM circuit was unaltered.

4.1 | Spontaneous activity and cortically-evoked responses of SNr neurons from SM and mPF territories

The present results show that the neurons recorded in mPF-SNr region had a more irregular firing pattern than those recorded in the SM-SNr region, displaying a greater number of cells exhibiting a burst firing pattern. These differences may be due to the different glutamatergic input that these two regions receive. It is important to note that SNr neuronal burst activity is mediated mainly by stimulation of

Cannabinoids differentially modulate cortical information transmission through the sensorimotor or medial prefrontal basal ganglia circuits

8. APPENDIX – Study I

FIGURE 5 Effect of systemic administration of Δ^9-THC (0.5 mg·kg^{-1}, i.v.) on cortico-nigral information transmission in SM and mPF BG circuits. (a) Top: raster plot and peristimulus time histogram showing a representative example of a triphasic response evoked in a SNr neuron by stimulation of the motor cortex under basal conditions. Bottom: after Δ^9-THC injection, the inhibitory and late excitatory components disappeared, with the early excitation remaining slightly diminished. Arrows indicate a stimulation artefact. (c) Top: raster plot and peristimulus time histogram showing a representative example of a triphasic response evoked in a SNr neuron by stimulation of the mPF cortex under basal conditions. Bottom: in this circuit, Δ^9-THC injection was able to reduce transmission through all three pathways. Arrows indicate a stimulation artefact. (b) Bar graphs showing the mean effect of Δ^9-THC (0.5 mg·kg^{-1}, i.v.) on cortically-evoked responses in SNr neurons (amplitude of early [EE; SM: $n = 7$; mPF: $n = 5$] and late [LE; SM: $n = 6$; mPF: $n = 9$] excitations and duration of inhibition [I; SM: $n = 5$; mPF: $n = 5$]) in SM and mPF circuits. Each bar represents the mean ± SEM of n rats. Each dot represents the value from one neuron before and after drug administration. *$P < 0.05$, Student's two-tailed paired t test to analyse the parameters of the evoked responses and repeated-measures two-way ANOVA to compare the effect of Δ^9-THC in SM and mPF circuits

NMDA receptors (Ibáñez-Sandoval et al., 2007; Shen & Johnson, 2006), which in the SNr comes from the STN (Ding, Li, & Zhou, 2013; Murer, Riquelme, Tseng, & Pazo, 1997; Tseng et al., 2000, 2001). Retrograde and anterograde labelling studies performed by Parent and Smith (1987) showed a significant number of subthalamonigral fibres in the medial part of the SNr, while a moderate number were found in the lateral part.

Regarding the cortically-evoked responses, the percentages of responding cells agree with previous findings (Aliane et al., 2009; Kolomiets et al., 2003; Maurice et al., 1999). The latency of the responses recorded in the mPF pathways was found to be higher than those in the SM ones, likely due to the distance that cortical information has to travel until reaching the SNr. In this way, in the mPF circuits, the cortical projections must reach the dorsomedial and ventral tiers of the striatum, whereas in the case of the SM circuits, the projections of the motor cortex reach the dorsolateral area of the striatum (McGeorge & Faull, 1989). Thus, the motor cortex would be closer to its targets in the striatum and the STN than in the mPF cortex, resulting in lower latency values for the SM circuits. Moreover, additional modulatory synapses may be influencing information

transmission through the different circuits. We found that the inhibitory response, which is related to the transmission through the direct trans-striatal pathway, had a longer duration in the SM than in the mPF circuits. This could be as a consequence of a higher activation of the SM circuits, since microdialysis studies have demonstrated a greater amount of glutamate coming from cortical afferents in the dorsal striatum than the ventral striatum (Gray, Rawls, Shippenberg, & McGinty, 1999; Pintor et al., 2004; Werkheiser, Rawls, & Cowan, 2006; Xi et al., 2006). In addition, binding experiments showed higher amounts of AMPA receptors in the dorsolateral striatum, in comparison to the dorsomedial striatum (Nicolle & Baxter, 2003).

4.2 | Effect of cannabinoids on cortico-nigral information transfer

The activation of CB$_1$ receptors located on presynaptic terminals leads to suppression of GABA and glutamate release in several brain areas, including BG nuclei (Gerdeman & Fernández-Ruiz, 2008; Wilson & Nicoll, 2002). Therefore, it is important to consider the different GABAergic and glutamatergic innervations of SM and mPF-BG

8. APPENDIX – Study I

Cannabinoids differentially modulate cortical information transmission through the sensorimotor or medial prefrontal basal ganglia circuits
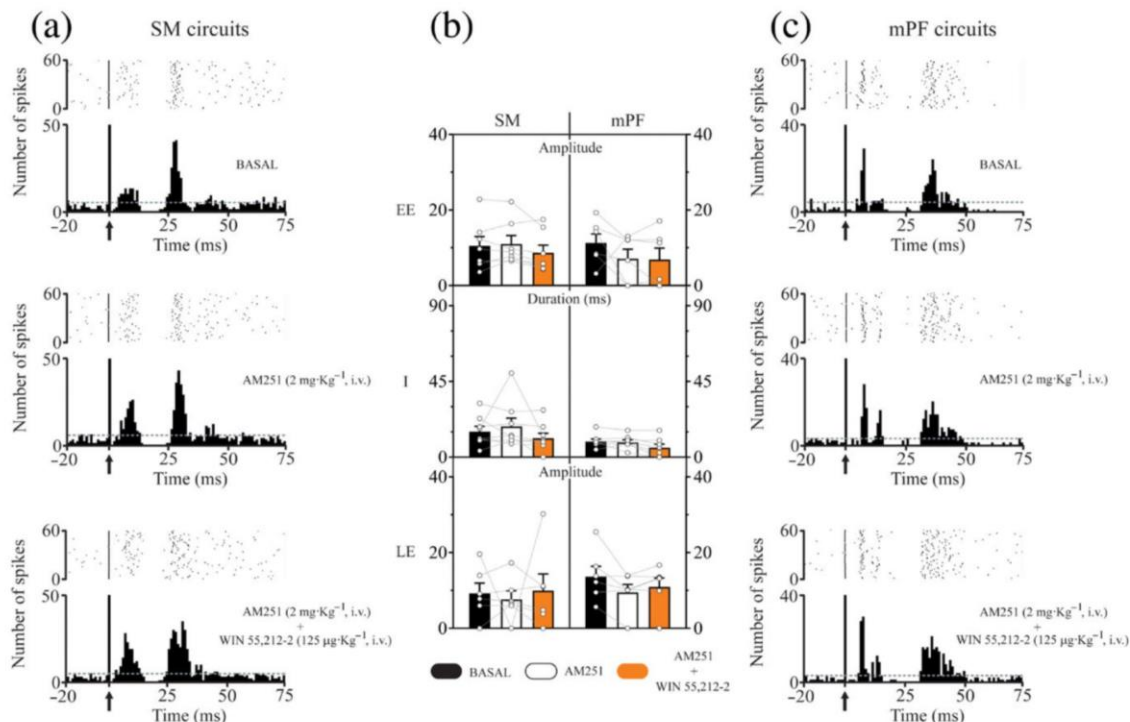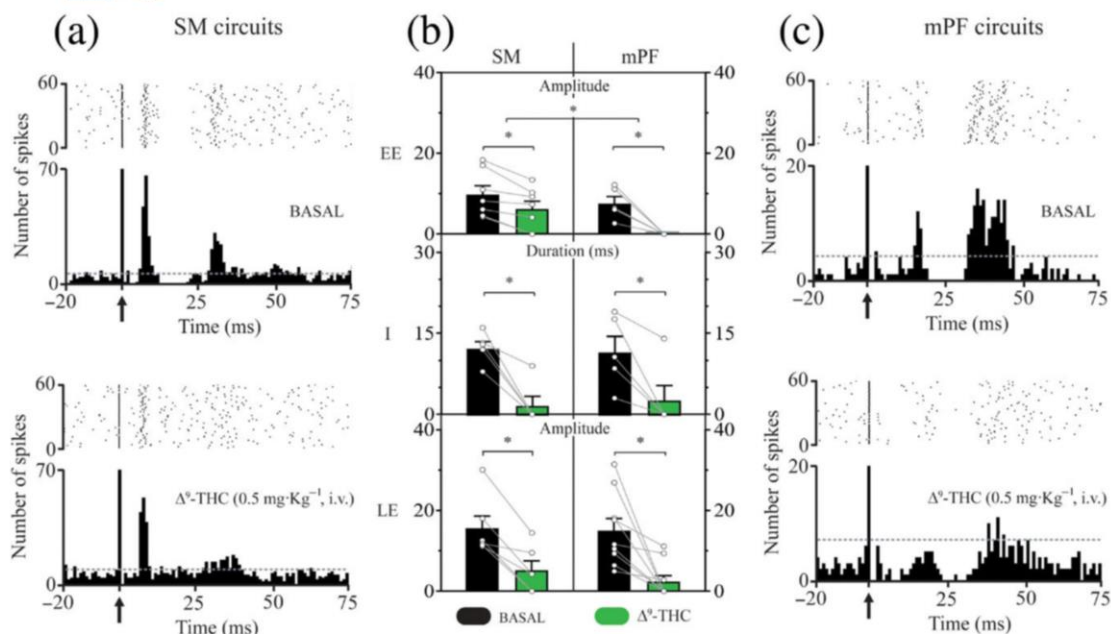
FIGURE 6 Blockade of Δ^9-THC-induced effects on cortico-nigral information transmission in SM and mPF BG circuits by pretreatment with the selective CB$_1$ antagonist AM251 (2 mg·kg^{-1}, i.v.). (a) Top: raster plot and peristimulus time histogram showing a representative example of a triphasic response evoked in a SNr neuron by stimulation of the motor cortex under basal conditions. AM251 administration did not modify the characteristics of the three components of the cortically-evoked response (middle) but blocked the effects mediated by Δ^9-THC (bottom). Arrows indicate a stimulation artefact. (c) Top: raster plot and peristimulus time histogram showing a representative example of a triphasic response evoked in a SNr neuron by stimulation of the mPF cortex under basal conditions. As in the SM circuit, AM251 administration did not modify the characteristics of the cortically-evoked triphasic response (middle) but blocked the effects induced by Δ^9-THC (bottom). Arrows indicate a stimulation artefact. (b) Bar graphs showing the mean effect of AM251 (2 mg·kg^{-1}, i.v.) and Δ^9-THC (0.5 mg·kg^{-1}, i.v.) on cortically-evoked responses in SNr neurons (amplitude of early [EE; SM: $n = 3$; mPF: $n = 6$] and late [LE; SM: $n = 3$; mPF: $n = 11$] excitations and duration of inhibition [I; SM: $n = 5$; mPF: $n = 11$]) in SM and mPF circuits. Each bar represents the mean ± SEM of n rats. Each dot represents the value from one neuron before and after drug administration

circuits mentioned previously, which, together with the fact that CB$_1$ receptors are also differently distributed along these circuits, may help to explain the cannabinoid-induced effects observed in the present study.

Our results show that the systemic administration of CB$_1$ receptor agonists profoundly disrupts the cortical information transmission along the BG circuits. These data are in line with previous in vivo and in vitro electrophysiological studies demonstrating that cannabinoid agonists inhibit GABAergic and glutamatergic neurotransmissions along the BG circuitry. Specifically, cannabinoids reduce corticostriatal (Gerdeman & Lovinger, 2001) and subthalamonigral glutamatergic neurotransmission (Sañudo-Peña & Walker, 1997; Szabo, Wallmichrath, Mathonia, & Pfreundtner, 2000), as well as striatopallidal and striatonigral GABAergic signalling (Miller & Walker, 1996; Wallmichrath & Szabo, 2002). However, the present results show that the modulatory role of CB$_1$ receptors on SM and mPF circuits of the BG is

different. In the SM circuits, after cannabinoid agonist administration (WIN 55,212-2 or Δ^9-THC), cortico-nigral information transmission via the direct and indirect trans-striatal pathways was strongly reduced. By contrast, the information transmitted via the hyperdirect trans-subthalamic pathway remained globally unchanged. Interestingly, in the mPF circuits, cannabinoid agonist administration induced a marked reduction in cortical information transfer in all the trans-BG pathways, including the trans-striatal and trans-subthalamic pathways.

The different effects of the cannabinoid drugs on cortico-nigral transmission through the hyperdirect pathway observed in both circuits, could be explained by considering the differential distribution of the CB$_1$ receptor within them. The regional comparison of CB$_1$ receptor expression in the cortex shows that mPF cortical areas have a higher expression of CB$_1$ receptors than SM cortical areas (Heng et al., 2011). Moreover, CB$_1$ receptor expression has been detected

Cannabinoids differentially modulate cortical information transmission
through the sensorimotor or medial prefrontal basal ganglia circuits

8. APPENDIX – Study I

in the STN, but no topographical variations in the expression between its motor and limbic/associative areas were demonstrated (Mailleux & Vanderhaeghen, 1992). Previous electrophysiological studies show that CB_1 receptor agonists have different effects on STN neurons from the motor territories and limbic/associative territories of the STN (Morera-Herreras, Ruiz-Ortega, & Ugedo, 2010). Therefore, differences in the sensitivity of the hyperdirect pathway to CB_1 receptor agonists may underlie differences in cortical CB_1 expression between mPF and SM cortical areas. These differences in CB_1 receptor expression along SM and mPF circuits could determine the site at which WIN 55,212-2 and Δ9-THC act. The regional comparison of CB_1 receptor expression at the cortical and striatal level indicates that SM areas of the striatum, which have a higher expression of the CB_1 receptor (dorsolateral territory) receive afferents from cortical areas with a low

expression (motor cortex). The opposite is observed in mPF areas of the striatum that show a low CB_1 receptor expression (ventromedial territory), which receive afferents from cortical areas with a high expression (mPF cortex; Van Waes et al., 2012). Based on this distribution and according to the hypothesis proposed by Van Waes et al. (2012), the cannabinoid agonist would largely inhibit the striatal GABA release in the SM circuits, while in the mPF circuits, the cortical glutamate release would be reduced. In our study, as hypothesized in Figure 7, in the SM circuits, both cannabinoid agonists tested, WIN 55,212-2 and $Δ^9$-THC, would inhibit the striatal GABA release more efficiently, interrupting cortico-nigral transmission at the level of the trans-striatal pathways. However, in the mPF circuit, the inhibition of cortical glutamate release induced by these drugs would lead to disruption of the cortical drive and, consequently, almost complete
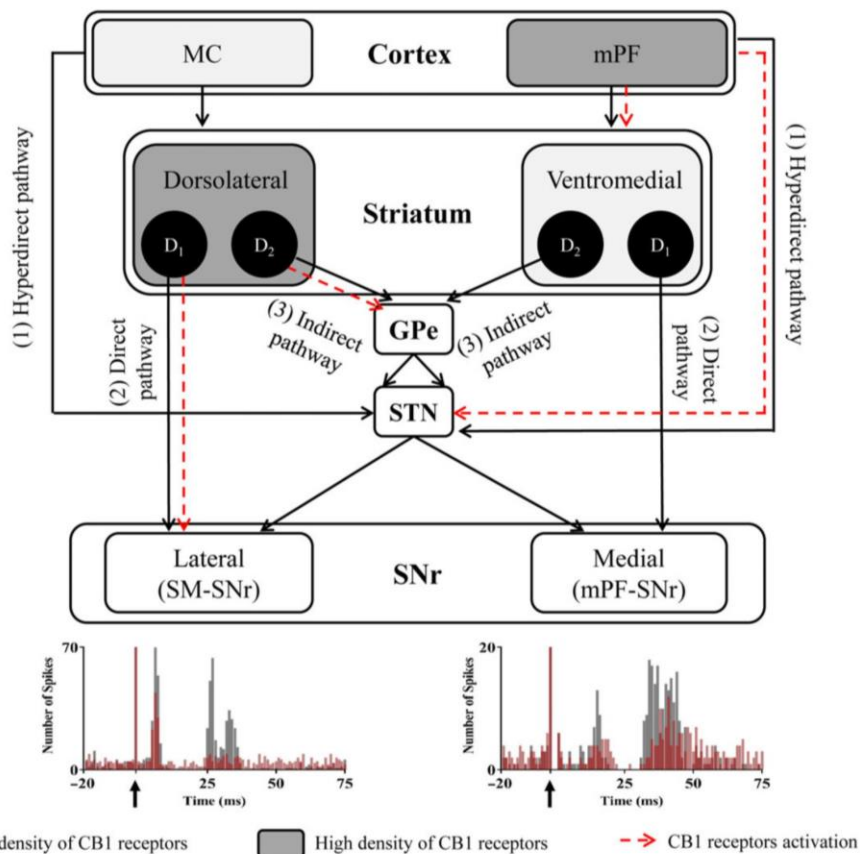
FIGURE 7 Simplified diagram explaining the effect of CB_1 receptor activation on cortico-nigral information transfer through the SM and mPF BG circuits. Under basal conditions, SM and mPF cortical information are transmitted to the SNr through three pathways: (1) cortex-subthalamus-SNr hyperdirect pathway (that evokes an early excitation in the SNr); (2) cortex-striatum-SNr direct pathway (that induces inhibition in the SNr), and (3) cortex-striatum-external *globus pallidus*-subthalamus-SNr indirect pathway (that induces late excitation in the SNr). The activation of CB_1 receptors by cannabinoid agonists (red dashed lines) mainly reduces the transmission through the trans-striatal direct and indirect pathways in SM circuits, whereas in mPF circuits, the activation of CB_1 receptors by cannabinoid agonists affects the corticostriatal and cortico-subthalamic transmissions more. D_1: medium spiny neurons expressing D_1 dopamine receptors; D_2: medium spiny neurons expressing D_2 dopamine receptors; GPe: external *globus pallidus*; MC: motor cortex; STN: subthalamic nucleus

8. APPENDIX – Study I

Cannabinoids differentially modulate cortical information transmission through the sensorimotor or medial prefrontal basal ganglia circuits

inhibition of the cortico-nigral information transfer through the three pathways.

Regarding the cannabinoid drugs tested, although both WIN 55,212-2 and Δ^9-THC activate CB_1 receptors and although the magnitude of the effects they induce is similar, their pharmacological profiles are different. The synthetic compound WIN 55,212-2 is a potent full CB_1/CB_2 agonist. However, Δ^9-THC is a partial CB_1/CB_2 agonist and GPR55 and GPR18 agonist, although it seems to exert its effects principally via CB_1 receptors (Pertwee, 2006). In fact, in the present study, all the effects observed seem to be mediated by the CB_1 receptor since they were blocked by the pretreatment with AM251, a selective CB_1 antagonist and GPR55/GPR18 agonist. Moreover, the administration of AM251 at the dose tested did not have any effect on the triphasic responses, indicating no tonic endocannabinoid control of these circuits.

4.3 | Functional considerations

Under normal conditions, BG output SNr neurons receive convergent synaptic input from the STN and striatum and exert a tonic inhibition on thalamic and brainstem structures. Thus, each SNr neuron receives stimulatory inputs from hyperdirect and indirect pathways (STN) as well as a direct inhibitory input from the striatum. In the SM circuit, hyperdirect and indirect pathways mediate the suppression of movement, while the direct pathway promotes movement (Bevan, Crossman, & Bolam, 1994). Our results show that after CB_1 activation, only the information through the hyperdirect pathway remained unaltered. Consequently, movement inhibition may result, which agrees with previous data showing that cannabinoids impair motor coordination, inducing hypokinesia, and catalepsy in rodents (Anderson, Anderson, Chase, & Walters, 1995; Crawley et al., 1993; de Lago, de Miguel, Lastres-Becker, Ramos, & Fernández-Ruiz, 2004; Navarro et al., 1993; Prescott, Gold, & Martin, 1992; Romero et al., 1995) as well as motor performance deficits in humans smoking marijuana (reviewed in Prashad & Filbey, 2017). Regarding the mPF circuit involved in decision making and goal-directed behaviour (Everitt & Robbins, 2005), after CB_1 activation, cortico-nigral information processing is disrupted almost completely. This mechanism may underlie the deficits in neurocognitive functioning that are well documented in frequent cannabis users (Grant et al., 2003; Schreiner & Dunn, 2012).

In summary, the cannabinoid system represents a promising target in the development of new therapies for several pathologies such as those related to motor disorders. Here, we show how CB_1 receptor agonists modulate the cortical-SNr transmission that comes from motor- and motivation-related cortical areas, which may contribute to a better understanding of the CB_1 receptor-mediated modulation of cortico-BG information processing.

ACKNOWLEDGEMENTS

CONFLICT OF INTEREST

The authors declare no conflicts of interest.

DECLARATION OF TRANSPARENCY AND SCIENTIFIC RIGOUR

This Declaration acknowledges that this paper adheres to the principles for transparent reporting and scientific rigour of preclinical research as stated in the *BJP* guidelines for Design & Analysis, and Animal Experimentation, and as recommended by funding agencies, publishers and other organisations engaged with supporting research.

ORCID

Teresa Morera-Herreras https://orcid.org/0000-0002-7601-4914

REFERENCES

Alexander, G. E., DeLong, M. R., & Strick, P. L. (1986). Parallel organization of functionally segregated circuits linking basal ganglia and cortex. *Annual Review of Neuroscience, 9*, 357–381. https://doi.org/10.1146/annurev.ne.09.030186.002041

Alexander, S. P. H., Christopoulos, A., Davenport, A. P., Kelly, E., Marrion, N. V., Peters, J. A., ... CGTP Collaborators (2017). The Concise Guide to PHARMACOLOGY 2017/18: G protein-coupled receptors. *British Journal of Pharmacology., 174*, S17–S129. https://doi.org/10.1111/bph.13878

Aliane, V., Pérez, S., Nieoullon, A., Deniau, J. M., & Kemel, M. L. (2009). Cocaine-induced stereotypy is linked to an imbalance between the medial prefrontal and sensorimotor circuits of the basal ganglia. *European Journal of Neuroscience, 30*(7), 1269–1279. https://doi.org/10.1111/j.1460-9568.2009.06907.x

Anderson, L. A., Anderson, J. J., Chase, T. N., & Walters, J. R. (1995). The cannabinoid agonists WIN 55,212-2 and CP 55,940 attenuate rotational behavior induced by a dopamine D1 but not a D2 agonist in rats with unilateral lesions of the nigrostriatal pathway. *Brain Research, 691*(1–2), 106–114. https://doi.org/10.1016/0006-8993(95)00645-7

Aristieta, A., Ruiz-Ortega, J. A., Miguelez, C., Morera-Herreras, T., & Ugedo, L. (2016). Chronic L-DOPA administration increases the firing rate but does not reverse enhanced slow frequency oscillatory activity and synchronization in *substantia nigra pars reticulata* neurons from 6-hydroxydopamine-lesioned rats. *Neurobiology of Disease, 89*, 88–100. https://doi.org/10.1016/j.nbd.2016.02.003

Bevan, M. D., Crossman, A. R., & Bolam, J. P. (1994). Neurons projecting from the entopeduncular nucleus to the thalamus receive convergent synaptic inputs from the subthalamic nucleus and the neostriatum in the rat. *Brain Research, 659*(1–2), 99–109. https://doi.org/10.1016/0006-8993(94)90868-0

Bossong, M. G., Mehta, M. A., van Berckel, B. N., Howes, O. D., Kahn, R. S., & Stokes, P. R. (2015). Further human evidence for striatal dopamine release induced by administration of Δ^9-tetrahydrocannabinol (THC): Selectivity to limbic striatum. *Psychopharmacology, 232*(15), 2723–2729. https://doi.org/10.1007/s00213-015-3915-0

Broyd, S. J., Greenwood, L. M., Croft, R. J., Dalecki, A., Todd, J., Michie, P. T., ... Solowij, N. (2013). Chronic effects of cannabis on sensory gating.
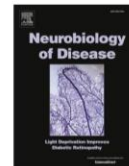
Cannabinoids differentially modulate cortical information transmission
through the sensorimotor or medial prefrontal basal ganglia circuits

8. APPENDIX – Study I

International Journal of Psychophysiology, 89(3), 381–389. https://doi.org/10.1016/j.ijpsycho.2013.04.015

Crawley, J. N., Corwin, R. L., Robinson, J. K., Felder, C. C., Devane, W. A., & Axelrod, J. (1993). Anandamide, an endogenous ligand of the cannabinoid receptor, induces hypomotility and hypothermia in vivo in rodents. *Pharmacology Biochemistry and Behavior*, 46(4), 967–972.

Curtis, M. J., Alexander, S., Cirino, G., Docherty, J. R., George, C. H., Giembycz, M. A., ... Ahluwalia, A. (2018). Experimental design and analysis and their reporting II: Updated and simplified guidance for authors and peer reviewers. *British Journal of Pharmacology*, 175(7), 987–993. https://doi.org/10.1111/bph.14153

Ding, S., Li, L., & Zhou, F. M. (2013). Presynaptic serotonergic gating of the subthalamonigral glutamatergic projection. *The Journal of Neuroscience*, 33(11), 4875–4885. https://doi.org/10.1523/JNEUROSCI.4111-12.2013

Edwards, C. R., Skosnik, P. D., Steinmetz, A. B., O'Donnell, B. F., & Hetrick, W. P. (2009). Sensory gating impairments in heavy cannabis users are associated with altered neural oscillations. *Behavioral Neuroscience*, 123(4), 894–904. https://doi.org/10.1037/a0016328

Everitt, B. J., & Robbins, T. W. (2005). Neural systems of reinforcement for drug addiction: From actions to habits to compulsion. *Nature Neuroscience*, 8(11), 1481–1489. https://doi.org/10.1038/nn1579. PubMed PMID: https://doi.org/info:pmid/16251991

Freund, T. F., Katona, I., & Piomelli, D. (2003). Role of endogenous cannabinoids in synaptic signaling. *Physiological Reviews*, 83(3), 1017–1066. https://doi.org/10.1152/physrev.00004.2003

Gerdeman, G., & Lovinger, D. M. (2001). CB1 cannabinoid receptor inhibits synaptic release of glutamate in rat dorsolateral striatum. *Journal of Neurophysiology*, 85(1), 468–471.

Gerdeman, G. L., & Fernández-Ruiz, J. (2008). The endocannabinoid system in the physiology and pathophysiology of the basal ganglia. In A. Kofalvi (Ed.), *Cannabinoids and the Brain* (pp. 423–483). New York, NY: Springer-Verlag.

Grant, I., Gonzalez, R., Carey, C. L., Natarajan, L., & Wolfson, T. (2003). Non-acute (residual) neurocognitive effects of cannabis use: A meta-analytic study. *Journal of the International Neuropsychological Society*, 9(5), 679–689. https://doi.org/10.1017/S1355617703950016

Gray, A. M., Rawls, S. M., Shippenberg, T. S., & McGinty, J. F. (1999). The κ-opioid agonist, U-69593, decreases acute amphetamine-evoked behaviors and calcium-dependent dialysate levels of dopamine and glutamate in the ventral striatum. *Journal of Neurochemistry*, 73(3), 1066–1074.

Haber, S. N. (2003). The primate basal ganglia: Parallel and integrative networks. *Journal of Chemical Neuroanatomy*, 26(4), 317–330.

Harding, S. D., Sharman, J. L., Faccenda, E., Southan, C., Pawson, A. J., Ireland, S., ... NC-IUPHAR (2018). The IUPHAR/BPS guide to pharmacology in 2018: Updates and expansion to encompass the new guide to Immunopharmacology. *Nucleic Acids Research*, 46, D1091–D1106. https://doi.org/10.1093/nar/gkx1121

Harkany, T., Mackie, K., & Doherty, P. (2008). Wiring and firing neuronal networks: Endocannabinoids take center stage. *Current Opinion in Neurobiology*, 18(3), 338–345. https://doi.org/10.1016/j.conb.2008.08.007

Heng, L., Beverley, J. A., Steiner, H., & Tseng, K. Y. (2011). Differential developmental trajectories for CB1 cannabinoid receptor expression in limbic/associative and sensorimotor cortical areas. *Synapse*, 65(4), 278–286. https://doi.org/10.1002/syn.20844

Ibáñez-Sandoval, O., Carrillo-Reid, L., Galarraga, E., Tapia, D., Mendoza, E., Gomora, J. C., ... Bargas, J. (2007). Bursting in *substantia nigra pars reticulata* neurons in vitro: Possible relevance for Parkinson disease. *Journal of Neurophysiology*, 98(4), 2311–2323. https://doi.org/10.1152/jn.00620.2007

Jin, X., & Costa, R. M. (2015). Shaping action sequences in basal ganglia circuits. *Current Opinion in Neurobiology*, 33, 188–196. https://doi.org/10.1016/j.conb.2015.06.011

Julian, M. D., Martin, A. B., Cuellar, B., Rodriguez De Fonseca, F., Navarro, M., Moratalla, R., & Garcia-Segura, L. M. (2003). Neuroanatomical relationship between type 1 cannabinoid receptors and dopaminergic systems in the rat basal ganglia. *Neuroscience*, 119(1), 309–318. https://doi.org/10.1016/S0306-4522(03)00070-8

Kilkenny, C., Browne, W., Cuthill, I. C., Emerson, M., & Altman, D. G. (2010). Animal research: Reporting in vivo experiments: The ARRIVE guidelines. *British Journal of Pharmacology*, 160, 1577–1579.

Kolomiets, B. P., Deniau, J. M., Glowinski, J., & Thierry, A. M. (2003). Basal ganglia and processing of cortical information: Functional interactions between trans-striatal and trans-subthalamic circuits in the *substantia nigra pars reticulata*. *Neuroscience*, 117(4), 931–938.

de Lago, E., de Miguel, R., Lastres-Becker, I., Ramos, J. A., & Fernández-Ruiz, J. (2004). Involvement of vanilloid-like receptors in the effects of anandamide on motor behavior and nigrostriatal dopaminergic activity: In vivo and in vitro evidence. *Brain Research*, 1007(1–2), 152–159. https://doi.org/10.1016/j.brainres.2004.02.016

Mailleux, P., & Vanderhaeghen, J.-J. (1992). Distribution of neuronal cannabinoid receptor in the adult rat brain: A comparative receptor binding radioautography and in situ hybridization histochemistry. *Neuroscience*, 48(3), 655–668.

Maurice, N., Deniau, J. M., Glowinski, J., & Thierry, A. M. (1999). Relationships between the prefrontal cortex and the basal ganglia in the rat: Physiology of the cortico-nigral circuits. *The Journal of Neuroscience*, 19(11), 4674–4681.

McGeorge, A. J., & Faull, R. L. (1989). The organization of the projection from the cerebral cortex to the striatum in the rat. *Neuroscience*, 29(3), 503–537.

Miller, A. S., & Walker, J. M. (1996). Electrophysiological effects of a cannabinoid on neural activity in the globus pallidus. *European Journal of Pharmacology*, 304(1–3), 29–35.

Morera-Herreras, T., Miguelez, C., Aristieta, A., Torrecilla, M., Ruiz-Ortega, J. A., & Ugedo, L. (2016). Cannabinoids and Motor Control of the Basal Ganglia: Therapeutic Potential in Movement Disorders. Cannabinoid in Health and Disease. *InTech*. https://doi.org/10.5772/62438.

Morera-Herreras, T., Ruiz-Ortega, J. A., Taupignon, A., Baufreton, J., Manuel, I., Rodriguez-Puertas, R., & Ugedo, L. (2010). Regulation of subthalamic neuron activity by endocannabinoids. *Synapse.*, 64(9), 682–698. https://doi.org/10.1002/syn.20778

Morera-Herreras, T., Ruiz-Ortega, J. A., & Ugedo, L. (2010). Two opposite effects of Δ^9-tetrahydrocannabinol on subthalamic nucleus neuron activity: Involvement of GABAergic and glutamatergic neurotransmission. *Synapse*, 64(1), 20–29. https://doi.org/10.1002/syn.20701

Murer, M. G., Riquelme, L. A., Tseng, K. Y., & Pazo, J. H. (1997). *Substantia nigra pars reticulata* single unit activity in normal and 60HDA-lesioned rats: Effects of intrastriatal apomorphine and subthalamic lesions. *Synapse*, 27(4), 278–293. https://doi.org/10.1002/(SICI)1098-2396(199712)27:4<278::AID-SYN2>3.0.CO;2-9

Navarro, M., Fernández-Ruiz, J. J., De Miguel, R., Hernández, M. L., Cebeira, M., & Ramos, J. A. (1993). Motor disturbances induced by an acute dose of Δ^9-tetrahydrocannabinol: Possible involvement of nigrostriatal dopaminergic alterations. *Pharmacology Biochemistry and Behavior*, 45(2), 291–298.

Nicolle, M. M., & Baxter, M. G. (2003). Glutamate receptor binding in the frontal cortex and dorsal striatum of aged rats with impaired attentional set-shifting. *European Journal of Neuroscience*, 18(12), 3335–3342.

8. APPENDIX – Study I

Cannabinoids differentially modulate cortical information transmission through the sensorimotor or medial prefrontal basal ganglia circuits

Parent, A., & Hazrati, L. N. (1995). Functional anatomy of the basal ganglia. I. The cortico-basal ganglia-thalamo-cortical loop. *Brain Res Brain Res Rev., 20*(1), 91–127.

Parent, A., & Smith, Y. (1987). Organization of efferent projections of the subthalamic nucleus in the squirrel monkey as revealed by retrograde labeling methods. *Brain Research, 436*(2), 296–310.

Pertwee, R. G. (2006). Cannabinoid pharmacology: The first 66 years. *British Journal of Pharmacology, 147*(Suppl 1), S163–S171. https://doi.org/10.1038/sj.bjp.0706406

Pintor, A., Galluzzo, M., Grieco, R., Pèzzola, A., Reggio, R., & Popoli, P. (2004). Adenosine A 2A receptor antagonists prevent the increase in striatal glutamate levels induced by glutamate uptake inhibitors. *Journal of Neurochemistry, 89*(1), 152–156.

Prashad, S., & Filbey, F. M. (2017). Cognitive motor deficits in cannabis users. *Current Opinion in Behavioral Sciences, 13*, 1–7. https://doi.org/10.1016/j.cobeha.2016.07.001

Prescott, W. R., Gold, L. H., & Martin, B. R. (1992). Evidence for separate neuronal mechanisms for the discriminative stimulus and catalepsy induced by Δ^9-THC in the rat. *Psychopharmacology (Berl), 107*(1), 117–124.

Romero, J., García, L., Cebeira, M., Zadrozny, D., Fernández-Ruiz, J. J., & Ramos, J. A. (1995). The endogenous cannabinoid receptor ligand, anandamide, inhibits the motor behavior: Role of nigrostriatal dopaminergic neurons. *Life Sciences, 56*(23–24), 2033–2040.

Sañudo-Peña, M. C., & Walker, J. M. (1997). Role of the subthalamic nucleus in cannabinoid actions in the *substantia nigra* of the rat. *Journal of Neurophysiology, 77*(3), 1635–1638.

Schreiner, A. M., & Dunn, M. E. (2012). Residual effects of cannabis use on neurocognitive performance after prolonged abstinence: A meta-analysis. *Experimental and Clinical Psychopharmacology, 20*(5), 420–429. https://doi.org/10.1037/a0029117

Shen, K. Z., & Johnson, S. W. (2006). Subthalamic stimulation evokes complex EPSCs in the rat *substantia nigra pars reticulata* in vitro. *The Journal of Physiology, 573*(Pt 3), 697–709. https://doi.org/10.1113/jphysiol.2006.110031

Solowij, N., & Battisti, R. (2008). The chronic effects of cannabis on memory in humans: A review. *Current Drug Abuse Reviews, 1*(1), 81–98.

Szabo, B., Wallmichrath, I., Mathonia, P., & Pfreundtner, C. (2000). Cannabinoids inhibit excitatory neurotransmission in the *substantia nigra pars reticulata*. *Neuroscience, 97*(1), 89–97.

Tremblay, L., Worbe, Y., Thobois, S., Sgambato-Faure, V., & Féger, J. (2015). Selective dysfunction of basal ganglia subterritories: From movement to behavioral disorders. *Movement Disorders, 30*(9), 1155–1170. https://doi.org/10.1002/mds.26199

Tseng, K. Y., Kasanetz, F., Kargieman, L., Pazo, J. H., Murer, M. G., & Riquelme, L. A. (2001). Subthalamic nucleus lesions reduce low frequency oscillatory firing of *substantia nigra pars reticulata* neurons in a rat model of Parkinson's disease. *Brain Research, 904*(1), 93–103.

Tseng, K. Y., Riquelme, L. A., Belforte, J. E., Pazo, J. H., & Murer, M. G. (2000). *Substantia nigra pars reticulata* units in 6-hydroxydopamine-lesioned rats: Responses to striatal D2 dopamine receptor stimulation and subthalamic lesions. *European Journal of Neuroscience, 12*(1), 247–256.

Van Waes, V., Beverley, J. A., Siman, H., Tseng, K. Y., & Steiner, H. (2012). CB1 cannabinoid receptor expression in the striatum: Association with corticostriatal circuits and developmental regulation. *Frontiers in Pharmacology, 3*, 21. https://doi.org/10.3389/fphar.2012.00021

Wallmichrath, I., & Szabo, B. (2002). Cannabinoids inhibit striatonigral GABAergic neurotransmission in the mouse. *Neuroscience, 113*, 671–682.

Werkheiser, J. L., Rawls, S. M., & Cowan, A. (2006). Icilin evokes a dose- and time-dependent increase in glutamate within the dorsal striatum of rats. *Amino Acids, 30*(3), 307–309. https://doi.org/10.1007/s00726-005-0306-6

Wilson, R. I., & Nicoll, R. A. (2002). Endocannabinoid signaling in the brain. *Science, 296*(5568), 678–682.

Xi, Z.-X., Gilbert, J. G., Peng, X.-Q., Pak, A. C., Li, X., & Gardner, E. L. (2006). Cannabinoid CB1 receptor antagonist AM251 inhibits cocaine-primed relapse in rats: Role of glutamate in the nucleus accumbens. *The Journal of Neuroscience, 26*(33), 8531–8536.

Zhang, X., Feng, Z. J., & Chergui, K. (2015). Induction of cannabinoid- and N-methyl-D-aspartate receptor-mediated long-term depression in the nucleus accumbens and dorsolateral striatum is region and age dependent. *The International Journal of Neuropsychopharmacology, 18*(4), pyu052. https://doi.org/10.1093/ijnp/pyu052

SUPPORTING INFORMATION

Additional supporting information may be found online in the Supporting Information section at the end of the article.

Dopaminergic denervation impairs cortical motor and associative/limbic information processing through the basal ganglia and its modulation by the CB₁ receptor

8. APPENDIX – Study II

Dopaminergic denervation impairs cortical motor and associative/limbic information processing through the basal ganglia and its modulation by the CB1 receptor

Mario Antonazzo [a,b], Sonia María Gomez-Urquijo [c,d], Luisa Ugedo [a,b], Teresa Morera-Herreras [a,b,*]

[a] Department of Pharmacology, Faculty of Medicine and Nursing, University of the Basque Country (UPV/EHU), Leioa 48940, Spain
[b] Neurodegenerative diseases Group, Biocruces Health Research Institute, Barakaldo, Bizkaia, Spain
[c] Department of Neurosciences, Faculty of Medicine and Nursing, University of the Basque Country (UPV/EHU), Leioa 48940, Spain
[d] Achucarro Basque Center for Neuroscience, Science Park of the University of the Basque Country (UPV/EHU), Leioa 48940, Spain

ARTICLE INFO

ABSTRACT

The basal ganglia (BG) are involved in cognitive/motivational functions in addition to movement control. Thus, BG segregated circuits, the sensorimotor (SM) and medial prefrontal (mPF) circuits, process different functional domains, such as motor and cognitive/motivational behaviours, respectively. With a high presence in the BG, the CB1 cannabinoid receptor modulates BG circuits. Furthermore, dopamine (DA), one of the principal neurotransmitters in the BG, also plays a key role in circuit functionality. Taking into account the interaction between DA and the endocannabinoid system at the BG level, we investigated the functioning of BG circuits and their modulation by the CB1 receptor under DA-depleted conditions. We performed single-unit extracellular recordings of *substantia nigra pars reticulata* (SNr) neurons with simultaneous cortical stimulation in sham and 6-hydroxydopamine (6-OHDA)-lesioned rats, together with immunohistochemical assays. We showed that DA loss alters cortico-nigral information processing in both circuits, with a predominant transmission through the hyperdirect pathway in the SM circuit and an increased transmission through the direct pathway in the mPF circuit. Moreover, although DA denervation does not change CB1 receptor density, it impairs its functionality, leading to a lack of modulation. These data highlight an abnormal transfer of information through the associative/limbic domains after DA denervation that may be related to the non-motor symptoms manifested by Parkinson's disease patients.

1. Introduction

Although, for a long time, the basal ganglia (BG) have been viewed exclusively as motor control structures, they are a highly organized network that integrates information from several cortical areas, conforming to segregated parallel anatomical circuits that process different functional domains. Thus, while sensorimotor (SM) circuits play a crucial role in motor functions, medial prefrontal (mPF) circuits are related to cognitive and motivational information processing (Alexander et al., 1986; Haber, 2003; Middleton and Strick, 2000; Parent and Hazrati, 1995). CB1 cannabinoid receptors are highly expressed in the BG, as well as in other parts of the brain (Herkenham et al., 1991; Köfalvi et al., 2005; Mailleux and Vanderhaeghen, 1992; Julián Romero et al., 2002; Tsou et al., 1998). Interestingly, CB1 receptor activation differentially modulates cortical information transfer through both circuits, decreasing SM information transmission through the trans-striatal pathways and profoundly hindering cortico-nigral transmission through the mPF circuits (Antonazzo et al., 2019). Some of the effects found after acute and chronic exposure to cannabis extracts, such as motor performance deficits (slower reaction time or inappropriate motor coordination) and neurocognitive functioning impairments (in memory, associative learning, task switching or attention) (Grant et al., 2003; Prashad and Filbey, 2017; Schreiner and Dunn, 2012), have been related to the activation of the CB1 receptor.

---

8. APPENDIX – Study II

Dopaminergic denervation impairs cortical motor and associative/limbic information processing through the basal ganglia and its modulation by the CB₁ receptor

Dopamine (DA), as one of the principal neurotransmitters in the BG, plays a key role in circuitry functionality (Tremblay et al., 2015). In fact, perturbations in DA neurotransmission at the level of the striatum contribute to maladaptive processing within the BG and lead not only to movement disorders, such as Parkinson's disease (PD), but also to several neuropsychiatric diseases (Tremblay et al., 2015). Substantial evidence supports neuroanatomical and direct/indirect functional interactions between the DA system and the endocannabinoid system in the BG: CB1 receptors form heteromers with DA receptors in striatal projection neurons (Ferré et al., 2009) cannabinoids increase nigrostriatal DA neuronal firing and synaptic DA release in the striatum, mainly through (Morera-Herreras et al., 2012) CB1 receptors present in GABAergic and glutamatergic terminals [for review see (García et al., 2016)] DA modulates endocannabinoid release in the striatum (Giuffrida et al., 1999; Patel et al., 2003); and there is altered endocannabinoid signalling in the BG after DA depletion [details in (Morera-Herreras et al., 2012)].

Considering these findings, we further investigated the impact of DA loss on cortical information transmission through the SM and mPF circuits of the BG and its regulation by the CB1 receptor. For this purpose, simultaneous cortical electrical stimulation and single-unit extracellular recordings of *substantia nigra pars reticulata* (SNr) neurons were carried out in anaesthetized sham and 6-hydroxydopamine (6-OHDA)-lesioned rats.

2. Materials and methods

2.1. Animals

Male Sprague-Dawley rats (160–215 g at the beginning of the experiments) were housed in groups of 4 under standard laboratory conditions (22 ± 1 °C, 55% ± 5% relative humidity, and 12:12 h light/dark cycle) with food and water provided ad libitum. The experimental protocols were reviewed and approved by the Local Ethical Committee for Animal Research of the University of the Basque Country (UPV/EHU, CEEA, ref. ES48/054000/6069). All of the experiments were performed in accordance with the European Community Council Directive on "The Protection of Animals Used for Scientific Purposes" (2010/63/EU) and with Spanish Law (RD 53/2013) for the care and use of laboratory animals.

2.2. Drugs

6-OHDA, desipramine hydrochloride, WIN 55,212-2 and chloral hydrate were obtained from Sigma-Aldrich. AM251 was obtained from Tocris Bioscience. Desipramine and chloral hydrate were prepared in 0.9% saline. 6-OHDA was dissolved in Milli-Q water containing 0.02% ascorbic acid. WIN 55,212-2 and AM251 were diluted in 1:1:18 cremophor/ethanol/saline solution. All drugs were prepared on the day of the experiment.

2.3. 6-Hydroxydopamine lesion

Unilateral 6-OHDA injection in the medial forebrain bundle (MFB) was performed, as previously described (Aristieta et al., 2016, 2019). Thirty minutes before stereotaxic surgery, rats were pretreated with desipramine (25 mg/kg, i.p.) in order to protect noradrenergic terminals from 6-OHDA toxicity. Rats were deeply anaesthetized with isoflurane inhalation (4% for induction; 1.5%–2% for maintenance) and placed in a stereotaxic frame (David Kopf® Instruments). Lesions were performed by two injections of 6-OHDA of 8.75 and 7 μg, respectively (3.5 μg/μl saline with 0.02% ascorbic acid) in the right medial forebrain bundle: 2.5 μl at anteroposterior (AP) −4.4 mm, mediolateral (ML) +1.2 mm and dorsoventral (DV) −7.8 mm, relative to bregma and dura with the toothbar set at −2.4, and 2 μl at AP −4.0 mm, ML +0.8 mm, and DV −8 mm, with toothbar at +3.4 (Paxinos and Watson, 2006). For the

administration of the neurotoxin a 10 μl-Hamilton syringe coupled to a pump at an infusion rate of 1 μl/min. Sham animals were similarly treated but instead of 6-OHDA received vehicle. Rats were randomized to receive either vehicle or 6-OHDA infusion. Electrophysiological experiments were performed 4–5 weeks after the lesion.

2.4. Cylinder test

Forelimb use asymmetry was assessed 4 weeks post-surgery as indicative of severe dopaminergic damage using the cylinder test, as previously described (Hernando et al., 2019). Rats were individually placed in a 20 cm diameter methacrylate cylinder and allowed to explore freely. Mirrors were placed behind the cylinder to allow a 360° view of the exploratory behavior. Each animal was left in place until at least 20 supporting front paw touches with open digits were done on the walls of the cylinder. The session was video-recorded for posterior analysis. Touches performed with the front limb contralateral or ipsilateral to the lesioned hemisphere were counted, and data expressed as the percentage of ipsilateral placement. Rats using the ipsilateral paw above 70% were considered to have severe damage of the dopaminergic system. Breakdown of these data into the different experimental groups is found in Table S1 and illustrated in the Fig. 1B.

2.5. Electrophysiological procedures

The electrophysiological procedures, schematically illustrated in Fig. 1, were performed as previously described (Antonazzo et al., 2019). Animals were anaesthetized with chloral hydrate (420 mg/kg, i.p.) for induction, followed by continuous administration (i.p.) of chloral hydrate at a rate of 115.5 mg/kg/h using a peristaltic pump to keep a steady level of anaesthesia. For additional drug administration, the right jugular vein was cannulated. The animal body temperature was maintained at ~37 °C for the entire experiment with a heating pad connected to a rectal probe. The rat was placed in a stereotaxic frame with its head secured in a horizontal orientation. The skull was exposed, and two 3-mm burr holes were drilled over the right SNr and the ipsilateral motor cortex (MC) or anterior cingulate cortex (ACC).

Single-unit extracellular recordings were made by an Omegadot single glass micropipette, pulled with an electrode puller (Narishige Scientific Instrument Lab., PE-2, Japan), broken back to a tip diameter of 1–2.5 μm under a light microscope and filled with 2% Pontamine Sky Blue in 0.5% sodium acetate. This electrode was lowered into the SM (5.8 mm posterior to Bregma, 2.5 mm lateral to midline, and 7–8 mm ventral to the dura mater) or mPF territory (5.4 mm posterior to Bregma, 1.8 mm lateral to midline, and 7–8 mm ventral to the dura mater) of the SNr. To evoke triphasic responses in SNr neurons, the MC (3.5 mm anterior to Bregma, 3.2 mm lateral to midline, and 1.6 mm ventral to the dura mater) or the ACC (2.9 mm anterior to Bregma, 0.6 mm lateral to midline, and 1.7 ventral to the dura mater) ipsilateral to the recording site, was stimulated at 1 Hz (pulse width, 600 μs; intensity, 1 mA) using coaxial stainless-steel electrodes (diameter, 250 μm; tip diameter, 100 μm; tip-to-barrel distance, 300 μm) during the recordings (Cibertec S. A.).

The signal from the recording electrode passed through an AxoClamp 2-B amplifier (Axon Instruments) bridge circuitry, amplified x100, and filtered at 300–3000 Hz with a high-input impedance amplifier (AMPLI64AC, Cibertec). The signal was monitored through an oscilloscope and an audio-monitor. Neuronal spikes were sampled at 25 kHz using a CED micro3 1401 analog-digital interface and a computer running Spike2 acquisition software (Cambridge Electronic Design, UK). SNr neurons were identified as non-dopaminergic by their classically defined electrophysiological characteristics: thin spikes (width, <2 ms) and ability to present relatively high-frequency discharges without decrease in spike amplitude (as described in Antonazzo et al. (2019)). Although multiple neurons were recorded in each animal in order to characterize the spontaneous and cortically evoked activity in both SM

2

Dopaminergic denervation impairs cortical motor and associative/limbic information processing through the basal ganglia and its modulation by the CB$_1$ receptor

8. APPENDIX – Study II

(caption on next page)

8. APPENDIX – Study II

Dopaminergic denervation impairs cortical motor and associative/limbic information processing through the basal ganglia and its modulation by the CB₁ receptor
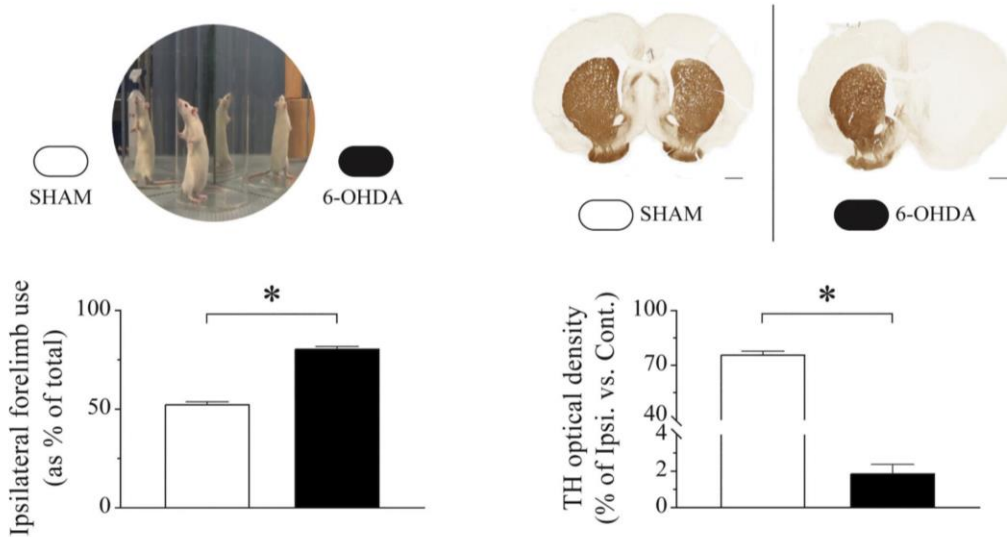
Fig. 1. Schematic illustration of electrophysiological recordings in SNr neurons from sensorimotor (SM) and medial prefrontal (mPF) territories, motor asymmetry and dopaminergic denervation in sham and 6-OHDA-lesioned rats.
A. Schematic horizontal sections of the rat brain showing the stimulation of the motor cortex (MC) or the anterior cingulate cortex (ACC), and a representative spike trace from SM-SNr or mPF-SNr neurons during single-unit recordings extracellular. The cortical information is transferred through the (Alexander et al., 1986) hyperdirect (cortex-STN-SNr, in blue), (Anderson et al., 2020) direct (cortex-striatum-SNr, in red) and (Antonazzo et al., 2019) indirect pathways (cortex-striatum-GP-STN-SNr, in green), inducing the characteristic triphasic response in SNr neurons, as illustrated in the peristimulus time histograms. Arrows indicate cortical stimulus application. Scale bar for spike traces is of 1 V and 1 ms. B. Left, video frame showing a rat performing the cylinder test. The mean percentage of ipsilateral forelimb use represented in the bar graph below shows that 6-OHDA-lesioned rats use more the forelimb ipsilateral to the lesioned side, indicating an important degree of motor asymmetry, and suggesting severe dopaminergic denervation. Right, representative brain slices showing TH immunostaining for both sham and 6-OHDA-lesioned rats. Note the severe striatal dopaminergic denervation in 6-OHDA rats, after infusion of the toxin in the MFB. The bar graph below shows the TH optical density (OD) mean percentage of variation, referring to the change in the hemisphere ipsilateral to the lesion vs. the contralateral side. As depicted in the brain slices above, 6-OHDA animals show a severe dopaminergic denervation. Slice scale bars are set to 1 mm. *P < 0.05, two-tailed unpaired Student's t-test. DL/DM striatum: dorsolateral/dorsomedial striatum; GP: *globus pallidus*; SNr: *substantia nigra pars reticulate*. (For interpretation of the references to colour in this figure legend, the reader is referred to the web version of this article.)

and mPF territories, only one SNr cell was pharmacologically studied per animal.

Firing parameters such as firing rate and coefficient of variation (CV) of SNr neurons were analysed offline using Spike2 software (version 7). The CV consisted on the ratio, expressed as a percentage, between the standard deviation and the mean of the neuron's inter-spike interval histogram. This histogram was made with 1 ms bins, and considering all the inter-spike intervals below 0.5 ms, given the relatively high firing rate of SNr neurons. The existence of burst firing in neurons was determined through a Spike2 script ("surprise.s2s"), based on the Poisson surprise algorithm. These parameters were analysed during time epochs of 150 s under basal conditions, or for 120 s once the drug was administered. Before data analysis, spike-sorting procedures were used just to discriminate electrical stimulation artifacts from actual spikes, and discard them to avoid any interference with posterior analysis. This procedures were done using the Spike2 software, and consisted in principal component analysis and template matching to help discriminate, and group stimulation artifacts and spikes waveforms separately. The few spare waveforms that left ungrouped after this were manually inspected and grouped accordingly. Given the nature of our recordings, only single-units were recorded, and thus all the spikes present in the recordings were from the same unit.

Peristimulus time histograms were generated from 180 stimulation trials using 1 ms bins. The criterion used to determine the existence of an excitatory response was a two-fold increase in the standard deviation over the pre-stimulus period, plus the mean number of spikes, for at least three consecutive bins. The amplitude of excitatory responses was quantified by calculating the difference between the mean number of spikes evoked within the time window of the excitation and the mean number of spikes occurring spontaneously before the stimulation. The duration of an inhibitory response corresponded to the time interval during which no spikes were observed for at least three consecutive bins.

To better describe information transmission through these circuits, we set latency ranges for each pathway based on the latencies of triphasic responses, since these inform of the transmission through the three pathways that constitute the circuits. Such ranges were set up to each cortically-evoked response (i.e. early excitation, EE; inhibition, INH, late excitation, LE), in each circuit (i.e. SM or mPF) and experimental group (i.e. sham or 6-OHDA). For each response, a range was set according to the minimum and maximum latency observed within the triphasic-respondent neurons of that circuit and experimental group (Table S2). Hence, cortically evoked responses whose latency was out of this range were excluded from the analyses of the cortically evoked responses, and neurons with no cortically evoked response within range were excluded from all the analysis (cortically evoked and spontaneous firing parameters).

As more than one neuron (1–15 per rat) was recorded per animal in the characterization of the SM and mPF circuits, electrophysiological parameters such as firing rate, coefficient of variation, and parameters related to cortically evoked responses (i.e. duration, latency and amplitude of the responses) were averaged per animal, so that every

animal had one value for each electrophysiological parameter.

2.6. Tyrosine hydroxylase immunohistochemistry

Immediately after the electrophysiological procedure, animals were transcardially perfused with a phosphate-buffered saline solution followed by 4% paraformaldehyde solution. Fixed brains were sliced at 40 μm by a freezing microtome (HM 430, Microm) and stored in a cryoprotective solution at −20 °C until further processing. Tyrosine hydroxylase (TH)-immunostaining was used to examine the degree of DA denervation in the striatum and the SNc as previously described (Aristieta et al., 2019, 2016). Free-floating sections were incubated in a 3% H_2O_2 + 10% MeOH solution prepared in potassium phosphate buffer saline with 0.1% Triton X-100 (KPBS-t) for 30 min. After that, sections were washed in KPBS and blocked with 5% normal goat serum (NGS) in KPBS-t during 1 h, and incubated with rabbit anti-TH (AB 152, 1:1000, Merck) primary antibody in 5% NGS-KPBS-t, at room temperature overnight. The sections were then washed in 2.5% NGS-KPBS-t, and incubated for 2 h with a biotinylated goat antibody against rabbit IgG (BA 1000, 1:200, Vector Laboratories) in 2.5% NGS-KPBS-t. Thereafter, sections were washed and incubated with an avidin–biotin–peroxidase complex (ABC kit, PK-6100, Vector Laboratories) and peroxidase activity was visualized with 0.05% 3,3′-diaminobenzidine (Sigma) and 0.03% H_2O_2. Finally, sections were mounted onto gelatin-coated slides, dehydrated, cleared with xylene and coverslipped. For the analysis, striatal sections from each animal (rostral, medial and caudal levels) were optically digitized using an EPSON V700 scanner at a resolution of 6400 ppp, and the mean optical density (OD) associated with the striatum was calculated using NIH-produced image analysis software ImageJ (Schindelin et al., 2012). The OD was expressed as a percentage of that of the contralateral intact side (100%) with the background associated with the corpus callosum set as 0%. Only animals with >90% DA degeneration were included in the analysis. Breakdown of these data into the different experimental groups is found in Table S1 and illustrated in the Fig. 1B.

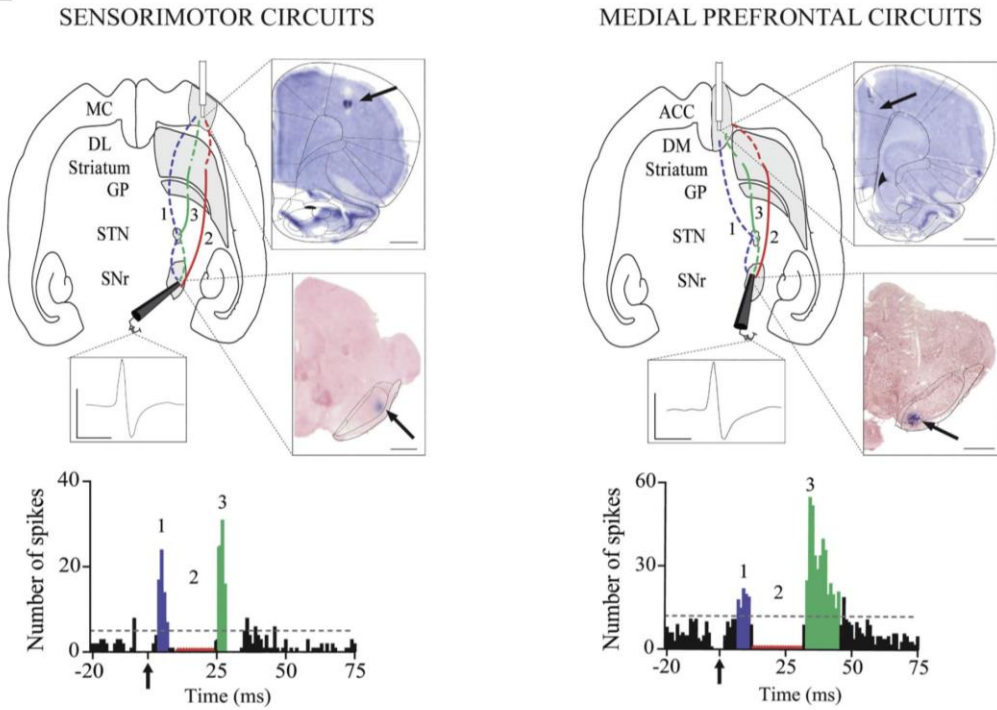*2.7. CB1 receptor immunohistochemistry*

Another series of animals (sham and 6-OHDA lesioned rats) were used to determine the expression of CB1 receptors within the BG. Rats were transcardially perfused with a phosphate-buffered saline solution followed by a mixture of 4% paraformaldehyde and 0.5% glutaraldehyde with 2 ml per litre of a saturated solution of picric acid in 0.1 M phosphate buffer (PB; pH 7.4). Brains were extracted and stored in fixative solution for one week. After fixation, brains were coronally cut at 50 μm by a cryotome.

Sections were preincubated in blocking solution containing 10% bovine serum albumin, 0.5% Triton X-100 and 0.1% sodium azide in Tris-HCl-buffered saline (TBS) for 30 min and then incubated in solution of primary goat antibody raised against CB1 cannabinoid receptor (CB1-Go-Af450 Frontier Institute Co.; RRID AB_257130) at a final dilution of

4

Dopaminergic denervation impairs cortical motor and
associative/limbic information processing through the basal
ganglia and its modulation by the CB₁ receptor

8. APPENDIX – Study II

2 μg/ml in 10% bovine serum albumin, 0.5% Triton X-100 and 0.1% sodium azide in TBS for 20 h. Afterwards, sections were rinsed in 1% bovine serum albumin and 0.5% Triton X-100 in TBS and incubated in biotinylated horse-anti-goat secondary antibody (Vector BA-9500) diluted 15 μg/ml in 1% bovine serum albumin and 0.5% Triton X-100 in tris buffered saline for 1 h. After secondary antibody incubation, sections were again rinsed in 1% bovine serum albumin and 0.5% Triton X-100 in TBS saline and reacted for 90 min in ABC complex diluted 1:1:50 in TBS. After several rinses in PB, the peroxidase reaction with 0.05% DAB and 0.003% H_2O_2 in PB was developed for 2 min. Sections were rinsed in PB, mounted onto gelatine-coated microscope slides, allowed to air dry, dehydrated in graded ethanol, cleared in xylene and coverslipped. Microscope slides with the reacted tissue were scanned with the 20× objective (NA 0.8; Carl-Zeiss) of a Pannoramic MIDI II (3DHISTECH) automatic slide scanner coupled to a CMOS camera (pco. edge 4.2, PCO), through an adapter with 1.6× magnification. Images were studied with FIJI software using the Bio-Formats plugin (Linkert et al., 2010; Schindelin et al., 2012).

For the analysis of the CB1 receptor density we defined the regions of interest (ROI) for each anatomo-functional division in each nucleus based on previous tracing, molecular and functional reports, in which compartmentalization of the analysed BG nuclei is made depending on the cortical information they process. Regarding cortex, we focused on the MC and the ACC since they were the target of cortical stimulation in electrophysiological experiments. BG nuclei receiving information from MC were considered to belong to the SM circuits, and those receiving ACC information to the mPF circuits of the BG. MC and ACC ROI's were made following a rat brain atlas (Paxinos and Watson, 2006). Cortical areas were analysed until 0.4 mm posterior to bregma, where they were considered small enough to be properly selected. Striatal SM and mPF territories were limited to those areas receiving afferences from MC and ACC, respectively (Heilbronner et al., 2016; McGeorge and Faull, 1989). Globus pallidus SM and mPF territories were defined based on calbindin expression patterns, which resembles SM and mPF striatal projections onto the *globus pallidus* (Rajakumar et al., 1994). SM-SNr and mPF-SNr territories were defined based on functional studies showing connectivity between motor or mPF cortices, respectively (Kolomiets et al., 2003). For frontal slices the olfactory tract, forceps minor or corpus callosum, were selected as background. For more caudal slices, the thalamus, geniculate nucleus or reticular formation, were used as background.

To analyze changes in CB1 receptor density between lesion group (sham vs. 6-OHDA) and territories (SM or mPF) of the analysed BG nuclei, background OD from each hemisphere was subtracted from ROI's OD's in their corresponding hemisphere. Then values from both hemispheres of the same slice, corresponding to a given nucleus and territory, were averaged between them; averaged values from all the slices in an animal were averaged, so each animal would have two values per nucleus: one value for the SM territory, and another for the mPF territory. These values corresponding to the same BG territory and nucleus were averaged by lesion group.

2.8. Statistical analysis of data

The data were analysed using the computer program GraphPad Prism (v. 5.01, GraphPad Software, Inc.) and SPSS (v. 25; IBM Corp.). Averages from each rat for firing rate, CV and parameters related to cortically evoked responses were analysed by a two-tailed unpaired Student's *t*-test when looking for differences between sham and 6-OHDA-lesioned animals in both circuits. Fisher's exact test was used to assess differences in the number of neurons presenting bursting patterns and cortically evoked patterns of response.

To assess the effects of WIN 55,212-2 on firing rate, CV and parameters related to cortically evoked responses before and after drug application (one neuron per animal), a repeated-measures two-way ANOVA was used. When allowable, Bonferroni *post-hoc* method was

used for correction of multiple comparisons. Fisher's exact test was used to assess differences in the number of neurons with burst firing before and after drug administration.

To determine the role of the CB1 receptor in the effect of WIN 55,212-2, the firing rate, CV, and cortically evoked responses pre-AM251, post-AM251 and post-AM251 + WIN 55,212-2, were compared using a repeated-measures one-way ANOVA in the SM circuits, and repeated-measures two-way ANOVA in the mPF circuits (one neuron per animal), both with Geisser-Greenhouse's correction if epsilon was below 0.75. When allowable, Bonferroni *post-hoc* method was used for correction of multiple comparisons. Differences in the number of neurons with burst firing were assessed with the chi-squared test.

CB1 receptor density averages from sham or 6-OHDA rats were compared using a two-way ANOVA (lesion × territory) to assess differences in CB1 receptor density between territories (SM and mPF) and lesion groups (sham and 6-OHDA). When allowable, Bonferroni *post-hoc* method was used for correction of multiple comparisons.

To assess differences in TH OD and ipsilateral forelimb use between sham and 6-OHDA rats a two-tailed unpaired Student's *t*-test was used.

The level of statistical significance was set at $P < 0.05$. Data are presented as group means ± the standard error of the mean (S.E.M.) of n rats, unless stated otherwise.

3. Results

3.1. Effect of dopaminergic denervation on SNr neuron activity from sensorimotor and prefrontal territories

All recorded cells exhibited the typical electrophysiological characteristics of GABAergic SNr neurons, including a narrow spike waveform and a relatively high firing rate (>7 Hz) with a regular pattern of discharge and response to cortical stimulation.

As summarized in Table 1, DA denervation differently affected SM-SNr and mPF-SNr neurons: the mean firing rate of mPF-SNr neurons was reduced in 6-OHDA-lesioned animals, while the mean firing rate of SM-SNr neurons in 6-OHDA-lesioned animals was not affected when compared to that of sham rats. Moreover, SM- and mPF-SNr neurons from lesioned animals presented a higher coefficient of variation than those from sham animals. In addition, the analysis of the firing pattern revealed that the number of neurons with bursts was increased in both SNr territories of the 6-OHDA-lesioned group.

As we previously showed, cortical stimulation of the MC or ACC evoked characteristic triphasic responses in SNr neurons that consisted of an early excitation followed by an inhibition and a late excitation (Antonazzo et al., 2019) (Fig. 1A). The presence of the early excitation is attributable to the activation of the so-called 'hyperdirect' cortico-subthalamo-nigral pathway. The activation of the 'direct' cortico-striato-nigral pathway give rise to the inhibition, and the late excitation derives from the activation of the 'indirect' cortico-striato-pallido-subthalamo-nigral pathway (Maurice et al., 1999). Different patterns of response can be observed in both SNr territories, yielding triphasic, biphasic or monophasic cortically evoked responses from the activation of the different pathways along the circuits. DA denervation induced changes in the percentage of neurons displaying different patterns of response in the SM-SNr territory (Table 2): the proportion of neurons displaying triphasic and biphasic (i.e., inhibition + late excitation) responses in SM-SNr neurons was reduced, in favour of more monophasic (i.e., early excitation) responses in the 6-OHDA-lesioned group. DA loss also altered patterns of response in mPF-SNr neurons, showing a greater amount of monophasic – inhibition – responses (Table 2). Overall, SM-SNr neurons displayed fewer inhibitions and late excitations, while the mPF-SNr neurons displayed only fewer late excitations after DA loss (Table 2).

DA denervation also affected the electrophysiological characteristics of cortically evoked responses in SNr neurons (Table 1). SM-SNr cells

8. APPENDIX – Study II

Dopaminergic denervation impairs cortical motor and associative/limbic information processing through the basal ganglia and its modulation by the CB₁ receptor

Table 1

Electrophysiological characteristics of the spontaneous and cortically-evoked responses in neurons from the sensorimotor (SM) and medial prefrontal (mPF) subdivisions of the *substantia nigra pars reticulata* (SNr) in sham and 6-OHDA-lesioned rats.

	SM-SNr		mPF-SNr	
	Sham (n = 21)	6-OHDA (n = 36)	Sham (n = 32)	6-OHDA (n = 41)
Firing rate (Hz)	21.2 ± 1.8	19.0 ± 1.2	24.8 ± 1.3	19.4 ± 1.0*
Coefficient of variation (%)	43.6 ± 2.4	70.3 ± 4.6*	49.0 ± 2.4	102.5 ± 5.9*
Burst firing neurons/ recorded neurons	51/98	91/115	126/187	144/160
Neurons exhibiting burst firing pattern (%)	52.0	79.1*	67.4	89.6*
Early excitation	n = 19	n = 27	n = 30	n = 28
Duration (ms)	5.3 ± 0.4	8.3 ± 1.0*	7.2 ± 0.7	6.4 ± 1.0
Latency (ms)	5.5 ± 0.4	5.7 ± 0.3	8.5 ± 0.6	13.7 ± 0.5*
Amplitude	14.4 ± 1.3	13.2 ± 0.8	8.2 ± 0.5	7.9 ± 0.8
Inhibition	n = 20	n = 29	n = 32	n = 38
Duration (ms)	19.8 ± 2.1	27.6 ± 4.6	11.5 ± 0.8	13.0 ± 1.7
Latency (ms)	12.1 ± 0.4	14.0 ± 0.4*	18.8 ± 0.4	20.8 ± 0.4*
Late excitation	n = 21	n = 29	n = 32	n = 38
Duration (ms)	6.0 ± 0.5	7.5 ± 0.7	11.2 ± 0.8	11.3 ± 0.9
Latency (ms)	27.1 ± 0.6	27.7 ± 0.7	33.4 ± 0.4	33.5 ± 0.5
Amplitude	17.9 ± 2.5	13.7 ± 1.5	15.4 ± 1.0	13.8 ± 0.8

Each value represents the mean ± S.E.M. of (n) recorded rats.

* $P < 0.05$ Sham vs. 6-OHDA (Firing rate, coefficient of variation and response parameters: two-tailed unpaired Student's *t*-test; neurons exhibiting burst firing pattern: Fisher's exact test).

Table 2

Percentage of occurrence the different patterns of responses evoked in *substantia nigra pars reticulata* (SNr) neurons by motor or medial prefrontal cortex stimulation in sham and 6-OHDA-lesioned animals.

	SM-SNr		mPF-SNr	
	Sham (n = 98)	6-OHDA (n = 115)	Sham (n = 187)	6-OHDA (n = 160)
Total no. neurons showing early excitation (%)	60.2	66.1	30.5	28.1
Total no. neurons showing inhibition (%)	75.5	51.3*	65.8	70.6
Total no. neurons showing late excitation (%)	65.3	46.1*	86.1	70.6*
Patterns of responses (%)				
Triphasic response	29.6	16.5*	19.8	11.9
Early excitation + Inhibition	21.4	22.6	3.2	5
Inhibition + Late excitation	16.3	3.5*	38	36.9
Early excitation + Late excitation	4.1	4.3	1.6	3.8
Early excitation	5.1	22.6*	5.9	7.5
Inhibition	8.2	8.7	4.8	16.9*
Late excitation	15.3	21.7	26.7	18.1

Each value represents the number of neurons exhibiting the response to cortical stimulation (% of n recorded neurons).

* $P < 0.05$ vs sham, Fisher's exact test.

from 6-OHDA-lesioned animals had early excitations with greater durations than those recorded from sham rats. In the case of mPF-SNr neurons, DA denervation increased the latency of the early excitation. Moreover, the inhibition appeared later in the SM- and mPF-SNr neurons of 6-OHDA-lesioned animals, as indicated by a higher latency. It is important to note that, when only triphasic responses were taken into account, only the differences in mPF-SNr neurons remained, while no differences in electrophysiological characteristics were found in SM-SNr neurons between groups (Table S2).

3.2. Effects of WIN 55,212-2 on cortico-nigral transmission through the sensorimotor circuits in sham and 6-OHDA-lesioned rats

The effect of the synthetic cannabinoid agonist WIN 55,212-2 (WIN) (125 µg/kg, i.v.) on the transfer of cortical information through the SM circuits in intact and 6-OHDA-lesioned rats was investigated. The dose of WIN was carefully selected to minimize any effects on the firing activity of SNr neurons, which could make the analysis of the cortically-evoked responses difficult. Thus, at the administered dose, WIN did not modify the SM-SNr neuron firing rate or the number of neurons with burst activity in the sham and 6-OHDA experimental groups, although some minor changes were observed regarding the regularity (Table S3).

According to our previous data (Antonazzo et al., 2019), in sham rats, systemic administration of WIN did not alter early excitation but diminished cortico-nigral transmission through the indirect pathway, as shown by a reduction in the amplitude of the late excitation. However, no statistically significant decrease was observed in the transmission through the direct pathway (Fig. 2). In contrast to that observed in the sham group, 6-OHDA lesions modified the effect of WIN on cortico-nigral transmission through the SM circuits, being the early excitation decreased after drug administration. However, cortico-nigral information transfer through the trans-striatal pathways was not affected after WIN administration in 6-OHDA-lesioned animals (Fig. 2).

The effects observed in sham rats were blocked by the previous administration of the CB1-selective antagonist AM251 (2 mg/kg, i.v.) (Fig. 3). AM251 alone did not modify the cortico-nigral information transfer (Fig. 3) or the spontaneous activity of SM-SNr neurons (Table S4).

3.3. Effects of WIN 55,212-2 on cortico-nigral transmission through the medial prefrontal circuits in sham and 6-OHDA-lesioned rats

We further explored the effect of WIN (125 µg/kg, i.v.) on cortico-nigral transmission through the mPF circuits in intact and 6-OHDA-lesioned rats. At the administered dose, WIN did not modify the mPF-SNr neuronal firing rate or the number of neurons displaying burst activity. Nevertheless, some minor changes were observed regarding regularity (Table S3).

As previously shown in control animals (Antonazzo et al., 2019), WIN administration dramatically impaired all cortically evoked responses, reducing the amplitude of the early and late excitations and the duration of the inhibition (Fig. 4). As in SM circuits, DA denervation induced changes in the way WIN modulates transmission through the mPF circuits. The administration of WIN reduced the amplitude of the early excitation but had no effect on cortical information transfer through the direct and indirect pathways (Fig. 4).

These effects were blocked by the previous administration of the CB1-selective antagonist AM251 (2 mg/kg, i.v.) in both sham and 6-OHDA-lesioned animals (Fig. 5). AM251 alone did not modify the cortico-nigral information transfer (Fig. 5) or the spontaneous activity of mPF-SNr neurons (Table S4).

3.4. CB1 receptor localization in the sensorimotor and prefrontal circuits of the basal ganglia in sham and 6-OHDA-lesioned rats

Finally, CB1 immunostaining was performed in all BG structures

6

Dopaminergic denervation impairs cortical motor and associative/limbic information processing through the basal ganglia and its modulation by the CB₁ receptor

8. APPENDIX – Study II

included in the SM and mPF circuits. The study of the mean OD obtained from all the slices through each structure, and the comparison between the divisions related to the SM and mPF circuits for every nucleus sampled revealed some differences. In the striatum from sham animals, the CB1-positive labelling in the lateral division related to the SM circuit was higher than in the mPF-related division. This difference was also statistically significant in 6-OHDA-lesioned animals (Fig. 6).

On the other hand, no statistically significant changes were found in the CB1 receptor immunostaining between sham and 6-OHDA-lesioned rats, in any of the analysed territories of the BG nuclei (Fig. 7).

4. Discussion

In the present study, we investigated the functioning of BG circuits and their modulation by the CB1 receptor under DA-depleted conditions. The results show that the DA deficit modifies the transmission through the SM and mPF circuits. Moreover, we observed an alteration at the level of CB1 receptors modulating cortico-BG information transfer in 6-OHDA-lesioned animals. Given the role of these circuits in motor and cognitive/motivational information processing, the present data may help researchers to understand the role of the cannabinoid system in motor and non-motor symptoms associated with the hypo-dopaminergic state.

4.1. Spontaneous and cortically evoked SNr neuron activity after DA denervation

According to our data, in DA-depleted animals, SNr neurons recorded in the mPF and SM regions exhibited alterations in spontaneous activity, displaying more irregular and burst firing patterns (Aristieta et al., 2016; Vegas-Suárez et al., 2020). However, only in the mPF-SNr neurons did we observe a significant reduction in the firing rate. In line with our results, Wang et al. (2010) showed a decreased firing rate and an increased CV and burst activity in mPF-SNr neurons in animals injected with 6-OHDA in the MFB. Regarding the SM territory, there is much more evidence supporting the hyperactive SNr neuronal discharge pattern after DA depletion, without changes in the firing rate (Aristieta et al., 2016; Maurice et al., 2015; Meissner et al., 2006; Murer et al., 1997; Tseng et al., 2000). Several studies suggest that there might be a mediolateral gradient in DA content in the SNr, with less DA in the SM-SNr and more DA in the mPF-SNr (Ciliax et al., 1995; Cragg et al., 1997; Rice et al., 1994, 1997; Weiss-Wunder and Chesselet, 1990). This suggestion is in accordance with the greater effect of DA denervation observed on the firing rate and pattern of mPF-SNr neurons. Our data suggest that mPF-SNr neurons rely more on DA for their normal function than SM-SNr neurons. The effects of DA denervation on SNr spontaneous activity likely involve an indirect mechanism, like modulation of pre-synaptic GABAergic or glutamatergic inputs, since SNr neurons lack

Fig. 2. Effect of systemic administration of WIN 55,212-2 (125 μg/kg, i.v.) on cortico-nigral information transmission in sensorimotor (SM) BG circuits in sham and 6-OHDA-lesioned animals.

A. Top, raster plot and peristimulus time histogram showing a representative example of a triphasic response evoked in an SM-SNr neuron from a sham rat through the stimulation of the motor cortex (MC) under basal conditions. Bottom, after WIN 55,212-2 injection, the inhibitory and late excitatory components disappeared, with the early excitation remaining unaltered. Arrows indicate cortical stimulus application. Dashed lines indicate the threshold for excitatory responses. C. Top, raster plot and peristimulus time histogram showing a representative example of a triphasic response evoked in an SM-SNr neuron from a 6-OHDA-lesioned animal through the stimulation of the motor cortex under basal conditions. Bottom, after WIN 55,212-2 injection, none of the three pathways experienced any change in transmission in 6-OHDA-denervated animals. Arrows indicate cortical stimulus application. Dashed lines indicate the threshold for excitatory responses. B. Bar graphs showing the mean effect of WIN 55,212-2 (125 μg/kg, i.v.) on cortically evoked responses in SM-SNr neurons (amplitude of early (EE; sham: n = 5; 6-OHDA: n = 6) and late (LE; sham: n = 5; 6-OHDA: n = 6) excitations and the duration of inhibition (INH; sham: n = 6; 6-OHDA: n = 6)) in SM circuits. Each bar represents the mean ± the S.E.M. of n rats. Each dot represents the value from one neuron before and after drug administration. *P < 0.05 before vs. after WIN, repeated-measures two-way ANOVA (Drug x Lesion).

8. APPENDIX – Study II

Dopaminergic denervation impairs cortical motor and associative/limbic information processing through the basal ganglia and its modulation by the CB₁ receptor

postsynaptic DA receptors (Yung et al., 1995). According to the classical BG organization model, the direct striatonigral pathway is under the control of DA projections via D1 receptors, whereas the striato-pallido-subthalamo-nigral indirect pathway is controlled via D2 receptors. Degeneration of nigrostriatal DA neurons results in a dramatic decrease of striatal DA level and, subsequently, in a supersensitivity of the striatal postsynaptic DA receptors affecting the direct and indirect pathways and triggering SNr neuron activity abnormalities (Galvan and Wichmann, 2008). Thus, in line with our previous data, SNr neurons recorded in the mPF and SM regions from 6-OHDA lesioned animals displayed more irregular and burst firing patterns, probably related with the well described hyperactivated subthalamic nucleus after DA depletion. Moreover, in mPF-SNr neurons we observed a significant reduction in the firing rate that might be due to an increase in the number of D2 receptors in the limbic striatum after striatal DA depletion, which activation inhibits SNr neuronal firing via their intracellular effects on G_i proteins (Lévesque et al., 1995).

In relation to the SM circuit, we show a prominent transmission through the hyperdirect trans-subthalamic pathway reflected by a greater mean duration and more monophasic early excitations. These data differ, at least in part, from the evidence available to date, although the heterogeneous results may depend on methodological differences like the use of different anaesthetic regime (chloral hydrate, urethane or awake animals) (Beyeler et al., 2010; Heckman et al., 2018; Kolomiets et al., 2003; Maurice et al., 1999; Sano and Nambu, 2019), or dopaminergic interruption method (6-OHDA lesion or pharmacological blockade) (Degos et al., 2005; Sano and Nambu, 2019). Moreover, the

degree of dopaminergic denervation, and time after the 6-OHDA injection, may also impact on results.

Degos et al. (2005) studied the effect of acute pharmacological blockade of DA transmission on circuit functionality, but by systemic injection of neuroleptics. They showed decreased transmission through the direct pathway and a reinforced transmission through the indirect pathway, without any change in the information transfer through the hyperdirect pathway. Using the 6-OHDA neurotoxin, other authors either have found no alterations (injected into the *substantia nigra pars compacta*) (Maurice et al., 2015) or have described early excitations as the predominant response after dopaminergic denervation (injected into the MFB, but recordings in awake mice) (Sano and Nambu, 2019). However, although this might be in accordance with our results, the authors also found an increase in transmission through the indirect pathway, concluding that only neuronal transduction through the direct pathway is diminished in PD. Predominant transmission through the hyperdirect pathway in the SM circuit observed in the present study, together with the hyperactivity of SM-SNr neurons, is consistent with the overactive state of the subthalamic nucleus extensively described under low DA conditions and has been related to the motor features of parkinsonism (Benabid et al., 1994; Bergman et al., 1994; Hassani et al., 1996; Steigerwald et al., 2008).

To our knowledge, the present is the first demonstration that DA denervation alters the cortically evoked responses in mPF-SNr neurons, leading to a predominant information transfer though the direct pathway, with a loss of efficacy in the transmission through the hyperdirect and indirect pathways (augmented latency of early excitations or
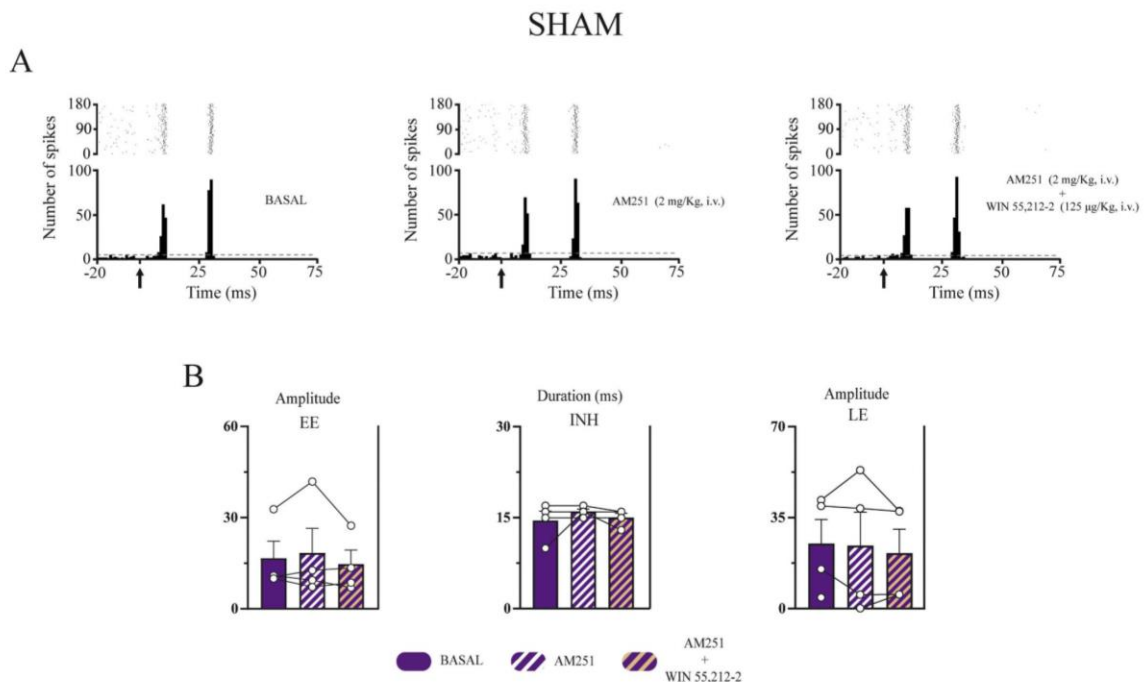
Fig. 3. Blockade of WIN 55,212-2-induced effects on cortico-nigral information transmission in sensorimotor (SM) BG circuits in sham animals by the previous administration of the CB1 selective antagonist AM251 (2 mg/kg, i.v.).
A. Left, raster plot and peristimulus time histogram showing a representative example of a triphasic response evoked in a SM-SNr neuron by stimulation of the motor cortex (MC) in a sham rat under basal conditions. AM251 administration did not modify the characteristics of the three components of the cortically evoked response (middle) but blocked the effects induced by WIN 55,212-2 (right). Arrows indicate cortical stimulus application. Dashed lines indicate threshold for excitatory responses. B. Bar graphs showing the mean effect of AM251 (2 mg/kg, i.v.) and WIN 55,212-2 (125 μg/kg, i.v.) on cortically evoked responses in SM-SNr neurons (amplitude of early (EE; n = 4) and late (LE; n = 4) excitations and duration of inhibition (INH; n = 4)) in SM circuits. Each bar represents the mean ± S.E.M. of n rats. Each dot represents the value from one neuron before and after drug administration.

Dopaminergic denervation impairs cortical motor and associative/limbic information processing through the basal ganglia and its modulation by the CB₁ receptor
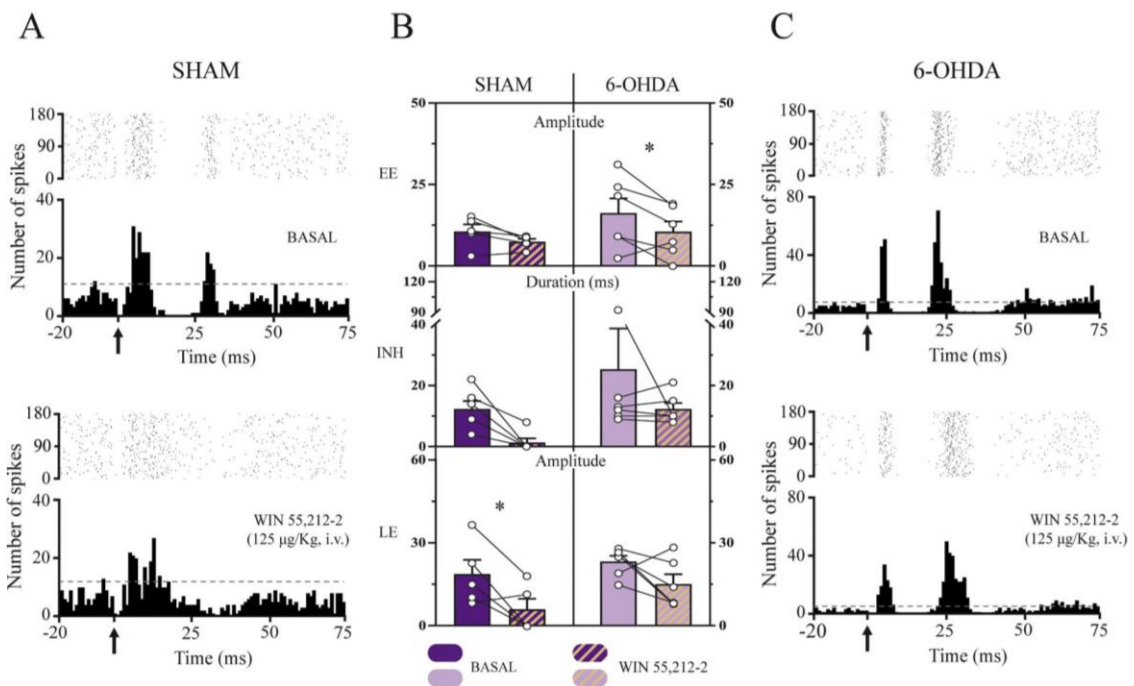
8. APPENDIX – Study II

Fig. 4. Effect of systemic administration of WIN 55,212-2 (125 μg/kg, i.v.) on cortico-nigral information transmission in medial prefrontal (mPF) BG circuits in sham and 6-OHDA-lesioned animals.

A. Top, raster plot and peristimulus time histogram showing a representative example of a triphasic response evoked in an mPF-SNr neuron from a sham rat through the stimulation of the anterior cingulate cortex (ACC) under basal conditions. Bottom, WIN 55,212-2 injection was able to reduce transmission through the three pathways. Arrows indicate cortical stimulus applic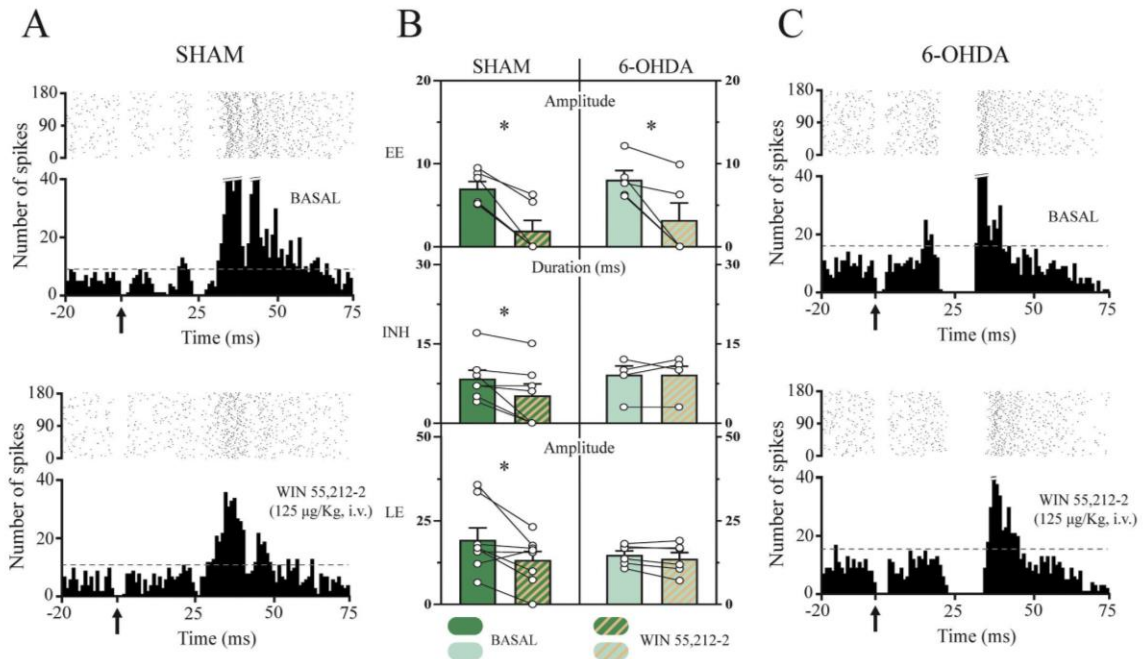ation. Dashed lines indicate the threshold for excitatory responses. C. Top, raster plot and peristimulus time histogram showing a representative example of a triphasic response evoked in an mPF-SNr neuron from a 6-OHDA-lesioned animal through the stimulation of the ACC under basal conditions. Bottom, after WIN 55,212-2 injection, only reduced transmission of the early excitation in 6-OHDA-denervated animals was observed. Arrows indicate cortical stimulus application. Dashed lines indicate the threshold for excitatory responses. B. Bar graphs showing the mean effect of WIN 55,212-2 (125 μg/kg, i.v.) on cortically evoked responses in mPF-SNr neurons (amplitude of early (EE; sham: n = 6; 6-OHDA: n = 8) and late (LE; sham: n = 8; 6-OHDA: n = 6) excitations and the duration of inhibition (INH; sham: n = 7; 6-OHDA: n = 5)) in mPF circuits. Each bar represents the mean ± the S.E.M. of n rats. Each dot represents the value from one neuron before and after drug administration. *$P < 0.05$ before vs. after WIN, repeated-measures two-way ANOVA (Drug x Lesion).

less late excitations). These data, together with the important modifications of the spontaneous activity of mPF-SNr neurons, indicate abnormal functionality inside associative and limbic territories of the BG. In fact, behavioural studies performed in similar PD models show cognitive dysfunctions, such as apathy (Anderson et al., 2020; Carvalho et al., 2013; Furlanetti et al., 2015) or depression-like behaviours (Winter et al., 2007; Zhang et al., 2011), that are linked to the BG and are present in PD patients (Tremblay et al., 2015). Thus, the alterations observed in this study in the mPF circuits after DA denervation might help understand the neurobiological components behind these motivational symptoms in PD patients.

Overall, our results indicate that DA depletion along with probable compensatory changes induced by DA denervation itself, lead to deficits in cortical information selection through the segregated anatomo-functional cortico-BG loops. In the mPF circuits, the information through the direct pathway is enhanced, while in the SM circuits, the enhancement takes place in the hyperdirect pathway. Although, in principle, these data would not be in line with studies showing striatal medium spiny neurons (MSN) hyperactivation (both those expressing D1 (dMSN) and those expressing D2 receptors (iMSN)) in animal models and PD patients (Fieblinger et al., 2014; Singh et al., 2016; Suarez et al., 2016), other factors could influence the output of the circuits seen in SNr neurons after cortical stimulation. Some studies point out alterations during hypodopaminergic states such as dendritic atrophy, spine pruning and reduced corticostriatal glutamatergic synapses in dMSN, iMSN or both MSN's that could be reducing cortical input on these neurons

(Fieblinger et al., 2014; Gagnon et al., 2017; Graves and Surmeier, 2019; Suarez et al., 2016). Moreover, functional studies show a decreased corticostriatal connectivity in dMSN's, and increased in iMSN's in a 6-OHDA model similar to ours, in line with the classical model of BG function in hypodopaminergic states (Escande et al., 2016; Mallet et al., 2006). Overall, this evidence would support the reduced percentage of neurons displaying direct pathway activation (inhibitory component of the cortically-evoked response in SNr neurons) that we observe in the SM circuits of 6-OHDA animals. However, the reduced transmission through the indirect pathway of the SM circuits in lesioned group is contradictory. Being the indirect pathway a polysynaptic pathway, interpretation of the effects of DA denervation grows in complexity, especially if we consider the impact of the DA loss in pallidal and subthalamic function (Chan et al., 2011; Magill et al., 2001; Miguelez et al., 2012). Moreover, one characteristic of the BG nuclei is the high synaptic convergence in its output nuclei. Mallet et al. (2006) showed that DA denervation increases the time window in which iMSN's respond to stimulation of the MC. This variability in the response time of iMSN's after cortical stimulation could make the summation of multiple inputs on neurons in downstream nuclei difficult, failing to engage neuronal activity efficiently, and provoke full transmission through the indirect pathway, reaching the SNr.

Regarding the mPF circuits, we observed only a decrease in the number of neurons showing a late excitation, related with decreased indirect pathway activation. Most of the studies discussed above address how BG physiology is altered in hypodopaminergic states with special

9

8. APPENDIX – Study II

Dopaminergic denervation impairs cortical motor and associative/limbic information processing through the basal ganglia and its modulation by the CB₁ receptor

emphasis on the SM territories, but few have addressed this same topic on the mPF territories of the BG. Some studies manifest substantial differences between SM and mPF territories. For instance, sensory- and limbic-related cortical areas preferentially innervate dMSN's, whilst motor-related areas innervate iMSN's (Wall et al., 2013). Moreover, functional studies have shown different forms of plasticity taking place under different conditions in SM and mPF territories of the striatum, besides differences in components from key striatal neurotransmitter systems (Arbuthnott and Wickens, 2007; Atwood et al., 2014; Braz et al., 2017; Herkenham et al., 1991). Together, this evidence calls for caution in extrapolating traits related with components from the SM circuits, into components from the mPF circuits. These differences could affect the way mPF circuits behaves, not only under physiological conditions, but also in pathological states, therefore stepping aside from what is expected from BG physiology under DA denervation.

The abnormal selectivity of information affecting motor, cognitive and motivational domains could be the neurophysiological impetus to the development of the motor and non-motor symptoms observed in PD, and it can be due to reduced anatomical and functional connectivity in cortico-BG networks, as demonstrated in PD patients and more evident for SM connections (Sharman et al., 2013).

4.2. Dysfunctional CB1-mediated modulation of cortico-BG information transmission

CB1-mediated modulation of cortical information transmission through the SM or mPF BG circuits is changed in 6-OHDA-lesioned animals. In agreement with our previous work in control animals (Antonazzo et al., 2019), administration of WIN in sham rats caused a reduction in the information transmission through the indirect pathway, without affecting the hyperdirect pathway in the SM circuits. Regarding the mPF circuits, administration of WIN in sham rats decreased information transmission through the three pathways. However, no statistically significant reduction of the transmission through the direct pathway was observed in this study in the SM circuits, in contrast to our previous work in control animals. This could be due to the extreme value present in the 6-OHDA dataset, which could likely be introducing noise, therefore confusing the statistical test. In support of this, data obtained here and in our previous work (Antonazzo et al., 2019) before and after WIN administration is similar, both mean and dispersion values (Before WIN: 12.3 ± 2.6 vs. 15.0 ± 1.5; After WIN: 3.5 ± 2.3 vs. 4.4 ± 2.1).

After dopaminergic denervation, the hyperdirect pathway in the SM circuits became sensitive to WIN administration. Previous work in our lab shows that administration of WIN in 6-OHDA-lesioned rats reduces
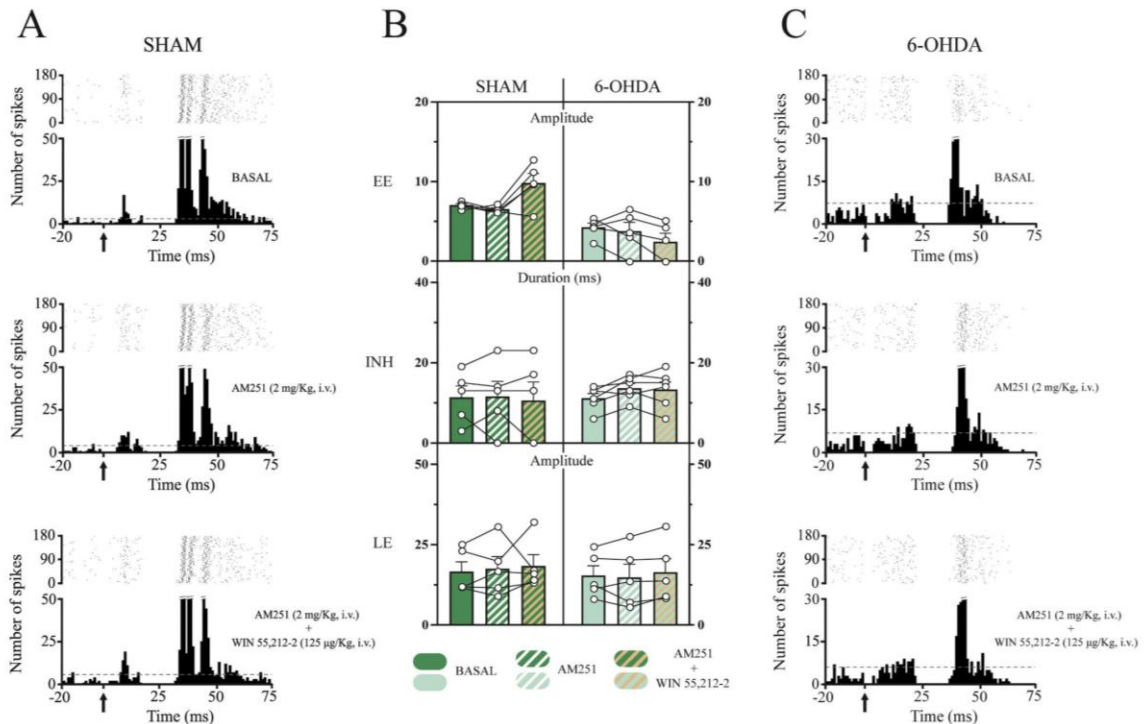

Fig. 5. Blockade of WIN 55,212-2-induced effects on cortico-nigral information transmission in medial prefrontal (mPF) BG circuits in sham and 6-OHDA-lesioned animals by the previous administration of the CB1 selective antagonist AM251 (2 mg/kg, i.v.).
A. Top, raster plot and peristimulus time histogram showing a representative example of a triphasic response evoked in a mPF-SNr neuron by stimulation of the anterior cingulate cortex (ACC) in a sham rat under basal conditions. AM251 administration did not modify the characteristics of the three components of the cortically evoked response (middle) but blocked the effects induced by WIN 55,212-2 (bottom). Arrows indicate cortical stimulus application. Dashed lines indicate threshold for excitatory responses. C. Top, raster plot and peristimulus time histogram showing a representative example of a triphasic response evoked in a mPF-SNr neuron by stimulation of the ACC in a 6-OHDA rat under basal conditions. AM251 administration did not modify the characteristics of the three components of the cortically evoked response (middle) but blocked the effects induced by WIN 55,212-2 (bottom). Arrows indicate cortical stimulus application. Dashed lines indicate threshold for excitatory responses. B. Bar graphs showing the mean effect of AM251 (2 mg/kg, i.v.) and WIN 55,212-2 (125 μg/kg, i.v.) on cortically evoked responses in mPF-SNr neurons (amplitude of early (EE; sham: n = 5; 6-OHDA: n = 5) and late (LE; sham: n = 5; 6-OHDA: n = 5) excitations and duration of inhibition (INH; sham: n = 5; 6-OHDA: n = 6) in mPF circuits. Each bar represents the mean ± S.E.M. of n rats. Each dot represents the value from one neuron before and after drug administration.

10

Dopaminergic denervation impairs cortical motor and associative/limbic information processing through the basal ganglia and its modulation by the CB₁ receptor

8. APPENDIX – Study II

Fig. 6. CB1 receptor immunoreactivity in the sensorimotor (SM) and medial prefrontal (mPF) basal ganglia territories in the cortex, striatum, globus pallidus and substantia nigra pars reticulate from sham and 6-OHDA-lesioned rats.

A. Representative sham rat (top) and 6-OHDA-lesioned (bottom) rats brain slices showing CB1 receptor immunoreactivity in the studied areas. SM and mPF analysed territories are marked in purple and green, respectively. B. Bar graphs showing the mean CB1 receptor optical density (OD) in the SM and mPF territories of the studied brain areas in sham and 6-OHDA-lesioned animals. Note that there is significantly less CB1 receptor immunoreactivity in the mPF territories of the striatum in both sham and 6-OHDA-lesioned animals compared to SM territories. Scale bars are set to 1 mm. Each bar represents the mean ± the S.E.M. of n rats. Each dot represents the averaged value from one rat. $*P < 0.05$ SM vs. mPF, repeated-measures two-way ANOVA (Territory × Lesion). (For interpretation of the references to colour in this figure legend, the reader is referred to the web version of this article.)
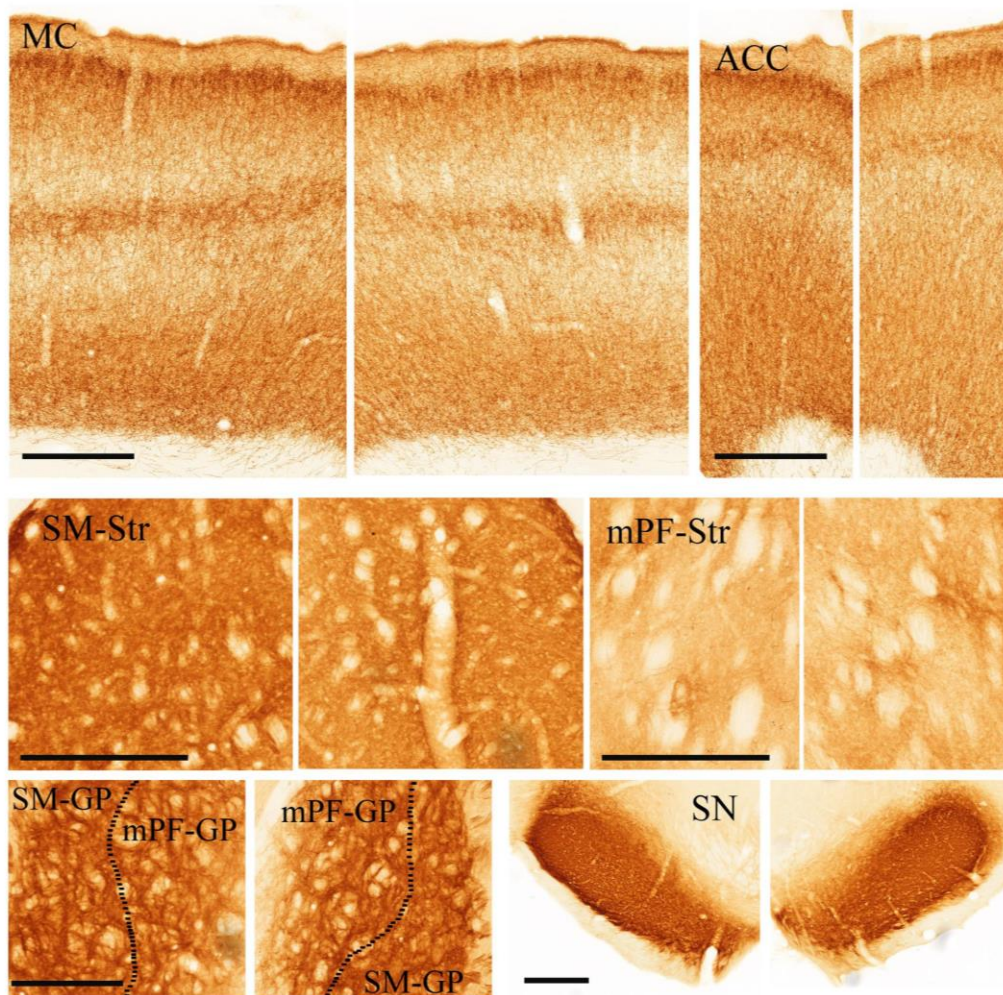
8. APPENDIX – Study II

Dopaminergic denervation impairs cortical motor and associative/limbic information processing through the basal ganglia and its modulation by the CB₁ receptor

Fig. 7. Regional distribution of CB1 receptor expression in the basal ganglia nuclei from 6-OHDA-lesioned rats.
Brain microphotographs of coronal sections showing the CB1 receptor immunohistochemistry. The first row shows the distribution of the CB1 receptor in the motor cortex (MC) and anterior cingulate cortex (ACC). Second row shows the sensorimotor territory (dorsolateral striatum; SM-Str) and the medial prefrontal territory (dorsomedial striatum; mPF-Str). Third row shows the globus pallidus divided in its sensorimotor (SM-GP) and medial prefrontal territory (mPF-GP), and the susbstantia nigra (SN). Studied areas are shown in pairs, being the pictures on the left from the lesioned hemisphere. Scale bars are set to 500 μm.

firing rate of subthalamic nucleus neurons (Morera-Herreras et al., 2011), which could explain the reduced transmission through the hyperdirect pathway after WIN administration in these circuits. In the mPF circuits, this pathway remains sensitive to WIN in the 6-OHDA group. However, trans-striatal pathways in both circuits became insensitive to WIN after DA denervation.

A possible explanation for the observed findings could be the alteration of CB1 receptor expression induced by DA depletion. For this reason, we decided to perform immunohistochemical assays to determine the precise territory-specific potential changes in each nucleus conforming the BG circuits. In sham animals, sub-territorial immuno-labelling analysis revealed predominant CB1 expression in the SM areas of the striatum compared to associative/limbic striatal regions. These data is consistent with previous work reported by other authors (A. G. Hohmann and Herkenham, 1999; Mailleux and Vanderhaeghen, 1992; Marsicano and Lutz, 1999; Matsuda et al., 1993; Van Waes et al., 2012;

Zimmer et al., 1999), overall suggesting that CB1 receptors located in these anatomical regions of the BG could predominantly regulate SM information processing, or at least to a greater extent than mPF receptors. In the SM areas of the striatum, and given the preferential location of the CB1 receptor on terminals (Irving et al., 2000), extensive location of the CB1 receptor in SM territories likely comes from MSN's axon collaterals. Therefore, contributions from striatal afferents to CB1 immunostaining in SM territories is probably minimal. Although the CB1 receptor is expressed in cortical areas projecting to SM territories of the striatum, this expression is modest, and located principally in non-pyramidal neurons (Heng et al., 2011; Mailleux and Vanderhaeghen, 1992). Moreover, midbrain dopaminergic neurons and thalamic neurons show negligible levels of CB1 expression (Herkenham et al., 1991; Mailleux and Vanderhaeghen, 1992). This is in line with the sparse CB1 presence in mPF territories of the striatum, where the expression of this receptor is also minimal (Hohmann and Herkenham, 2000; Van Waes

Dopaminergic denervation impairs cortical motor and associative/limbic information processing through the basal ganglia and its modulation by the CB₁ receptor

8. APPENDIX – Study II

et al., 2012). In this case, sparse CB1 immunostaining would likely come from afferences like mPF cortical areas, and to some extent hippocampus and amygdala where CB1 receptor is highly expressed (Herkenham et al., 1991; Mailleux and Vanderhaeghen, 1992; Voorn et al., 2004). Overall, contribution to CB1 immunostaining from striatal interneurons is probably low since they represent <3% of the total number of striatal neurons, regardless that some of them express CB1 receptor (Hohmann and Herkenham, 2000; Martín et al., 2008; Oorschot et al., 2002).

Additionally, we did not find any topographical difference in CB1 receptor expression under conditions of low DA, although the higher CB1 expression in the striatal SM area was preserved compared to the mPF. In agreement with our observations, using the unilateral-MFB 6-OHDA rat model, no changes in CB1 receptor binding in the BG have been described, measured by [³H]-WIN-55,212-2 autoradiography 7–10 weeks after the lesion (Romero et al., 2000), by immunohisto-chemistry at different post-lesion time points (Walsh et al., 2010), or by mRNA in situ hybridization histochemistry (Zeng et al., 1999). More recently, similar results have been reported in MPTP parkinsonian monkeys (Rojo-Bustamante et al., 2018). Data coming from *post-mortem* brain tissue of PD patients are inconclusive, showing increased (Lastres-Becker et al., 2001) or no changes (Farkas et al., 2012) in CB1 receptor binding or decreased receptor expression measured through mRNA (Hurley et al., 2003).

Taking into account these results, we can conclude that, in our experimental conditions, CB1 receptor expression in BG nuclei is not affected by DA denervation, indicating that the loss of cannabinoid modulation of cortico-BG circuits could be due to a mechanism related to an alteration of CB1 receptor functionality. In this aspect, current evidence also shows some discrepancies, describing increased activation of GTP-binding proteins in PD patients treated with L-DOPA and MPTP marmosets (Lastres-Becker et al., 2001) as well as no changes in 6-OHDA-lesioned rats (Romero et al., 2000). In our experimental model, and according to the observed results, we hypothesize that after 4–5 weeks of DA depletion induced by unilateral-MFB 6-OHDA injection, CB1 receptor hyposensitivity occurs within the cortico-BG circuits, which could explain the lack of the modulation of these networks.

5. Conclusions

In summary, the present study allows us to better understand the non-motor functions of the BG and highlights not only dysfunctional motor information processing though the cortico-BG circuits but also abnormal information transfer through the associative/limbic domains after DA loss. This unusual mPF BG circuitry functionality could be related to the cognitive deficits and behavioural disorders that occur in PD. Therefore, the targeting of limbic/associative BG circuits and the restoration of CB1 functionality could constitute a promising target for the treatment of these non-motor symptoms manifested by PD patients.

CRediT authorship contribution statement

Mario Antonazzo: Data curation, Formal analysis, Investigation, Visualization, Writing - original draft, Writing - review & editing. **Sonia María Gomez-Urquijo:** Investigation, Visualization, Writing - original draft, Writing - review & editing. **Luisa Ugedo:** Funding acquisition, Project administration, Supervision, Writing - original draft, Writing -

review & editing. **Teresa Morera-Herreras:** Conceptualization, Funding acquisition, Project administration, Supervision, Writing - original draft, Writing - review & editing.

Declaration of Competing Interest

None.

Appendix A. Supplementary data

Supplementary data to this article can be found online at https://doi.org/10.1016/j.nbd.2020.105214.

References

Alexander, G.E., DeLong, M.R., Strick, P.L., 1986. Parallel organization of functionally segregated circuits linking basal ganglia and cortex. Annu. Rev. Neurosci. 9 (1), 357–381. https://doi.org/10.1146/annurev.ne.09.030186.002041.

Anderson, C., Sheppard, D., Dorval, A.D., 2020. Parkinsonism and subthalamic deep brain stimulation dysregulate behavioral motivation in a rodent model. Brain Res. 1736, 146776. https://doi.org/10.1016/j.brainres.2020.146776.

Antonazzo, M., Gutierrez-Ceballos, A., Bustinza, I., Ugedo, L., Morera-Herreras, T., 2019. Cannabinoids differentially modulate cortical information transmission through the sensorimotor or medial prefrontal basal ganglia circuits. Br. J. Pharmacol. 176 (8), 1156–1169. https://doi.org/10.1111/bph.14613.

Arbuthnott, G.W., Wickens, J., 2007. Space, time and dopamine. Trends Neurosci. 30 (2), 62–69. https://doi.org/10.1016/j.tins.2006.12.003.

Aristieta, A., Ruiz-Ortega, J.A., Miguelez, C., Morera-Herreras, T., Ugedo, L., 2016. Chronic L-DOPA administration increases the firing rate but does not reverse enhanced slow frequency oscillatory activity and synchronization in substantia nigra pars reticulata neurons from 6-hydroxydopamine-lesioned rats. Neurobiol. Dis. 89, 88–100. https://doi.org/10.1016/J.NBD.2016.02.003.

Aristieta, A., Ruiz-Ortega, J.A., Morera-Herreras, T., Miguelez, C., Ugedo, L., 2019. Acute L-DOPA administration reverses changes in firing pattern and low frequency oscillatory activity in the entopeduncular nucleus from long term L-DOPA treated 6-OHDA-lesioned rats. Exp. Neurol. 322, 113036. https://doi.org/10.1016/j.expneurol.2019.113036.

Atwood, B.K., Kupferschmidt, D.A., Lovinger, D.M., 2014. Opioids induce dissociable forms of long-term depression of excitatory inputs to the dorsal striatum. Nat. Neurosci. 17 (4), 540–548. https://doi.org/10.1038/nn.3652.

Benabid, A.L., Pollak, P., Gross, C., Hoffmann, D., Benazzouz, A., Gao, D.M., Laurent, A., Gentil, M., Perret, J., 1994. Acute and long-term effects of subthalamic nucleus stimulation of Parkinson's disease. Stereotact. Funct. Neurosurg. 62 (1–4), 76–84. https://doi.org/10.1159/000098600.

Bergman, H., Wichmann, T., Karmon, B., DeLong, M.R., 1994. The primate subthalamic nucleus. II. Neuronal activity in the MPTP model of parkinsonism. J. Neurophysiol. 72 (2), 507–520. https://doi.org/10.1152/jn.1994.72.2.507.

Beyeler, A., Kadiri, N., Navailles, S., Boujema, M.B., Gonon, F., Moine, C.L., Gross, C., De Deurwaerdère, P., 2010. Stimulation of serotonin2C receptors elicits abnormal oral movements by acting on pathways other than the sensorimotor one in the rat basal ganglia. Neuroscience 169 (1), 158–170. https://doi.org/10.1016/j.neuroscience.2010.04.061.

Braz, B.Y., Belforte, J.E., Murer, M.G., Galiñanes, G.L., 2017. Properties of the corticostriatal long term depression induced by medial prefrontal cortex high frequency stimulation in vivo. Neuropharmacology 121, 278–286. https://doi.org/10.1016/j.neuropharm.2017.05.001.

Carvalho, M.M., Campos, F.L., Coimbra, B., Pêgo, J.M., Rodrigues, C., Lima, R., Rodrigues, A.J., Sousa, N., Salgado, A.J., 2013. Behavioral characterization of the 6-hydroxidopamine model of Parkinson's disease and pharmacological rescuing of non-motor deficits. Mol. Neurodegener. 8 (1), 14. https://doi.org/10.1186/1750-1326-8-14.

Chan, C.S., Glajch, K.E., Gertler, T.S., Guzman, J.N., Mercer, J.N., Lewis, A.S., Goldberg, A.B., Tkatch, T., Shigemoto, R., Fleming, S.M., Chetkovich, D.M., Osten, P., Kita, H., Surmeier, D.J., 2011. HCN channelopathy in external globus pallidus neurons in models of Parkinson's disease. Nat. Neurosci. 14 (1), 85–92. https://doi.org/10.1038/nn.2692.

Ciliax, B.J., Heilman, C., Demchyshyn, L.L., Pristupa, Z.B., Ince, E., Hersch, S.M., Niznik, H.B., Levey, A.I., 1995. The dopamine transporter: immunochemical characterization and localization in brain. J. Neurosci. 15 (3), 1714–1723. https://doi.org/10.1523/JNEUROSCI.15-03-01714.1995.

8. APPENDIX – Study II

Dopaminergic denervation impairs cortical motor and
associative/limbic information processing through the basal
ganglia and its modulation by the CB₁ receptor

Cragg, S.J., Rice, M.E., Greenfield, S.A., 1997. Heterogeneity of electrically evoked dopamine release and reuptake in substantia Nigra, ventral tegmental area, and striatum. J. Neurophysiol. 77 (2), 863–873. https://doi.org/10.1152/jn.1997.77.2.863.

Degos, B., Deniau, J.-M., Thierry, A.-M., Glowinski, J., Pezard, L., Maurice, N., 2005. Neuroleptic-induced catalepsy: electrophysiological mechanisms of functional recovery induced by high-frequency stimulation of the subthalamic nucleus. J. Neurosci. 25 (33), 7687–7696. https://doi.org/10.1523/JNEUROSCI.1056-05.2005.

Escande, M.V., Taravini, I.R.E., Zold, C.L., Belforte, J.E., Murer, M.G., 2016. Loss of homeostasis in the direct pathway in a mouse model of asymptomatic Parkinson's disease. J. Neurosci. 36 (21), 5686–5698. https://doi.org/10.1523/JNEUROSCI.0492-15.2016.

Farkas, S., Nagy, K., Jia, Z., Harkany, T., Palkovits, M., Donohou, S.R., Pike, V.W., Halldin, C., Máthé, D., Csiba, L., Gulyás, B., 2012. The decrease of dopamine D 2/D 3 receptor densities in the putamen and nucleus caudatus goes parallel with maintained levels of CB 1 cannabinoid receptors in Parkinson's disease: a preliminary autoradiographic study with the selective dopamine D 2/D 3 ant. Brain Res. Bull. 87 (6), 504–510. https://doi.org/10.1016/j.brainresbull.2012.02.012.

Ferré, S., Goldberg, S.R., Lluis, C., Franco, R., 2009. Looking for the role of cannabinoid receptor heteromers in striatal function. Neuropharmacology 56 (Suppl. 1), 226–234. https://doi.org/10.1016/j.neuropharm.2008.06.076.

Fieblinger, T., Graves, S.M., Sebel, L.E., Alcacer, C., Plotkin, J.L., Gertler, T.S., Chan, C.S., Heiman, M., Greengard, P., Cenci, M.A., Surmeier, D.J., 2014. Cell type-specific plasticity of striatal projection neurons in parkinsonism and L-DOPA-induced dyskinesia. Nat. Commun. 5 (1), 5316. https://doi.org/10.1038/ncomms6316.

Furlanetti, L.L., Coenen, V.A., Aranda, I.A., Döbrössy, M.D., 2015. Chronic deep brain stimulation of the medial forebrain bundle reverses depressive-like behavior in a hemiparkinsonian rodent model. Exp. Brain Res. 233 (11), 3073–3085. https://doi.org/10.1007/s00221-015-4375-9.

Gagnon, D., Petryszyn, S., Sanchez, M.G., Bories, C., Beaulieu, J.M., De Koninck, Y., Parent, A., Parent, M., 2017. Striatal neurons expressing D1 and D2 receptors are morphologically distinct and differently affected by dopamine denervation in mice. Sci. Rep. 7 (1), 41432. https://doi.org/10.1038/srep41432.

Galvan, A., Wichmann, T., 2008. Pathophysiology of parkinsonism. Clin. Neurophysiol. 119 (7), 1459–1474. https://doi.org/10.1016/j.clinph.2008.03.017.

García, C., Palomo-Garo, C., Gómez-Gálvez, Y., Fernández-Ruiz, J., 2016. Cannabinoid–dopamine interactions in the physiology and physiopathology of the basal ganglia. Br. J. Pharmacol. 173 (13), 2069–2079. https://doi.org/10.1111/bph.13215.

Giuffrida, A., Parsons, L.H., Kerr, T.M., Rodríguez de Fonseca, F., Navarro, M., Piomelli, D., 1999. Dopamine activation of endogenous cannabinoid signaling in dorsal striatum. Nat. Neurosci. 2 (4), 358–363. https://doi.org/10.1038/7268.

Grant, I., Gonzalez, R., Carey, C.L., Natarajan, L., Wolfson, T., 2003. Non-acute (residual) neurocognitive effects of cannabis use: a meta-analytic study. J. Int. Neuropsychol. Soc. 9 (5), 679–689. https://doi.org/10.1017/S1355617703950016.

Graves, S.M., Surmeier, D.J., 2019. Delayed spine pruning of direct pathway spiny projection neurons in a mouse model of Parkinson's disease. Front. Cell. Neurosci. 13, 32. https://doi.org/10.3389/fncel.2019.00032.

Haber, S.N., 2003. The primate basal ganglia: parallel and integrative networks. J. Chem. Neuroanat. 26 (4), 317–330. https://doi.org/10.1016/j.jchemneu.2003.10.003.

Hassani, O.K., Mouroux, M., Féger, J., 1996. Increased subthalamic neuronal activity after nigral dopaminergic lesion independent of disinhibition via the globus pallidus. Neuroscience 72 (1), 105–115. https://doi.org/10.1016/0306-4522(95)00535-8.

Heckman, P.R.A., Schweimer, J.V., Sharp, T., Prickaerts, J., Blokland, A., 2018. Phosphodiesterase 4 inhibition affects both the direct and indirect pathway: an electrophysiological study examining the tri-phasic response in the substantia nigra pars reticulata. Brain Struct. Funct. 223 (2), 739–748. https://doi.org/10.1007/s00429-017-1518-8.

Heilbronner, S.R., Rodriguez-Romaguera, J., Quirk, G.J., Groenewegen, H.J., Haber, S. N., 2016. Circuit-based corticostriatal homologies between rat and primate. Biol. Psychiatry 80 (7), 509–521. https://doi.org/10.1016/j.biopsych.2016.05.012.

Heng, L., Beverley, J.A., Steiner, H., Tseng, K.Y., 2011. Differential developmental trajectories for CB1 cannabinoid receptor expression in limbic/associative and sensorimotor cortical areas. Synapse 65 (4), 278–286. https://doi.org/10.1002/syn.20844.

Herkenham, M., Lynn, A.B., de Costa, B.R., Richfield, E.K., 1991. Neuronal localization of cannabinoid receptors in the basal ganglia of the rat. Brain Res. 547 (2), 267–274. https://doi.org/10.1016/0006-8993(91)90970-7.

Hernando, S., Requejo, C., Herran, E., Ruiz-Ortega, J.A., Morera-Herreras, T., Lafuente, J. V., Gainza, E., Pedraz, J.L., Igartua, M., Hernandez, R.M., 2019. Beneficial effects of n-3 polyunsaturated fatty acids administration in a partial lesion model of Parkinson's disease: the role of glia and Nrf2 regulation. Neurobiol. Dis. 121, 252–262. https://doi.org/10.1016/j.nbd.2018.10.001.

Hohmann, A.G., Herkenham, M., 1999. Localization of central cannabinoid CB1 receptor messenger RNA in neuronal subpopulations of rat dorsal root ganglia: a double-label in situ hybridization study. Neuroscience 90 (3), 923–931. https://doi.org/10.1016/S0306-4522(98)00524-7.

Hohmann, Andrea G., Herkenham, M., 2000. Localization of cannabinoid CB1 receptor mRNA in neuronal subpopulations of rat striatum: a double-label in situ hybridization study. Synapse 37 (1), 71–80. https://doi.org/10.1002/(SICI)1098-2396(200007)37:1<71::AID-SYN8>3.0.CO;2-K.

Hurley, M.J., Mash, D.C., Jenner, P., 2003. Expression of cannabinoid CB1 receptor mRNA in basal ganglia of normal and parkinsonian human brain. J. Neural Transm. (Vienna) 110 (11), 1279–1288. https://doi.org/10.1007/s00702-003-0033-7.

Irving, A.J., Coutts, A.A., Harvey, J., Rae, M.G., Mackie, K., Bewick, G.S., Pertwee, R.G., 2000. Functional expression of cell surface cannabinoid CB(1) receptors on presynaptic inhibitory terminals in cultured rat hippocampal neurons. Neuroscience 98 (2), 253–262. https://doi.org/10.1016/s0306-4522(00)00120-2.

Köfalvi, A., Rodrigues, R.J., Ledent, C., Mackie, K., Vizi, E.S., Cunha, R.A., Sperlágh, B., 2005. Involvement of cannabinoid receptors in the regulation of neurotransmitter release in the rodent striatum: a combined immunochemical and pharmacological analysis. J. Neurosci. 25 (11), 2874–2884. https://doi.org/10.1523/JNEUROSCI.4232-04.2005.

Kolomiets, B.P., Deniau, J.M., Glowinski, J., Thierry, A.M., 2003. Basal ganglia and processing of cortical information: functional interactions between trans-striatal and trans-subthalamic circuits in the substantia nigra pars reticulata. Neuroscience 117 (4), 931–938.

Lastres-Becker, I., Cebeira, M., De Ceballos, M.L., Zeng, B.Y., Jenner, P., Ramos, J.A., Fernández-Ruiz, J.J., 2001. Increased cannabinoid CB1 receptor binding and activation of GTP-binding proteins in the basal ganglia of patients with Parkinson's syndrome and of MPTP-treated marmosets. Eur. J. Neurosci. 14 (11), 1827–1832. https://doi.org/10.1046/j.0953-816X.2001.01812.x.

Lévesque, D., Martres, M.P., Diaz, J., Griffon, N., Lammers, C.H., Sokoloff, P., Schwartz, J.C., 1995. A paradoxical regulation of the dopamine D3 receptor expression suggests the involvement of an anterograde factor from dopamine neurons. Proc. Natl. Acad. Sci. 92 (5), 1719–1723. https://doi.org/10.1073/pnas.92.5.1719.

Linkert, M., Rueden, C.T., Allan, C., Burel, J.-M., Moore, W., Patterson, A., Loranger, B., Moore, J., Neves, C., Macdonald, D., Tarkowska, A., Sticco, C., Hill, E., Rossner, M., Eliceiri, K.W., Swedlow, J.R., 2010. Metadata matters: access to image data in the real world. J. Cell Biol. 189 (5), 777–782. https://doi.org/10.1083/jcb.201004104.

Magill, P.J., Bolam, J.P., Bevan, M.D., 2001. Dopamine regulates the impact of the cerebral cortex on the subthalamic nucleus–globus pallidus network. Neuroscience 106 (2), 313–330. https://doi.org/10.1016/S0306-4522(01)00281-0.

Mailleux, P., Vanderhaeghen, J.J., 1992. Localization of cannabinoid receptor in the human developing and adult basal ganglia. Higher levels in the striatonigral neurons. Neurosci. Lett. 148 (1–2), 173–176. https://doi.org/10.1016/0304-3940(92)90832-R.

Mallet, N., Ballion, B., Moine, C.L., Gonon, F., 2006. Cortical inputs and GABA interneurons imbalance projection neurons in the striatum of parkinsonian rats. J. Neurosci. 26 (14), 3875–3884. https://doi.org/10.1523/JNEUROSCI.4439-05.2006.

Marsicano, G., Lutz, B., 1999. Expression of the cannabinoid receptor CB1 in distinct neuronal subpopulations in the adult mouse forebrain. Eur. J. Neurosci. 11 (12), 4213–4225. https://doi.org/10.1046/j.1460-9568.1999.00847.x.

Martín, A.B., Fernandez-Espejo, E., Ferrer, B., Gorriti, M.A., Bilbao, A., Navarro, M., Rodriguez de Fonseca, F., Moratalla, R., 2008. Expression and function of CB 1 receptor in the rat striatum: localization and effects on D 1 and D 2 dopamine receptor-mediated motor behaviors. Neuropsychopharmacology 33 (7), 1667–1679. https://doi.org/10.1038/sj.npp.1301558.

Matsuda, L.A., Bonner, T.I., Lolait, S.J., 1993. Localization of cannabinoid receptor mRNA in rat brain. J. Comp. Neurol. 327 (4), 535–550. https://doi.org/10.1002/cne.903270406.

Maurice, N., Deniau, J.-M., Glowinski, J., Thierry, A.-M., 1999. Relationships between the prefrontal cortex and the basal ganglia in the rat: physiology of the Cortico-Nigral circuits. J. Neurosci. 19 (11), 4674–4681. https://doi.org/10.1523/JNEUROSCI.19-11-04674.1999.

Maurice, N., Deltheil, T., Melon, C., Degos, B., Mourre, C., Amalric, M., Goff, L.K.L., 2015. Bee venom alleviates motor deficits and modulates the transfer of cortical information through the basal ganglia in rat models of Parkinson's disease. PLoS One 10 (11). https://doi.org/10.1371/journal.pone.0142838.

McGeorge, A.J., Faull, R.L., 1989. The organization of the projection from the cerebral cortex to the striatum in the rat. Neuroscience 29 (3), 503–537.

Meissner, W., Ravenscroft, P., Reese, R., Harnack, D., Morgenstern, R., Kupsch, A., Klitgaard, H., Bioulac, B., Gross, C.E., Bezard, E., Boraud, T., 2006. Increased slow oscillatory activity in substantia nigra pars reticulata triggers abnormal involuntary movements in the 6-OHDA-lesioned rat in the presence of excessive extracellular striatal dopamine. Neurobiol. Dis. 22 (3), 586–598. https://doi.org/10.1016/j.nbd.2006.01.009.

Middleton, F.A., Strick, P.L., 2000. Basal ganglia output and cognition: evidence from anatomical, behavioral, and clinical studies. Brain Cogn. 42 (2), 183–200. https://doi.org/10.1006/brcg.1999.1099.

Miguelez, C., Morin, S., Martinez, A., Goillandeau, M., Bezard, E., Bioulac, B., Baufreton, J., 2012. Altered pallido-pallidal synaptic transmission leads to aberrant firing of globus pallidus neurons in a rat model of Parkinson's disease. J. Physiol. 590 (22), 5861–5875. https://doi.org/10.1113/jphysiol.2012.241331.

Morera-Herreras, T., Ruiz-Ortega, J.A., Linazasoro, G., Ugedo, L., 2011. Nigrostriatal denervation changes the effect of cannabinoids on subthalamic neuronal activity in rats. Psychopharmacology 214 (2), 379–389. https://doi.org/10.1007/s00213-010-2043-0.

Morera-Herreras, T., Miguelez, C., Aristieta, A., Ruiz-Ortega, J.Á., Ugedo, L., 2012. Endocannabinoid modulation of dopaminergic motor circuits. Front. Pharmacol. 3, 110. https://doi.org/10.3389/fphar.2012.00110.

Murer, M.G., Riquelme, L.A., Tseng, K.Y., Pazo, J.H., 1997. Substantia nigra pars reticulata single unit activity in normal and 60HDA-lesioned rats: effects of intrastriatal apomorphine and subthalamic lesions. Synapse 27 (4), 278–293. https://doi.org/10.1002/(SICI)1098-2396(199712)27:4<278::AID-SYN2>3.0.CO;2-9.

Oorschot, D.E., Tunstall, M.J., Wickens, J.R., 2002. Local connectivity between striatal spiny projection neurons: a re-evaluation. In: Nicholson, L.F.B., Faull, R.L.M. (Eds.),

14

Dopaminergic denervation impairs cortical motor and associative/limbic information processing through the basal ganglia and its modulation by the CB₁ receptor

8. APPENDIX – Study II

The Basal Ganglia VII. Springer US. https://doi.org/10.1007/978-1-4615-0715-4_42 (pp. 421–434).

Parent, A., Hazrati, L.N., 1995. Functional anatomy of the basal ganglia. I. The cortico-basal ganglia-thalamo-cortical loop. Brain Res. Rev. 20 (1), 91–127. https://doi.org/10.1016/0165-0173(94)00007-C.

Patel, S., Rademacher, D.J., Hillard, C.J., 2003. Differential regulation of the endocannabinoids anandamide and 2-arachidonylglycerol within the limbic forebrain by dopamine receptor activity. J. Pharmacol. Exp. Ther. 306 (3), 880–888. https://doi.org/10.1124/jpet.103.054270.

Paxinos, G., Watson, C., 2006. The Rat Brain in Stereotaxic Coordinates, Vol. 2. Academic Press. https://books.google.com/books?id=0prYfdDbh58C&pgis=1.

Prashad, S., Filbey, F.M., 2017. Cognitive motor deficits in cannabis users. Curr. Opin. Behav. Sci. 13, 1–7. https://doi.org/10.1016/j.cobeha.2016.07.001.

Rajakumar, N., Rushlow, W., Naus, C.C.G., Elisevich, K., Flumerfelt, B.A., 1994. Neurochemical compartmentalization of the globus pallidus in the rat: an immunocytochemical study of calcium-binding proteins. J. Comp. Neurol. 346 (3), 337–348. https://doi.org/10.1002/cne.903460303.

Rice, M.E., Richards, C.D., Nedergaard, S., Hounsgaard, J., Nicholson, C., Greenfield, S. A., 1994. Direct monitoring of dopamine and 5-HT release in substantia nigra and ventral tegmental area in vitro. Exp. Brain Res. 100 (3), 395–406. https://doi.org/10.1007/BF02738400.

Rice, M.E., Cragg, S.J., Greenfield, S.A., 1997. Characteristics of electrically evoked somatodendritic dopamine release in substantia nigra and ventral tegmental area in vitro. J. Neurophysiol. 77 (2), 853–862. https://doi.org/10.1152/jn.1997.77.2.853.

Rojo-Bustamante, E., Abellanas, M.A., Clavero, P., Thiolat, M.L., Li, Q., Luquin, M.R., Bezard, E., Aymerich, M.S., 2018. The expression of cannabinoid type 1 receptor and 2-arachidonoyl glycerol synthesizing/degrading enzymes is altered in basal ganglia during the active phase of levodopa-induced dyskinesia. Neurobiol. Dis. 118, 64–75. https://doi.org/10.1016/j.nbd.2018.06.019.

Romero, J., Berrendero, F., Pérez-Rosado, A., Manzanares, J., Rojo, A., Fernández-Ruiz, J.J., de Yebenes, J.G., Ramos, J.A., 2000. Unilateral 6-hydroxydopamine lesions of nigrostriatal dopaminergic neurons increased CB1 receptor mRNA levels in the caudate-putamen. Life Sci. 66 (6), 485–494. https://doi.org/10.1016/S0024-3205(99)00618-9.

Romero, Julián, Lastres-Becker, I., De Miguel, R., Berrendero, F., Ramos, J.A., Fernández-Ruiz, J., 2002. The endogenous cannabinoid system and the basal ganglia: biochemical, pharmacological, and therapeutic aspects. Pharmacol. Ther. 95 (2), 137–152. https://doi.org/10.1016/S0163-7258(02)00253-X.

Sano, H., Nambu, A., 2019. The effects of zonisamide on L-DOPA–induced dyskinesia in Parkinson's disease model mice. Neurochem. Int. 124, 171–180. https://doi.org/10.1016/j.neuint.2019.01.011.

Schindelin, J., Arganda-Carreras, I., Frise, E., Kaynig, V., Longair, M., Pietzsch, T., Preibisch, S., Rueden, C., Saalfeld, S., Schmid, B., Tinevez, J.-Y., White, D.J., Hartenstein, V., Eliceiri, K., Tomancak, P., Cardona, A., 2012. Fiji: an open-source platform for biological-image analysis. Nat. Methods 9 (7), 676–682. https://doi.org/10.1038/nmeth.2019.

Schreiner, A.M., Dunn, M.E., 2012. Residual effects of cannabis use on neurocognitive performance after prolonged abstinence: a meta-analysis. Exp. Clin. Psychopharmacol. 20 (5), 420–429. https://doi.org/10.1037/a0029117.

Sharman, M., Valabregue, R., Perlbarg, V., Marrakchi-Kacem, L., Vidailhet, M., Benali, H., Brice, A., Lehéricy, S., 2013. Parkinson's disease patients show reduced cortical-subcortical sensorimotor connectivity. Mov. Disord. 28 (4), 447–454. https://doi.org/10.1002/mds.25255.

Singh, A., Mewes, K., Gross, R.E., DeLong, M.R., Obeso, J.A., Papa, S.M., 2016. Human striatal recordings reveal abnormal discharge of projection neurons in Parkinson's disease. Proc. Natl. Acad. Sci. U. S. A. 113 (34), 9629–9634. https://doi.org/10.1073/pnas.1606792113.

Steigerwald, F., Pötter, M., Herzog, J., Pinsker, M., Kopper, F., Mehdorn, H., Deuschl, G., Volkmann, J., 2008. Neuronal activity of the human subthalamic nucleus in the parkinsonian and nonparkinsonian state. J. Neurophysiol. 100 (5), 2515–2524. https://doi.org/10.1152/jn.90574.2008.

Suarez, L.M., Solis, O., Aguado, C., Lujan, R., Moratalla, R., 2016. L-DOPA oppositely regulates synaptic strength and spine morphology in D1 and D2 striatal projection neurons in dyskinesia. Cereb. Cortex 26 (11), 4253–4264. https://doi.org/10.1093/cercor/bhw263.

Tremblay, L., Worbe, Y., Thobois, S., Sgambato-Faure, V., Féger, J., 2015. Selective dysfunction of basal ganglia subterritories: from movement to behavioral disorders. Mov. Disord. 30 (9), 1155–1170. https://doi.org/10.1002/mds.26199.

Tseng, K.Y., Riquelme, L.A., Belforte, J.E., Pazo, J.H., Murer, M.G., 2000. Substantia nigra pars reticulata units in 6-hydroxydopamine-lesioned rats: responses to striatal D2 dopamine receptor stimulation and subthalamic lesions. Eur. J. Neurosci. 12 (1), 247–256. https://doi.org/10.1046/j.1460-9568.2000.00910.x.

Tsou, K., Brown, S., Sañudo-Peña, M.C., Mackie, K., Walker, J.M., 1998. Immunohistochemical distribution of cannabinoid CB1 receptors in the rat central nervous system. Neuroscience 83 (2), 393–411. https://doi.org/10.1016/S0306-4522(97)00436-3.

Van Waes, V., Beverley, J.A., Siman, H., Tseng, K.Y., Steiner, H., 2012. CB1 cannabinoid receptor expression in the striatum: association with Corticostriatal circuits and developmental regulation. Front. Pharmacol. 3, 21. https://doi.org/10.3389/fphar.2012.00021.

Vegas-Suárez, S., Pisanò, C.A., Requejo, C., Bengoetxea, H., Lafuente, J.V., Morari, M., Miguelez, C., Ugedo, L., 2020. 6-Hydroxydopamine lesion and levodopa treatment modify the effect of buspirone in the substantia nigra pars reticulata. Br. J. Pharmacol. 177 (17), 3957–3974. https://doi.org/10.1111/bph.15145.

Voorn, P., Vanderschuren, L.J.M.J., Groenewegen, H.J., Robbins, T.W., Pennartz, C.M.A., 2004. Putting a spin on the dorsal-ventral divide of the striatum. Trends Neurosci. 27 (8), 468–474. https://doi.org/10.1016/j.tins.2004.06.006.

Wall, N.R., De La Parra, M., Callaway, E.M., Kreitzer, A.C., 2013. Differential innervation of direct- and indirect-pathway striatal projection neurons. Neuron 79 (2), 347–360. https://doi.org/10.1016/j.neuron.2013.05.014.

Walsh, S., Mnich, K., Mackie, K., Gorman, A.M., Finn, D.P., Dowd, E., 2010. Loss of cannabinoid CB1receptor expression in the 6-hydroxydopamine-induced nigrostriatal terminal lesion model of Parkinson's disease in the rat. Brain Res. Bull. 81 (6), 543–548. https://doi.org/10.1016/j.brainresbull.2010.01.009.

Wang, Y., Zhang, Q.J., Liu, J., Ali, U., Gui, Z.H., Hui, Y.P., Chen, L., Wang, T., 2010. Changes in firing rate and pattern of GABAergic neurons in subregions of the substantia nigra pars reticulata in a rat model of Parkinson's disease. Brain Res. 1324, 54–63. https://doi.org/10.1016/j.brainres.2010.02.008.

Weiss-Wunder, L.T., Chesselet, M.-F., 1990. Heterogeneous distribution of cytochrome oxidase activity in the rat substantia nigra: correlation with tyrosine hydroxylase and dynorphin immunoreactivities. Brain Res. 529 (1), 269–276. https://doi.org/10.1016/0006-8993(90)90837-2.

Winter, C., von Rumohr, A., Mundt, A., Petrus, D., Klein, J., Lee, T., Morgenstern, R., Kupsch, A., Juckel, G., 2007. Lesions of dopaminergic neurons in the substantia nigra pars compacta and in the ventral tegmental area enhance depressive-like behavior in rats. Behav. Brain Res. 184 (2), 133–141. https://doi.org/10.1016/j.bbr.2007.07.002.

Yung, K.K.L., Bolam, J.P., Smith, A.D., Hersch, S.M., Ciliax, B.J., Levey, A.I., 1995. Immunocytochemical localization of D1 and D2 dopamine receptors in the basal ganglia of the rat: light and electron microscopy. Neuroscience 65 (3), 709–730. https://doi.org/10.1016/0306-4522(94)00536-E.

Zeng, B.Y., Dass, B., Owen, A., Rose, S., Cannizzaro, C., Tel, B.C., Jenner, P., 1999. Chronic L-DOPA treatment increases striatal cannabinoid CB1 receptor mRNA expression in 6-hydroxydopamine-lesioned rats. Neurosci. Lett. 276 (2), 71–74. https://doi.org/10.1016/S0304-3940(99)00762-4.

Zhang, X., Egeland, M., Svenningsson, P., 2011. Antidepressant-like properties of sarizotan in experimental parkinsonism. Psychopharmacology 218 (4), 621–634. https://doi.org/10.1007/s00213-011-2356-7.

Zimmer, A., Steiner, H., Bonner, T.I., Zimmer, A.M., Kitai, S.T., 1999. Altered gene expression in striatal projection neurons in CB1 cannabinoid receptor knockout mice. Proc. Natl. Acad. Sci. U. S. A. 96 (10), 5786–5790. https://doi.org/10.1073/pnas.96.10.5786.

> CHAPTER EIGHT

Therapeutic potential of cannabinoids as neuroprotective agents for damaged cells conducing to movement disorders

Mario Antonazzo[a,b], María Botta[c], Harkaitz Bengoetxea[d], José Ángel Ruiz-Ortega[a,b,c], Teresa Morera-Herreras[a,b,*]

[a]Department of Pharmacology, Faculty of Medicine and Nursing, University of the Basque Country (UPV/EHU), Leioa, Spain
[b]Neurodegenerative Diseases Group, BioCruces Bizkaia Health Research Institute, Barakaldo, Bizkaia, Spain
[c]Department of Pharmacology, Faculty of Pharmacy, University of the Basque Country (UPV/EHU), Vitoria-Gasteiz, Spain
[d]Department of Neurosciences, Faculty of Medicine and Nursing, University of the Basque Country (UPV/EHU), Leioa, Spain
*Corresponding author: e-mail address: teresa.morera@ehu.eus

Contents

Abstract

The basal ganglia (BG), an organized network of nuclei that integrates cortical information, play a crucial role in controlling motor function. In fact, movement disorders such as Parkinson's disease (PD) and Huntington's disease (HD) are caused by the degeneration of specific structures within the BG. There is substantial evidence supporting the idea that cannabinoids may constitute novel promising compounds for the treatment of movement disorders as neuroprotective and anti-inflammatory agents. This potential therapeutic role of cannabinoids is based, among other qualities, on their capacity to reduce oxidative injury and excitotoxicity, control calcium influx and limit the toxicity of reactive microglia. The mechanisms involved in these effects are related to CB1 and CB2 receptor activation, although some of the effects are CB receptor independent.

229

Thus, taking into account the aforementioned properties, compounds that act on the endocannabinoid system could be useful as a basis for developing disease-modifying therapies for PD and HD.

Abbreviations

2–AG	2-arachidonoyl glycerol
3–NP	3-nitropropionic acid
6–OHDA	6-hydroxydopamine
Δ^9-THC	Δ^9-tetrahydrocannabinol
ACEA	arachidonyl-2′-chloroethylamide
AEA	arachidonoyl ethanolamide
BG	basal ganglia
CAG	cytosine-adenine-guanine
CBD	cannabidiol
CNS	central nervous system
COX-2	cyclooxygenase 2
DAGLα	diacylglycerol lipase α
ECS	endocannabinoid system
FAAH	fatty acid amide hydrolase
GABA	gamma aminobutyric acid
HD	Huntington's disease
HTT	Huntingtin protein
IL	interleukin
iNOS	inducible nitric oxide synthase
LPS	lipopolysaccharide
MAGL	monoacylglycerol lipase
MPTP	1-methyl-4-phenyl-1,2,3,6-tetrahydropyridine
MSN	medium spiny neuron
NAPE-PLD	N-acyl-phosphatidylethanolamine-hydrolysing phospholipase D
NO	nitric oxide
PPAR	peroxisome proliferator-activated receptor
PD	Parkinson's disease
ROS	reactive oxygen species
SNpc	*substantia nigra pars compacta*
SNpr	*substantia nigra pars reticulata*
TNF-α	tumor necrosis factor-α
TRPV1	transient receptor potential vanilloid type 1
VTA	ventral tegmental area
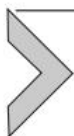
1. The endocannabinoid signaling system and its distribution in the basal ganglia

Preparations of the cannabis plant have been used as medicinal drugs by various cultures and civilizations for thousands of years. The identification of more than 60 compounds known as cannabinoids that are present in

the plant *Cannabis sativa* led to the investigation and discovery of the endocannabinoid system (ECS). The ECS comprises lipid-signaling endogenous ligands named endocannabinoids (eCBs), biosynthesizing and degrading enzymes, and their associated receptors and is broadly distributed in the central and peripheral nervous systems (Castillo, Younts, Chávez, & Hashimotodani, 2012).

The best-characterized eCBs in the central nervous system (CNS) are 2-arachidonoyl glycerol (2-AG) and arachidonoyl ethanolamide (AEA, also known as anandamide) (Devane et al., 1992; Sugiura, Kishimoto, Oka, & Gokoh, 2006). The main degradative enzyme for 2-AG in the brain, monoacylglycerol lipase (MAGL), is located presynaptically (Gulyas et al., 2004) and is the crucial element for the control of 2-AG signaling (Hashimotodani, Ohno-Shosaku, & Kano, 2007). In contrast, diacylglycerol lipase α (DAGLα) is localized in postsynaptic neurons (Katona & Freund, 2008), and it is required for Ca^{2+}-dependent 2-AG production and eCB-mediated synaptic plasticity (Tanimura et al., 2010). Postsynaptic depolarization and intracellular Ca^{2+} influx also promote AEA production. One of the main enzymes that synthesizes AEA in the brain is N-acyl-phosphatidylethanolamine-hydrolysing phospholipase D (NAPE-PLD), which can be expressed both post- and presynaptically (Cristino et al., 2008), whereas fatty acid amide hydrolase (FAAH) is mainly implicated in AEA catabolism (Varvel, Cravatt, Engram, & Lichtman, 2006).

The effects of eCBs are primarily mediated by their interaction with two well-characterized $G_{i/o}$ protein-coupled cannabinoid receptor subtypes, CB1 and CB2 (Castillo et al., 2012). Activation of these receptor subtypes inhibits adenylyl cyclase and some voltage-dependent calcium channels and activates mitogen-activated protein kinases (MAPK) and inwardly rectifying potassium channels. In the brain, the concentration of 2-AG is higher than that of AEA, and 2-AG acts as a full agonist, whereas AEA acts as a partial agonist at cannabinoid receptors, suggesting that cannabinoid regulation in the brain is elicited mainly by 2-AG (Sugiura et al., 2006). In addition, eCBs can also interact with other receptors such as the transient receptor potential vanilloid type 1 (TRPV1) cation channel, the GTP-binding protein-coupled receptor GPR55, the abnormal-CBD receptor and the peroxisome proliferator-activated receptor (PPAR).

CB1 and CB2 receptors are widely expressed throughout the body, and countless brain functions, including anxiety, mood, cognition, motor control, feeding behavior and pain, as well as pathophysiological processes such as Parkinson's disease (PD) and dyskinesias, are regulated at least in part

through these receptors. The CB1 receptor resides in axon terminal endings, but substantial functional evidence confirms that it is also expressed on somata (Fitzgerald, Shobin, & Pickel, 2012). This receptor is highly expressed in the CNS, including the cortex, cerebellum, hippocampus and especially the basal ganglia (BG). The BG, an organized network of sub-cortical nuclei that connects the cortex and the thalamus, display the highest levels of both mRNA expression and CB1 receptor (Romero et al., 2002). The striatum (Calabresi, Picconi, Tozzi, Ghiglieri, & Di Filippo, 2014), as well as other regions such as the *globus pallidus*, the *entopeduncular nucleus* and the *substantia nigra pars reticulata* (SNpr), which receive striatal efferent outputs, have high levels of CB1 receptor binding sites (Muñoz-Arenas et al., 2015; Sierra et al., 2015). CB1 receptors are presynaptically located in striatonigral (direct striatal efferent pathway) and striatopallidal (indirect striatal efferent pathway) projection neurons (Kofalvi, 2005). These neurons use gamma-aminobutyric acid (GABA) as a neurotransmitter. Other markers that are co-expressed with GABA in these pathways include glutamic acid decarboxylase, prodynorphin, substance P, preproenkephalin, and D1 and D2 dopaminergic receptors (Hohmann & Herkenham, 2000). In contrast, intrinsic striatal neurons, which contain acetylcholine or somatostatin, do not express CB1 receptors (Hohmann & Herkenham, 2000). Moreover, CB1 receptors have been observed in glutamatergic cor-ticostriatal afferents (Gerdeman & Lovinger, 2001; Kofalvi, 2005) and in subthalamopallidal and/or subthalamonigral projections (Dasilva, Grieve, Cudeiro, & Rivadulla, 2014; Mailleux & Vanderhaeghen, 1992). Apart from neuronal populations, CB1 receptors are also expressed on glial cells, but their density is lower than that observed on neurons (Bilkei-Gorzo et al., 2018).

On the other hand, CB2 receptors are more predominant in peripheral tissues and cells of the immune system (B lymphocytes, natural killer cells, monocytes, neutrophils, T8 lymphocytes, and T4 lymphocytes) (Munro, Thomas, & Abu-Shaar, 1993; Navarrete, García-Gutiérrez, Aracil-Fernández, Lanciego, & Manzanares, 2018). CB2 receptors are also expressed in the CNS, especially in the dorsal vagal motor nucleus, the nucleus ambiguus and the spinal trigeminal nucleus (Núñez et al., 2008; Van Sickle et al., 2005). In addition, although early attempts to identify CB2 receptors in the CNS under basal conditions failed, this paradigm has changed in the last decade. For the first time, Van Sickle et al. (2005) revealed that CB2 receptors are expressed in neurons of the brainstem of

mice, rats and ferrets under normal conditions. Following this pioneering work, subsequent studies have characterized the expression of CB2 receptors in several brain regions, including the cortex, BG (striatum, SNpr), amygdala, hippocampus and ventral tegmental area (VTA) (Gong et al., 2006; Onaivi et al., 2006; Zhang et al., 2014). In these brain regions, CB2 receptors were detected in microglia (Cabral, Raborn, Griffin, Dennis, & Marciano-Cabral, 2008) and in neurons (Zhang et al., 2014). Thus, the presence of CB2 receptors has been described in cortical, hippocampal, pallidal and mesencephalic neurons (Lanciego et al., 2011) as well as in the amygdala and striatum (Brusco, Tagliaferro, Saez, & Onaivi, 2008; Onaivi et al., 2006). Because other studies did not localize these receptors in healthy brains, the localization of CB2 receptors in the CNS remains controversial. The disagreement among authors on this point may be due in part to the lack of specificity of the antibodies used. To circumvent this methodological limitation, new genetic strategies based on mouse lines that express enhanced green fluorescent protein under the control of the CB2 promoter have been developed (López et al., 2018).

Various pharmacological, neurochemical and electrophysiological studies indicate that eCBs function largely through retrograde signaling in which postsynaptic activity induces eCB production and release with backward transmission across the synapse to depress presynaptic neurotransmitter release (Castillo et al., 2012). In the BG, eCBs tend to decrease GABAergic and glutamatergic transmission by activating CB1 receptors (Benarroch, 2007). Moreover, eCBs interfere with the dopaminergic system (reviewed in Morera-Herreras, Miguelez, Aristieta, Ruiz-Ortega, & Ugedo, 2012), affecting dopamine release and modulating the firing activity of dopaminergic neurons (Solinas, Justinova, Goldberg, & Tanda, 2006). Although nigrostriatal dopaminergic neurons seem not to express CB1 receptors (Piomelli, 2003), the activation or the blockade of the ECS directly affects the functionality of these cells (Fernández-Ruiz, Hernández, & Ramos, 2010). These actions are mediated by the CB1 receptor, which is expressed in neuronal subpopulations that are located in the vicinity and are connected to dopaminergic neurons such as GABAergic, glutamatergic, and opioidergic neurons (van der Stelt & Di Marzo, 2003). In addition, the stimulation of dopamine receptors increases the levels of striatal AEA, which may serve as an inhibitory feedback signal countering dopamine-induced motor activity (Ferrer, Asbrock, Kathuria, Piomelli, & Giuffrida, 2003). However, additional mechanisms could explain the modulation of dopaminergic

transmission by eCBs, since some eCBs interact with other receptors such as TRPV1, which is expressed on nigrostriatal terminals and on tyrosine hydroxylase-positive neurons in the *substantia nigra pars compacta* (SNpc) (Mezey et al., 2000; Starowicz, Nigam, & Di Marzo, 2007).

2. Mechanisms underlying neuroprotection by cannabinoids

The ECS is targeted by compounds that have specific biological and therapeutic effects; these effects include, among others, limitation of neuronal damage by reduction of excitotoxicity, neuroinflammation, oxidative stress and calcium influx. Accordingly, cannabinoids are emerging as potential neuroprotective compounds in progressive neurodegenerative pathologies (Fernández-Ruiz, Romero, & Ramos, 2015). In fact, pharmacological manipulation of the ECS has revealed neuroprotective effects in some experimental models of neurodegenerative diseases, suggesting that this therapeutic strategy could be useful in modifying the progression of such pathologies (Fernández-Ruiz et al., 2010).

The molecular mechanisms underlying the neuroprotective action of cannabinoids are diverse (summarized in the Fig. 1). On one hand, such neuroprotection is related to a direct action on the ECS by activation of CB1 and CB2 (Ramirez, 2005), TRPV1 (Baek et al., 2018) or GPR55 receptors (Kallendrusch et al., 2013). On the other hand, neuroprotection by cannabinoids could also be mediated by activating targets outside the ECS, such as nuclear receptors of the PPAR family (Fidaleo, Fanelli, Ceru, & Moreno, 2014), transcription factors (Fernández-Ruiz et al., 2013), serotonin 1A receptors (Pazos et al., 2013) and the adenosine signaling pathway (Castillo, Tolón, Fernández-Ruiz, Romero, & Martinez-Orgado, 2010). The broad spectrum of activity of cannabinoid compounds may be important in its use as a neuroprotective agent since multi-targeted designed drugs have been shown to be very promising tools in preclinical studies testing neuroprotective and disease-modifying agents (Geldenhuys & Van der Schyf, 2013).

2.1 Neuroprotection directly related to CB receptors

Substantial evidence supports the idea that excitotoxicity plays a key role in neuronal damage in neurodegenerative diseases. In this sense, CB1 receptors can provide a neuroprotective effect by normalizing glutamate homeostasis. CB1 receptors are located at neuronal glutamatergic terminals, and their

activation by cannabinoid agonists reduces glutamate release, thereby limiting glutamatergic excitotoxicity (Mechoulam, Panikashvili, & Shohami, 2002; van der Stelt et al., 2002). In parallel with their antiglutamatergic effect, cannabinoids, by reducing the activation of NMDA receptors and the subsequent opening of voltage-sensitive calcium channels, can diminish calcium influx, thereby avoiding the activation of destructive pathways linked to high intracellular levels of this ion (Demuth & Molleman, 2006; Fowler et al., 2003).

Furthermore, the activation of CB1 receptors provides neuroprotection by inducing an enhancement of the blood supply after neuronal damage, an effect that could be of special interest in ischemic episodes. The mechanism implicated in this effect is related to a decrease in the generation of endothelium-derived mediators (endothelin-1 or nitric oxide (NO)) that induce vasoconstriction of injured tissues after ischemia (Chen et al., 2000).

In addition to their aforementioned beneficial effects, cannabinoids are also able to regulate the immunological processes that are clearly involved in neuronal damage, including local inflammatory events related to the activation of glial cells. In fact, many studies suggest that glial activation, along with neuroinflammation (microglial activation, astrogliosis or infiltration of immune cells), contributes to the initiation or progression of neurodegenerative processes. The activation of CB1 receptors leads to modulation of the levels of neurotrophins and anti-inflammatory mediators. Thus, cannabinoid ligands acting on CB1 receptors can create favorable conditions for the regeneration of damaged neurons by decreasing tumor necrosis factor-α (TNF-α) and interleukin-12 (IL-12) levels and increasing IL-10 levels (Smith, Terminelli, & Denhardt, 2000). Together with CB1 receptors, CB2 receptors are also implicated in these neuroprotective effects, since their activation inhibits the production of chemokines by astrocytes (Sheng, Hu, Ni, Rock, & Peterson, 2009). Moreover, the activation of CB2 receptors reduces the proliferation and migration of microglial cells at lesion sites (Walter et al., 2003) and reduces the production of TNF-α by inhibiting the activation of NF-κB (Oh et al., 2010), a transcription factor that is important in regulating pro-inflammatory responses.

Apart from the classical CB receptors, recent studies suggest that TRPV1 receptors may be a promising neuroprotective target. Capsaicin is able to protect neurons against neurotoxicity by specific activation of astrocytic TRPV1 receptors, which leads to reduced microglial activation and reduces consequent oxidative stress (Baek et al., 2018). In contrast, other authors have shown that overactivation of TRPV1 leads to neurotoxicity by

increasing intracellular calcium levels or disrupting mitochondrial function (Kim et al., 2005). Therefore, further investigations are necessary to clarify the role of TRPV1 in neurodegeneration/neuroprotection.

Although its function in the brain is still poorly understood, the GPR55 receptor represents a putative receptor for various cannabinoids and has been proposed as a novel neuroprotective target. Thus, GPR55 receptor activation by lysophosphatidylinositol exerts a neuroprotective effect in excitotoxically lesioned rat organotypic cultures. However, the mechanisms behind GPR55 activation in microglia have yet to be unraveled (Kallendrusch et al., 2013).

2.2 Neuroprotection not directly related to CB receptors

Due to their antioxidant properties, cannabinoids can provide neuroprotection through mechanisms that are not directly related to their action at classical CB receptors. Phytocannabinoids such as Δ^9-tetrahydrocannabinol (Δ^9-THC), cannabinol and cannabidiol (CBD), as well as synthetic cannabinoids such as nabilone and HU-211, may protect against brain damage by restoring the equilibrium between oxidative and antioxidant mechanisms that is altered during neurodegenerative processes. In fact, during degeneration, a deficiency in endogenous antioxidant mechanisms and high levels of reactive oxygen species (ROS) have been described (Marsicano, Moosmann, Hermann, Lutz, & Behl, 2002). This neuroprotective potential of cannabinoids is related to their ability to reduce excessive production of these ROS by acting as scavengers and antagonizing lipid peroxidation (Chen & Buck, 2000; Hampson, Grimaldi, Axelrod, & Wink, 1998).

Further studies attempting to elucidate the exact mechanism underlying these antioxidant effects have suggested that, in addition to their particular chemical structure containing phenolic groups, the mechanism of action of cannabinoids may also be related to the activation of PPAR receptors. In fact, CBD exerts both antioxidant and anti-inflammatory effects through the activation of these receptors (Iuvone, Esposito, De Filippis, Scuderi, & Steardo, 2009; O'Sullivan, 2016). In particular, CBD inhibits the synthesis and release of a number of pro-inflammatory molecules, including cytokines, NO, and GFAP protein, from activated glial cells (Esposito et al., 2007) through a PPARγ receptor-mediated mechanism (Scuderi, Steardo, & Esposito, 2014). This effect is associated with the inhibition of p38 MAP kinase and the regulation of NF-κB, which controls the expression of genes that encode pro-inflammatory enzymes

(Esposito et al., 2006). Moreover, CBD regulates the microglial cell migration that plays a crucial role in the propagation of the neuroinflammatory response, preventing the recruitment of microglial cells to lesion sites (Walter et al., 2003). Nevertheless, it is known that CBD can enhance endogenous AEA signaling by inhibiting its intracellular degradation by FAAH or by decreasing eCB transport (Bisogno et al., 2001; Leweke et al., 2012). Consequently, CBD could provide neuroprotection by increasing eCB effects that are mediated by CB1 and CB2 receptor activation.

In addition, HU–211 is also able to act on postsynaptic NMDA glutamatergic receptors; it may decrease the intracellular concentration of calcium by closing voltage-dependent calcium channels, thereby also promoting a neuroprotective effect that is not mediated by CB receptor activation (Hansen et al., 2002; Nadler, Mechoulam, & Sokolovsky, 1993).

CB1 receptor
↓ Glutamate release
↓ Calcium influx
↑ Blood supply
↓ Pro-inflammatory mediators (TNF-α, IL-12)
↑ Anti-inflammatory mediators (IL-10)

CB2 receptor
↓ Proliferation of glial cells
↓ Migration of glial cells
↓ Production of chemokines by astrocytes
↓ Pro-inflammatory mediators (TNF-α)

TRPV1
↓ Microglial activation by astrocytic TRPV1 receptor stimulation
↓ Oxidative stress
Protection against excitotoxicity?

Neuroprotection

GPR55
Protection against excitotoxicity?

Other mechanisms
↓ ROS (action as scavengers)
↓ Lipid peroxidation
↓ eCBs degradation and transport
↓ Pro-inflammatory mediators (PPARγ receptors related mechanism)
↓ Microglial cell migration

Fig. 1 Summary of the different mechanisms proposed for the neuroprotection exerted by cannabinoids. Abbreviations: eCBs, endocannabinoids; IL, interleukin; PPAR, peroxisome proliferator-activated receptor; ROS, Reactive oxygen species; TNF, tumor necrosis factor; TRPV1, transient receptor potential vanilloid type 1.

3. Cannabinoids as neuroprotective agents in neurodegenerative disorders

Due to the aforementioned pharmacological properties of the cannabinoids, compounds that target the ECS could be useful as neuroprotective tools in neurodegenerative disorders such as PD or Huntington's disease (HD) in which specific structures within the BG degenerate. Current

pharmacological treatments for both pathologies focus on restoring normal motor functionality and ameliorating symptoms but are not able to arrest or slow down the progression of neurodegeneration. Therefore, the search for disease-modifying therapies is of primary interest in the treatment of PD and HD.

3.1 Neuroprotective effect of cannabinoids in Parkinson's disease

PD is the second most common neurodegenerative disorder after Alzheimer's disease. It is an age-related pathology that is present in 1–2% of the population over 60 years of age (Massano & Bhatia, 2012; Nussbaum & Ellis, 2003). Although the most notorious symptoms of PD include motor alterations such as bradykinesia, resting tremors, rigidity and postural instability, non-motor alterations (e.g., dementia and depression) are also present (reviewed in Poewe & Mahlknecht, 2010). The two main physiopathological hallmarks of PD are the accumulation of α-synuclein aggregates and the degeneration of dopaminergic neurons in the SNpc (reviewed in Thomas, 2009), leading to dopamine depletion. This will affect the functionality of the BG, key nuclei in voluntary movement and other processes, as they are strongly modulated by dopamine (reviewed in Gerfen & Surmeier, 2011). In recent decades, there has been an increase in our understanding of the pathological pathways that underlie PD development. This knowledge has suggested several targets for neuroprotective intervention in PD such as neuroinflammation, excitotoxicity, mitochondrial function and oxidative stress, among others (reviewed in Schapira, Olanow, Greenamyre, & Bezard, 2014). The ECS has been suggested as an appropriate target system for increasing neuroprotection because it is able to modulate some of the pathological features observed in PD patients' brains and in animal models (reviewed in Fernández-Ruiz et al., 2011) (summarized in Table 1).

Neuroinflammation occurs mainly through glial activation, which is thought to be a key contributor to dopaminergic degeneration (Kaur, Gill, Bansal, & Deshmukh, 2017; Lull & Block, 2010). Glial activation occurs both in patients and in animal models of PD and is due to the subsequent increase in the levels of various pro-inflammatory agents such as IL-1β, TNF-α, inducible nitric oxide synthase (iNOS) and cyclooxygenase 2 (COX-2) (Ouchi et al., 2005; Ramsey & Tansey, 2014; Teismann & Schulz, 2004).

Table 1 Neuroprotective effects of the endocannabinoid system modulation in Parkinson's disease.

Parkinson's disease

1. Reduction of neuroinflammation	
CB1 activation	↓Microglial activation ↓Production of pro-inflammatory agents (IL-1β, TNF-α, iNOs, COX-2)
CB1 blockade	↑Activated astrocytes in SNpc
CB2 activation	↓Glial cell number ↓Production of pro-inflammatory agents (IL-1β, TNF-α, iNOs, NO)
MAGL inhibition	↑Glial cell number ↑Levels of GDNF ↑Production of anti-inflammatory mediators (TGF-β)
2. Reduction of excitotoxicity	
CB1 activation	↓Excitotoxicity by inhibiting glutamate release
FAAH inhibition	Prevention against excitotoxicity
3. Modulation of mitochondrial function	
PPAR-γ activation	↑Mitochondrial biogenesis
CB1 activation	↑Mitochondrial biogenesis ↑Mitochondrial function ↑Number of mitochondria
4. Reduction of oxidative stress	
CB1 activation	↓Expresión of microglial NADPH oxidase in an MPTP animal model ↓ROS ↓Lipid peroxidation
CB2 activation	↓Myeloperoxidase-positive astrocytes ↑Antioxidant enzyme activity ↑Antioxidant agents
PPAR-γ activation	↓ROS
FAAH inhibition	↓ROS ↓Lipid peroxidation ↓Protein carbonylation

Abbreviations: COX-2, cyclooxygenase 2; FAAH, fatty acid amide hydrolase; GDNF, Glial cell-derived neurotrophic factor; IL, interleukin; iNOS, inducible nitric oxide synthase; MAGL, monoacylglycerol lipase; MPTP, 1-methyl-4-phenyl-1,2,3,6-tetrahydropyridine; NO, nitric oxide; PPAR, peroxisome proliferator-activated receptor; ROS, reactive oxygen species; SNpc, substantia nigra pars compacta; TGF, Transforming growth factor; TNF, tumor necrosis factor

Several reports show the promising ability of cannabinoids to reduce neuroinflammation in PD models. *In vivo* CB1 activation diminished dopaminergic neuronal damage caused by the neurotoxin 1-methyl-1,2,3, 6-tetrahydropyridine (MPTP), decreased microglial activation, and reduced IL-1β, TNF-α and iNOS levels (Chung et al., 2011). However, other reports showed that these protective effects of cannabinoids against MPTP toxicity were independent of CB1 receptor activation (Price et al., 2009). Arachidonyl-2′-chloroethylamide (ACEA), a CB1-selective agonist, prevented neuronal death in an *in vitro* lipopolysaccharide (LPS)-induced inflammation model (Vrechi, Crunfli, Costa, & Torrão, 2018). In another report, rimonabant, a CB1 antagonist, increased the survival of SNpc dopaminergic neurons after striatal injection of 6-hydroxydopamine (6-OHDA). It was shown to have no effect on microglial activation but to increase the number of activated astrocytes in the SNpc (Cerri et al., 2014). The CB2 receptor agonist JWH-133 prevented MPTP-induced neurodegeneration and reduced the production of IL-1β, TNF-α and iNOS by activated microglia (Chung et al., 2016). Other publications also provide evidence for a role of the CB2 receptor in preventing neurodegeneration, reducing levels of inflammatory factors and decreasing glial cell numbers in animal models of PD (Javed, Azimullah, Haque, & Ojha, 2016; Ojha, Javed, Azimullah, & Haque, 2016) and in decreasing inflammatory markers in an LPS-induced inflammation model *in vitro* (Malek, Popiolek-Barczyk, Mika, Przewlocka, & Starowicz, 2015). In addition to receptors, eCB metabolic enzymes may also have potential as therapeutic targets. The MAGL inhibitor JZL184 partially prevented MPTP-induced neuronal damage *in vivo*; it also increased glial cell numbers and levels of GDNF and TGF-β, an anti-inflammatory cytokine (Fernández-Suárez et al., 2014). Moreover, cannabinoids had no neuroprotective effect in *in vitro* PD models when glia were not present, suggesting that their modulatory effect on glial activity is the main mechanism responsible for the neuroprotection offered by these compounds (Chung et al., 2011; Lastres-Becker, Molina-Holgado, Ramos, Mechoulam, & Fernández-Ruiz, 2005).

Neuroinflammation can contribute to glutamate release and thereby promote glutamate-related processes. Moreover, aggregated α-synuclein present in the brains of PD patients is known to increase glutamate-induced synaptic currents. Thus, excitotoxicity occurs due to the overstimulation of glutamatergic receptors. Furthermore, activation of glutamate receptors located on microglia causes the release of pro-inflammatory cytokines, feeding neuroinflammation, glutamate-related excitotoxicity, and subsequent

neuronal loss. Although not the reason for the initial neuronal decay, this process contributes to dopaminergic degeneration in PD (reviewed in Ambrosi, Cerri, & Blandini, 2014).

As mentioned above, cannabinoids can regulate glutamate release, thus providing a way to reduce excitotoxicity (Domenici, 2006; Takahashi & Castillo, 2006). Δ^9-THC and AEA were shown to reduce the excitotoxicity induced by ouabain *in vivo* through activation of the CB1 receptor. In the same experimental model, modulation of TPRV1 activity also reduced excitotoxicity (van der Stelt et al., 2001; Veldhuis et al., 2003). Moreover, WIN 55,212-2 and AEA, CB1/CB2 receptor agonists, prevented neuronal death in *in vitro* models of excitotoxicity (Rangel-López et al., 2015; Serpa, Pinto, Bernardino, & Cascalheira, 2015). Other reports have suggested that BDNF might be a key to CB1-mediated protection against excitotoxicity (Blázquez et al., 2015; Khaspekov et al., 2004). Regulation of eCB metabolism might also be useful in fighting excitotoxicity in PD, considering that FAAH inhibition was shown to prevent excitotoxicity in various excitotoxic models both *in vivo* and *in vitro* (Aguilera-Portillo et al., 2019; Karanian et al., 2007; Naidoo et al., 2011).

Cannabinoids can also modulate mitochondrial function and, therefore, oxidative stress through a variety of mechanisms; thus, they represent potential therapeutic tools for reducing such processes in PD. PD patients display mitochondrial dysfunction that is reflected in reduced activity of complex I of the mitochondrial respiratory electron transport chain. Moreover, some complex I inhibitors have been used to recreate PD in animal models, and some mutations linked to PD are involved in mitochondrial function. This mitochondrial dysfunction is linked to ROS production, which causes further mitochondrial and cellular damage leading to apoptosis and thus contributes to neuronal degeneration in PD (reviewed in Schapira, 2008).

Some cannabinoids may have positive effects on mitochondrial biogenesis and function. For instance, Δ^9-THC is able to restore the levels of proteins involved in mitochondrial biogenesis and protect cells from MPTP toxicity *in vitro* in a PPAR-γ-dependent manner (Carroll, Zeissler, Hanemann, & Zajicek, 2012; Zeissler et al., 2016). In *in vivo* and *in vitro* models of cerebral ischemia, activation of the CB1 receptor was shown to increase the number of mitochondria as well as to enhance the expression of markers of mitochondrial biogenesis and function (Bai et al., 2017; Cai et al., 2017; Ma et al., 2015). Furthermore, CBD reversed the dopaminergic impairment caused by 6-OHDA injection in an animal model (Lastres-Becker et al., 2005) and had positive effects on mitochondrial function

and oxidative stress in *in vitro* models of various pathological states (Liu et al., 2014; Sun, Hu, Wu, & Zhang, 2017; Yang et al., 2014). One clinical trial investigated the possible neuroprotective effects of CBD in PD patients and found no differences in the neuroprotection parameters that were assessed (Chagas et al., 2014). The limitations of this study were its small sample size and, possibly, the short treatment duration used to evaluate changes in PD progression.

Finally, oxidative stress induced *in vivo* in a rotenone PD model was reduced by administration of *Cannabis sativa* extracts, although no protection against dopaminergic degeneration was observed (Abdel-Salam et al., 2015). Both CB1 and CB2 receptors seem to be involved in the antioxidant activity of cannabinoids. WIN 55,212-2 offered protection against neurodegeneration, reduced lipid peroxidation and protein carbonylation *in vivo* after MPTP treatment (Escamilla-Ramírez et al., 2017), and reduced ROS and lipid peroxidation *in vitro* after quinolinic acid insult (Rangel-López et al., 2015). Activation of the CB1 receptor resulted in reduced expression of microglial NADPH oxidase and decreased DNA and protein oxidative damage in an MPTP animal model of PD (Chung et al., 2011). CB2 receptor activation reduced the number of myeloperoxidase-positive astrocytes and increased antioxidant enzyme activity levels and the levels of antioxidant molecules in animal models of PD (Chung et al., 2016; Javed et al., 2016). Δ^9-THC also prevented dopaminergic lesions after 6-OHDA injection *in vivo* (Lastres-Becker et al., 2005) and reduced ROS production in an *in vitro* model of PD through PPARγ activation (Carroll et al., 2012; Zeissler et al., 2016). URB597, a FAAH inhibitor, also exerted neuroprotective effects against neuronal death induced by 6-OHDA and MPTP *in vivo* by reducing lipid peroxidation, protein carbonylation and ROS (Escamilla-Ramírez et al., 2017; Maya-López, Ruiz-Contreras, et al., 2017; Pelição et al., 2016). Moreover, some cannabinoids have intrinsic structural antioxidant properties that also contribute to their effectiveness as antioxidant agents (Marsicano et al., 2002).

3.2 Neuroprotective effect of cannabinoids in Huntington's disease

HD is a rare autosomal-dominant progressive neurodegenerative disorder caused by a mutation in the IT15 gene (*HTT*) that encodes the huntingtin protein (HTT). The mutation consists of an extension of the trinucleotide cytosine-adenine-guanine (CAG) repeat (>39 CAG repeats) that yields an abnormally long polyglutamine sequence in the N-terminus of HTT

(pathogenic HTT) (MacDonald et al., 1993). The neuropathological consequence of this mutation is the specific degeneration of striatal GABAergic medium spiny neurons (MSNs) (Reiner et al., 1988) and, to a lesser extent, of glutamatergic pyramidal neurons in the cerebral cortex (Hedreen, Peyser, Folstein, & Ross, 1991; Heinsen et al., 1994). The neurodegeneration leads to motor abnormalities, the early stages of which are characterized by chronic movements and cognitive deterioration; the advanced stages are associated with parkinsonian-like symptoms such as bradykinesia and rigidity (Berardelli et al., 1999). Although the molecular mechanisms underlying neuronal degeneration and disease onset in HD have not been elucidated in detail, some authors have demonstrated that mitochondrial dysfunction, energy depletion, excitotoxicity, oxidative damage, protein aggregation and neuroinflammation play important roles in the neuronal loss that occurs in HD (for review, see Borrell-Pagès, Zala, Humbert, & Saudou, 2006).

There is substantial evidence supporting the idea that the ECS in the BG becomes hypofunctional in HD. In fact, progressive loss of CB1 receptors in murine animal models of HD has been reported (Bisogno, Martire, Petrosino, Popoli, & Di Marzo, 2008; Dowie et al., 2009; Glass, Van Dellen, Blakemore, Hannan, & Faull, 2004; McCaw et al., 2004). These observations are consistent with *post mortem* autoradiographic studies of brain tissue sections from HD patients that show a notable decrease in CB1 receptor levels in MSNs of the caudate and putamen at early stages of the disease (Denovan-Wright & Robertson, 2000; Glass, Dragunow, & Faull, 2000; Van Laere et al., 2010). This could very likely be due to inhibition of CB1 transcription mediated by the mutant HTT (Laprairie et al., 2014). Interestingly, a massive and progressive loss of CB1 receptors occurs prior to the neurodegeneration of MSNs and the onset of motor symptoms (Dowie et al., 2009; McCaw et al., 2004). These data suggest that activation of CB1 receptors may modify the progression of HD.

The hypothesis that CB1 receptors may modify the progression of HD has been intensively investigated, mainly in preclinical experimental models of the disease. In these models, most of the neuroprotective actions observed were mediated via CB1 cannabinoid receptors. Because these receptors are located both presynaptically and postsynaptically at neuronal glutamatergic terminals, their activation by cannabinoid agonists would be expected to lead to decreased glutamate release and thus to limit excitotoxicity (Sagredo et al., 2007). In fact, administration of the CB1 receptor agonist WIN 55,212-2 to an intrastriatal quinolinic acid-injected rat model of HD preserved striatal neurons by decreasing glutamate-mediated

Table 2 Neuroprotective effects of the endocannabinoid system modulation in Huntington's disease

Huntington's disease

1. Reduction of excitotoxicity	
CB1 activation	↓Glutamate-mediated excitotoxicity
2. Attenuation of glial toxicity	
CB2 activation	↓Reactive microglial cells ↓Production of pro-inflammatory cytokines (TNF-α) ↓ROS ↓NO ↑Production of neurotrophins and anti-inflammatory mediators (IL-10, IL-1 antagonist)
3. Antioxidant/antiinflammatory properties	
Chemical structure	↓ROS (action as scavengers)
PPAR-γ activation	Interference with the NF-κB signaling pathway Induction of antioxidant enzymes

Abbreviations: IL, interleukin; NF-κB, nuclear factor-κB; NO, nitric oxide; PPAR, peroxisome proliferator-activated receptor; ROS, reactive oxygen species; TNF, tumor necrosis factor

excitotoxicity (Table 2). This effect was blocked by the CB1 receptor antagonist AM251, demonstrating that it was CB1-dependent (Pintor et al., 2006). Similarly, administration of Δ^9-THC or WIN 55,212-2 had a neuroprotective effect against striatal neurotoxicity in rats lesioned with the mitochondrial toxin 3-nitropropionic acid (3-NP) (Lastres–Becker et al., 2004; Maya-López, Colín-González, et al., 2017). Using the same HD model in mice, Díaz–Alonso et al. (2016) found that a novel cannabigerol derivative, VCE-003.2, also prevented loss of MSNs. Additionally, in the R6/2 mutant mouse model, activation of CB1 receptors by the administration of Δ^9-THC also protected MSNs from death (Blázquez et al., 2011). In contrast, in double-mutant animals (CB1 receptor-deficient R6/2 mutant mice), striatal degeneration was exacerbated due to increased excitotoxic damage and decreased levels of brain-derived neurotrophic factors (Blázquez et al., 2011; Chiarlone et al., 2014; Mievis, Blum, & Ledent, 2011). Rescue of CB1 gene expression by striatal injection of a recombinant adeno-associated viral vector encoding the CB1 receptor normalized the HD pathology characteristic of this mouse model (Blázquez et al., 2015; Naydenov et al., 2014).

Overall, the foregoing evidence indicates that CB1 receptor stimulation could be a promising neuroprotective tool for delaying HD progression. Although substantial loss of CB1 receptor-containing striatal neurons occurs in advanced stages of the disease (Fernández-Ruiz et al., 2015), it was recently demonstrated that the neuroprotective effect of such stimulation is predominantly due to the specific activation of CB1 receptors located on corticostriatal terminals, which are preserved during the progression of the disease (Chiarlone et al., 2014).

Cannabinoid compounds have also been shown to exert neuroprotective effects in HD by selectively activating CB2 receptors (Table 2). This cannabinoid receptor subtype is poorly abundant in the striatum in conditions of health, but its overexpression has been described both in HD patients and in animal models of the disease (Fernández-Ruiz, Pazos, García-Arencibia, Sagredo, & Ramos, 2008; Fernández-Ruiz et al., 2007; Palazuelos et al., 2009). Upregulation of CB2 receptors occurs in glial cells, including astrocytes, and is especially marked in striatal reactive microglia (Fernández-Ruiz et al., 2010, 2007). CB2 receptors may control the influence of reactive microglia on neurons by reducing the release of pro-inflammatory cytokines, ROS or NO and, moreover, by promoting the production of neurotrophins and anti-inflammatory mediators (IL-10 or IL-1 receptor antagonists) (reviewed in Navarro et al., 2016). In this way, the compensatory overexpression of CB2 receptors exerts a beneficial effect in HD, protecting striatal neurons from neuroinflammatory injury. In fact, genetic ablation of the CB2 receptor in R6/2 mice exacerbates microglial activation, aggravates motor abnormalities and accelerates the onset of the disease (Bouchard et al., 2012; Palazuelos et al., 2009). Consistent with these findings, selective pharmacological stimulation of CB2 receptors has a neuroprotective effect on striatal neurons in various animal models of HD such as quinolinic acid-lesioned mice and malonate-lesioned rats (Palazuelos et al., 2009; Sagredo et al., 2009).

Finally, cannabinoids such as Δ^9-THC and CBD have been shown to exert neuroprotective action in the 3-NP lesioned rat model of HD due to antioxidant mechanisms that are independent of CB1/CB2 receptor activation (Sagredo et al., 2007, 2011) (Table 2). These effects seem to be related to a scavenging action on ROS that is probably due to the phenolic structures of these phytocannabinoids. In addition, recent evidence demonstrates that cannabinoids also produce beneficial effects by activating PPAR-γ in transgenic R6/2 and 3-NP-lesioned mice (reviewed in Fernández-Ruiz, Gómez-Ruiz, García, Hernández, & Ramos, 2017).

Despite the vast amount of preclinical evidence indicating that cannabinoids may be a promising neuroprotective agent in HD, the clinical studies conducted to date have focused on evaluating the potential role of cannabinoids in the alleviation of specific symptoms without determining their effect on disease progression. In a double-blind, randomized, crossover, placebo-controlled pilot clinical trial, administration of Sativex® to 25 HD patients for 12 weeks failed to improve symptomatology, produce molecular changes in biomarkers or slow disease progression (López-Sendón Moreno et al., 2016). However, in a more recent study, seven HD patients showed improved dystonia and motor scores after cannabinoid drug administration (Sativex®, nabilone or dronabinol) (Saft et al., 2018). In these studies, cannabinoids were safe and well-tolerated and were associated with a low incidence of adverse effects. Additional clinical trials are warranted to assess the potential value of cannabinoid-based therapies in halting or slowing the progression of neurodegeneration in HD. Nevertheless, the authors suggest that in future studies, higher doses and/or longer treatment periods will be needed.

4. Concluding remarks

The solid preclinical evidence that has been presented to date demonstrates the neuroprotective properties of cannabinoid compounds and shows that these compounds represent promising drugs for delaying the progression of neurodegenerative diseases associated with cytotoxicity-induced neuronal and glial damage. The neuroprotective "multi-target" approach offered by cannabinoids must now be evaluated and validated in clinical trials. Such trials could offer a framework for the development of novel disease-modifying therapies in the treatment of PD or HD.

References

Abdel-Salam, O. M. E., Youness, E. R., Khadrawy, Y. A., Mohammed, N. A., Abdel-Rahman, R. F., Omara, E. A., et al. (2015). The effect of cannabis on oxidative stress and neurodegeneration induced by intrastriatal rotenone injection in rats. *Comparative Clinical Pathology*, *24*(2), 359–378. https://doi.org/10.1007/s00580-014-1907-9.

Aguilera-Portillo, G., Rangel-López, E., Villeda-Hernández, J., Chavarría, A., Castellanos, P., Elmazoglu, Z., et al. (2019). The pharmacological inhibition of fatty acid amide hydrolase prevents excitotoxic damage in the rat striatum: Possible involvement of CB1 receptors regulation. *Molecular Neurobiology*, *56*, 844–856. https://doi.org/10.1007/s12035-018-1129-2.

Ambrosi, G., Cerri, S., & Blandini, F. (2014). A further update on the role of excitotoxicity in the pathogenesis of Parkinson's disease. *Journal of Neural Transmission*, *121*(8), 849–859. https://doi.org/10.1007/s00702-013-1149-z.

Baek, J. Y., Jeong, J. Y., Kim, K. I., Won, S.-Y., Chung, Y. C., Nam, et al. (2018). Inhibition of microglia-derived oxidative stress by ciliary neurotrophic factor protects dopamine neurons in vivo from MPP + neurotoxicity. *International Journal of Molecular Sciences, 19*(11), 3543. https://doi.org/10.3390/ijms19113543.

Bai, F., Guo, F., Jiang, T., Wei, H., Zhou, H., Yin, H., et al. (2017). Arachidonyl-2-Chloroethylamide alleviates cerebral ischemia injury through glycogen synthase kinase-3β-mediated mitochondrial biogenesis and functional improvement. *Molecular Neurobiology, 54*(2), 1240–1253. https://doi.org/10.1007/s12035-016-9731-7.

Benarroch, E. (2007). Endocannabinoids in basal ganglia circuits: Implications for Parkinson disease. *Neurology, 69*(3), 306–309. https://doi.org/10.1212/01.wnl.0000267407.79757.75.

Berardelli, A., Noth, J., Thompson, P. D., Bollen, E. L. E. M., Currà, A., Deuschl, G., et al. (1999). Pathophysiology of chorea and bradykinesia in Huntington's disease. *Movement Disorders, 14*(3), 398–403. https://doi.org/10.3989/cyv.2007.v46.i1.260.

Bilkei-Gorzo, A., Albayram, O., Ativie, F., Chasan, S., Zimmer, T., Bach, K., et al. (2018). Cannabinoid 1 receptor signaling on GABAergic neurons influences astrocytes in the ageing brain. *PLoS One, 13*(8), e0202566. https://doi.org/10.1371/journal.pone.0202566.

Bisogno, T., Hanuš, L., De Petrocellis, L., Tchilibon, S., Ponde, D. E., Brandi, I., et al. (2001). Molecular targets for cannabidiol and its synthetic analogues: Effect on vanilloid VR1 receptors and on the cellular uptake and enzymatic hydrolysis of anandamide. *British Journal of Pharmacology, 134*(4), 845–852. https://doi.org/10.1038/sj.bjp.0704327.

Bisogno, T., Martire, A., Petrosino, S., Popoli, P., & Di Marzo, V. (2008). Symptom-related changes of endocannabinoid and palmitoylethanolamide levels in brain areas of R6/2 mice, a transgenic model of Huntington's disease. *Neurochemistry International, 52*(1), 307–313. https://doi.org/10.1016/j.neuint.2007.06.031.

Blázquez, C., Chiarlone, A., Bellocchio, L., Resel, E., Pruunsild, P., García-Rincón, D., et al. (2015). The CB1cannabinoid receptor signals striatal neuroprotection via a PI3K/Akt/mTORC1/BDNF pathway. *Cell Death and Differentiation, 22*(10), 1618–1629. https://doi.org/10.1038/cdd.2015.11.

Blázquez, C., Chiarlone, A., Sagredo, O., Aguado, T., Pazos, M. R., Resel, E., et al. (2011). Loss of striatal type 1 cannabinoid receptors is a key pathogenic factor in Huntington's disease. *Brain, 134*(1), 119–136. https://doi.org/10.1093/brain/awq278.

Borrell-Pagès, M., Zala, D., Humbert, S., & Saudou, F. (2006). Huntington's disease: From huntingtin function and dysfunction to therapeutic strategies. *Cellular and Molecular Life Sciences, 63*(22), 2642–2660. https://doi.org/10.1007/s00018-006-6242-0.

Bouchard, J., Truong, J., Bouchard, K., Dunkelberger, D., Desrayaud, S., Moussaoui, S., et al. (2012). Cannabinoid receptor 2 signaling in peripheral immune cells modulates disease onset and severity in mouse models of Huntington's disease. *Journal of Neuroscience, 32*(50), 18259–18268. https://doi.org/10.1523/JNEUROSCI.4008-12.2012.

Brusco, A., Tagliaferro, P., Saez, T., & Onaivi, E. S. (2008). Postsynaptic localization of CB2 cannabinoid receptors in the rat hippocampus. *Synapse, 62*(12), 944–949. https://doi.org/10.1002/syn.20569.

Cabral, G. A., Raborn, E. S., Griffin, L., Dennis, J., & Marciano-Cabral, F. (2008). CB 2 receptors in the brain: Role in central immune function. *British Journal of Pharmacology, 153*(2), 240–251. https://doi.org/10.1038/sj.bjp.0707584.

Cai, M., Yang, Q., Li, G., Sun, S., Chen, Y., Tian, L., et al. (2017). Activation of cannabinoid receptor 1 is involved in protection against mitochondrial dysfunction and cerebral ischaemic tolerance induced by isoflurane preconditioning. *British Journal of Anaesthesia, 119*(6), 1213–1223. https://doi.org/10.1093/bja/aex267.

Calabresi, P., Picconi, B., Tozzi, A., Ghiglieri, V., & Di Filippo, M. (2014). Direct and indirect pathways of basal ganglia: A critical reappraisal. *Nature Neuroscience, 17*(8), 1022–1030. https://doi.org/10.1038/nn.3743.

Mario Antonazzo et al.

Carroll, C. B., Zeissler, M. L., Hanemann, C. O., & Zajicek, J. P. (2012). Δ9-tetrahydrocannabinol (Δ9-THC) exerts a direct neuroprotective effect in a human cell culture model of Parkinson's disease. *Neuropathology and Applied Neurobiology, 38*(6), 535–547. https://doi.org/10.1111/j.1365-2990.2011.01248.x.

Castillo, A., Tolón, M. R., Fernández-Ruiz, J., Romero, J., & Martinez-Orgado, J. (2010). The neuroprotective effect of cannabidiol in an in vitro model of newborn hypoxic-ischemic brain damage in mice is mediated by CB2and adenosine receptors. *Neurobiology of Disease, 37*(2), 434–440. https://doi.org/10.1016/j.nbd.2009.10.023.

Castillo, P. E., Younts, T. J., Chávez, A. E., & Hashimotodani, Y. (2012). Endocannabinoid signaling and synaptic function. *Neuron, 76*(1), 70–81. https://doi.org/10.1016/j.neuron.2012.09.020.

Cerri, S., Levandis, G., Ambrosi, G., Montepeloso, E., Antoninetti, G. F., Franco, R., et al. (2014). Neuroprotective potential of adenosine A2Aand cannabinoid CB1receptor antagonists in an animal model of Parkinson disease. *Journal of Neuropathology and Experimental Neurology, 73*(5), 414–424. https://doi.org/10.1097/NEN.0000000000000064.

Chagas, M. H. N., Zuardi, A. W., Tumas, V., Pena-Pereira, M. A., Sobreira, E. T., Bergamaschi, M. M., et al. (2014). Effects of cannabidiol in the treatment of patients with Parkinson's disease: An exploratory double-blind trial. *Journal of Psychopharmacology, 28*(11), 1088–1092. https://doi.org/10.1177/0269881114550355.

Chen, Y., & Buck, J. (2000). Cannabinoids protect cells from oxidative cell death: A receptor-independent mechanism. *The Journal of Pharmacology and Experimental Therapeutics, 293*(3), 807–812. https://doi.org/10.1016/0306-4573(95)80035-R.

Chen, Y., McCarron, R. M., Ohara, Y., Bembry, J., Azzam, N., Lenz, F. A., et al. (2000). Human brain capillary endothelium: 2-Arachidonoglycerol (endocannabinoid) interacts with endothelin-1. *Circulation Research, 87*(4), 323–327. https://doi.org/10.1161/01.RES.87.4.323.

Chiarlone, A., Bellocchio, L., Blazquez, C., Resel, E., Soria-Gomez, E., Cannich, A., et al. (2014). A restricted population of CB1 cannabinoid receptors with neuroprotective activity. *Proceedings of the National Academy of Sciences of the United States of America, 111*(22), 8257–8262. https://doi.org/10.1073/pnas.1400988111.

Chung, Y. C., Bok, E., Huh, S. H., Park, J.-Y., Yoon, S.-H., Kim, S. R., et al. (2011). Cannabinoid receptor type 1 protects nigrostriatal dopaminergic neurons against MPTP neurotoxicity by inhibiting microglial activation. *The Journal of Immunology, 187*(12), 6508–6517. https://doi.org/10.4049/jimmunol.1102435.

Chung, Y. C., Shin, W. H., Baek, J. Y., Cho, E. J., Baik, H. H., Kim, S. R., et al. (2016). CB2 receptor activation prevents glial-derived neurotoxic mediator production, BBB leakage and peripheral immune cell infiltration and rescues dopamine neurons in the MPTP model of Parkinson's disease. *Experimental and Molecular Medicine, 48*(1), e205. https://doi.org/10.1038/emm.2015.100.

Cristino, L., Starowicz, K., De Petrocellis, L., Morishita, J., Ueda, N., Guglielmotti, V., et al. (2008). Immunohistochemical localization of anabolic and catabolic enzymes for anandamide and other putative endovanilloids in the hippocampus and cerebellar cortex of the mouse brain. *Neuroscience, 151*(4), 955–968. https://doi.org/10.1016/j.neuroscience.2007.11.047.

Dasilva, M., Grieve, K. L., Cudeiro, J., & Rivadulla, C. (2014). Anandamide activation of CB1 receptors increases spontaneous bursting and oscillatory activity in the thalamus. *Neuroscience, 265*, 72–82. https://doi.org/10.1016/j.neuroscience.2014.01.049.

Demuth, D. G., & Molleman, A. (2006). Cannabinoid signalling. *Life Sciences, 78*, 549–563. https://doi.org/10.1016/j.lfs.2005.05.055.

Denovan-Wright, E. M., & Robertson, H. A. (2000). Cannabinoid receptor messenger RNA levels decrease in a subset of neurons of the lateral striatum, cortex and hippocampus of transgenic Huntington's disease mice. *Neuroscience, 98*(4), 705–713. https://doi.org/10.1016/S0306-4522(00)00157-3.

Devane, W. A., Hanuš, L., Breuer, A., Pertwee, R. G., Stevenson, L. A., Griffin, G., et al. (1992). Isolation and structure of a brain constituent that binds to the cannabinoid receptor. *Science*, *258*(5090), 1946–1949. https://doi.org/10.1126/science.1470919.

Díaz-Alonso, J., Paraíso-Luna, J., Navarrete, C., Del Río, C., Cantarero, I., Palomares, B., et al. (2016). VCE-003.2, a novel cannabigerol derivative, enhances neuronal progenitor cell survival and alleviates symptomatology in murine models of Huntington's disease. *Scientific Reports*, *6*(1), 29789. https://doi.org/10.1038/srep29789.

Domenici, M. R. (2006). Cannabinoid receptor type 1 located on presynaptic terminals of principal neurons in the forebrain controls glutamatergic synaptic transmission. *Journal of Neuroscience*, *26*(21), 5794–5799. https://doi.org/10.1523/JNEUROSCI.0372-06.2006.

Dowie, M. J., Bradshaw, H. B., Howard, M. L., Nicholson, L. F. B., Faull, R. L. M., Hannan, A. J., et al. (2009). Altered CB1 receptor and endocannabinoid levels precede motor symptom onset in a transgenic mouse model of Huntington's disease. *Neuroscience*, *163*(1), 456–465. https://doi.org/10.1016/j.neuroscience.2009.06.014.

Escamilla-Ramírez, A., García, E., Palencia-Hernández, G., Colín-González, A. L., Galván-Arzate, S., Túnez, I., et al. (2017). URB597 and the cannabinoid WIN55,212-2 reduce behavioral and neurochemical deficits induced by MPTP in mice: Possible role of redox modulation and NMDA receptors. *Neurotoxicity Research*, *31*(4), 532–544. https://doi.org/10.1007/s12640-016-9698-1.

Esposito, G., De Filippis, D., Maiuri, M. C., De Stefano, D., Carnuccio, R., & Iuvone, T. (2006). Cannabidiol inhibits inducible nitric oxide synthase protein expression and nitric oxide production in β-amyloid stimulated PC12 neurons through p38 MAP kinase and NF-κB involvement. *Neuroscience Letters*, *399*(1–2), 91–95. https://doi.org/10.1016/j.neulet.2006.01.047.

Esposito, G., Scuderi, C., Savani, C., Steardo, L., De Filippis, D., Cottone, P., et al. (2007). Cannabidiol in vivo blunts β-amyloid induced neuroinflammation by suppressing IL-1β and iNOS expression. *British Journal of Pharmacology*, *151*(8), 1272–1279. https://doi.org/10.1038/sj.bjp.0707337.

Fernández-Ruiz, J., Gómez-Ruiz, M., García, C., Hernández, M., & Ramos, J. A. (2017). Modeling neurodegenerative disorders for developing cannabinoid-based neuroprotective therapies. In *Vol. 593*. *Methods in enzymology* (pp. 175–198). Academic Press. https://doi.org/10.1016/bs.mie.2017.06.021.

Fernández-Ruiz, J., Hernández, M., & Ramos, J. A. (2010). Cannabinoid-dopamine interaction in the pathophysiology and treatment of CNS disorders. *CNS Neuroscience & Therapeutics*, *16*(3), e72–e91. https://doi.org/10.1111/j.1755-5949.2010.00144.x.

Fernández-Ruiz, J., Moreno-Martet, M., Rodríguez-Cueto, C., Palomo-Garo, C., Gomez-Cañas, M., Valdeolivas, S., et al. (2011). Prospects for cannabinoid therapies in basal ganglia disorders. *British Journal of Pharmacology*, *163*(7), 1365–1378. https://doi.org/10.1111/j.1476-5381.2011.01365.x.

Fernández-Ruiz, J., Pazos, M. R., García-Arencibia, M., Sagredo, O., & Ramos, J. A. (2008). Role of CB2 receptors in neuroprotective effects of cannabinoids. *Molecular and Cellular Endocrinology*, *286*(1–2 Suppl. 1), S91–S96. https://doi.org/10.1016/j.mce.2008.01.001.

Fernández-Ruiz, J., Romero, J., & Ramos, J. A. (2015). Endocannabinoids and neurodegenerative disorders: Parkinson's disease, Huntington's chorea, Alzheimer's disease, and others. In R. G. Pertwee (Ed.), *Endocannabinoids* (pp. 233–259). Cham: Springer International Publishing. https://doi.org/10.1007/978-3-319-20825-1_8.

Fernández-Ruiz, J., Romero, J., Velasco, G., Tolón, R. M., Ramos, J. A., & Guzmán, M. (2007). Cannabinoid CB2 receptor: A new target for controlling neural cell survival? *Trends in Pharmacological Sciences*, *28*(1), 39–45. https://doi.org/10.1002/aqc.967.

Fernández-Ruiz, J., Sagredo, O., Pazos, M. R., García, C., Pertwee, R., Mechoulam, R., et al. (2013). Cannabidiol for neurodegenerative disorders: Important new clinical

applications for this phytocannabinoid? *British Journal of Clinical Pharmacology*, 75(2), 323–333. https://doi.org/10.1111/j.1365-2125.2012.04341.x.

Fernández-Suárez, D., Celorrio, M., Riezu-Boj, J. I., Ugarte, A., Pacheco, R., González, H., et al. (2014). The monoacylglycerol lipase inhibitor JZL184 is neuroprotective and alters glial cell phenotype in the chronic MPTP mouse model. *Neurobiology of Aging*, 35(11), 2603–2616. https://doi.org/10.1016/j.neurobiolaging.2014.05.021.

Ferrer, B., Asbrock, N., Kathuria, S., Piomelli, D., & Giuffrida, A. (2003). Effects of levodopa on endocannabinoid levels in rat basal ganglia: Implications for the treatment of levodopa-induced dyskinesias. *European Journal of Neuroscience*, 18(6), 1607–1614. https://doi.org/10.1046/j.1460-9568.2003.02896.x.

Fidaleo, M., Fanelli, F., Ceru, M., & Moreno, S. (2014). Neuroprotective properties of peroxisome proliferator-activated receptor alpha (PPARα) and its lipid ligands. *Current Medicinal Chemistry*, 21(24), 2803–2821. https://doi.org/10.2174/0929867321666140303143455.

Fitzgerald, M. L., Shobin, E., & Pickel, V. M. (2012). Cannabinoid modulation of the dopaminergic circuitry: Implications for limbic and striatal output. *Progress in Neuro-Psychopharmacology and Biological Psychiatry*, 38(1), 21–29. https://doi.org/10.1016/j.pnpbp.2011.12.004.

Fowler, C. J., Jonsson, K.-O., Andersson, A., Juntunen, J., Järvinen, T., Vandevoorde, S., et al. (2003). Inhibition of C6 glioma cell proliferation by anandamide, 1-arachidonoylglycerol, and by a water soluble phosphate ester of anandamide: Variability in response and involvement of arachidonic acid. *Biochemical Pharmacology*, 66(5), 757–767.

Geldenhuys, W. J., & Van der Schyf, C. J. (2013). Rationally designed multi-targeted agents against neurodegenerative diseases. *Current Medicinal Chemistry*, 20(13), 1662–1672. https://doi.org/10.2174/09298673113209990112.

Gerdeman, G., & Lovinger, D. M. (2001). CB1 cannabinoid receptor inhibits synaptic release of glutamate in rat dorsolateral striatum. *Journal of Neurophysiology*, 85(1), 468–471.

Gerfen, C. R., & Surmeier, D. J. (2011). Modulation of striatal projection systems by dopamine. *Annual Review of Neuroscience*, 34(1), 441–466. https://doi.org/10.1146/annurev-neuro-061010-113641.

Glass, M., Dragunow, M., & Faull, R. L. M. (2000). The pattern of neurodegeneration in Huntington's disease: A comparative study of cannabinoid, dopamine, adenosine and GABA(A) receptor alterations in the human basal ganglia in Huntington's disease. *Neuroscience*, 97(3), 505–519. https://doi.org/10.1016/S0306-4522(00)00008-7.

Glass, M., Van Dellen, A., Blakemore, C., Hannan, A. J., & Faull, R. L. M. (2004). Delayed onset of Huntington's disease in mice in an enriched environment correlates with delayed loss of cannabinoid CB1 receptors. *Neuroscience*, 123(1), 207–212. https://doi.org/10.1016/S0306-4522(03)00595-5.

Gong, J. P., Onaivi, E. S., Ishiguro, H., Liu, Q. R., Tagliaferro, P. A., Brusco, A., et al. (2006). Cannabinoid CB2 receptors: Immunohistochemical localization in rat brain. *Brain Research*, 1071(1), 10–23. https://doi.org/10.1016/j.brainres.2005.11.035.

Gulyas, A. I., Cravatt, B. F., Bracey, M. H., Dinh, T. P., Piomelli, D., Boscia, F., et al. (2004). Segregation of two endocannabinoid-hydrolyzing enzymes into pre- and postsynaptic compartments in the rat hippocampus, cerebellum and amygdala. *European Journal of Neuroscience*, 20(2), 441–458. https://doi.org/10.1111/j.1460-9568.2004.03428.x.

Hampson, A. J., Grimaldi, M., Axelrod, J., & Wink, D. (1998). Cannabidiol and (−)9-tetrahydrocannabinol are neuroprotective antioxidants. *Proceedings of the National Academy of Sciences of the United States of America*, 95(14), 8268–8273. https://doi.org/10.1073/pnas.95.14.8268.

Hansen, H. H., Azcoitia, I., Pons, S., Romero, J., García-Segura, L. M., Ramos, J. A., et al. (2002). Blockade of cannabinoid CB1receptor function protects against in vivo disseminating brain damage following NMDA-induced excitotoxicity. *Journal of Neurochemistry*, *82*(1), 154–158. https://doi.org/10.1046/j.1471-4159.2002.00961.x.

Hashimotodani, Y., Ohno-Shosaku, T., & Kano, M. (2007). Presynaptic Monoacylglycerol lipase activity determines basal endocannabinoid tone and terminates retrograde endocannabinoid signaling in the Hippocampus. *Journal of Neuroscience*, *27*(5), 1211–1219. https://doi.org/10.1523/JNEUROSCI.4159-06.2007.

Hedreen, J. C., Peyser, C. E., Folstein, S. E., & Ross, C. A. (1991). Neuronal loss in layers V and VI of cerebral cortex in Huntington's disease. *Neuroscience Letters*, *133*(2), 257–261. https://doi.org/10.1016/0304-3940(91)90583-F.

Heinsen, H., Strik, M., Bauer, M., Luther, K., Ulmar, G., Gangnus, D., et al. (1994). Cortical and striatal neurone number in Huntington's disease. *Acta Neuropathologica*, *88*(4), 320–333. https://doi.org/10.1007/BF00310376.

Hohmann, A. G., & Herkenham, M. (2000). Localization of cannabinoid CB1receptor mRNA in neuronal subpopulations of rat striatum: A double-label in situ hybridization study. *Synapse*, *37*(1), 71–80. https://doi.org/10.1002/(SICI)1098-2396(200007)37:1<71::AID-SYN8>3.0.CO;2-K.

Iuvone, T., Esposito, G., De Filippis, D., Scuderi, C., & Steardo, L. (2009). Cannabidiol: A promising drug for neurodegenerative disorders? *CNS Neuroscience and Therapeutics*, *15*(1), 65–75. https://doi.org/10.1111/j.1755-5949.2008.00065.x.

Javed, H., Azimullah, S., Haque, M. E., & Ojha, S. K. (2016). Cannabinoid type 2 (CB2) receptors activation protects against oxidative stress and neuroinflammation associated dopaminergic neurodegeneration in rotenone model of parkinson's disease. *Frontiers in Neuroscience*, *10*, 321. https://doi.org/10.3389/fnins.2016.00321.

Kallendrusch, S., Kremzow, S., Nowicki, M., Grabiec, U., Winkelmann, R., Benz, A., et al. (2013). The G protein-coupled receptor 55 ligand l-α-lysophosphatidylinositol exerts microglia-dependent neuroprotection after excitotoxic lesion. *Glia*, *61*(11), 1822–1831. https://doi.org/10.1002/glia.22560.

Karanian, D. A., Karim, S. L., Wood, J. T., Williams, J. S., Lin, S., Makriyannis, A., et al. (2007). Endocannabinoid enhancement protects against Kainic acid-induced seizures and associated brain damage. *Journal of Pharmacology and Experimental Therapeutics*, *322*(3), 1059–1066. https://doi.org/10.1124/jpet.107.120147.

Katona, I., & Freund, T. F. (2008). Endocannabinoid signaling as a synaptic circuit breaker in neurological disease. *Nature Medicine*, *14*(9), 923–930. https://doi.org/10.1038/nm.f.1869.

Kaur, K., Gill, J. S., Bansal, P. K., & Deshmukh, R. (2017). Neuroinflammation—a major cause for striatal dopaminergic degeneration in Parkinson's disease. *Journal of the Neurological Sciences*, *381*, 308–314. https://doi.org/10.1016/j.jns.2017.08.3251.

Khaspekov, L. G., Verca, M. S. B., Frumkina, L. E., Hermann, H., Marsicano, G., & Lutz, B. (2004). Involvement of brain-derived neurotrophic factor in cannabinoid receptor-dependent protection against excitotoxicity. *European Journal of Neuroscience*, *19*(7), 1691–1698. https://doi.org/10.1111/j.1460-9568.2004.03285.x.

Kim, S. R., Lee, D. Y., Chung, E. S., Oh, U. T., Kim, S. U., & Jin, B. K. (2005). Transient receptor potential Vanilloid subtype 1 mediates cell death of mesencephalic dopaminergic neurons in vivo and in vitro. *Journal of Neuroscience*, *25*(3), 662–671. https://doi.org/10.1523/JNEUROSCI.4166-04.2005.

Kofalvi, A. (2005). Involvement of cannabinoid receptors in the regulation of neurotransmitter release in the rodent striatum: A combined immunochemical and pharmacological analysis. *Journal of Neuroscience*, *25*(11), 2874–2884. https://doi.org/10.1523/JNEUROSCI.4232-04.2005.

Lanciego, J. L., Barroso-Chinea, P., Rico, A. J., Conte-Perales, L., Callén, L., Roda, E., et al. (2011). Expression of the mRNA coding the cannabinoid receptor 2 in the pallidal complex of *Macaca fascicularis*. *Journal of Psychopharmacology*, *25*(1), 97–104. https://doi.org/10.1177/0269881110367732.

Laprairie, R. B., Warford, J. R., Hutchings, S., Robertson, G. S., Kelly, M. E. M., & Denovan-Wright, E. M. (2014). The cytokine and endocannabinoid systems are co-regulated by NF-κB p65/RelA in cell culture and transgenic mouse models of Huntington's disease and in striatal tissue from Huntington's disease patients. *Journal of Neuroimmunology*, *267*(1–2), 61–72. https://doi.org/10.1016/j.jneuroim.2013.12.008.

Lastres-Becker, I., Bizat, N., Boyer, F., Hantraye, P., Fernández-Ruiz, J., & Brouillet, E. (2004). Potential involvement of cannabinoid receptors in 3-nitropropionic acid toxicity in vivo. *Neuroreport*, *15*(15), 2375–2379. https://doi.org/10.1097/00001756-200410250-00015.

Lastres-Becker, I., Molina-Holgado, F., Ramos, J. A., Mechoulam, R., & Fernández-Ruiz, J. (2005). Cannabinoids provide neuroprotection against 6-hydroxydopamine toxicity in vivo and in vitro: Relevance to Parkinson's disease. *Neurobiology of Disease*, *19*(1–2), 96–107. https://doi.org/10.1016/j.nbd.2004.11.009.

Leweke, F. M., Piomelli, D., Pahlisch, F., Muhl, D., Gerth, C. W., Hoyer, C., et al. (2012). Cannabidiol enhances anandamide signaling and alleviates psychotic symptoms of schizophrenia. *Translational Psychiatry*, *2*(3), e94. https://doi.org/10.1038/tp.2012.15.

Liu, H., Song, Z., Liao, D., Zhang, T., Liu, F., Zhuang, K., et al. (2014). Neuroprotective effects of trans-Caryophyllene against Kainic acid induced seizure activity and oxidative stress in mice. *Neurochemical Research*, *40*(1), 118–123. https://doi.org/10.1007/s11064-014-1474-0.

López, A., Aparicio, N., Pazos, M. R., Grande, M. T., Barreda-Manso, M. A., Benito-Cuesta, I., et al. (2018). Cannabinoid CB2receptors in the mouse brain: Relevance for Alzheimer's disease. *Journal of Neuroinflammation*, *15*(1), 158. https://doi.org/10.1186/s12974-018-1174-9.

López-Sendón Moreno, J. L., García Caldentey, J., Trigo Cubillo, P., Ruiz Romero, C., García Ribas, G., Alonso Arias, M. A. A., et al. (2016). A double-blind, randomized, cross-over, placebo-controlled, pilot trial with Sativex in Huntington's disease. *Journal of Neurology*, *263*(7), 1390–1400. https://doi.org/10.1007/s00415-016-8145-9.

Lull, M. E., & Block, M. L. (2010). Microglial activation and chronic neurodegeneration. *Neurotherapeutics*, *7*(4), 354–365. https://doi.org/10.1016/j.nurt.2010.05.014.

Ma, L., Jia, J., Niu, W., Jiang, T., Zhai, Q., Yang, L., et al. (2015). Mitochondrial CB1 receptor is involved in ACEA-induced protective effects on neurons and mitochondrial functions. *Scientific Reports*, *5*(1), 12440. https://doi.org/10.1038/srep12440.

MacDonald, M. E., Ambrose, C. M., Duyao, M. P., Myers, R. H., Lin, C., Srinidhi, L., et al. (1993). A novel gene containing a trinucleotide repeat that is expanded and unstable on Huntington's disease chromosomes. *Cell*, *72*(6), 971–983. https://doi.org/10.1016/0092-8674(93)90585-E.

Mailleux, P., & Vanderhaeghen, J. J. (1992). Distribution of neuronal cannabinoid receptor in the adult rat brain: A comparative receptor binding radioautography and in situ hybridization histochemistry. *Neuroscience*, *48*(3), 655–668. https://doi.org/10.1016/0306-4522(92)90409-U.

Malek, N., Popiolek-Barczyk, K., Mika, J., Przewlocka, B., & Starowicz, K. (2015). Anandamide, acting via CB2 receptors, alleviates LPS-induced neuroinflammation in rat primary microglial cultures. *Neural Plasticity*, *2015*, 130639. https://doi.org/10.1155/2015/130639.

Marsicano, G., Moosmann, B., Hermann, H., Lutz, B., & Behl, C. (2002). Neuroprotective properties of cannabinoids against oxidative stress: Role of the cannabinoid receptor CB1. *Journal of Neurochemistry*, *80*(3), 448–456. https://doi.org/10.1046/j.0022-3042.2001.00716.x.

Massano, J., & Bhatia, K. P. (2012). Clinical approach to Parkinson's disease: Features, diagnosis, and principles of management. *Cold Spring Harbor Perspectives in Medicine*, *2*(6), a008870. https://doi.org/10.1101/cshperspect.a008870.

Maya-López, M., Colín-González, A. L., Aguilera, G., de Lima, M. E., Colpo-Ceolin, A., Rangel-López, E., et al. (2017). Neuroprotective effect of WIN55,212-2 against 3-nitropropionic acid-induced toxicity in the rat brain: Involvement of CB1 and NMDA receptors. *American Journal of Translational Research*, *9*(2), 261–274. Retrieved from http://www.ncbi.nlm.nih.gov/pubmed/28337258.

Maya-López, M., Ruiz-Contreras, H. A., de Jesús Negrete-Ruíz, M., Martínez-Sánchez, J. E., Benítez-Valenzuela, J., Colín-González, A. L., et al. (2017). URB597 reduces biochemical, behavioral and morphological alterations in two neurotoxic models in rats. *Biomedicine and Pharmacotherapy*, *88*, 745–753. https://doi.org/10.1016/j.biopha.2017.01.116.

McCaw, E. A., Hu, H., Gomez, G. T., Hebb, A. L. O., Kelly, M. E. M., & Denovan-Wright, E. M. (2004). Structure, expression and regulation of the cannabinoid receptor gene (CB1) in Huntington's disease transgenic mice. *European Journal of Biochemistry*, *271*(23–24), 4909–4920. https://doi.org/10.1111/j.1432-1033.2004.04460.x.

Mechoulam, R., Panikashvili, D., & Shohami, E. (2002). Cannabinoids and brain injury: Therapeutic implications. *Trends in Molecular Medicine*, *8*(2), 58–61. https://doi.org/10.1016/S1471-4914(02)02276-1.

Mezey, E., Toth, Z. E., Cortright, D. N., Arzubi, M. K., Krause, J. E., Elde, R., et al. (2000). Distribution of mRNA for vanilloid receptor subtype 1 (VR1), and VR1-like immunoreactivity, in the central nervous system of the rat and human. *Proceedings of the National Academy of Sciences of the United States of America*, *97*(7), 3655–3660. https://doi.org/10.1073/pnas.97.7.3655.

Mievis, S., Blum, D., & Ledent, C. (2011). Worsening of Huntington disease phenotype in CB1 receptor knockout mice. *Neurobiology of Disease*, *42*(3), 524–529. https://doi.org/10.1016/j.nbd.2011.03.006.

Morera-Herreras, T., Miguelez, C., Aristieta, A., Ruiz-Ortega, J. Á., & Ugedo, L. (2012). Endocannabinoid modulation of dopaminergic motor circuits. *Frontiers in Pharmacology*, *3*, 110. https://doi.org/10.3389/fphar.2012.00110.

Muñoz-Arenas, G., Paz-Bermúdez, F., Báez-Cordero, A., Caballero-Florán, R., González-Hernández, B., Florán, B., et al. (2015). Cannabinoid CB1 receptors activation and coactivation with D2 receptors modulate GABAergic neurotransmission in the globus pallidus and increase motor asymmetry. *Synapse*, *69*(3), 103–114. https://doi.org/10.1002/syn.21796.

Munro, S., Thomas, K. L., & Abu-Shaar, M. (1993). Molecular characterization of a peripheral receptor for cannabinoids. *Nature*, *365*(6441), 61–65. https://doi.org/10.1038/365061a0.

Nadler, V., Mechoulam, R., & Sokolovsky, M. (1993). Blockade of 45Ca2+ influx through the N-methyl-d-aspartate receptor ion channel by the non-psychoactive cannabinoid HU-211. *Brain Research*, *622*(1–2), 79–85. https://doi.org/10.1016/0006-8993(93)90804-V.

Naidoo, V., Nikas, S. P., Karanian, D. A., Hwang, J., Zhao, J., Wood, J. A. T., et al. (2011). A new generation fatty acid amide hydrolase inhibitor protects against kainate-induced excitotoxicity. *Journal of Molecular Neuroscience*, *43*(3), 493–502. https://doi.org/10.1007/s12031-010-9472-4.

Navarrete, F., García-Gutiérrez, M. S., Aracil-Fernández, A., Lanciego, J. L., & Manzanares, J. (2018). Cannabinoid CB1 and CB2 receptors, and Monoacylglycerol lipase gene expression alterations in the basal ganglia of patients with Parkinson's disease. *Neurotherapeutics*, *15*(2), 1–11. https://doi.org/10.1007/s13311-018-0603-x.

Navarro, G., Morales, P., Rodríguez-Cueto, C., Fernández-Ruiz, J., Jagerovic, N., & Franco, R. (2016). Targeting cannabinoid CB2 receptors in the central nervous system. Medicinal chemistry approaches with focus on neurodegenerative disorders. *Frontiers in Neuroscience*, *10*(Sep), 406. https://doi.org/10.3389/fnins.2016.00406.

Naydenov, A. V., Sepers, M. D., Swinney, K., Raymond, L. A., Palmiter, R. D., & Stella, N. (2014). Genetic rescue of CB1receptors on medium spiny neurons prevents loss of excitatory striatal synapses but not motor impairment in HD mice. *Neurobiology of Disease*, *71*, 140–150. https://doi.org/10.1016/j.nbd.2014.08.009.

Núñez, E., Benito, C., Tolón, R. M., Hillard, C. J., Griffin, W. S. T., & Romero, J. (2008). Glial expression of cannabinoid CB2 receptors and fatty acid amide hydrolase are beta amyloid-linked events in Down's syndrome. *Neuroscience*, *151*(1), 104–110. https://doi.org/10.1016/j.neuroscience.2007.10.029.

Nussbaum, R. L., & Ellis, C. E. (2003). Alzheimer's disease and Parkinson's disease. *New England Journal of Medicine*, *348*(14), 1356–1364. https://doi.org/10.1056/NEJM2003ra020003.

O'Sullivan, S. E. (2016). An update on PPAR activation by cannabinoids. *British Journal of Pharmacology*, *173*(12), 1899–1910. https://doi.org/10.1111/bph.13497.

Oh, Y. T., Lee, J. Y., Lee, J., Lee, J. H., Kim, J. E., Ha, J., et al. (2010). Oleamide suppresses lipopolysaccharide-induced expression of iNOS and COX-2 through inhibition of NF-κB activation in BV2 murine microglial cells. *Neuroscience Letters*, *474*(3), 148–153. https://doi.org/10.1016/j.neulet.2010.03.026.

Ojha, S., Javed, H., Azimullah, S., & Haque, M. E. (2016). β–Caryophyllene, a phytocannabinoid attenuates oxidative stress, neuroinflammation, glial activation, and salvages dopaminergic neurons in a rat model of Parkinson disease. *Molecular and Cellular Biochemistry*, *418*(1–2), 59–70. https://doi.org/10.1007/s11010-016-2733-y.

Onaivi, E. S., Ishiguro, H., Gong, J. P., Patel, S., Perchuk, A., Meozzi, P. A., et al. (2006). Discovery of the presence and functional expression of cannabinoid CB2 receptors in brain. *Annals of the New York Academy of Sciences*, *1074*(1), 514–536. https://doi.org/10.1196/annals.1369.052.

Ouchi, Y., Yoshikawa, E., Sekine, Y., Futatsubashi, M., Kanno, T., Ogusu, T., et al. (2005). Microglial activation and dopamine terminal loss in early Parkinson's disease. *Annals of Neurology*, *57*(2), 168–175. https://doi.org/10.1002/ana.20338.

Palazuelos, J., Aguado, T., Pazos, M. R., Julien, B., Carrasco, C., Resel, E., et al. (2009). Microglial CB2 cannabinoid receptors are neuroprotective in Huntington's disease excitotoxicity. *Brain*, *132*(11), 3152–3164. https://doi.org/10.1093/brain/awp239.

Pazos, M. R., Mohammed, N., Lafuente, H., Santos, M., Martínez-Pinilla, E., Moreno, E., et al. (2013). Mechanisms of cannabidiol neuroprotection in hypoxic-ischemic newborn pigs: Role of 5HT1Aand CB2 receptors. *Neuropharmacology*, *71*, 282–291. https://doi.org/10.1016/j.neuropharm.2013.03.027.

Pelição, R., Santos, M. C., Freitas-Lima, L. C., Meyrelles, S. S., Vasquez, E. C., Nakamura-Palacios, E. M., et al. (2016). URB597 inhibits oxidative stress induced by alcohol binging in the prefrontal cortex of adolescent rats. *Neuroscience Letters*, *624*, 17–22. https://doi.org/10.1016/j.neulet.2016.04.068.

Pintor, A., Tebano, M. T., Martire, A., Grieco, R., Galluzzo, M., Scattoni, M. L., et al. (2006). The cannabinoid receptor agonist WIN 55,212-2 attenuates the effects induced by quinolinic acid in the rat striatum. *Neuropharmacology*, *51*(5), 1004–1012. https://doi.org/10.1016/j.neuropharm.2006.06.013.

Piomelli, D. (2003). The molecular logic of endocannabinoid signalling. *Nature Reviews Neuroscience*, *4*(11), 873–884. https://doi.org/10.1038/nrn1247.

Poewe, W., & Mahlknecht, P. (2010). The clinical progression of Parkinson's disease. *Parkinsonism & Related Disorders*, *15*(Suppl. 4), S28–S32. https://doi.org/10.1016/S1353-8020(09)70831-4.

Price, D. A., Martinez, A. A., Seillier, A., Koek, W., Acosta, Y., Fernandez, E., et al. (2009). WIN55,212-2, a cannabinoid receptor agonist, protects against nigrostriatal cell loss in the 1-methyl-4-phenyl-1,2,3,6-tetrahydropyridine mouse model of Parkinson's disease. *European Journal of Neuroscience*, *29*(11), 2177–2186. https://doi.org/10.1111/j.1460-9568.2009.06764.x.

Ramirez, B. G. (2005). Prevention of Alzheimer's disease pathology by cannabinoids: Neuroprotection mediated by blockade of microglial activation. *Journal of Neuroscience*, *25*(8), 1904–1913. https://doi.org/10.1523/JNEUROSCI.4540-04.2005.

Ramsey, C. P., & Tansey, M. G. (2014). A survey from 2012 of evidence for the role of neuroinflammation in neurotoxin animal models of Parkinson's disease and potential molecular targets. *Experimental Neurology*, *256*, 126–132. https://doi.org/10.1016/j.expneurol.2013.05.014.

Rangel-López, E., Colín-González, A. L., Paz-Loyola, A. L., Pinzón, E., Torres, I., Serratos, I. N., et al. (2015). Cannabinoid receptor agonists reduce the short-term mitochondrial dysfunction and oxidative stress linked to excitotoxicity in the rat brain. *Neuroscience*, *285*, 97–106. https://doi.org/10.1016/j.neuroscience.2014.11.016.

Reiner, A., Albin, R. L., Anderson, K. D., D'Amato, C. J., Penney, J. B., & Young, A. B. (1988). Differential loss of striatal projection neurons in Huntington disease. *Proceedings of the National Academy of Sciences of the United States of America*, *85*(15), 5733–5737. https://doi.org/10.1073/pnas.85.15.5733.

Romero, J., Lastres-Becker, I., De Miguel, R., Berrendero, F., Ramos, J. A., & Fernández-Ruiz, J. (2002). The endogenous cannabinoid system and the basal ganglia: Biochemical, pharmacological, and therapeutic aspects. *Pharmacology and Therapeutics*, *95*(2), 137–152. https://doi.org/10.1016/S0163-7258(02)00253-X.

Saft, C., Von Hein, S. M., Lucke, T., Thiels, C., Peball, M., Djamshidian, A., et al. (2018). Cannabinoids for treatment of dystonia in Huntington's disease. *Journal of Huntington's Disease*, *7*(2), 167–173. https://doi.org/10.3233/JHD-170283.

Sagredo, O., García-Arencibia, M., De Lago, E., Finetti, S., Decio, A., & Fernández-Ruiz, J. (2007). Cannabinoids and neuroprotection in basal ganglia disorders. *Molecular Neurobiology*, *36*(1), 82–91. https://doi.org/10.1007/s12035-007-0004-3.

Sagredo, O., González, S., Aroyo, I., Pazos, M. R., Benito, C., Lastres-Becker, I., et al. (2009). Cannabinoid CB2 receptor agonists protect the striatum against malonate toxicity: Relevance for Huntington's disease. *Glia*, *57*(11), 1154–1167. https://doi.org/10.1002/glia.20838.

Sagredo, O., Pazos, M. R., Satta, V., Ramos, J. A., Pertwee, R. G., & Fernández-Ruiz, J. (2011). Neuroprotective effects of phytocannabinoid-based medicines in experimental models of Huntington's disease. *Journal of Neuroscience Research*, *89*(9), 1509–1518. https://doi.org/10.1002/jnr.22682.

Schapira, A. H. (2008). Mitochondria in the aetiology and pathogenesis of Parkinson's disease. *The Lancet Neurology*, *7*(1), 97–109. https://doi.org/10.1016/S1474-4422(07)70327-7.

Schapira, A. H. V., Olanow, C. W., Greenamyre, J. T., & Bezard, E. (2014). Slowing of neurodegeneration in Parkinson's disease and Huntington's disease: Future therapeutic perspectives. *The Lancet*, *384*(9942), 545–555. https://doi.org/10.1016/S0140-6736(14)61010-2.

Scuderi, C., Steardo, L., & Esposito, G. (2014). Cannabidiol promotes amyloid precursor protein ubiquitination and reduction of beta amyloid expression in SHSY5YAPP + cells through PPARγ involvement. *Phytotherapy Research*, *28*(7), 1007–1013. https://doi.org/10.1002/ptr.5095.

Serpa, A., Pinto, I., Bernardino, L., & Cascalheira, J. F. (2015). Combined neuroprotective action of adenosine A1 and cannabinoid CB1 receptors against NMDA-induced excitotoxicity in the hippocampus. *Neurochemistry International*, *87*, 106–109. https://doi.org/10.1016/j.neuint.2015.06.005.

Sheng, W. S., Hu, S., Ni, H. T., Rock, R. B., & Peterson, P. K. (2009). WIN55,212-2 inhibits production of CX3CL1 by human astrocytes: Involvement of p38 MAP kinase. *Journal of Neuroimmune Pharmacology*, *4*(2), 244–248. https://doi.org/10.1007/s11481-009-9147-5.

Sierra, S., Luquin, N., Rico, A. J., Gómez-Bautista, V., Roda, E., Dopeso-Reyes, I. G., et al. (2015). Detection of cannabinoid receptors CB1 and CB2 within basal ganglia output neurons in macaques: Changes following experimental parkinsonism. *Brain Structure and Function, 220*(5), 2721–2738. https://doi.org/10.1007/s00429-014-0823-8.

Smith, S. R., Terminelli, C., & Denhardt, G. (2000). Effects of cannabinoid receptor agonist and antagonist ligands on production of inflammatory cytokines and anti-inflammatory interleukin-10 in endotoxemic mice. *The Journal of Pharmacology and Experimental Therapeutics, 293*(1), 136–150. Retrieved from http://www.ncbi.nlm.nih.gov/pubmed/10734163.

Solinas, M., Justinova, Z., Goldberg, S. R., & Tanda, G. (2006). Anandamide administration alone and after inhibition of fatty acid amide hydrolase (FAAH) increases dopamine levels in the nucleus accumbens shell in rats. *Journal of Neurochemistry, 98*(2), 408–419. https://doi.org/10.1111/j.1471-4159.2006.03880.x.

Starowicz, K., Nigam, S., & Di Marzo, V. (2007). Biochemistry and pharmacology of endovanilloids. *Pharmacology and Therapeutics, 114*(1), 13–33. https://doi.org/10.1016/j.pharmthera.2007.01.005.

Sugiura, T., Kishimoto, S., Oka, S., & Gokoh, M. (2006). Biochemistry, pharmacology and physiology of 2-arachidonoylglycerol, an endogenous cannabinoid receptor ligand. *Progress in Lipid Research, 45*(5), 405–446. https://doi.org/10.1016/j.plipres.2006.03.003.

Sun, S., Hu, F., Wu, J., & Zhang, S. (2017). Cannabidiol attenuates OGD/R-induced damage by enhancing mitochondrial bioenergetics and modulating glucose metabolism via pentose-phosphate pathway in hippocampal neurons. *Redox Biology, 11*, 577–585. https://doi.org/10.1016/j.redox.2016.12.029.

Takahashi, K. A., & Castillo, P. E. (2006). The CB1 cannabinoid receptor mediates glutamatergic synaptic suppression in the hippocampus. *Neuroscience, 139*(3), 795–802. https://doi.org/10.1016/j.neuroscience.2006.01.024.

Tanimura, A., Yamazaki, M., Hashimotodani, Y., Uchigashima, M., Kawata, S., Abe, M., et al. (2010). The endocannabinoid 2-Arachidonoylglycerol produced by diacylglycerol lipase α mediates retrograde suppression of synaptic transmission. *Neuron, 65*(3), 320–327. https://doi.org/10.1016/j.neuron.2010.01.021.

Teismann, P., & Schulz, J. B. (2004). Cellular pathology of Parkinson's disease: Astrocytes, microglia and inflammation. *Cell and Tissue Research, 318*(1), 149–161. https://doi.org/10.1007/s00441-004-0944-0.

Thomas, B. (2009). Parkinson's disease: From molecular pathways in disease to therapeutic approaches. *Antioxidants & Redox Signaling, 11*(9), 2077–2082. https://doi.org/10.1089/ars.2009.2697.

van der Stelt, M., & Di Marzo, V. (2003). The endocannabinoid system in the basal ganglia and in the mesolimbic reward system: Implications for neurological and psychiatric disorders. *European Journal of Pharmacology, 480*(1–3), 133–150. https://doi.org/10.1016/j.ejphar.2003.08.101.

van der Stelt, M., Veldhuis, W. B., Bär, P. R., Veldink, G. A., Vliegenthart, J. F. G., & Nicolay, K. (2001). Neuroprotection by Δ^9-tetrahydrocannabinol, the main active compound in marijuana, against Ouabain-induced in vivo excitotoxicity. *The Journal of Neuroscience, 21*(17), 6475–6479. https://doi.org/10.1523/JNEUROSCI.21-17-06475.2001.

van der Stelt, M., Veldhuis, W. B., Maccarrone, M., Bär, P. R., Nicolay, K., Veldink, G. A., et al. (2002). Acute neuronal injury, excitotoxicity, and the endocannabinoid system. *Molecular Neurobiology, 26*(2–3), 317–346. https://doi.org/10.1385/MN:26:2-3:317.

Van Laere, K., Casteels, C., Dhollander, I., Goffin, K., Grachev, I., Bormans, G., et al. (2010). Widespread decrease of type 1 cannabinoid receptor availability in Huntington disease in vivo. *Journal of Nuclear Medicine: Official Publication, Society of Nuclear Medicine, 51*(9), 1413–1417. https://doi.org/10.2967/jnumed.110.077156.

Van Sickle, M. D., Duncan, M., Kingsley, P. J., Mouihate, A., Urbani, P., Mackie, K., et al. (2005). Neuroscience: Identification and functional characterization of brainstem cannabinoid CB2 receptors. *Science, 310*(5746), 329–332. https://doi.org/10.1126/science.1115740.

Varvel, S. A., Cravatt, B. F., Engram, A. E., & Lichtman, A. H. (2006). Fatty acid amide hydrolase (−/−) mice exhibit an increased sensitivity to the disruptive effects of anandamide or oleamide in a working memory water maze task. *The Journal of Pharmacology and Experimental Therapeutics, 317*(1), 251–257. https://doi.org/10.1124/jpet.105.095059.

Veldhuis, W. B., van der Stelt, M., Wadman, M. W., van Zadelhoff, G., Maccarone, M., Fezza, F., et al. (2003). Neuroprotection by the endogenous cannabinoid anandamide and arvanil against *in vivo* excitotoxicity in the rat: Role of vanilloid receptors and lipoxygenases. *The Journal of Neuroscience, 23*(10), 4127–4133. https://doi.org/10.1523/JNEUROSCI.23-10-04127.2003.

Vrechi, T. A., Crunfli, F., Costa, A. P., & Torrão, A. S. (2018). Cannabinoid receptor type 1 agonist ACEA protects neurons from death and attenuates endoplasmic reticulum stress–related apoptotic pathway signaling. *Neurotoxicity Research, 33*(4), 846–855. https://doi.org/10.1007/s12640-017-9839-1.

Walter, L., Franklin, A., Witting, A., Wade, C., Xie, Y., Kunos, G., et al. (2003). Nonpsychotropic cannabinoid receptors regulate microglial cell migration. *The Journal of Neuroscience, 23*(4), 1398–1405. https://doi.org/10.1523/JNEUROSCI.23-04-01398.2003.

Yang, L., Rozenfeld, R., Wu, D., Devi, L. A., Zhang, Z., & Cederbaum, A. (2014). Cannabidiol protects liver from binge alcohol-induced steatosis by mechanisms including inhibition of oxidative stress and increase in autophagy. *Free Radical Biology and Medicine, 68*, 260–267. https://doi.org/10.1016/j.freeradbiomed.2013.12.026.

Zeissler, M.-L., Eastwood, J., McCorry, K., Hanemann, O. C., Zajicek, J. P., & Carroll, C. B. (2016). Delta-9-tetrahydrocannabinol protects against MPP+ toxicity in SH-SY5Y cells by restoring proteins involved in mitochondrial biogenesis. *Oncotarget, 7*(29), 46603–46614. https://doi.org/10.18632/oncotarget.10314.

Zhang, H.-Y., Gao, M., Liu, Q.-R., Bi, G.-H., Li, X., Yang, H.-J., et al. (2014). Cannabinoid CB 2 receptors modulate midbrain dopamine neuronal activity and dopamine-related behavior in mice. *Proceedings of the National Academy of Sciences, 111*(46), E5007–E5015. https://doi.org/10.1073/pnas.1413210111.